DURABILITY OF PULP FIBER-CEMENT COMPOSITES

A Dissertation
Presented to
The Academic Faculty

by

Benjamin J. Mohr

In Partial Fulfillment
of the Requirements for the Degree
Doctor of Philosophy in Civil Engineering

Georgia Institute of Technology

August 2005

Copyright © 2005 by Benjamin J. Mohr

Durability of Pulp Fiber-Cement Composites

Approved by:

Dr. Kimberly Kurtis, Advisor
School of Civil and Environmental Engineering
Georgia Institute of Technology

Dr. Laurence Jacobs
School of Civil and Environmental Engineering
Georgia Institute of Technology

Dr. Hiroki Nanko
Institute of Paper Science and Technology at Georgia Tech
Georgia Institute of Technology

Dr. Arun Gokhale
School of Materials Science and Engineering
Georgia Institute of Technology

Dr. Lawrence Kahn
School of Civil and Environmental Engineering
Georgia Institute of Technology

Date Approved: July 6, 2005

ACKNOWLEDGEMENTS

I would like to thank everyone who has made it possible for me to complete my Ph.D. experience. Without the help of all who have assisted me over the past four years, this work would not have been possible. I owe much appreciation to my advisor, Dr. Kimberly Kurtis, for her guidance, support, and patience. Her insights and direction have been invaluable to my experience. I am grateful to Dr. Hiroki Nanko who has taught me the art of microscopy and for always being a source of unlimited information. I would also like to thank Dr. Joseph Biernacki for all his help in using the ESEM and providing feedback on the work conducted under his supervision. I also owe thanks to Dr. Lawrence Kahn for always meeting with me and for providing feedback. Special thanks to Dr. Laurence Jacobs and Dr. Arun Gokhale for providing useful insights. In addition, I would like to thank Shaobo Pan at IPST for preparing the pulp used in this research.

NSF and the IPST member companies have provided the financial support to make this research possible. Any opinions, findings, and conclusions or recommendations expressed in this material are those of the authors and do not necessarily reflect the views of the sponsors.

Over the course of my research, the following undergraduates have assisted me with unbridled enthusiasm and patience: Anne Bradford, Anthony Fisher, Ford Burgher, Roberto Blackman, and Laura Premenko. I am grateful of my officemates and friends, past and present – Nabil El-Ashkar, Nikhila Naik, Mauricio Lopez, Courtney Collins, Krissy Thibodeaux, Joy Justice, Jeff Kock, Scott Canfield, Brian Smith, and Jason

McCormick – for providing me with feedback and personal encouragement. Victor Garas and Marcus Millard should also be thanked for putting up with me during my last semesters. Special thanks to CEE staff, Antionette Keith and Ken Thomas, who have always assisted me with everything administrative and facilities associated.

I would also like to thank my parents for their support and for at least attempting to understand what I do. And finally, very special thanks to my wife, Kathy, who through her enduring love, understanding, and patience provided me with the strength and motivation to make this all possible.

TABLE OF CONTENTS

LIST OF TABLES

LIST OF FIGURES

SUMMARY

Wood pulp fibers are a unique reinforcing material as they are non-hazardous, renewable, and readily available at relatively low cost compared to other commercially available fibers. Today, pulp fiber-cement composites can be found in products such as extruded non-pressure pipes and non-structural building materials, mainly thin-sheet products. Although natural fibers have been used historically to reinforce various building materials, little scientific effort has been devoted to the examination of natural fibers to reinforce engineering materials until recently. The need for this type of fundamental research has been emphasized by widespread awareness of moisture-related failures of some engineered materials; these failures have led to the filing of national- and state-level class action lawsuits against several manufacturers.

Thus, if pulp fiber-cement composites are to be used for exterior structural applications, the effects of cyclical wet/dry (rain/heat) exposure on performance must be known. Pulp fiber-cement composites have been tested in flexure to examine the progression of strength and toughness degradation. Based on scanning electron microscopy (SEM), environmental scanning electron microscopy (ESEM), energy dispersive spectroscopy (EDS), a three-part model describing the mechanisms of progressive degradation has been proposed: (1) initial fiber-cement/fiber interlayer debonding, (2) reprecipitation of crystalline and amorphous ettringite within the void space at the former fiber-cement interface, and (3) fiber embrittlement due to reprecipitation of calcium hydroxide filling the spaces within the fiber cell wall structure.

Finally, as a means to mitigate kraft pulp fiber-cement composite degradation, the effects of partial portland cement replacement with various supplementary cementitious materials (SCMs) has been investigated for their effect on mitigating kraft pulp fiber-cement composite mechanical property degradation (i.e., strength and toughness losses) during wet/dry cycling. SCMs have been found to be effective in mitigating composite degradation through several processes, including a reduction in the calcium hydroxide content, stabilization of monosulfate by maintaining pore solution pH, and a decrease in ettringite reprecipitation accomplished by increased binding of aluminum in calcium aluminate phases and calcium in the calcium silicate hydrate (C-S-H) phase.

In conclusion, the degradation of pure portland cement paste composites containing pulp fibers was found to be very significant. Contrary to ACI 544 recommendations, fibers containing relatively high lignin contents (*i.e.*, TMP fibers) exhibited a slower progression of degradation as compared to low-lignin fibers, such as bleached kraft pulp fibers. The degradation of these composites can be mitigated through the addition of SCMs as a partial weight replacement for portland cement.

CHAPTER 1

INTRODUCTION

Though the use of natural materials to reinforce brittle materials has been around since the use of straw to reinforce mud blocks, the incorporation of cellulosic fibers into cement-based materials has recently received renewed interest because of their renewability and because of the benefits to mechanical behavior. Although they typically do not contribute additional tensile or flexural (first crack) strength, the use of cellulosic fibers to reinforce cement-based matrices can improve toughness, ductility, flexural capacity after cracking, and crack resistance as compared to unreinforced cement-based materials. Since cement-based materials are inherently weak in tension, fibers provide a means of controlling crack growth through several mechanisms, such as the introduction of closure stresses across a microcrack and crack tip deflection. Thus, cracks remain microcracks, rather than coalescencing into macrocracks, which can lead to failure.

Fiber-reinforced cement-based materials have been used in many aspects of construction. Steel, polymers, and cellulosic fibers are the most commonly used to reinforce cement-based materials, which may range from cement paste to mortar to concrete. Within the framework of the research presented in the following chapters, our discussion will be exclusive to cellulosic fibers used to reinforce both cement paste and mortar.

Currently, cellulosic fiber reinforced cementitious materials are most widely used for exterior products such as siding and roofing materials, for residential construction. Previously, this class of construction composites contained asbestos fibers. Asbestos fibers were used due to their high strength-to-weight ratio. However, due to the carcinogenic nature of asbestos, alternative fibers were sought and cellulosic fibers, including pulp fibers, were determined to be a viable alternative.

In the United States, wood pulp fibers are used to reinforce cementitious materials, due to their abundance. In other parts of the world, sisal, jute, and other cellulosic fibers are used where their abundance is plentiful. Wood pulp fiber is a unique reinforcing material as it is non-hazardous, renewable, and readily available at relatively low cost compared to other commercially available fibers [MacVicar et al., 1999]. As a result of these various advantages, pulp fiber-cement composites have found practical applications in recent decades in the commercial market as a replacement for hazardous asbestos fibers. Today, pulp fiber-cement composites can be found in products such as extruded non-pressure pipes and non-structural building materials, mainly thin-sheet products [ACI 544, 1996]. Fiber-cement siding has been called “tomorrow’s growth product” [Kurpiel, 1998] and as of the late 1990’s, shares 7-10% of the North American siding market [Kurpiel, 1997]. This percentage has increased to approximately 20% in the United States as of 2005 [Hojaji, 2005].

However, the replacement of asbestos with cellulosic fibers is not without its own sustainability concerns. Thus, to ensure the satisfactory performance of fiber-cement materials, improved understanding of their expected long-term performance is essential. In particular, adequate understanding of the effects of moisture fluctuations

expected during exterior exposure on performance over time is critical to ensure durability of fiber-cement composites and to gain market acceptance for these materials. Although cellulosic fibers have been used historically to reinforce various building materials, little scientific effect has been devoted to the examination of cellulosic fibers to reinforce engineering materials until recently [ACI 544, 1996]. The need for this type of fundamental research has been emphasized by widespread awareness of moisture-related failures of some engineering wood siding products; these failures have lead to the filing of national- and state-level class action lawsuits against several manufacturers [NAHBRC, 2000]. With the poor durability of engineered wood materials used for residential construction, homeowners and builders may be more reluctant to embrace new construction materials, including fiber-cement products. In addition, some complaints have been lodged against manufacturers of fiber-cement roofing materials. According to Graham [2000], the National Roofing Contractors Association (NRCA) has received frequent complaints regarding premature deterioration, including surface crazing, breakage, cracking, delamination, softening, and discoloration, of pulp fiber-reinforced composite shingles produced by a number of manufacturers.

Because of these concerns, the main focus of this research is to investigate the durability of pulp fiber-cement composites when subjected to simulated heat/rain (*i.e.*, wet/dry cycling) conditions. In this manner, the incorporation of pulp fibers has led to durability and sustainability concerns. Other important aspects that will be discussed include means of improving the sustainability of new construction through the addition of pulp fibers to the cement-based materials. It is through this research that a more comprehensive understanding of the infrastructure sustainability will be ascertained.

Thus, the following chapters will discuss the background, results, and conclusions of this research program. Chapter 2 will begin by giving a thorough overview of the existing literature concerning cellulosic fiber reinforcement of cement-based materials, including compressive strength, flexure strength, shrinkage, and durability aspects. Chapter 3 discusses the research methodology used for the various aspects of this project, from mechanical testing to microstructural characterization. Chapter 4 begins with mechanical testing and microstructural characterization results assessing kraft pulp fiber modifications and differences in pulp fiber types. Based on these results, a novel three-part progressive degradation mechanism is proposed. Using an array of innovative characterization techniques such as environmental scanning electron microscopy, the proposed model is verified. Previous research has investigated the durability of these composites only prior to and after wet/dry cycling. Thus, this progressive degradation model is believed to be the first and most comprehensive evaluation of the progressive mechanisms involved with composite durability during wet/dry cycling. Once the mechanisms were elucidated, methods were utilized in order to mitigate the degradation that was observed. Chapter 5 will discuss one such approach to kraft pulp fiber-cement composite degradation through the use of supplementary cementitious materials as a partial weight replacement for portland cement. Though cellulosic fibers have typically been used for thin-sheet products such as fiber-cement siding, there is a push to incorporate these fibers into larger structural concrete members. Though there are many aspects associated with using cellulosic fibers in concrete, one aspect – internal curing / autogenous shrinkage mitigation – was investigated in Chapter 6. This is believed to be the first evaluation of wood-derived materials applied to internal

curing of high-strength concrete. Lastly, Chapter 7 will provide an overview of the major research findings presented in Chapters 4 – 6. In addition, research is proposed that will be the basis for future grants and proposals.

CHAPTER 2

LITERATURE REVIEW

The current literature concerning pulp fiber characteristics, pulp fiber fiber-cement composite properties, and composite durability will be reviewed herein. While many types of cellulosic fibers have been studied for their respective benefit in improving the properties of cement-based materials, the focus of this research has been on wood pulp fibers. Thus, the literature discussed here will be limited to those cement-based composites incorporating only wood pulp fibers, where applicable.

2.1 Pulp Fiber Characteristics

2.1.1 Pulp Fiber Chemical Composition

Cellulose, $(C_6H_{10}O_5)_n$, accounts for the largest mass percent (typically 45-50%) of a cellulosic fiber [Bledzki and Gassan, 1999]. It is typically found with the cell walls of a cellulosic fiber. The general chemical structure of this linear unbranched polymer, composed of glucose mers, $C_6H_{12}O_6$, [Young *et al*., 1998; Illston and Domone, 2001], can be seen in Figure 2-1. The mechanical properties of cellulosic fibers are largely dependent upon the degree of cellulose polymerization, crystallinity (which may vary between 65 and 90% in wood), cellulose cell wall structure, and cellulose content. For

the most part, as the amount of cellulose increases, the fiber tensile strength and modulus of elasticity increase linearly. In addition, the hydroxyl side groups of the cellulose molecule act to create microfibrils and are largely responsible for the hygroscopic nature of cellulosic fibers [Young *et al*., 1998].

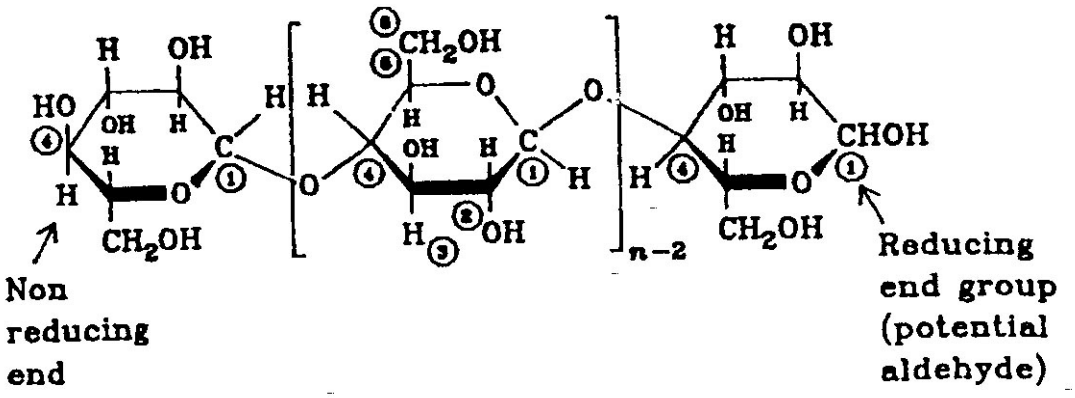

Figure 2-1. General physical structure of cellulose [Nevell and Zeronian, 1985].

Lignin makes up 20-30% of the wood structure by mass. It is composed of complex polymers, primarily phenyl propane, that bind the wood fiber together [Young *et al*., 1998], as seen in Figure 2-2. The structure of lignin is three-dimensional and largely amorphous. The degree of polymerization of lignin varies from fiber to fiber, given the same fiber type. Lignin is predominately found in the fiber middle lamella, though it can be found throughout the fiber, acting to bind the individual cells together. Lignin is also responsible for imparting stiffness in wood [Illston and Domone, 2001]. For the most

part, lignin is the least understood component of cellulosic fibers. Though lignin is relatively variable and amorphous, it has been used as a chemical additive to concrete as a cement hydration retarder in certain forms.

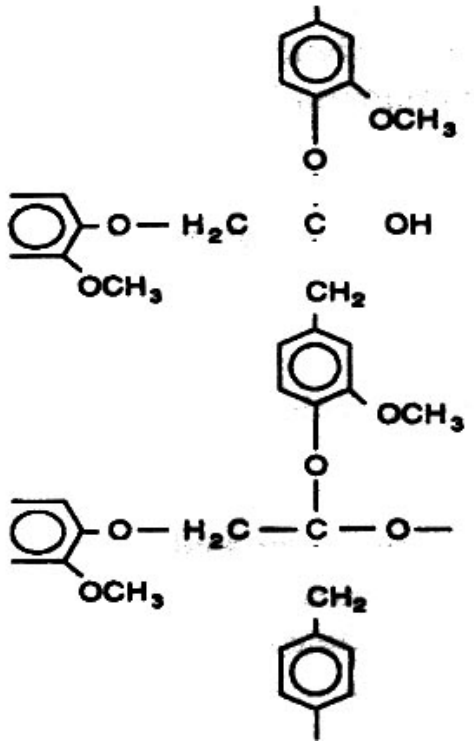

Figure 2-2. General physical structure of lignin [Nevell and Zeronian, 1985].

Hemicelluloses generally account for 20-25% by mass of cellulosic fibers. Hemicelluloses are also predominately found in the fiber cell walls concentrated away from the middle lamella. Contrary to its name, hemicelluloses differ greatly from cellulose in that hemicelluloses are branched polymers composed of several different

non-glucose sugar mers, typically galactose, mannose and/or xylose [Illston and Domone, 2001]. Hemicelluloses are amorphous, with a degree of polymerization on the order of 150-200 [Young *et al*., 1998]. Furthermore, the structure of hemicelluloses varies from plant to plant due to the relative amounts of various sugars, unlike cellulose, but generally has a form as seen in Figure 2-3.

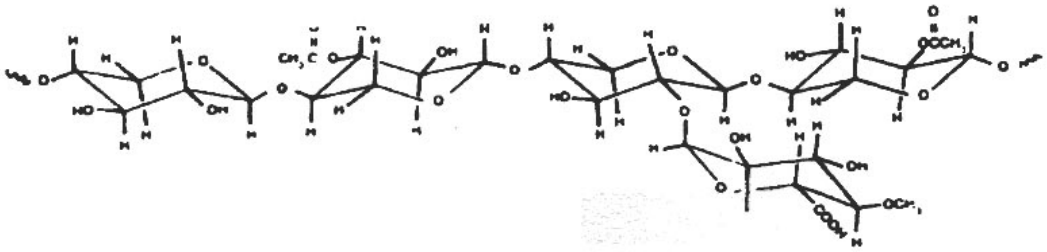

Figure 2-3. General physical structure of hemicelluloses [Nevell and Zeronian, 1985].

The last chemical component of wood is the extractives. Extractives compose up to 10% of the fiber by mass but do not form part of the fiber physical structure. Instead, these organic compounds give certain properties to the wood, such as color, odor, taste [Young *et al*., 1998], and decay and insect resistance [Illston and Domone, 2001]. Most of these extractives have little commercial value, but some waxes, such as rubber and resin have significant economic value [Illston and Domone, 2001]. Certain extractives such as polysaccharides and tannic acids may be incompatible with cement-based materials. Within the pulp industry, it is known that plywood concrete formwork

derived from certain wood materials can cause concrete setting problems due to the presence of these extractives.

2.1.2 Pulp Fiber Physical Structure

A cellulosic fiber consists of 4 distinct layers. Figure 2-4 illustrates a typical fiber cross-section, including the middle lamella (lignin-rich layer that holds together the neighboring fiber cells), primary wall, S1-S3 layers, and the fiber lumen. The primary wall, S1, S2, and S3 layers have relative thicknesses of 1-2, 10-22, 70-90, and 2-8%, respectively [Young *et al*., 1998].

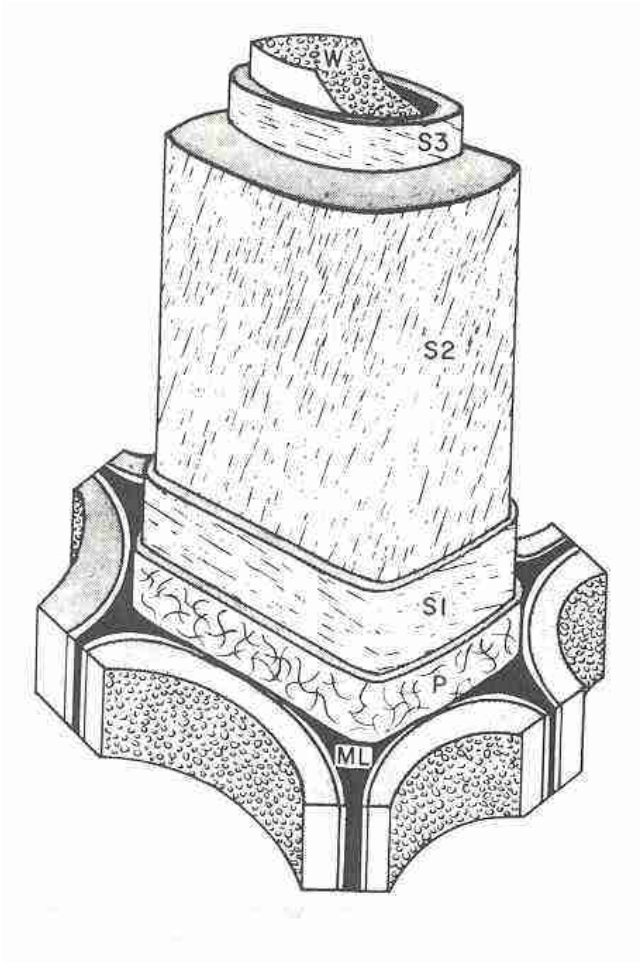

Figure 2-4. Pulp fiber physical structure.

Within the secondary wall layers, the helix or spiral angle of a fiber describes the orientation of microfibrils with respect to the longitudinal axis of the fiber. Fiber microfibrils are considered to be oriented "bundles" of fiber cells located within the fiber cell walls (S1, S2, S3) as seen in Figure 2-4. The helix angle (Figure 2-5) is directly related to the tensile strength and stiffness of a fiber and can be used to model those fiber mechanical properties along with the fiber cellulose content. The S2 layer is typically

thought to provide the fibers with the largest percentage of strength due to its relatively large thickness and small helix angle.

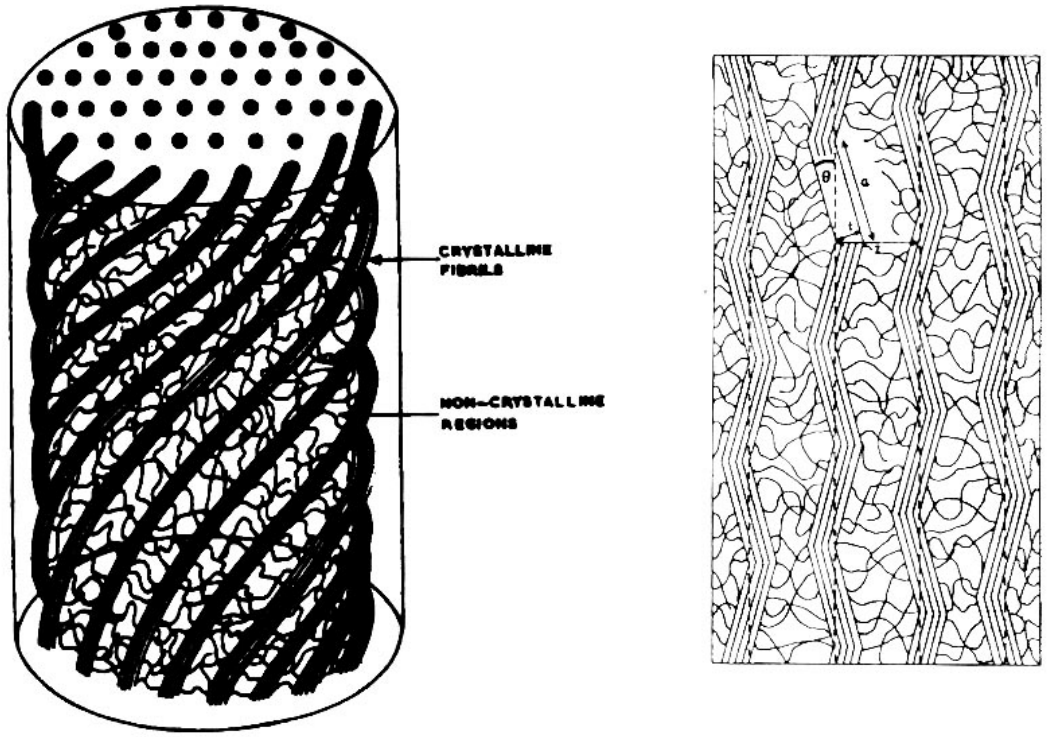

Figure 2-5. Helix angle of S1 layer in 3D and 2D views [Hearle and Sparrow, 1979].

Typically, 90% of the volume of wood consists of the longitudinally aligned cells – tracheids – previously mentioned. However, the remaining 10% consists of cells, called parenchyma, oriented transversely. These cells are responsible for the transport of nutrients through the cell structure. In addition, the tracheids and parenchyma are

interconnected by pits that allow for liquid movement between closely aligned, parallel fiber cells [Young *et al*., 1998].

2.1.3 Kraft (Chemical) Processing

Chemical pulp processes are also referred to as kraft pulping and constitute the largest portion of pulps manufactured. During the chemical soaking in NaOH and Na_2S and processing of kraft fibers, most of lignin and hemicelluloses is removed. Because of this, kraft pulp fibers are generally considered to be of the highest quality in terms of strength and bleached brightness potential [Thorp and Kocurek, 1998]. However, these important qualities come at the cost of a low yield potential of approximately 45-55% and high operating and capital costs compared to the other pulp processes. Additionally, any required refining (beating) must be done separately and at increased costs.

2.1.4 Thermomechanical Processing

Mechanical pulps are made without chemical processing and thus only require mechanical energy, and often heat, to produce pulps with distinct properties often used in newsprint paper. High-temperature refined fibers, also known as thermomechanical pulp (TMP) generally produce yields of 80-90% and are significantly cheaper than kraft pulps to produce. Typically, TMP fibers cost approximately 20% less than kraft fibers. Furthermore, post-processing refining is often not required as the TMP processes create the same effect as the refining operation after kraft pulping. Unlike bleached kraft fibers,

TMP fibers contain lignin. The resulting mechanical pulp contains approximately 25-31% lignin by mass compared to 3-8% for unbleached kraft pulp and 0-1% for bleached kraft pulp [Stenius, 2000].

Generally, however, fibers with lower lignin and hemicelluloses content, such as kraft pulp fibers, have been favored for use in cement-based composites, because of the potential for alkali degradation of these components [ACI 544, 1996]. Though mechanical pulps appear to be attractive in terms of their high yields and low costs, the mechanical properties of the TMP fibers suffer, compared to kraft fibers. Lastly, TMP fiber specific gravity is typically assumed to be 0.5, as compared to 1.5 for softwood kraft fibers. The specific gravity of TMP fibers is lower than that of kraft fibers since TMP fibers have an open lumen, whereas the kraft fiber lumen is collapsed. This aspect is important to consider when proportioning a pulp fiber-cement mix design.

2.2 Wood Pulp Fiber-Cement Composite Properties

2.2.1 Fresh Properties

2.2.1.1 Workability

All fibers are expected to decrease the workability (*i.e.*, flow) of a cementitious mix. Detrimental effects to flow can often be offset by the use of superplasticizers. However, the use of superplasticizers may have an adverse effect of early age properties of cement-based materials, including increased set time and decreased cohesiveness.

Thus, it is important to understand the effect of fiber incorporation on workability to identify any areas of concern.

Soroushian and Marikunte [1990] found that the flow (as measured by ASTM C 230) of a cement paste mix tended to decrease slightly with the incorporation of kraft pulp fibers. However, in the study by Soroushian and Marikunte [1990], the water-to-cement ratio was increased with increasing fiber mass fractions. Therefore, a definitive conclusion cannot be drawn from their work regarding the effect of pulp fiber addition on workability. However, it can be concluded that at a water-to-cement ratio of 0.35, hardwood kraft fibers (average length of 0.9 mm) decreased flow more so than softwood kraft fibers (average length of 3.0 mm) at a 1% fiber mass fraction. At a 2% fiber mass fraction (water-to-cement ratio of 0.40), there was no difference in measured flow between the softwood and hardwood kraft fibers.

Additionally, the incorporation of 1 and 2% mechanical pulp fibers by mass led to a 12.2-14.9% and a 6.1% increased flow, respectively, as compared to the two kraft fiber types at the same water-to-cement ratios. Additionally, Soroushian and Marikunte [1992] have shown that cement paste containing mechanical pulp fibers actually increases flow when compared to the control (without fibers) and at the same water-to-cement ratio (without using superplasticizers). However, no justification was given concerning the increased flow of cement pastes containing mechanical pulps.

Using concrete, Naik *et al*. [2004] have shown that the incorporation of relatively low fiber mass fractions (*i.e.*, less than 1%) can significantly reduce slump. It was found that the concrete slump without fibers was approximately 235 mm. With the

incorporation of up to 0.8% fibers by mass, slump decrease by as much as 170 mm using approximately the same mix proportions (water-to-cement ratio of 0.47).

2.2.1.2 Setting Time

As discussed previously, lignin is a well-known cement hydration retarder and is a component of lignosulfate hydration retarding chemical admixtures. Therefore, the incorporation of pulp fibers to a cementitious matrix may present some incompatibilities. Since pulp fibers contain organic polymers, it is possible that these polymers may adversely influence cement hydration. It is possible that the incorporation of pulp fibers may slightly lengthen setting time of cement paste samples. This effect should be more pronounced when lignin-rich fibers, such as TMP, are used.

Results by Soroushian and Marikunte [1990, 1991, 1992, 1994] using ASTM C 403 (penetration resistance) show that the initial set of cement pastes containing softwood and hardwood kraft fibers does not appear to be altered. However, the final set time was slightly increased. Using mechanical pulp fibers, both initial and final set times were significantly increased. Furthermore, as the fiber content increased, setting times increased in accordance. This appears to indicate that the pulp fiber chemical composition does play a role in cement hydration.

Even though these results indicate adverse effects on cement hydration with the use of pulp fibers, more research needs to be done to determine the cause of delayed setting. It is possible that pulp fibers contain certain chemicals, such as lignin, that influence cement hydration. In addition, it is also possible that pulp fibers may absorb

and/or desorb water from the cement matrix (or the atmosphere), altering localized water-to-cement ratios and thus, influencing setting times. Thus, to isolate the effect of pulp fibers on cement hydration, it is suggested that heat of hydration studies (Section 2.2.1.3) may be more appropriate for determining actual incompatibilities between pulp fibers and cement hydration.

2.2.1.3 Heat of Hydration

Since cement hydration is exothermic, calorimetry can be used to measure changes in cement hydration, due to the incorporation of additional materials, such as pulp fibers. Heat of hydration is also important for massive concrete sections where thermal expansions and contractions may induce cracking. Thus, by measuring the heat of hydration of cement samples with pulp fibers, the overall heat evolved and the rate of cement hydration can be measured. Previously, in Section 2.2.1.2, it was shown that the incorporation of kraft pulp and TMP fibers was found to delay setting of cement paste. It was suggested that calorimetry measurements of heat of hydration may be a more appropriate method to assess the compatibility of pulp fibers in a cement matrix.

Research by Bilba *et al*. [2003] has shown that as the amount of lignin-rich cellulosic fibers added to a cement paste sample increases, the peak heat of hydration temperature decreased. However, the time to reach this temperature was not affected by the presence of these cellulosic fibers. The overall heat evolved and the length of heat evolution was not recorded, thus restricting interpretations of these data. These data are important to understand the overall effect of fiber addition.

Hofstrand *et al*. [1984] have also shown that the addition of wood particles, rich in lignin, significantly lowers the maximum hydration heat. There is also a marked delay in the maximum hydration heat as compared to the cement paste control sample. It was also noted that heat of hydration curves varied depending upon the wood species being used. These variations may be due to the chemical composition of the fibers, which was not reported in this study. In the study by Hofstrand *et al*. [1984], overall heat of hydration values were not reported. It is also unclear from the research methodology if the water-to-cement ratio was kept constant for each composite and if any superplasticizer was used. Similar results were achieved by Moslemi and Lim [1984] and Lee *et al*. [1987].

However, all the previous work has concentrated on wood particles, not kraft or thermomechanical pulp fibers. Since pulp fibers contain some lignin, a well-known cement hydration retarder, it is possible that cement hydration as a whole may be slightly affected by the incorporation of pulp fibers. If the fiber lignin does have an effect, TMP fibers, containing 25-31% lignin by mass, should have the greatest impact on the observed heat of hydration curves. In addition, the use of bleached kraft fibers (0-1% lignin) should a negligible impact on hydration due to their minimal lignin content.

Pulp fibers are hydrophilic and can slowly release water back into the matrix as the internal relative humidity of the sample decreases (self-desiccation). Thus, it is also possible to observe changes in the length of initial cement hydration (*i.e.*, internal curing) via heat of hydration. Overall, the research presented here may be slightly misleading as to the compatibility of pulp fibers in a cement matrix. Since TMP or kraft fibers were not

specifically used, it is difficult to draw any specific conclusions based on the work presented here.

2.2.2 Shrinkage

2.2.2.1 Plastic Shrinkage

Plastic shrinkage occurs in fresh concrete due to the evaporation of water from the surface of the concrete causing negative capillary stresses and volume contractions [Cabrera *et al*., 1992]. If the evaporation gradient between the surface and interior of the concrete is significant, plastic shrinkage cracking can occur on the concrete surface prior to final set. Water absorption by formwork and subbase materials can also lead to plastic shrinkage cracking. The incorporation of hydrophilic fibers may reduce the effects of surface evaporation by retaining moisture and acting to restrain surface cracking.

From the literature, there are several restrained plastic shrinkage test methods. All test methods have shown varying degrees of success. Often, only certain rich concrete mixes with high water-to-cement ratios will show plastic shrinkage cracking. Plastic shrinkage cracking is also highly dependent upon environmental conditions (*i.e.*, wind speed and humidity). Currently, no standard exists as a guideline for conducting plastic shrinkage tests.

Balaguru [1994] evaluated the effectiveness of several types of fibers in reducing the plastic shrinkage cracking of concrete slabs with stress risers. Results indicated that cellulose fibers added at a dosage rate of 3 lb/yd^3 were much less effective

than equivalent dosage rates of polypropylene or polyethylene fibers in minimizing the overall average crack area. The differences in shrinkage area are attributed to the smaller aspect ratio of pulp fibers as compared to the polymeric fibers. In addition, fibers were less effective in reducing the average crack width for lean concrete mixes as compared to rich mixes. It is possible that the fiber-cement bond strength is enhanced in richer concrete mixes, leading to greater crack closure stresses induced by the fibers.

Soroushian and Ravanbakhsh [1998] used a test method with risers for end restraint and stress increase to determine the performance of normal and high-performance concrete with and without 0.06% cellulose fibers by volume to concrete. The pulp fiber volume fraction is equivalent to a typical polypropylene dosage rate of 0.5 lb/yd^3 of concrete. Statistically significant results indicated that cellulose fibers reduced the average crack area by 52.3% (109 to 52 mm^2) and the average maximum crack width by 46.3% (1.08 to 0.58 mm^2) for normal concrete (water-to-cement ratio of 0.55, 422 kg/m^3 cement, 844 kg/m^3 both natural sand and 25mm aggregate) after 3 hours from casting. Similar results were obtained for the high-performance concrete mix (water-to-cement ratio of 0.42, 505 kg/m^3 cement, 1045 kg/m^3 25mm aggregate, and 590 kg/m^3 natural sand) where the cellulose fibers reduced the average crack area by 44.7% (16.1 to 8.9 mm^2) and the average maximum crack width by 46.2% (0.13 to 0.07 mm).

Soroushian [2000] has also established that the incorporation of 0.2% pulp fibers by volume has reduced the plastic shrinkage maximum crack width of concrete from approximately 0.14 mm to 0.02 mm.

However, additional work is necessary to compare the effectiveness of pulp fibers to polypropylene fibers, which are more typically used in practice. That is, it

should be determined if pulp fiber reinforced concrete specimens require higher volume fractions to achieve similar crack resistance to that of polypropylene reinforced concrete. Since pulp fibers can be produced at a fraction of the cost of polypropylene fibers, higher volume fractions could be more economical, while achieving equivalent results, compared to other fiber types.

Additionally, more research is needed to establish if there is an upper limit on fiber volume fractions. In other words, is there a maximum threshold fiber volume fraction where the use of a higher volume fraction does not produce any additional benefit.

2.2.2.2 Autogenous Shrinkage

It is well known that the products of cement hydration occupy a smaller volume than the original reactants. This reduction is known as chemical shrinkage and is usually notated as a volume reduction (mL) per gram of cement. Thus, cement pastes will exhibit a reduction in volume from the addition of water to cement until setting. Once final set has occurred and the cement paste has formed a semi-rigid skeleton, continued cement hydration will lead to increases in pore sizes as net volumetric changes are restrained.

After set and without an external water source, increases in porosity and reductions in internal relative humidity will create capillary surface tensions in the pore structure. These surface tensions will lead to tensile stresses in the microstructure. These internal stresses cause cement paste deformations, also known as autogenous

deformations. These deformations are typically shrinkage and are also referred to autogenous shrinkage in most cases.

Autogenous deformations are defined as isothermal linear deformations that occur without any moisture migration (*i.e.*, no mass change). Certain shrinkage-reducing admixtures may minimize this deformation due to a decrease in capillary surface tension and an increase in the cement paste relative humidity, thus changing the cement paste internal drying characteristics. Autogenous deformations have only recently been considered as a significant problem.

It was found in 1940, that autogenous shrinkage strains after setting were only on the order of 50-100 με for normal concrete [Davis, 1940]. Thus, for over 40 years, autogenous deformations were largely neglected. However, with the advent of high-performance concrete (HPC) in the 1980's, containing low water-to-cement ratios and typically silica fume, early-age cracking has occurred with greater frequency. In HPC cement pastes, autogenous shrinkage strains after setting can reach upwards of a thousand microstrain within 3-7 days and several thousand microstrain within a few months. The two aspects of HPC that make it so attractive are also the reasons that it is so susceptible to early-age deformations and cracking. Low water-to-cement ratio and silica fume (or other SCMs) will greatly refine the pore structure of the cement paste. Refinement of the paste pore system will create greater internal capillary stresses after set, leading to increased autogenous shrinkage.

Several approaches have been undertaken to mitigate autogenous shrinkage. One approach has concentrated on using water-entraining materials to release water during self-desiccation, thus maintaining the internal RH of the cement paste and

lowering the capillary tension. This method is also known as internal or autogenous curing and has been investigated using lightweight aggregate particles saturated with water [Weber and Reinhardt, 1997; Bentz and Snyder, 1999], super absorbent polymers (SAPs) [Jensen and Hansen, 2001; Jensen and Hansen, 2002; Jensen and Lura, 2003], and other materials [Jensen and Lura, 2003].

From the available literature, no research efforts have considered effects of cellulose-based fibers or powder on the autogenous deformations of cement-based composites. Pulp fibers are expected to contribute both to internal restraint and internal curing, while pulp powders will not provide any restraint.

2.2.2.3 Free Shrinkage

Free shrinkage is a measure of the drying shrinkage of cement-based materials. In this particular test, specimens are stored after demolding so that they are unrestrained and thus do not typically exhibit cracking. However, large free shrinkage strains could correlate to increased cracking tendency upon restraint.

Results by Sarigaphuti *et al*. [1993] indicate that the incorporation of 0.5% pulp or polypropylene fibers by volume did not have an observed effect on free shrinkage. Additional work by El-Ashkar [2002a] has shown that the used of a pulp fiber volume fraction greater than 0.25% led to increased free shrinkage of mortar specimens. This additional shrinkage attributed to pulp fiber shrinkage – upon releasing water – that may be contributing to increased mortar bar shrinkage.

Thus, it seems the free shrinkage of cement-based specimens is independent of the incorporation of fibers. This may be due to the concept that fibers typically are primarily beneficial after cracking. However, ASR literature shows that fibers do minimize expansive strains due to internal restraint. Though, in the case of free shrinkage, the fibers are being placed in compressive loading and may not assist in restraining the compressive strains.

Though it appears that this particular shrinkage measurement technique is not applicable to fiber-reinforced cement-based materials, it is possible that pulp fibers may themselves lead to increased free shrinkage at sufficient fiber volume fractions [Toledo Filho *et al*., 2004]. Since pulp fibers are hygroscopic and release moisture during drying, they exhibit some measure of shrinkage. Thus, pulp fibers may actually contribute to composite shrinkage. However, this effect may not be appreciable since longitudinal swelling and shrinkage of pulp fibers is typically on the order of 2-5%. The majority of pulp fiber dimensional change is in the radial direction where swelling and shrinkage may be as high as 135% for kraft fibers.

More research is warranted to assess how fiber shrinkage influences composite free shrinkage. The effect of pulp fiber shrinkage should be isolate to determine if the pulp fibers are causing increased free shrinkage. In addition, if the pulp fibers are the primary cause of increased free shrinkage, what effect do these fibers have on drying shrinkage? This will be addressed in the following section.

2.2.2.4 Drying (Restrained) Shrinkage

Restrained shrinkage has been used to evaluate drying shrinkage, which is induced shrinkage due to moisture loss from concrete specimens, after setting. While the observed restrained shrinkage primarily consists of drying shrinkage, it may also include plastic, chemical, and autogenous shrinkage. However, all constitutive shrinkage mechanisms are typically minimal. Plastic shrinkage is only evident prior to setting due to excess evaporation in large specimens. In the restrained ring shrinkage tests, evaporation is minimized. Chemical and autogenous shrinkage is expected to be minimal within the range of water-to-cement ratios typically used for these tests.

Restrained shrinkage is most commonly assessed using a restrained ring shrinkage apparatus [AASHTO P 34-99, 2003; ASTM C 1581, 2004]. However, regardless of shrinkage mechanisms, the addition of fibers to concrete is known to delay the onset of initial cracking and decreasing the maximum crack width/area.

Voigt *et al*. [2004] have shown that the addition of steel and polypropylene fibers delay the time of first visible crack from 15 days to as much as 27 days. In addition, the maximum crack widths were decreased by more than a factor of two. It was also shown that increases in the number of fibers per unit volume/area and the fiber surface area led to decreases in the maximum crack width.

Sarigaphuti *et al*. [1993] have also shown that the addition of fibers ($V_f = 0.5\%$) to concrete can delay the onset of cracking. In this study, the control concrete specimens (water-to-cement ratio of 0.55) cracked after 8 days, while the pulp fiber-reinforced rings delayed cracking by up to 6 days. Polypropylene reinforced concrete delayed the onset

of cracking by only 3 days. Also, average crack widths at 42 days were reduced from 0.98 mm to as small as 0.25 mm.

Similar results were achieved by Soroushain [2000] using 0.2% pulp fibers by volume. It appeared that the onset of cracking was delayed by several days in the pulp fiber-reinforced concrete. Cracking initiated after approximately 22-23 days for the control sample and about 25-26 days for the pulp fiber concrete sample. The maximum crack width was also reduced, from approximately 0.2 mm to 0.85 mm.

2.2.3 Mechanical Properties

2.2.3.1 Compressive Strength

For the most part, compressive strength has not been thoroughly considered. Relatively little research is available from the current literature, compared to the tremendous amount of bending and tensile test results. If these composites are to be used for any application requiring compressive load carrying capacity, the effect of compressive strength changes due to fiber addition must be taken into account. Though it is difficult to compare various research studies due to widely varying experimental procedures, relative changes within studies can be directly compared.

Lin *et al*. [1994] reported cement paste (ASTM Type III cement) reinforced with 4% pulp fibers by mass (~5.5% by volume) exhibited significant losses in 28 day compressive strength (as measured by ASTM C 109) with curing at 100% RH, 25 °C. The compressive strength of composites containing hardwood kraft, softwood kraft, and

recycled kraft (newspaper) fibers was 55.9, 44.5, and 48.1 MPa, respectively, as compared to 108.7 MPa for the control without fibers.

Furthermore, Soroushian and Marikunte [1990] reported cement paste compressive strengths (tested according to ASTM C 873) of approximately 53, 58, and 61 MPa for mechanical pulp, softwood kraft, and hardwood kraft, respectively, at a 1% fiber mass fraction compared to 70 MPa for the control sample without fibers. At a 2% fiber mass, compressive strengths were approximately 40, 52, and 52 MPa, respectively. Thus, it can be seen that the mechanical pulp led to lower compressive strengths. In addition, as the fiber volume fraction increased, the composite compressive strength decreased.

Blankenhorn *et al*. [2001] reported similar results using the same experimental procedure and fiber types. At 28 days, the control strength was 95.5 MPa, but the incorporation of hardwood kraft, softwood kraft, and recycled kraft (newspaper) led to compressive strengths of 49.3, 51.7, and 43.3 MPa. Additionally, this study investigated fiber treatment methods to improve the compressive strength of pulp fiber-cement composites. However, not much success was reported as the maximum compressive strength obtained was only 55.8 MPa using a 10% alkylalkoxysilane treatment. Fiber treatments including an acrylic treatment did not produce appreciable improvements and in some cases, led to a further reduction in compressive strength. Additional fiber treatments by Pehanich *et al*. [2004] included sodium silicate, potassium silicate, and silane (aqueous silica). Only the silicate treatments produce encouraging results, though compressive strengths were significantly less than that of the control.

El-Ashkar [2002a] concluded that softwood kraft fiber volume fractions up to 1.2% did not significantly affect mortar compressive strength, compared to plain mortar. Addition of 2% fibers by volume led to an 18-34% reduction in mortar compressive strength. Furthermore, concrete with up to a 1% softwood kraft fiber volume fraction did not exhibit any significant compressive strength changes, compared to plain concrete. However, higher fiber volume fraction concrete mixes were not tested, so it is possible that higher fiber volume fractions may be possible without sacrificing compressive strength.

Sarigaphuti *et al*. [1993] has shown that concrete mixed with softwood kraft and hardwood fibers at volume fractions of 0.5% did not exhibit any compressive strength changes at 28 days. In this study, it appeared that compressive strength is independent of fiber length as shown by the use of hardwood fibers and varying percentages of summerwood and springwood fibers of the softwood variety. Fiber lengths were 0.7mm for hardwood fibers and varied from 1.33-4.40mm for softwood fiber varieties. All cellulose fibers proved more effective than polypropylene fibers with lengths of 11 mm. It should be noted that the incorporation of polypropylene fibers to concrete also led to a reduction in compressive strength on the same order as that of the pulp fibers.

Cellulose fibers also outperformed polypropylene fibers in a study by Soroushian and Ravanbakhsh [1999]. It was observed that cellulose fibers were effective in increasing the early age strength of high-early strength (HES) concrete, comparing to plain HES concrete, while inclusion of polypropylene fibers led to lower compressive strengths. It should be noted that the HES mixes in this study included a $CaCl_2$ cement hydration accelerant. The compatibility of cellulose fibers with cement mixes appears to

be greatly enhanced with this addition of $CaCl_2$ as previously shown by Lee and Hong [1986]. In that study, composite mixes exposed to $CaCl_2$ exhibited higher compressive strengths. Without $CaCl_2$, the use of some varieties of Southern kraft pulp fibers led to significantly lower compressive strengths compared to the typical Southern Pine kraft fibers used. However, with the addition of 3% $CaCl_2$, the compressive strengths of cement pastes with various Southern kraft fibers could not be differentiated. This seems to indicate that the use of $CaCl_2$ with cellulose fibers not only increases the compressive strength of the mixes up to at least 28 days, but also improves the compatibility of certain cellulose fiber species with cement.

Despite the observed results, the mechanism for decreased compressive strength is relatively unknown. It may be related to the pulp fiber retarding cement hydration due to the presence of lignin. Sections 2.2.1.2 and 2.2.1.3 reviewed the existing work concerning cement hydration in the presence of pulp fibers and found the pulp fibers containing lignin may delay the onset of setting and reduce the heat of hydration of a sample. Additionally, the incorporation of any type of fibers tends to increase the air content of a cement mixture. Air content likely increases due to poor compaction and reduced workability. Lastly, the pulp fibers may act as pre-existing microcracks that allow for accelerated crack propagation during compressive loading.

However, the reduction in compressive strength due to the incorporation of cellulosic fibers has been overcome with the partial replacement of cement with silica fume and slag [de Gutierrez *et al*., 2004].

2.2.3.2 Flexural Strength

2.2.3.2.1 Effect of Fiber Volume/Mass Fraction

Many research efforts have taken into consideration the effect of varying fiber contents on the bending strength of cement composites [Andonian *et al*., 1979; Coutts, 1987a, 1987b; Coutts and Kightly, 1982; Coutts and Warden, 1985, 1990; El-Ashkar, 2002; Soroushian and Marikunte, 1990, 1992, 1995]. The overall trend from the available literature indicates that as the fiber volume fraction increases, so does the flexural first crack and peak strength. However, it is difficult to differentiate first crack strength from peak strength in the literature. Generally, the strength of a composite was referred to as the flexural strength without any explanation. For this work, it was assumed that flexural strength is equivalent to the peak strength of the composite in flexure.

Andonian *et al*. [1979] appear to have performed the only published experimental work assessing the effect of fiber volume/mass fraction on first crack strength. In that study, fiber mass fractions of 2-10% were evaluated. First crack strength results indicate that a continual increase in first crack strength occurs with increasing fiber mass fractions. Furthermore, from the data, it appears that the first crack strength begins to level off at a fiber mass fraction of 10%; however, larger fiber contents were not tested.

More research is needed to evaluate the effect of fiber volume fraction on the first crack strength of cement composites. It is possible that increases in fiber contents

effectively replace a portion of cement and thus lower the first crack strength, in addition to the problems of poor dispersion as will be discussed later. Additionally, an optimal fiber content should be determined and compared to the optimal content for peak strength values.

The leveling off in strength with higher fiber contents also appears to occur for peak strength. In the previous study, an optimum fiber mass fraction of 6% produced the greatest peak strength values. Similar results were achieved by Coutts [1987a, 1987b] and Coutts and Warden [1985]. Those results indicated an optimum fiber mass fraction of approximately 8% in mortar samples. Additional results by Coutts and Warden [1990] appear to indicate that a 20% fiber mass fraction produced optimal peak strengths.

These variations in optimal peak strength are most likely due to different fiber types and manufacturing methods. In theory, there should not be an optimal fiber content. However, poor dispersion and increased void contents that occur with higher fiber contents tend to lower peak strengths. High optimal fiber contents are assumed to be indicator of good dispersion and low amounts of entrapped air voids. It is expected that the slurry-dewatering manufacturing method should allow for the use of higher fiber contents than a cast-in-place method.

2.2.3.2.2 Effect of Pulping Process

Though mechanical pulps appear to be attractive in terms of their high yields and low costs, the mechanical properties of the TMP fibers suffer compared to kraft fibers. Several research efforts have considered the use of TMP for fiber-cement

composites. The flexural/peak strength of TMP fiber-reinforced composites was found to be significantly less than composites with softwood or hardwood kraft fibers [Campbell and Coutts, 1980; Simatupang and Lange, 1987; Soroushian and Marikunte, 1990, 1992; Soroushian *et al*., 1994] for low volume/mass fractions and water-to-cement ratios greater than approximately 0.32. This strength reduction is possibly due to the presence of lignin and extractives present on the surface of TMP fibers that slow the hydration of cement around the fibers resulting in a very weak fiber-cement matrix interface bond [Campbell and Coutts, 1980]. In addition, since TMP fibers are much shorter than kraft fibers, less fiber pull-out occurs, leasing to lower post-cracking toughening.

At fiber mass fractions greater than 5% and water-to-cement ratios less than 0.32, TMP composite flexural/peak strength was found to be greater than that of kraft pulp composites. This may be due to the greater workability of fresh TMP cement mixes due to the shorter and stiffer fibers that tend not to clump, as compared to fresh kraft pulp cement mixes. It should be noted that these published results only indicate flexural/peak strength data for TMP fiber composites up to 28 days.

It is suggested that later-age flexural strength tests be conducted to see if this inhibitory effect only slows the localized cement hydration or completely prevents further fiber-cement bonding. Thus, TMP composite flexural strength with different matrix ages should be done.

2.2.3.2.3 Effect of Kraft Pulp Species

For kraft pulp fibers, there are generally considered to be two fiber types – those derived from softwood species and those derived from hardwood species. The chemical compositions of the two fiber types are very similar, with softwoods containing slightly more lignin and less cellulose and hemicellulose. Furthermore, hardwood species exhibit shorter fiber lengths and smaller diameters compared to softwood fiber species. Composites reinforced with softwood fibers exhibit higher flexural strengths than with hardwood fibers regardless of the fiber volume/mass fraction [Campbell and Coutts, 1980; Soroushian and Marikunte, 1990, 1992]. However, Marikunte and Soroushian [1994] have shown that there is no significant difference in flexural strength between the two types of kraft fibers. These results appear to be independent of the composite manufacturing technique, whether slurry-dewatering or cast-in-place.

2.2.3.2.4 Effect of Fiber Bleaching

Bleaching is typically done to pulp to improve the brightness/whiteness of pulp for paper applications. In addition, bleaching largely removes lignin, a polymer that binds the fiber cells together, from the fiber. Typical bleached kraft fibers contain 70-80% cellulose and 20-30% hemicellulose, while unbleached fibers typically consist of 65-75% cellulose, 17-32% hemicellulose, and 3-8% lignin [Stenius, 2000]. The use of lignin in cement admixtures, such as lignosulfates, is known to have a retarding effect on cement hydration. Therefore, the removal of lignin from the fiber is suspected of

improving fiber-cement bonding, by increasing the amount of hydration products in the fiber-cement interface.

Improvements in fiber-cement bonding are suspected in increasing the flexural strength of a fiber cement composites. Results by Mai *et al*. [1983] using autoclaved Wisakraft fiber-cement composites manufactured by the slurry-dewatering method indicate an increased flexural/peak strength for bleached fiber composites compared to unbleached fiber composites. The composites contained an approximate fiber mass fraction of 8% (approximate fiber volume fraction of 5.3%). Increases in peak strength were in the range of 10.9-25.2% depending on the testing condition and composite specimen orientation during the manufacturing process.

2.2.3.2.5 Effect of Fiber Beating

Beating of the pulp fibers fibrillates the S1 layer and breaks down the mat structure of the fiber [Coutts, 1984, 1987a]. Fibrils are formed from the fiber surface, thereby increasing the fiber surface area. By increasing the amount of fiber surface area, beaten fibers may exhibit increased fiber-cement bonding characterized by higher strength but lower toughness values and decreased tendency for fiber pull-out compared to unbeaten fibers. However, the reduction in fiber length that may occur can present a competing effect by decreasing the post-cracking toughness, due to shorter fiber pull-out lengths [Coutts, 1987b].

The freeness of a beaten fiber is an arbitrary number measuring the rate at which water drains from a fiber-water slurry. TAPPI 207 specifies the measuring of the rate at which water drains from a slurry containing 1 liter of water and 3 grams of fibers. The level of beating or refinement is given as a Canadian Standard Freeness (CSF) value. A high CSF value, generally greater than 700 mL, is indicative of unbeaten fibers. On the other hand, CSF values less than 200 mL generally indicate that the fibers that are well beaten [Coutts, 1984]. Intermediate CSF values range from 500-550 mL.

Several research efforts have studied the effect of beating on flexural strength for composites manufacturing by the slurry-dewatering method [Campbell and Coutts, 1980; Coutts and Kightly, 1982; Vinson and Daniel, 1990; Soroushian *et al*., 1995]. However, the most extensive study on the effect of beating was conducted by Coutts [1984]. In this study, the effect of beating was evaluated at several different CSF values. The cement paste composites were manufactured using the slurry-dewatering method with fiber mass fractions ranging from 2-14%. Unfortunately, this manufacturing process does not allow for a specific determination of the composite water-to-cement ratio. For first crack strength, it was found that an optimum fiber mass fraction of 10% (approximately 7% fiber volume fraction) was achieved for all beating levels. Also, a fiber CSF value of approximately 550 mL appeared to produce optimum conditions regardless of fiber content.

The optimum fiber fraction and CSF value may change with the incorporation of fibers in specimens made by cast-in-place methods. These changes may occur due to an increased void volume present in cast-in-place specimens, relative to slurry-dewatering methods. This appears to be an accurate assessment given the results by El-

Ashkar [2002a]. At fiber volume fractions of 0.6%, 1.2%, and 2.0%, beaten (CSF = 464mL) softwood fiber-reinforced cement mortar flexure specimens show significant decreases in flexural strength compared to unbeaten softwood fiber composites.

2.2.3.3 Flexural Toughness

Improvements to the toughness and ductility of cement-based materials have been the driving cause for the incorporation of fibers. Ductility is defined as the ability of a material to sustain load after initial cracking and is measured as the total strain experienced at failure. For cement-based materials, fibers provide this ductility to overcome the inherent disadvantages of cement materials. Upon cracking, fibers are able to bridge the initial crack and hold the crack together until the fibers either pull-out from the cement matrix or fracture.

Even though much research has concentrated on evaluating the toughness of fiber-cement composites, there is no clear method for measuring ductility. Perhaps the most common method for evaluating toughness is the JCI-SF4 method developed in Japan. Toughness is defined in this method as the area under the load-deflection curve up to a deflection equal to the span length divided by 150.

However, certain deficiencies exist within testing equipment during initial loading within the linear elastic region. Due to differences in loading systems, the slope of the linear elastic region may vary for the same material if tested on various testing systems. Therefore, to reduce measurement error, toughness may be quantified as "post-cracking toughness" or as the area under the load-deflection curve *after* the first crack.

2.2.3.3.1 Effect of Fiber Volume/Mass Fraction

Similar to the previously presented flexural strength results, composite toughness has been demonstrated to significantly improve as the fiber volume fraction increases [Andonian *et al*., 1979; Coutts and Kightly, 1982; Coutts and Warden, 1985, 1990; Coutts, 1987a, 1987b; Soroushian and Marikunte, 1990, 1992, 1995; El-Ashkar, 2002]. However, toughness seems to be less sensitive to poor fiber dispersion as optimal fiber mass fractions for toughness are generally 2-4% greater than that observed from the peak strength data.

2.2.3.3.2 Effect of Pulping Process

Similar to bending strength results, reported bending toughness values for TMP fiber-cement composites are lower than kraft pulp composites. Mortar results by Soroushian *et al*. [1994] show TMP composite toughness, measured by JCI-SF4, to be 25.1% and 21.4% lower than softwood and hardwood fiber composite toughness, respectively. The composites were manufactured using cast-in-place methods and were reinforced with a fiber mass fraction of 2% (approximate fiber volume fraction of 1.33%).

Additional data by Soroushian and Marikunte [1990,1992] suggest that kraft fiber-cement composite exhibit approximately 25% and 75% greater toughness values than TMP fiber-cement composites with 1% and 2% fibers by mass (0.67% and 1.33% fiber by volume), respectively. In this case, the composites were made using the slurry-

dewatering method. Thus, it appears that the slurry-dewatering method produces composites with greater toughness than cast-in-place methods. The increased toughness is most likely due to increased fiber-cement bonding.

It can be seen that as the volume fraction of fibers increases, so does the difference between TMP and kraft fiber composite toughness values. It also appears that cement paste composites are more susceptible to larger toughness differences. The mechanism for lower TMP fiber-cement composites toughness is unclear. It is suggested that the shorter fiber lengths of TMP accounts for the majority of differences. The longer kraft fibers allow for longer fiber pull-out lengths and greater frictional energy dissipation, both of which improve the toughness behavior of a cement-based composite.

2.2.3.3.3 Effect of Kraft Pulp Species

It was previously noted that hardwood kraft fibers tend to have shorter fiber lengths and smaller fiber diameters compared to softwood kraft fibers. Furthermore, hardwood fibers generally have a smaller aspect ratio than softwood fibers. Thus, it is expected that if the toughness of a fiber-cement composite is solely dependent on the fiber length or aspect ratio, softwood fibers would be more effective than hardwood fibers in improving the toughness of cement-based composites.

In most studies, softwood fiber-cement composites exhibit higher toughness values than composites with hardwood fibers [Coutts, 1987a; Soroushian and Marikunte, 1994; Marikunte and Soroushian, 1994]. Results by Coutts [1987a] most adequately illustrate the differences between fiber types with varying composite fiber content. As

the composite fiber content was increased, the toughness of composites with either fiber type increased, as expected. Furthermore, it should also be noted that with increasing fiber contents, the differences between the fiber types becomes more prominent. Therefore, it appears that toughness is dependent upon the fiber aspect ratio.

Though the following section will describe the effect of beating and shortened fiber lengths, a more definite and quantitative research effort must be done with different fibers, varying aspect ratios, and similar manufacturing methods to identify the degree of toughness dependence on aspect ratio. Toughness may also be related to the fiber helix angle and the fiber chemical composition. It is suggested that other cellulosic fibers that have similar helix angles and chemical compositions as kraft fibers be used at identical fiber volume fractions to develop a fiber aspect ratio versus composite bending toughness plot.

2.2.3.3.4 Effect of Fiber Bleaching

Since fiber bleaching largely removes the lignin present in a fiber, it is expected that bleached fibers will exhibit increased fiber-cement bonding, since lignin may retard local cement hydration around the fiber. It is difficult to predict whether increased fiber-cement bonding would improve toughness. If the bonding is too strong, fiber failure will be dominated by fiber fracture. On the other hand, if no chemical or physical bond is present, the composite will no show any improvements in toughness.

Results by Mai *et al*. [1983] show improvements of 7-29%, depending on the curing condition, for unbleached fiber-cement composite toughness as compared to

bleached fibers. The composites were manufactured using the slurry-dewatering method with a fiber mass fraction of 8% (fiber volume fraction of 5.33%).

More research needs to be conducted to evaluate the trend in bleached and unbleached fiber-cement toughness values for varying fiber volume fraction. An optimum fiber volume fraction may be present for each fiber treatments. Furthermore, the effect of age must be investigated to monitor changes in fiber-cement bonding with increased cement hydration.

2.2.3.3.5 Effect of Fiber Beating

Similar to the effect of bleaching, the effect of fiber beating on composite toughness may be largely dependent on the fiber-cement bonding. Another effect of fiber beating is the shortening of fiber lengths. This may also contribute to decreased toughness due to shorter fiber pull-out lengths. In the previous sections, it was noted that a lesser degree of fiber-cement bonding and longer fiber lengths produced higher composite toughness values. This hypothesis seems to be valid for fiber mass fraction less than 8% (fiber volume fraction of 5.33%) [Coutts and Kightly, 1982; Coutts, 1984; Vinson and Daniel, 1990]. Unbeaten (CSF>700mL) fiber-cement composites exhibited greater toughness values than beaten fiber-cement composites at fiber mass fractions of 2-8%. At fiber mass fractions of 10-14%, cement composite toughness appears to be optimized at intermediate CSF values around 500 mL.

An explanation is given by Vinson and Daniel [1990] to explain how higher contents of unbeaten fibers do not perform in the same manner as lesser contents, *i.e.*,

beaten fiber-cement composite exhibit greater ductility than unbeaten fiber-cement composites. It was suggested that poor fiber dispersion of the longer unbeaten fibers at higher fiber volume fractions leads to decreases in composite toughness. Shorter fibers tend not to clump as readily and therefore, disperse in the composite more effectively.

2.2.4 Composite Microstructure

Though an abundance of literature on composite mechanical properties has been published, less data are available concerning the microstructure of fiber-cement composites. Scanning electron microscopy of fracture surfaces and polished samples is typical of microstructural studies. In this section, the available literature will be reviewed. Composite microstructure has significant durability implications as will be discussed later. Thus, it is imperative to understand the microstructure prior to any exposure conditions.

Based on the published information, composite microstructure tends to vary depending upon the manufacturing method, whether slurry-dewatering or cast-in-place. The slurry-dewatering, due to pressure applied to the sample, is expected to exhibit a denser matrix and thus increased fiber-cement bonding, as compared to the cast-in-place method.

Thus, the cellulosic fiber-cement matrix interface and the near-interface region are of primary concern when discussing the composite microstructure. It is well-known that a strong fiber-cement bond will lead to improved flexural strength, but decreased toughness and vice versa. Cellulosic fibers are organic and are considered to be

somewhat incompatible in terms of chemically bonding to an inorganic material, such as that of a cement matrix [Coutts, 1983]. Therefore, fiber-cement bonding is typically considered to be of a physical nature.

However, chemical bonding has later been proposed as a means to explain composite fracture behavior at different relative humidities [Coutts and Kightly, 1984]. When tested wet, fiber-cement composite fracture surfaces exhibited long pulled out fibers. On the other hand, samples tested oven dry exhibited fiber fracture with short fiber pull-out lengths.

To explain this behavior, it has been suggested that hydrogen bonding and/or hydroxide bridges are formed between the cement matrix and cellulosic fibers. The cement matrix contains metal hydroxyl groups, such as Ca-OH, Si-OH, and Al-OH. Cellulosic fibers contain covalent hydroxyl groups of the following nature: C-OH. Therefore, hydrogen bonding has been theorized as the main form of chemical bonding between the matrix and fibers.

When wet, it is hypothesized that the hydrogen bonds are broken by insertion of water molecules between the bonds [Coutts and Kightly, 1984]. Therefore, fibers tend to pull out during composite bending, rather than fracturing due to a strong fiber-cement bond. However, fiber swelling while in the wet state may present a competing effect by creating additional physical friction force with the cement matrix. However, for the most part, this imparted frictional force is overcome by the lack of chemical bonding between the fiber and matrix.

Though the fiber-cement bonding mechanisms are important for the mechanical properties of fiber-cement composites, the fiber interfacial region appears to have greater

implications for the overall performance of such a composite. For slurry-dewatered composites, the interface region has been found to be dense, with no calcium hydroxide present [Coutts, 1987c; Savastano *et al*., 2003, 2004]. However, composites cast in place have shown somewhat porous interface transition zones up to 100 μm thick containing large calcium hydroxide crystals [Savastano and Agopyan, 1999]. It is thought that during the dewatering process, excess water is forced from the cellulosic fibers, creating a dense interface zone. With normal cast-in-place methods, water tends to settle around the fibers due to their hygroscopic nature. This creates a zone of increased water-to-cement ratio and thus, increased porosity. Since calcium hydroxide is the most soluble component of cement hydration, it will preferentially migrate to porous regions and recrystallize during composite curing.

Regardless of the interfacial region bonding mechanisms, the pulping process appears to influence fiber failure mechanisms during composite cracking. It was found that mechanically pulped fibers tend to pull out of a cement matrix, with little fiber fracture observed [Davies *et al*., 1981; Savastano *et al*., 2003]. As for kraft pulped fibers, fiber fracture and fiber pull-out was observed, dependent upon the testing conditions, as discussed previously.

2.3 Wet/Dry Cycling Durability

Wet/dry cycling has been used in laboratory testing to replicate rain and heat conditions in the field and is widely applied as an accelerated exposure method. The goal of this method is alternatively fill and empty the capillary pore structure of the composite,

thus exposing the fibers to the alkaline pore solution and then removing any degraded fiber components. If pulp fiber-cement composites are to be used for applications where performance must be ensured after environmental exposure, the effects of cyclical wetting and drying on performance must be known.

2.3.1 Mechanical Testing

2.3.1.1 Kraft Pulp Distributed Fiber-Cement Composites

As discussed previously, kraft pulp fibers have been preferred for fiber-cement applications for their superior mechanical properties and alkali resistance as compared to thermomechanical pulp fibers. Thus, the majority of published research has employed kraft pulped cellulosic fibers. Despite the abundance of literature in relation to these fiber-cement composites, there does not appear to be a consensus concerning the composite mechanical performance after exposure to wet/dry cycling.

Using sisal fiber-mortar composites, Gram [1983] found significant losses in post-cracking peak strength and toughness with wet/dry cycling. The majority of these losses occurred by 12 wet/dry cycles. On the other hand, Soroushian *et al*. [1994a] found that the flexural strength of kraft pulp fiber-mortar composites *increased* with wet/dry cycling. Additionally, flexural toughness was found to significantly decrease, particularly by 20 wet/dry cycles. Results obtained by Toledo Filho *et al*. [2003] using sisal and coconut fibers, and El-Ashkar *et al*. [2002b] and Akers and Studinka [1989] using kraft pulp fibers, indicate that though a reduction in toughness occurred with

wet/dry cycling, an increase in first crack strength was observed. These differences cannot be directly explained at this time, but may be related to differing experimental methods. That is, in [Akers and Studinka, 1989; El-Ashkar *et al*., 2002; Toledo Filho *et al*., 2003], samples subjected to exposure were tested at later ages than the control samples. Therefore, matrix strength improvements with increasing age due to continued cement hydration were not considered and may account for the first crack strength increases with increased wet/dry exposure. The differences between peak (flexural) strength trends with wet/dry cycling warrants further investigation of the influence of wet/dry cycling on mechanical performance.

Marikunte and Soroushian [1994] concluded that the mechanical properties of fiber-cement composite were adversely affected after 25 wet/dry cycles compared to control specimens (*i.e.*, zero wet/dry cycles). However, it is unclear from the published data, if progressive damage occurs to fiber-cement composites with wet/dry cycling. That is, how do the mechanical properties, such as strength and toughness, differ after 25 wet/dry cycles as compared to a fiber-cement composite exposed to 5, 10, or 15 wet/dry cycles? It is important to examine the progression of degradation to understand and predict changes in performance with exposure.

2.3.1.1.1 Effect of Supplementary Cementitious Materials (SCMs)

Efforts to improve the durability of cellulosic fiber-reinforced cement materials subjected to wet/dry cycling have largely concentrated on the addition of SCMs. The use of artificial pozzolans has been shown to delay or minimize composite degradation. It is

thought that durability improvements occur due to a lowering of the pore solution pH, removal of excess CH through the formation of supplementary C-S-H, and refinement of the pore structure (matrix densification). All of these mechanisms are thought to minimize composite degradation due to wet/dry cycling. However, the mechanism(s) for the improved durability have yet to be established.

Silica fume, used at relatively large amounts (*i.e.*, 30% or greater replacement of cement by weight) appears to significantly minimize composite degradation due to wet/dry cycling [Gram, 1983; Bergstrom and Gram, 1984; Tolêdo Filho *et al*., 2003]. Silica fume replacements of 17% and 33% of cement by weight reduced the pore water pH from 13.2 to 12.9 and 12.0, respectively [Gram, 1983]. Partial replacement of portland cement with 40% slag by weight by Tolêdo Filho *et al*. [2003] did not significantly improve the sisal fiber mortar composite durability after 46 wet/dry cycles. Additionally, Gram [1983] has also shown that replacement of cement with 70% slag by weight only reduced the pore solution pH from 13.2 to 13.0 and did not improve the durability of sisal fiber mortar composites after 120 wet/dry cycles. Using rice-husk ash, Ziraba *et al*. [1985] concluded that 45% replacement of portland cement by weight minimized sisal fiber-mortar composite degradation due to wet/dry cycling by reducing the pore solution pH by 15-20%. No other SCM replacements (including fly ash and metakaolin) have been previously investigated as a means of minimizing composite degradation.

Despite improvements in composite durability with certain cement replacements, there is no existing information about the mechanism of improved durability. That is, how significant a role does the cement pore solution play? Does the

permeability of the composite affect durability? Which is more important – pore solution chemistry or composite permeability? Or are durability improvements based on a combination of the two? Also, how is cement hydration altered by lowering the pore solution pH? These questions must be answered before establishing any criteria or recommendations for improving pulp fiber-cement composite durability.

2.3.1.1.2 Effect of Water-to-Cement Ratio

The effect of varying the water-to-cement ratio has been investigated to identify the role in which composite permeability and matrix densification play a role in composite degradation due to wet/dry cycling. To date, there has been no available literature concerning this particular aspect. Other attempted methods to reduce permeability include the use of polymer has varied. However, the incorporation of all these techniques can modify the matrix chemical composition and/or dramatically increase the cost of such a product. Thus, variations in water-to-cement ratio were chosen to isolate and evaluate the role of composite permeability as changes in the water-to-cement ratio can greatly influence matrix permeability.

2.3.1.2 Thermomechanical Pulp Distributed Fiber-Cement Composites

Traditionally, kraft pulp fibers have been used as reinforcement in cement-based materials containing pulp fibers. A potential lower-cost alternative to kraft pulp fibers are thermomechanical pulp (TMP) fibers. The mechanical properties of some TMP

reinforced cement-based materials have been examined. Campbell and Coutts [1994a] found that thermomechanical pulp (TMP) fiber-cement composites exhibited lower flexural strength than kraft pulp fiber composites at moderate water-to-cement ratios (*i.e.*, 0.33-0.45) and low fiber contents (*i.e.*, mass fractions less than 5%). Additionally, Soroushian and Marikunte [1992] have shown that the strength and toughness of composites reinforced with TMP were lower than respective fiber volumes of kraft pulp.

However, the anticipated durability of TMP fiber-cement composites to wet/dry exposure has been much less extensively studied. Soroushian *et al*. [1994a] found that mechanical pulp composites exhibited a faster progression of composition degradation during wet/dry cycling compared to kraft pulp fibers.

Because of the potential economic advantages associated with TMP fibers, a more thorough evaluation of thermomechanical pulp fiber-cement composite properties prior to and after wet/dry exposure appears warranted.

2.3.1.3 *Aligned Pulp Fiber Sheet Composites*

The relatively low cost of pulp fibers makes them attractive for reinforcing cement-based materials. However, one obstacle to the practical use of these fibers is their poor dispersion in portland cement-based materials. Reinforcement using aligned pulp fiber sheets, rather than discrete fibers, could avoid the problems with workability and fiber dispersion commonly associated with fiber reinforcement.

By reinforcing cement-based materials with sheets comprised of aligned pulp fibers additional benefits may be had in terms of tailoring the composite design for the

desired mechanical behavior. That is, the functionality of the reinforcement can be tailored to achieve specific performance characteristics in structural and non-structural cement-based materials. For example, by aligning the pulp fibers, strength and stiffness in fiber-cement products can be enhanced directionally. Basic laminated plate theory can be used to infer the mechanical properties of aligned discontinuous fiber composites at various fiber orientations. In unidirectional aligned discontinuous fiber composites, the composite strength and stiffness is generally greatest in the fiber direction, and significantly less in the cross-fiber direction [Gibson, 1994; Herakovich, 1998]. On the other hand, randomly oriented discontinuous fiber composites exhibit three-dimensional isotropy. In other words, the strength and stiffness of this type of composite can only be varied by changing the fiber volume fraction and fiber aspect ratio, given the same fiber and matrix material. Fiber aspect ratio (l/d) plays a significant role in the performance of randomly distributed fiber composites, but has also been shown to have only a negligible effect on composite strength and stiffness in unidirectional aligned discontinuous fiber composites subjected to off-axis stresses. Lastly, another possible benefit of using pulp fiber sheet reinforcement is that the reinforcement can be placed only where needed. That is, the pulp fiber reinforcement could be located near the base of a concrete section to provide additional flexural capacity, tensile strength, and toughness. Located near the surface of the section, the fiber reinforcement might provide additional resistance to surface cracking, which may result from over-finishing, shrinkage, salt crystallization, or cyclic freezing and thawing, for example.

Previous research by Mu and Meyer [2002] has shown that fiber meshes of AR-glass, PVA, and polypropylene were more effective than their respective equivalent

volumes of randomly distributed fibers at improving flexural strength and toughness of composite members. These results would be expected according to laminated plate theory. In the face of an oncoming crack, more oriented fibers are able to bridge the crack than if the fibers were randomly distributed. In that case, only a small number of fibers are able to bridge the crack. Furthermore, of those fibers bridging the crack, not all fibers will be oriented at 0º relative to the stress direction. As discussed previously, as the fiber orientation is increased from 0º, reductions in composite strength and stiffness occur [Gibson, 1994; Herakovich, 1998]. From laminated plate theory, this result expected considering that the fibers carry the stress across a crack. Thus, additional fibers in the direction of the principle stress will yield greater composite strength and stiffness. Since randomly distributed fiber composites contain fibers throughout their sections (*i.e.*, in regions experiencing tension or compression, in flexure), it can be expected that composite strength and stiffness will increase by concentrating the fibers in regions expected to experience tension.

2.3.2 Microstructural Characterization

Several mechanisms have been proposed to explain losses in mechanical performance (*i.e.*, strength and ductility) [Bentur and Akers, 1989]. These mechanisms include:

- Alkaline hydrolysis leading to a reduction in the cellulose degree of polymerization,
- Dissolution of lignin and hemicellulose,
- Fiber embrittlement/mineralization,

- Microbiological attack.

The leading theory to date has been the fiber embrittlement mechanism. It has been observed that embrittlement of the fibers is caused by cement hydration product formation within the middle lamella of the fiber during wet/dry cycling [Bentur and Akers, 1989]. Once the fibers become mineralized, fiber fracture becomes the main fiber failure mode, as seen in Figures 2-6 – 2-9. The loss of energy dissipation during fiber pull-out accounts for significant decreases in toughness values.

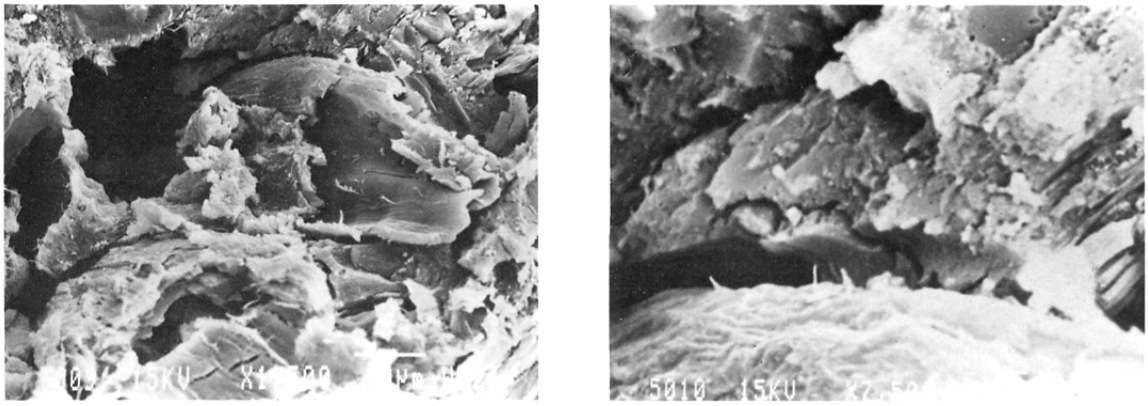

Figure 2-6. SEM micrograph of pulp fiber-cement composite fracture surface after wet/dry cycling [Bentur and Akers, 1989].

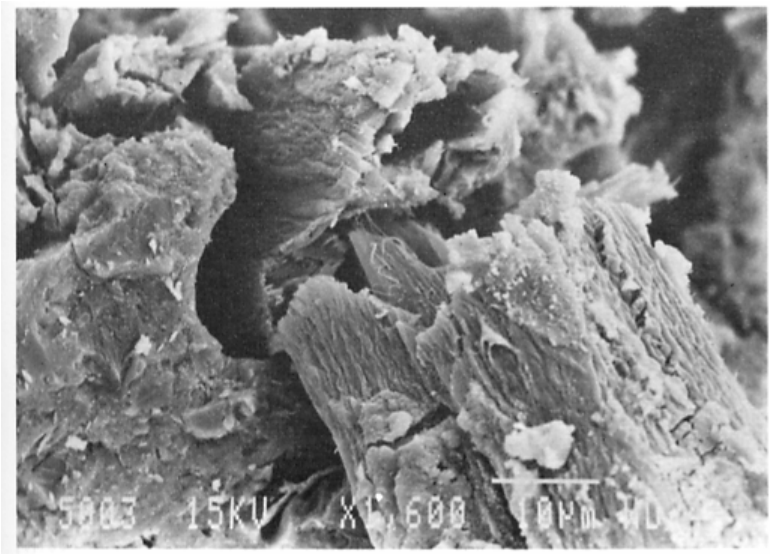

Figure 2-7. SEM micrograph of pulp fiber-cement composite fracture surface after wet/dry cycling [Bentur and Akers, 1989].

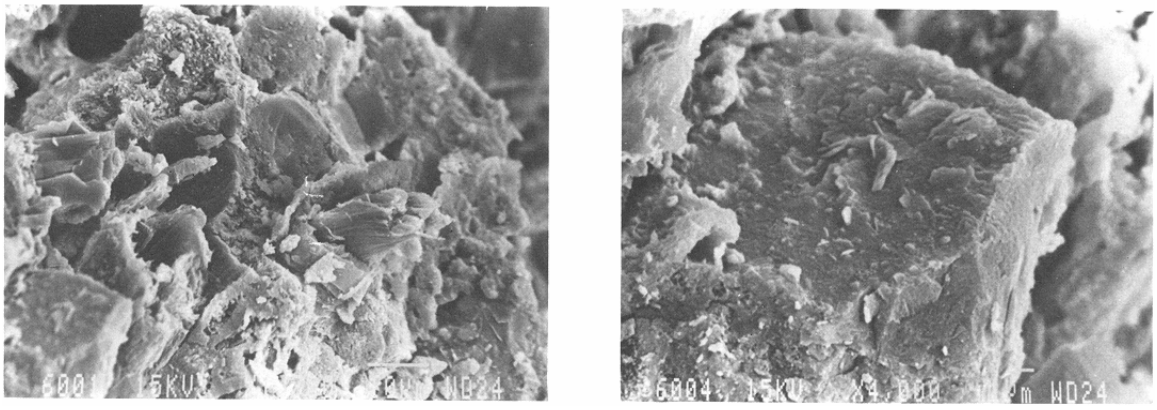

Figure 2-8. SEM micrograph of pulp fiber-cement composite fracture surface after wet/dry cycling [Bentur and Akers, 1989].

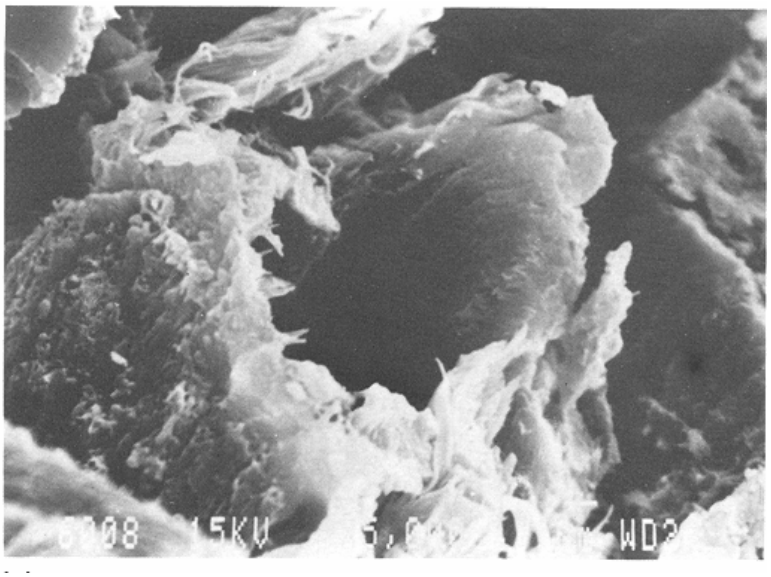

Figure 2-9. SEM micrograph of pulp fiber-cement composite fracture surface after wet/dry cycling [Bentur and Akers, 1989].

After wet/dry cycling, it has been observed that cellulosic fibers debond from the surrounding matrix, creating a void space [Toledo Filho *et al*., 2000], as seen in Figure 2-10. In addition, chemical element mapping of polished composite surfaces by Toledo Filho *et al*. [2000] has shown an increase in calcium, sulfur, and silicon concentrations within and around cellulosic fibers when subjected to 25 wet/dry cycles, as illustrated in Figure 2-11.

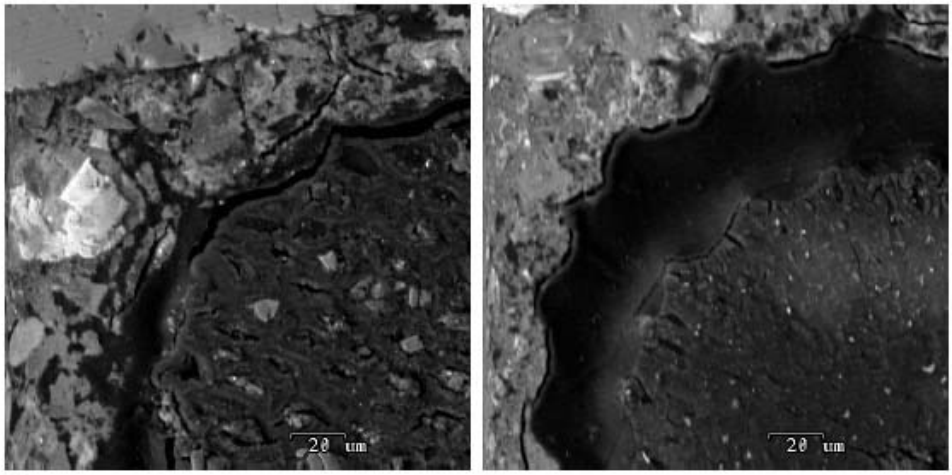

Figure 2-10. SEM BSE elemental map of transition zone around sisal fibers. (a) Prior to cycling. (b) After 25 wet/dry cycles [Tolêdo Filho *et al*., 2000].

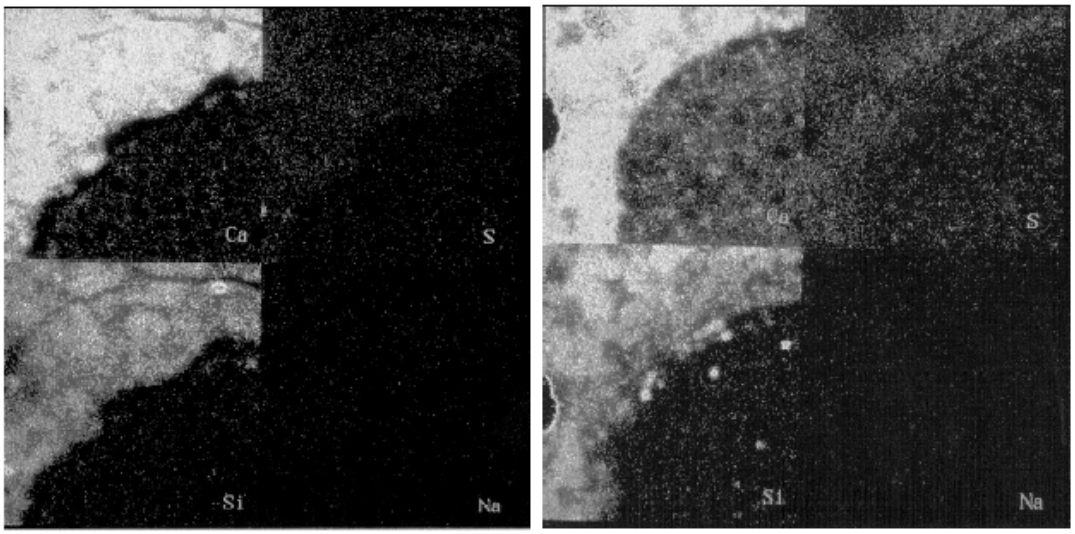

Figure 2-11. SEM BSE elemental map of transition zone around sisal fibers. (a) Prior to cycling. (b) After 25 wet/dry cycles [Tolêdo Filho *et al*., 2000].

This debonding of the cellulosic fibers from the matrix may explain decreases in mechanical strength that have been previously mentioned. Furthermore, the precipitation of inorganic elements within the fiber likely leads to the mineralization and subsequent embrittlement of the fiber. However, no published results are available concerning the progression of this degradation. That is, does the degradation occur progressively or is damage isolates to the first few wet/dry cycles. Thus, it appears that further research is needed to quantitatively examine the progression of composite degradation with wet/dry cycling. Hence, the majority of the results and discussion presented in Chapter 4 will provide insight into the progression of degradation and provide mechanism to explain this behavior.

CHAPTER 3

RESEARCH METHODOLOGY

3.1 Wet/Dry Cycling

3.1.1 Materials

3.1.1.1 Cement Paste Matrix

Fiber-cement beams were made with a water-to-cementitious materials ratio of 0.60 (unless otherwise noted) using commercially available ASTM Type I portland cement and deionized water (resistivity of 18.2 MΩ·m). Oxide analysis and Bogue potential composition for the cement are listed in Table 3-1. ADVA Flow, a carboxylated polyether superplasticizer obtained from Grace Construction Products, was used at a maximum dosage rate of 6.15 μL per gram of cement to aid workability.

Table 3-1. Oxide analysis (mass percent) and Bogue potential composition for ASTM Type I portland cement.

Oxide	Type I portland cement
SiO_2	20.17
Al_2O_3	5.34
Fe_2O_3	3.85
CaO	63.93
MgO	0.91
Na_2O	0.05
K_2O	0.35
TiO_2	0.35
Mn_2O_3	0.08
P_2O_5	0.07
SrO	0.07
BaO	0.02
SO_3	4.00
Loss on ignition	0.80
Insoluble residue	0.05
C_3S	54.16
C_2S	16.97
C_3A	7.64
C_4AF	11.70

Some composites contained supplementary cementitious materials (SCMs) used as a partial replacement for portland cement by weight. These SCMs included the following: (1) silica fume (SF), (2) ground granulated blast furnace slag (SL), (3) Class F fly ash (FA), (4) Class C fly ash (CA), (5) metakaolin (MK), and (6) proprietary blend of diatomaceous earth/volcanic ash (DEVA).

Force 10,000 D densified silica fume was obtained from Grace Construction Products. The ground granulated blast furnace slag was provided by Holcim in Birmingham, AL. The two metakaolins used in this study, MK235 (Kaorock) and MK349 (Kaorock F), were provided by Thiele Kaolin Company in Sandersville, GA. Raw and calcined DEVA blends were obtained from Western Pozzolan in Doyle, CA. The metakaolins and DEVA blends differ primarily in their surface area. The oxide analysis and surface area of these SCMs is presented in Table 3-2.

Table 3-2. Oxide analysis (mass percent) and particle surface area of supplementary cementitious materials.

Oxide	Silica fume	Slag	Class C fly ash	Class F fly ash	Metakaolin (MK235)	Metakaolin (MK349)	DEVA blend - raw	DEVA blend - calcined
SiO_2	97.12	39.43	31.27	56.37	51.37	52.10	69.25	70.65
Al_2O_3	0.01	9.09	17.43	28.47	44.60	44.03	15.37	14.66
Fe_2O_3	0.05	0.51	6.76	6.00	0.46	0.92	5.98	5.88
CaO	0.37	35.76	28.40	1.17	0.23	0.47	1.86	1.83
MgO	0.28	12.10	5.22	1.01	0.03	0.13	0.84	0.85
Na_2O	0.04	0.14	1.62	0.24	0.39	0.02	2.01	1.87
K_2O	0.58	0.37	0.37	2.81	0.07	0.14	1.72	1.65
TiO_2	0.02	0.33	1.46	1.54	1.99	1.42	0.59	0.58
Mn_2O_3	0.04	0.56	0.08	0.04	0.01	0.01	0.07	0.06
P_2O_5	0.08	0.02	0.99	0.27	0.19	0.17	0.18	0.22
SrO	0.01	0.05	0.44	0.12	0.01	0.01	0.05	0.04
BaO	0.00	0.08	0.70	0.13	0.01	0.02	N/A	N/A
ZnO	N/A	N/A	N/A	N/A	N/A	N/A	0.02	0.02
SO_3	0.04	1.55	2.81	0.05	0.14	0.00	0.31	0.10
Loss on ignition	1.36	0.01	2.45	1.79	0.51	0.56	1.65	1.59
Moisture	0.43	0.12	0.20	0.14	0.19	0.34	0.12	1.43
Surface Area (m^2/g)					11.1	25.4	2.654	0.999

3.1.1.2 Mortar Matrix

Composite beams were made with a water-to-cement ratio of 0.50 and a sand-to-cement ratio of 1.0 using commercially available ASTM Type I portland cement, deionized water (resistivity = 18.2 MΩ·m), and natural siliceous sand (fineness modulus = 1.80), obtained from Brown Brothers Quarry in Junction City, GA. Oxide analysis and Bogue potential composition for the cement are listed in Table 3-1.

3.1.1.3 Discrete Fibers

Kraft pulp and TMP fibers were used as reinforcement at a 4% fiber volume fraction in the cement paste. The kraft pulp fibers were Slash Pine softwoods obtained from Buckeye Technologies in Plant City, Florida. Four types of kraft pulp samples were used to evaluate the effect of fiber processing, *i.e.*, beating, bleaching, and initial drying state. Table 3-3 lists the fiber treatments investigated for each pulp fiber sample group along with the respective ash and moisture contents, which were determined according to methods described in TAAPI T211 [2002] and T412 [2002], respectively. Beaten pulp fibers were beaten using a laboratory Valley beater to a Canadian Standard Freeness (CSF) of 550 mL. With the exception of the never-dried fibers, fibers were received in dry, compacted form prior to being fluffed. The never-dried fibers were received in moist, fluffed form. All kraft pulp fibers were treated by a process described in [Kurtis *et al.*, 2001; El-Ashkar *et al.*, 2003] to improve dispersion. This process involves treating the fibers with cationic starch and fly ash to improve their dispersion during mixing.

Table 3-3. Kraft pulp fiber modification treatments investigated.

Fiber	Drying State	Bleaching	Beating	Ash Content[a]	Moisture Content[b]
A	Never-dried	Unbleached	Unbeaten	49.01%	47.30%
B	Once-dried	Bleached	Beaten	60.37%	48.90%
C	Once-dried	Bleached	Unbeaten	41.25%	45.85%
D	Never-dried	Bleached	Unbeaten	48.79%	46.40%

[a] per TAPPI T211 [2002].
[b] per TAPPI T412 [2002].

TMP southern Loblolly Pine fibers were obtained from Augusta Newsprint Company in Augusta, GA. The TMP fibers did not require surface treatment to achieve good dispersion. The improved dispersion of the TMP fibers is likely due to their stiffer fiber cell wall and shorter fiber length (~1-2 mm for TMP versus ~5-8 mm for kraft pulp of these species), which results from the mechanical action used during TMP pulping.

The volume fraction of fibers was kept constant throughout all wet/dry cycling durability mixes, regardless of fiber type. Thus, it should be noted that the mass fractions for the fiber types did vary due to differences in the fiber specific gravity. A specific gravity of 0.5 was assumed for the TMP fibers, as compared to 1.5 for the softwood kraft fibers. The specific gravity of TMP fibers is lower than that of kraft fibers since TMP fibers have an open lumen, whereas the kraft fiber lumen is collapsed. In terms of mass fractions incorporating the differences in specific gravity, the mass fractions of kraft and TMP fibers used were 6% and 2%, respectively.

3.1.1.4 Aligned Fiber Sheets

Aligned fiber sheets were prepared with a basis weight of 30 g/m^2 using the four kraft fiber types listed in Table 3-3. The fibers were obtained from Buckeye Technologies in Plant City, FL. This particular basis weight (thickness) corresponds to an equivalent distributed fiber volume fraction of 0.0787%. The corresponding equivalent distributed fiber volume fraction was calculated by first converting the fiber sheet weight per unit specimen size to an appropriate fiber sheet volume knowing the specific gravity of the fibers used. Then, the equivalent volume fraction was simply determined by dividing the volume of the fiber sheet by the total specimen volume.

Fiber sheets were manufactured using a dynamic sheet former. A dynamic sheet former prepares uniform fiber sheets by spraying a pulp suspension inside a rotating drum. Water is drained from the sheet by centrifugal force. Fiber alignment can be controlled by varying the rotational velocity of the drum. Fiber sheet basis weight can be varied by using different concentrations of pulp slurry.

3.1.2 Sample Preparation

3.1.2.1 Distributed Fiber-Cement Composites

Pastes were prepared by mixing the pulp fiber and approximately 50% of the water and the entirety of the superplasticizer for 3 minutes at 60 rpm in a 1.5L-capacity Hobart mixer to ensure separation of the fibers. Subsequently, the cement was added,

followed by the remaining water. Mixing continued at 120 rpm for another 5 minutes to allow for uniform fiber dispersion. For composites containing one or more SCMs, the SCMs were added prior to the cement and mixed for 3 minutes.

It should be noted that this methodology is a cast-in-place method as opposed to slurry-dewatering or autoclaving. Cement paste samples were used to isolate the effect of wet/dry cycling on composite durability, negating effects such as the presence of aggregate on composite behavior.

Flexure specimens were cast in two layers in 2.54 x 2.54 x 30.5 cm (1 x 1 x 12 inch) brass molds. After each layer was placed, the mix was tamped to minimize entrapped air. After the second layer was placed and the samples finished, they were placed in a curing box at 22±2° C and 90±5% RH. After 24 hours, the samples were demolded, cut with a masonry saw to a 10.2 cm (4 inch) length, and placed in a limewater curing tank at 18±2° C until wet/dry cycling or testing commenced.

3.1.2.2 Aligned Fiber Sheet Mortar Composites

Mortars were prepared by mixing the cement and sand for 3 minutes at 60 rpm in a 1.5L-capacity Hobart mixer. Subsequently, the water was slowly added and mixing continued at 60 rpm for another 5 minutes. Flexure specimens were cast in 2.54 x 2.54 x 30.5 cm (1 x 1 x 12 inch) brass molds. A predetermined mass of mortar was initially added to the mold, tamped and vibrated to level the mortar surface such that two-thirds of the mold was filled. The precut fiber sheet was then placed in the mold and lightly tamped to remove trapped air voids beneath the fiber sheet. Then, the remaining mortar

was slowly added to the mold, taking care to keep the fiber sheet plane. After finishing, the molds were placed in a curing box at 22±2° C and 90±5% RH. After 24 hours, the samples were demolded, cut with a masonry saw to a 10.2 cm (4 inch) length, and placed in a limewater curing tank at 18±2° C until wet/dry cycling or testing commenced.

3.1.3 Wet/Dry Cycle Definition

To determine the time to saturation and drying, a hysteresis percent mass change versus time curve, similar to Tolêdo Filho *et al.* [2000, 2003], was developed. The mass was measured to monitor mass loss and gain during wet/dry cycling. When the mass stabilized (*i.e.*, mass change of less than 1% over a period of three hours), the sample was assumed to be either dry or saturated, depending upon the exposure. The percent mass change over time for each fiber type when subjected to wet/dry cycling is shown in Figure 3-1. Thus, it was determined that a 48-hour cycle length was appropriate to allow for dry and saturated conditions in these fiber-cement beams.

Therefore, a wet/dry cycle was defined for this research as 23 hours and 30 minutes drying in an oven at 60±5° C and 20±5% RH, air drying at 22±5° C and 60±5% RH for 30 minutes, 23 hours and 30 minutes soaking in water at 20±2° C, and air drying at 22±5° C and 60±5% RH for 30 minutes. Air drying of samples was allowed between saturation and drying to avoid unrealistic thermal shock and subsequent microcracking. Mechanical testing was performed after the 30 minutes at 22±5° C and 60±5% RH preceded by 23 hours and 30 minutes of soaking.

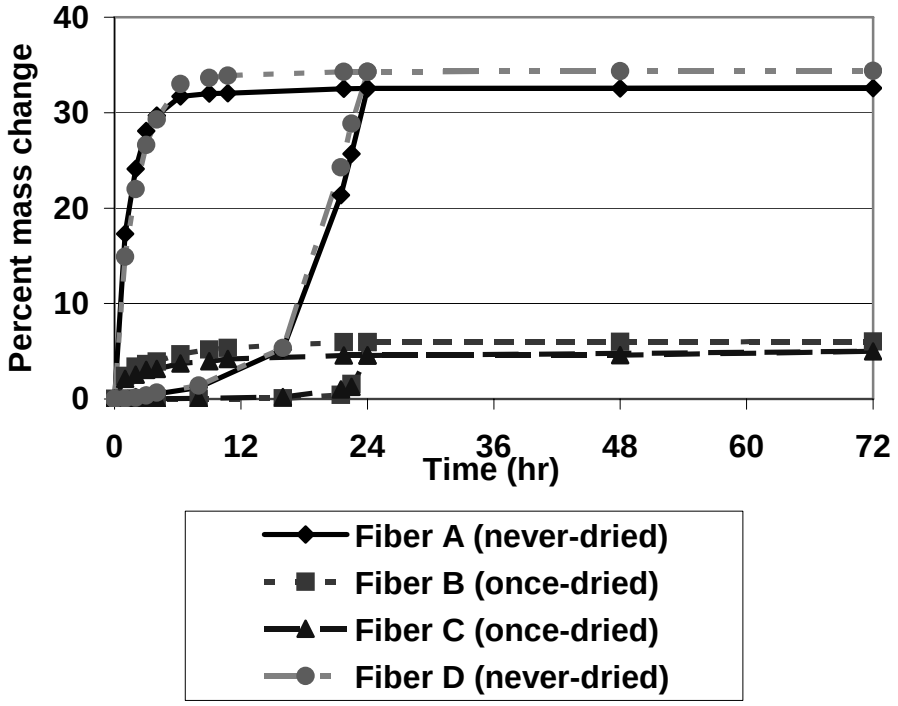

Figure 3-1. Determination of wet/dry cycle length.

3.1.4 Mechanical Testing

The 2.54 x 2.54 x 10.2 cm (1 x 1 x 4 inch) samples were tested in center-point bending with a span of 7.6 cm (3 inches). The span-to-depth ratio of 3 was chosen to comply with ASTM C 348 [2002] and C 293 [2002]. Tests were performed in triplicate using a 98 kN (22 kip) screw driven test frame (Satec model 22EMF) with a crosshead displacement of 0.1 mm/min. The testing setup can be seen in Figure 3-2. The deflection was captured using an electronic deflectometer (Epsilon model 3540-012M-ST), placed

under the center point of the beam. The test was controlled using the deflection system to better capture the post-cracking behavior of the beams.

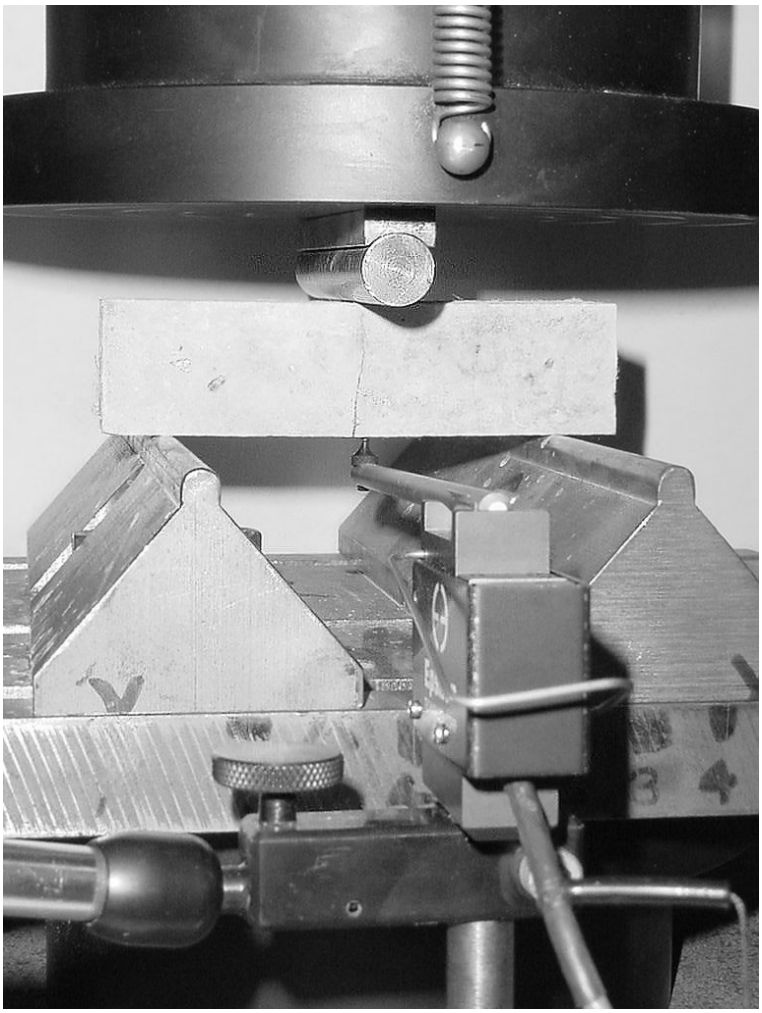

Figure 3-2. Experimental flexure testing set-up.

Toughness was defined as the post-cracking toughness or the area under the load-deflection curve beyond first cracking. This definition is necessary because beams subjected to a low number of cycles exhibited load-deflection toughening after cracking, while those beams subjected to a larger number of wet/dry cycles exhibited load-deflection softening after cracking (Figure 3-3a). In the absence of post-cracking toughening, the peak strength will be equal to the first crack strength. Peak strength values take into consideration the toughening of the composite after cracking (Figure 3-3b).

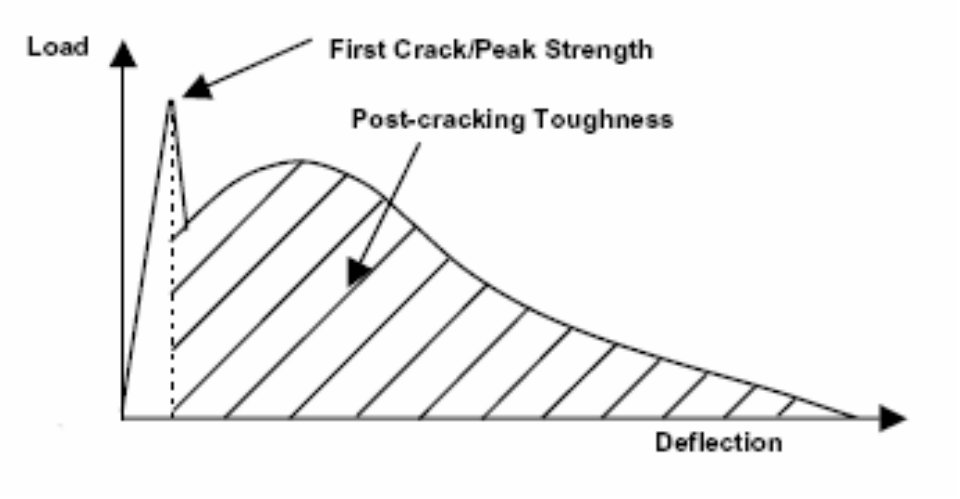

(a)

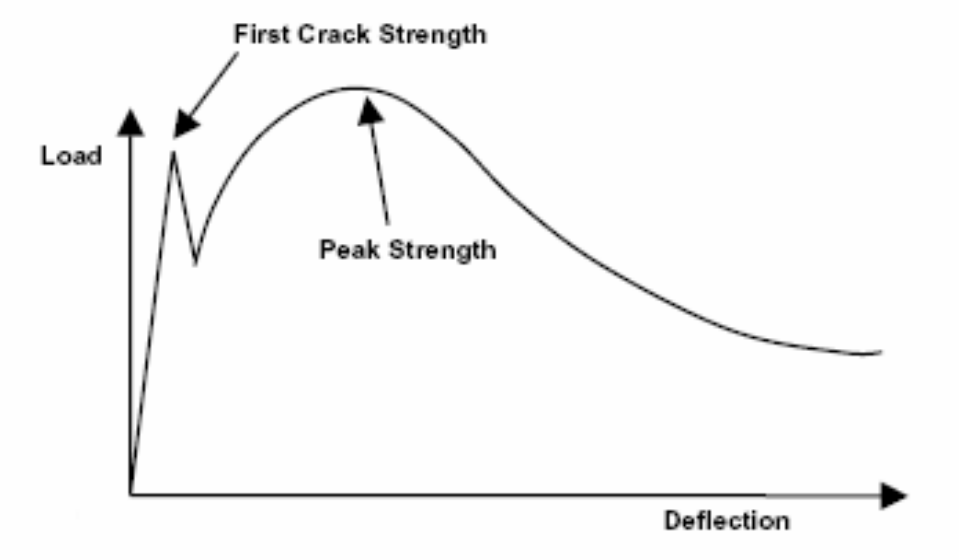

(b)

Figure 3-3. Definition of first crack strength, peak strength, and post-cracking toughness. (a) Post-cracking softening where first crack strength is equal to peak strength. (b) Post-cracking toughening where first crack strength is less than the peak strength.

3.1.5 Microstructural Characterization

3.1.5.1 Sample Storage

After mechanical testing, the specimens were soaked in ethanol for 24 hours and oven-dried at 105° C for 48 hours to dehydrate the sample and prevent additional cement hydration. Following dehydration, samples were stored in sealed containers to minimize carbonation.

3.1.5.2 Backscattered Electron (BSE) Imaging Sample Preparation

Additionally, to determine the approximate chemical composition of the matrix C-S-H, epoxy impregnated and polished composite samples were prepared for backscattered electron (BSE) imaging. Microscopy samples were cut using an Allied High Tech 4 variable speed wafering saw. Ethanol was used as the cutting lubricant. Samples were cut to a maximum thickness of 5 mm. After cutting, samples were labeled and placed in an oven at 105 °C for 1 hour to dry the ethanol.

Epoxy impregnation was accomplished using a Buehler vacuum impregnation system. EPO-THIN hardener and resin were used at a mix ratio of 100:36. Potted samples were demolded after 24 hours. Samples were allowed for cure for several more days.

Potted samples were initially manually polished using a Buehler Economet 4 variable speed grinder-polisher. Samples were progressively polished at grit sizes of 240,

320, and 600 for 2 minutes each. Automatic final polishing was accomplished on a Buehler VECTOR grinder-polisher with 5 and 1 μm diamond aerosol sprays. Samples were cleaned with ethanol after each polishing step.

3.1.5.3 Scanning Electron Microscopy (SEM)

Microstructural characterization of composite fracture surfaces was employed using a JSM 6400 scanning electron microscope in secondary electron (SE) mode. Fracture surface samples were removed from the center of the composites, mounted on SEM stubs, and coated with osmium by the method developed by Kubotsu and Ueda [1980]. Osmium coating was used to prevent charging of the sample and to improve the contrast and maximum resolution of the observed fracture surfaces, as compared to conventional gold coating.

3.1.5.4 Environmental Scanning Electron Microscopy (ESEM)

ESEM has numerous benefits over standard scanning electron microscopy. With ESEM, conductive coating of samples is not necessary. Despite the lack of coating, a high electron accelerating voltage can be easily achieved. Thus, it is possible to achieve an accelerating voltage greater than 25 kV with the non-conductive cement-based samples in the ESEM. Furthermore, the lack of coating is beneficial as it does not alter the specimen microstructure and apparent chemical composition. Thus, energy dispersive spectroscopy (EDS) is easily facilitated on uncoated samples. Typically, gold

or carbon coating can interfere with EDS measurements if the coating is too thick. Special care must also be taken to avoid using a coating that may give false EDS readings, such as using a carbon coating and measuring relative carbon intensities from a sample.

Microstructural observations were conducted on a FEI Quanta 200 environmental scanning electron microscope (ESEM) in a gaseous (water vapor) environment. *In situ* microscopic wet/dry cycling observations were made by mounting specimens on a thermocoupled stage. Specimen wetting and drying was accomplished by maintaining a constant stage temperature of 5° C and changing the water vapor pressure from 4 to 6 Pa in order to modify the localized relative humidity from 10% to 100% RH. Fracture surface samples exposed to *in situ* saturation were removed from the composite such that the sample thickness was several millimeters to ensure adequate water vapor condensation above the samples.

3.1.5.5 Energy Dispersive Spectroscopy (EDS)

Initially, a Monte Carlo simulation, Figure 3-4, was run to determine an appropriate accelerating voltage (*i.e.*, 10 kV) as to not account for any hydration products within the fiber lumen. An accelerating voltage of 10 kV led to a maximum interaction depth of approximately 1.5 μm which is less than the fiber cell wall thickness. Thus, the EDS results encompass only hydration products apparent on the fiber surface and within the fiber cell wall.

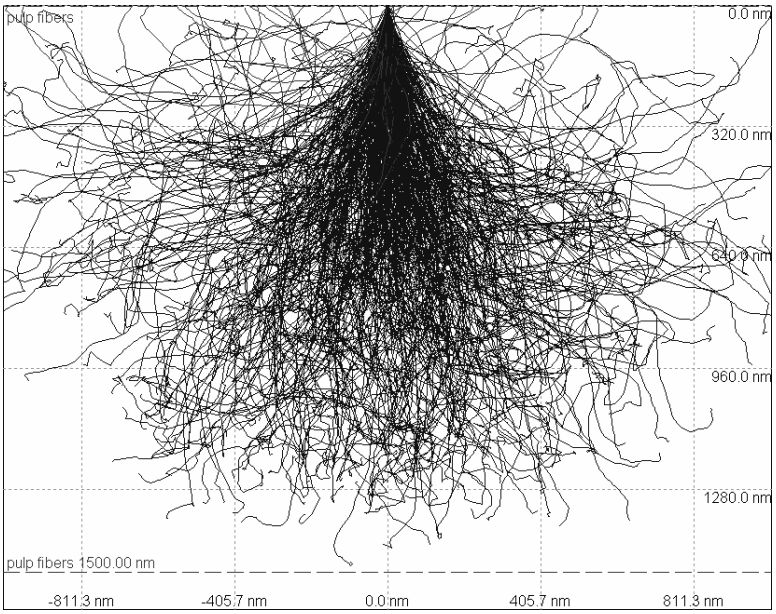

Figure 3-4. Monte Carlo simulation.

Spectroscopy was accomplished using an EDAX SUTW detector. All EDS spectra were collected at an accelerating voltage of 10.0 kV and a water vapor pressure of 93.3 Pa (0.70 Torr). EDS measurements were standardized against a blast furnace slag with a previously known chemical composition, as in Richardson *et al.* [2002]. The standard was compared against a synthetic ettringite sample to verify the correct quantization. Conditions varied to obtain adequate ESEM images or EDS spectra collection.

For the composite fracture surfaces, several EDS spot analyses were conducted on each observed fiber in secondary electron (SE) mode. One data point represents the average chemical composition of an observed fiber. Twenty fibers on each fracture surface were observed.

Polished and epoxy impregnated composites samples were imaged in backscattered electron (BSE) mode. Samples were examined for C-S-H primary and trace compositions. Fifty data points were acquired for each sample examined.

Since most EDS measurements were conducted on fracture surfaces (as opposed to flat polished samples), the results may be considered semi-quantitative. However, for this work, only relative changes in chemical composition were of primarily interest. Thus, the facilitation of fracture surfaces for EDS analyses was appropriate for this work.

3.1.5.6 Laser Scanning Confocal Microscopy (LSCM)

Confocal microscopy has generally been used in biological fields and in materials science However, LSCM has emerged as a tool for cement-based materials microcharacterization [Kurtis *et al.*, 2002]. For this research program, LSCM has been used to quantitatively evaluate composite fracture surface characteristics. LSCM observations were conducted on an argon laser (λ = 488-514 nm) Leica Confocal TCS NT. Fracture surfaces were observed in reflected light mode using a H PLAN 20x/0.40 ∞/1.8 Q/B objective lens (magnification = 400X).

For this research, eight 500 x 500 μm areas were imaged for each sample. At each point, the sample area was focused through the eyepieces with all settings to "visual." Once the area was in focus, all settings were made to "confocal." With the original microscope software, the reflective mode was chosen. Upon initial scanning at a voltage of 435 V, an initial and final z-scan point were chosen to indicate the top and bottom focus planes that were observed during confocal scanning. For this particular

research, a step size of 5 μm was chosen to optimize resolution and time. Finally, upon completion of the series scanning, fractography measurements were be determined.

Fractography of composite fracture surface was investigated as a means to correlate fracture surface characteristics to composite post-cracking toughness. Quantitative measurements included fracture surface roughness number and fractal dimension. These factors were conducted to evaluate the effectiveness of the fibers in improving composite toughness. Fracture surface roughness was determined by the actual surface area to the projected surface area ratio [Kurtis *et al.*, 2002].

In addition, by evaluating the fractal dimension, changes in composite surface roughness as a function of wet/dry cycling can be assessed. In other words, the effect of wet/dry cycling induced microcracking altering surface roughness. By separating out the effect of fibers on fractal dimension calculations, the effect of SCMs and wet/dry cycling on matrix roughness can be deduced. The fractal dimension was determined by drawing a line across specific areas – those including fibers or without. Along the user-defined line, a z-profile was exported to a spreadsheet program. The fractal dimension was determined using the line method, as opposed to the box method.

3.1.5.7 Differential Scanning Calorimetry (DSC)

Differential scanning calorimetry was used as a means of phase identification within the kraft pulp fiber-cement composites containing supplementary cementitious materials. This method was also used for semi-quantitative analysis of hydration products, particularly calcium hydroxide ($Ca(OH)_2$).

Samples were prepared by cutting a slice from composites previously tested in flexure. The area of these samples was initially 25.4x25.4mm. However, due to carbonation (as indicated by phenolphelin indicator), the edges of the slice were removed to minimize the amount of carbonated materials. The resulting slice had a surface area of approximately 10x10mm. Samples were then ground in ethanol and dried for 4 hours at 80º C to removed capillary and pore water from the sample. After drying, samples were stored in sealed tubes for no more than 18 hours until characterization commenced.

A TA Instruments 2010 DSC was used for these experiments. Samples were encapsulated in aluminum samples pans containing approximately 10-15 mg of finely ground composite material. Due to the heating range capabilities of this particular apparatus (<700º C), calcium carbonate (carbonated calcium hydroxide) could not be resolved. Thus, care was taken during sample preparation to minimize calcium carbonate in the sample prior to analysis, as discussed in the preceding paragraph. The time between exposure to atmospheric conditions and DSC testing was approximately 16 hours for all samples tested. Thus, the amount of calcium carbonate in all samples should be fairly consistent and may be considered negligible for relative, semi-quantitative analysis.

During DSC testing, samples were maintained in a nitrogen atmosphere at a flow rate of 40 mL/min. Samples were heated from room temperature to approximately 650º C at 10º C/min. The reference aluminum sample pan remained empty.

The heat of enthalpy for all endothermic peaks were defined by the area contained within the peak. The peak area was bounded by a chord connecting the onset

point of the leading and trailing tangents. All numerical calculations were conducted using TA Instruments Universal Analysis v2.5H software.

3.2 Heat of Hydration / Isothermal Calorimetry

Cement paste samples were prepared with a water-to-cement ratio of 0.50 and 3% fibers/powder by mass. ASTM Type I portland cement and deionized water (resistivity of 18.2 MΩ·m) was used. Oxide analysis and Bogue potential composition for the cement are listed in Table 3-4. Unbleached kraft, bleached kraft and TMP fibers as well as wood and cellulose (bleached kraft) powders were evaluated.

Pastes were prepared by mixing the fibers or powder and the entirety of the water for 1 minute with a hand mixer. Subsequently, the cement was added and mixing continued for another 4 minutes. After zeroing the mass of the polyethylene ampules, 18-20 grams of paste was added to the ampule. The time between the end of mixing and placement of ampule in the calorimeter was 2 minutes. No superplasticizer was not added to avoid influencing cement hydration.

Hydration data was obtained using an 8-channel Thermometric TAM Air calorimeter. Samples were maintained at 25.0±0.1° C and automatic measurements were recorded every 2 minutes for 7 days, disregarding the first 10 minutes of data due to heat generated during ampule placement.

Table 3-4. Oxide analysis (mass percent) and Bogue potential composition for ASTM Type I LaFarge portland cement.

Oxide	Type I portland cement
SiO_2	21.26
Al_2O_3	4.79
Fe_2O_3	3.14
CaO	64.10
MgO	2.35
Na_2O	0.02
K_2O	0.36
TiO_2	0.19
Mn_2O_3	0.04
P_2O_5	0.03
SrO	0.03
BaO	0.04
SO_3	2.63
Loss on ignition	1.04
Insoluble residue	0.11
C_3S	55.24
C_2S	19.28
C_3A	7.38
C_4AF	9.54

3.3 Setting Time / Autogenous Deformation

3.3.1 Materials

High performance cement pastes were prepared with a water-to-cementitious materials (w/cm) ratio of 0.30, ASTM Type I portland cement, 10% metakaolin by mass of cement, and deionized water (resistivity of 18.2 MΩ·m) were used. The metakaolin (*Kaorock*) was provided by Thiele Kaolin Company in Sandersville, Georgia. Oxide analysis and Bogue potential composition for the cement are listed in Table 3-4 and oxide analysis of metakaolin is listed in Table 3-2. Metakaolin was chosen as it was previously found to induce more autogenous shrinkage than silica fume [Justice *et al.*, 2005].

The wood powder, obtained from J. Rettenmaier in Schoolcraft, Michigan, has an average fiber length of approximately 0.5-1.0 mm. The two types of cellulose powders have average fiber lengths of 10 μm (*Vitacel*) and 700 μm (*Arbocel*) and were also obtained from J. Rettenmaier in Schoolcraft, Michigan. The fiber length of the unbleached kraft fibers is approximately 4-5 mm while average thermomechanical (TMP) fiber length is 1-2 mm. The TMP of Loblolly pine was obtained from Augusta Newsprint Company in Augusta, Georgia. The unbleached kraft pulp of Slash pine was obtained from Buckeye Technologies in Plant City, Florida. LiquiBlock 80HS superabsorbent polymers (sodium salt of cross-linked polyacrylic acid) have a particle size distribution of 1-100 μm and were obtained from Emerging Technologies, Inc. in Greensboro, North Carolina.

The internal curing materials were added at differing fiber mass fractions in order to entrain equivalent amounts of water. It has been previously shown [Jensen and Hansen, 2001; Bentz *et al.*, 2005] that at a basic (no supplementary cementitious materials) water-to-cement ratio of 0.30, additional entrained water approximately equal to 0.050 ($w/c_e = 0.050$) should mitigate autogenous shrinkage by providing enough water to prevent self-desiccation. For this research, this critical water entrainment dosage has been used. However, the addition of metakaolin creates a worst-case scenario for autogenous shrinkage. Thus, the actual critical water entrainment value may be higher than 0.050 due to increased chemical shrinkage/self-desiccation.

Based on image analysis during environmental scanning electron microscopy (ESEM), it was found that the average cement pore solution absorption capacity (k) of the TMP fibers and wood powder was 3.3, while $k_{average} = 1.0$ for the kraft fibers and cellulose powders. These differences are illustrated in Figures 3-5 and 3-6. For the SAPs, the absorption capacity was assumed to be 10.0, based on [Jensen and Hansen, 2002; Jensen and Lura, 2003].

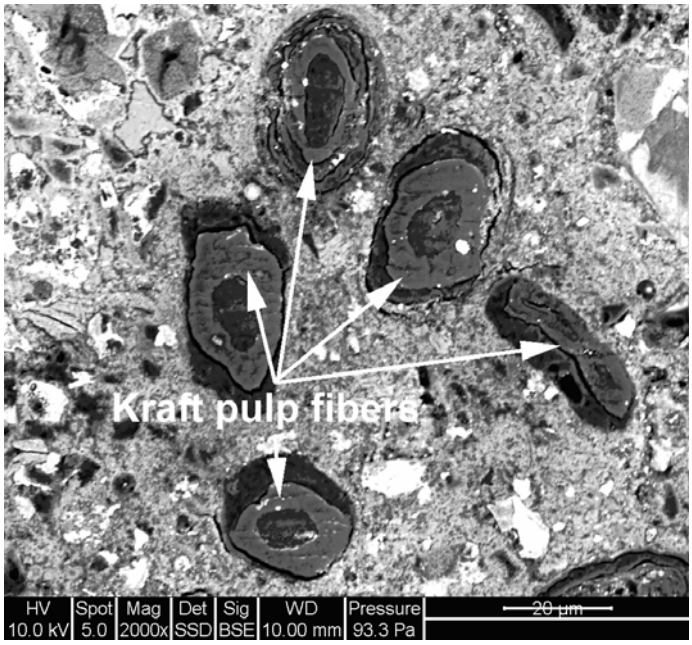

Figure 3-5. Environmental scanning electron microscopy (ESEM) micrograph of kraft pulp fibers ($k_{average}$ = 1.0).

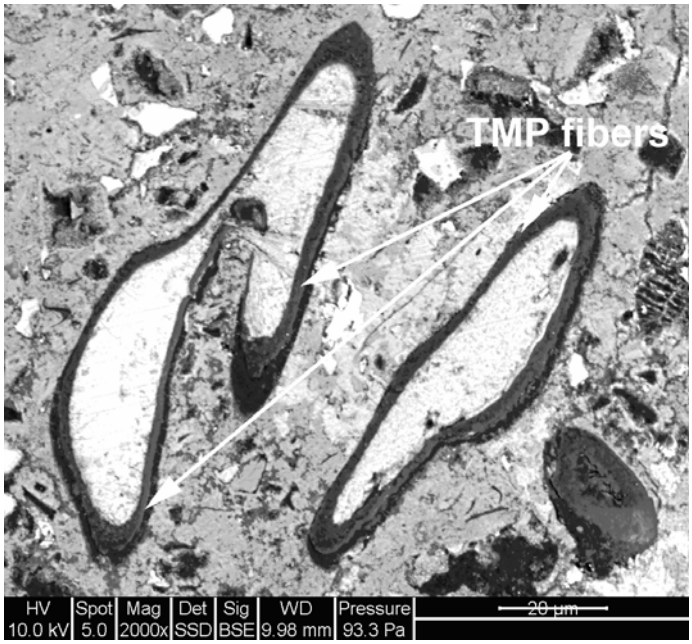

Figure 3-6. Environmental scanning electron microscopy (ESEM) micrograph of TMP fibers ($k_{average}$ = 3.3).

However, though wood powder has the same average absorption capacity as TMP fibers (*i.e.*, 3.3), this material has been shown in Figure 3-7 to release water during drying twice as fast as TMP fibers. This occurs as the shorter wood powders have, on average, twice as many open ends as the longer TMP fibers. In other words, for the wood powders and TMP fibers, water release rate is inversely proportional to fiber length (*i.e.*, shorter fiber length leads to increased release rate).

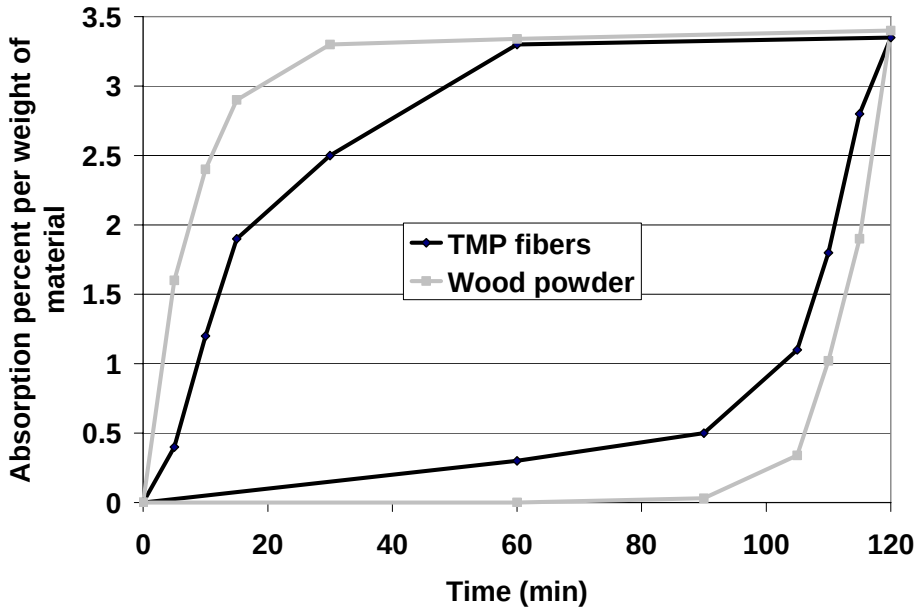

Figure 3-7. Moisture isotherms for TMP fibers and wood powder.

Thus, the TMP fibers and SAPs were added at dosages such that $w/cm_e = 0.025$, 0.050, 0.075, and 0.100. These entrained water dosage rates corresponded to material mass fractions of 0.75, 1.5, 2.25, 3.0% and 0.25, 0.50, 0.75, 1.0%, respectively.

In addition, wood powder was added at dosages of 1.5, 3.0, and 4.5% by mass corresponding to water entrainment values of 0.050, 0.10, and 0.15. Cellulose powders and kraft pulp fibers proved to be difficult to mix at low mass fractions, as expected. In addition, these materials only absorb their exact mass in water (*i.e.*, $k_{average}$=1.0). The maximum dosage rate possible was 1.0%, corresponding to $w/cm_e = 0.010$.

3.3.2 Sample Preparation

Pastes were prepared by mixing the internal curing materials and approximately 50% of the water for 3 minutes at 60 rpm in a 1.5L-capacity Hobart mixer to ensure separation of the materials, particularly the wood-derived fibers and powders. Subsequently, the cement was added, followed by the remaining water. Mixing continued at 120 rpm for another 5 minutes to allow for uniform dispersion. ADVA Flow superplasticizer, obtained from WR Grace, was added at a dosage rate of 1.5-2.0 μL/g cement for all mixes. The superplasticizer dosage rate was kept consistent as to minimize capillary water surface tension differences.

Autogenous deformation was measured by the technique described by Jensen and Hansen [1995]. This technique involves taking frequent linear deformation measurements of cement paste sealed in a rigid polyethylene mold with low friction, as seen in Figure 3-8. Measurements began at final set (as determined by Vicat needle penetration – ASTM C 191 [2003]) and continued periodically along a logarithmic scale. The initial measurement was taken at final set to exclude plastic deformation.

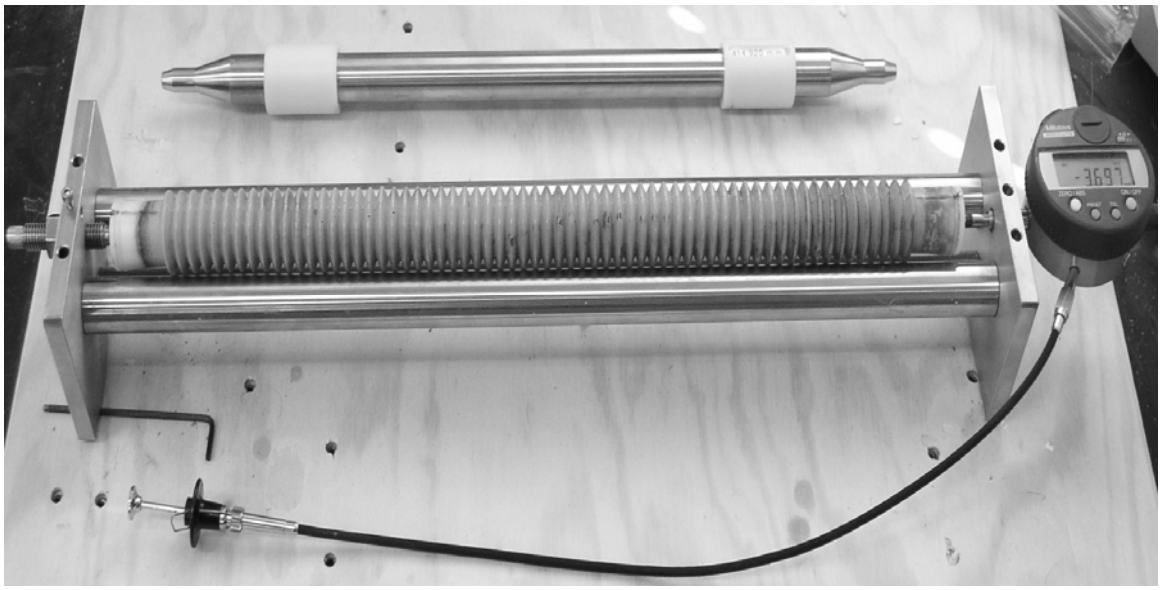

Figure 3-8. Corrugated polyethylene mold and measurement comparator used for autogenous shrinkage.

CHAPTER 4

WET / DRY CYCLING - FIBER MODIFICATIONS

Much of the research effort spent measuring durability and long-term performance of fiber-cement composites has focused on two key issues: (1) potential for fiber degradation in the alkaline cement paste and (2) changes in measured mechanical properties at high humidity. Addressing issue (1) above, research has shown that composites containing fibers with larger amounts of lignin may be more susceptible to attack by alkalis, producing composites more sensitive to weathering and aging [Pederson, 1980; Harper, 1982; Charman and Vautair, 1986; Gram 1986; Marikunte and Soroushian, 1994]. By selecting fibers with a low lignin content, such as kraft pulp fibers, such deterioration is expected to be largely avoided [ACI 544, 1996]. Addressing issue (2) above, research evidence has shown the cellulose fiber-reinforced cement-based materials display lower strengths and stiffnesses when tested wet, but increased toughness (energy absorbed before failure) as compared to when tested oven dry [Mai *et al.*, 1983; Coutts and Kightly, 1984]. Increases in moisture content appear to weaken the fiber-cement matrix bonding, encouraging fiber pull-out due to debonding, rather than rupture. The decreased strength in flexure is believed to be a result of the decreased bond strength, while increased toughness is believed to result from increasing energy consumption during fiber pull-out [ACI 544, 1996]. While it is clear that the moisture state will influence composite performance, significantly less research has been

performed to address the effect of cyclical wetting and drying (and resulting cyclical fiber swelling and shrinkage) on the performance of fiber-cement composites. Such conditions are expected when fiber-cement composites are subjected to external exposures during service.

In a test of accelerated aging (which included wet/dry cycling and CO_2 exposure), MacVicar *et al.* [1999] found that the compressive strength of a single type of commercially available fiber-cement composites actually increased due to decreased matrix porosity on increasing exposure. While this research is a valuable contribution to the knowledge base describing long-term durability of these types of materials, the scope of testing performed (*i.e.*, exposure conditions examined, materials tested) is limited. Also, importantly, the test program of MacVicar and co-workers did not report changes in flexural performance, elastic modulus, and toughness of the material resulting from aging; these properties are more sensitive than compressive strength to cracking induced during debonding. Soroushian and co-workers, who have published widely on the development and testing of fiber-cement materials, report significant decreases (40% or more) in flexural toughness after 25 wet/dry cycles as compared to samples not exposed to wet/dry cycling [Marikunte and Soroushian, 1994]. However, data were only reported for 0 and 25 wet/dry cycles. It is worthwhile to measure the change in toughness with respect to the number of wet/dry cycles, including intermediate cycles, as well as any influence of fiber processing to limit fiber swelling and degradation. Clearly, further research is required (1) to assess the effects of cyclical changes in moisture content on fiber-cement bonding and (2) to determine if any changes to the fiber chemistry or morphology will produce fiber-cement composites with enhanced performance in

external service environments. Results from this phase of research have been published [Mohr *et al.,* 2005a, 2005b]. Thus, if such composites are to be increasingly used for applications where performance must be ensured after environmental exposure, the durability of these composites must be thoroughly investigated.

4.1 Fiber Modifications

With the selection of an experiment designed to eliminate the effects of continued cement hydration on measured strength, the focus of this investigation was to isolate the influence of variations in fiber processing to determine if these variations affect fiber-cement composite behavior during progressive wet/dry cycling. That is, can certain processes, *i.e.*, beating, bleaching, initial drying state and pulping, be used to minimize degradation of fiber-cement composite strength and/or toughness due to wet/dry cycling? These fiber processes are known to change the chemical and physical structure of the fiber.

4.1.1 Effect of Wet/Dry Cycling

Samples were tested at 0, 1, 2, 5, 10, 15, and 25 wet/dry cycles to measure the progression of damage, if any, resulting from increasing number of cycles. Figure 4-1 illustrates typical load-deflection curves after 0, 5, 10, and 25 cycles. It can be seen that there is a 43.5-52.0% loss of first crack strength, a 50.8-72.4% loss of peak strength, and

a 97.5-98.8% loss of post-cracking toughness after 25 wet/dry cycles. The majority of strength and toughness loss occurs within the first two to five cycles.

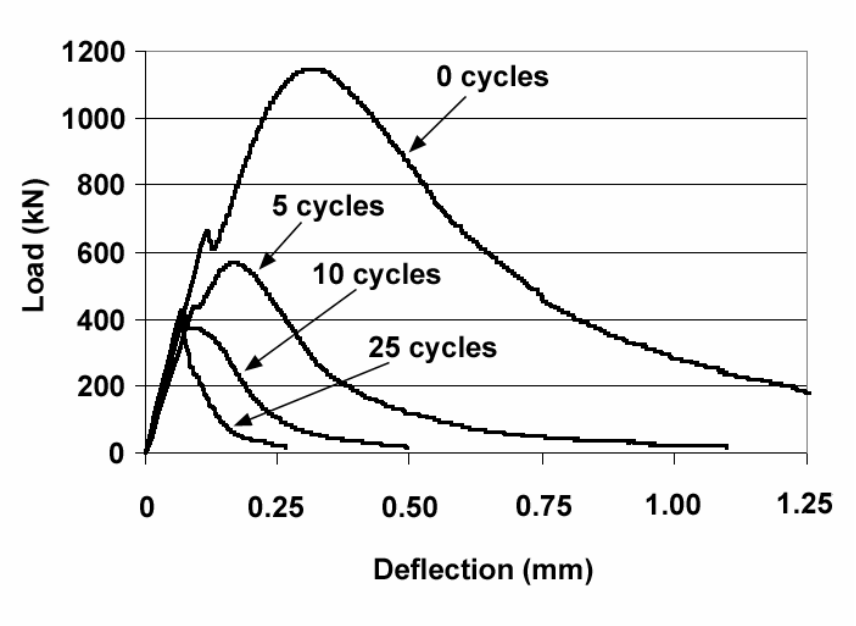

Figure 4-1. Typical load-deflection curves for kraft pulp fiber-cement composites.

With the exception of the unbleached kraft fiber (fiber A) composite, average first crack and peak strength values were lowest between five and ten cycles. For these samples containing bleached kraft fibers (fibers B-D), first crack strength decreased by 53.6-60.3% and peak strength decreased by 59.2-78.2% upon reaching the minimum values as compared to samples not exposed to wet/dry cycling (*i.e.*, zero cycles). However, after 25 cycles, values for first crack and peak strength increased relative to these minimum values by 20.6-38.8%.

Average post-cracking toughness values, with the exception of the composites containing unbleached kraft fibers (fiber A), reached minimum values after 15 cycles. These were 98.1-98.5% lower than those samples not exposed to cycling. However, after 25 cycles, post-cracking toughness increased by 2-32% relative to the minimum values after 15 cycles. In these samples, the lowest strength and toughness measured during this evaluation occurred after 25 cycles.

SEM micrographs of fracture surfaces, Figure 4-2 – 4-4, show the progression of damage with wet/dry cycling. Without cycling, Figure 4-2, fibers regularly extend approximately 600-1000 μm from the fracture surface. Thus, in the absence of wet/dry cycling, fiber pull-out appears to be the predominant mode of failure. Examination of fracture surfaces after 25 cycles, such as shown in Figure 4-4, shows that the predominant mode of failure after this period of exposure is fiber fracture. This suggests that after 25 wet/dry cycles, the fiber becomes brittle, most likely due to mineralization of the fibers. Energy dispersive spectroscopy (EDS) of SEM backscattered electron imaging by Tolêdo Filho *et al.* [2000] and Savastano and Agopyan [1999] confirm the transport of cement hydration products, primarily $Ca(OH)_2$, within the lumen and voids of fibers, as well as around the fibers due to wet/dry cycling. Similar observations of cement hydration product deposits were made during this work.

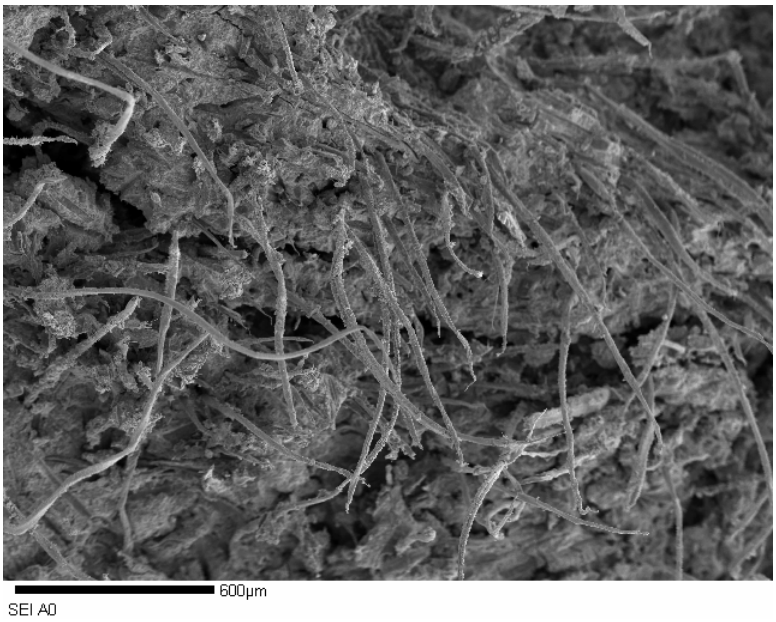

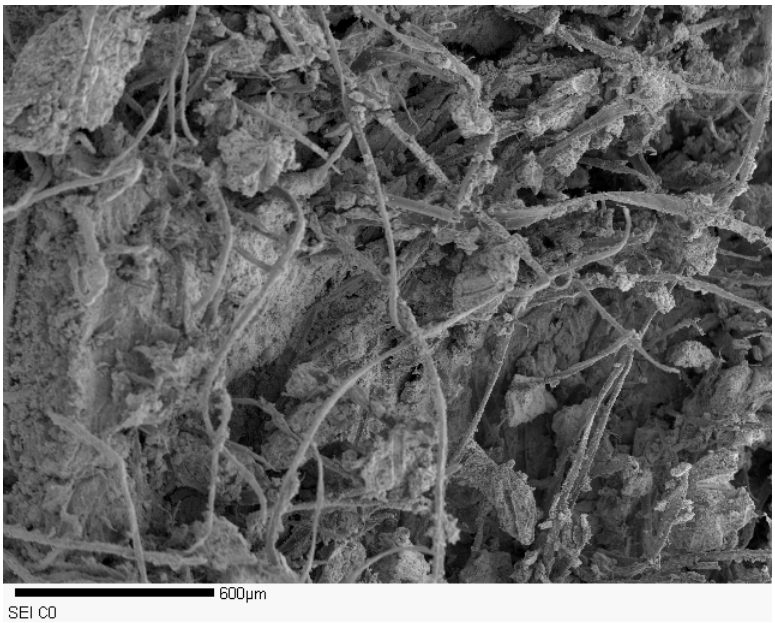

Figure 4-2. SEM micrographs of kraft pulp fiber-cement composite fracture surfaces without cycling.

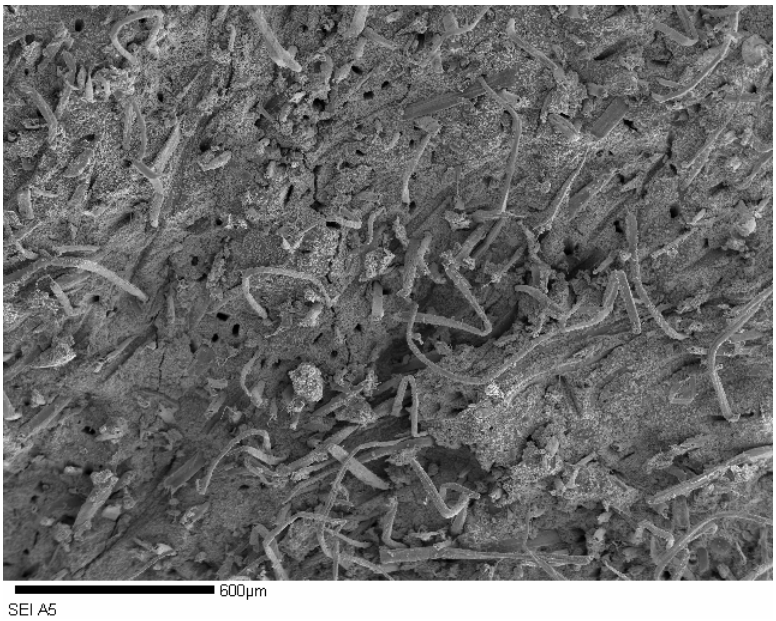

Figure 4-3. SEM micrographs of kraft pulp fiber-cement composite fracture surfaces after 5 cycles.

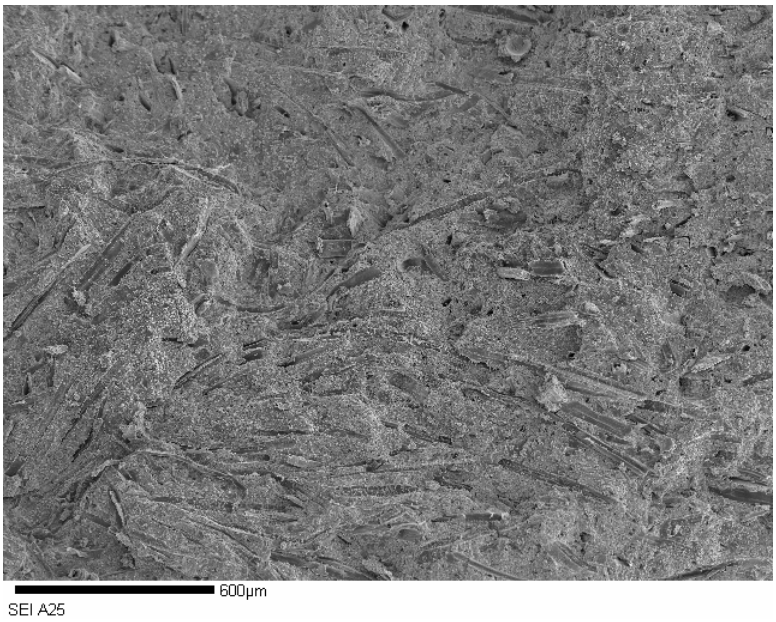

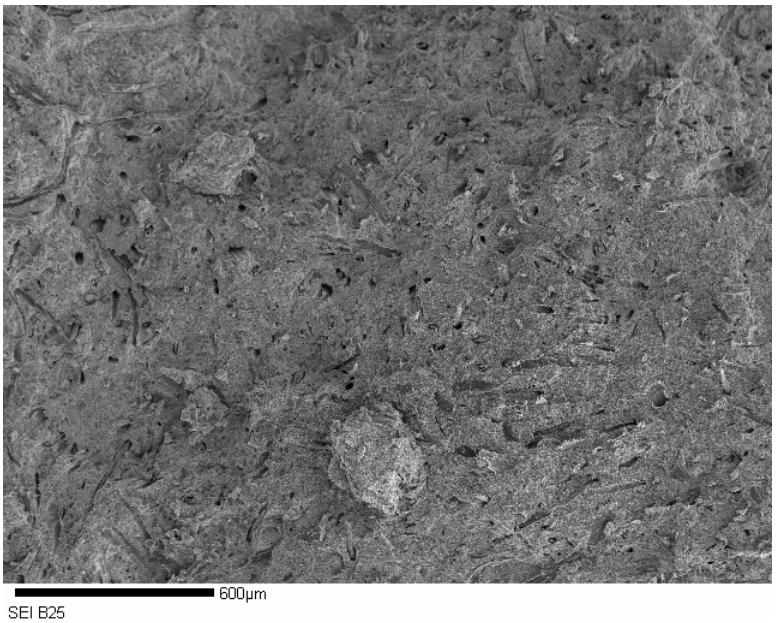

Figure 4-4. SEM micrographs of kraft pulp fiber-cement composite fracture surfaces after 25 cycles.

Since the majority of loss in flexural performance was found by mechanical testing to occur within the first 5 wet/dry cycles, it is worthwhile to observe fracture surfaces after 5 wet/dry cycles. Examination of fracture surfaces of these samples, such as in Figure 4-3, shows that fiber pull-out remains the predominant mode of failure, as was observed with no wet/dry exposure. However, the fiber pull-out length is significantly less (*i.e.*, approximately 100-400 μm after 5 wet/dry cycles as compared to 600-1000 μm in the control). Even though the majority of strength and toughness losses were measured after 5 wet/dry cycles, examination of SEM micrographs, such as Figures 4-3 and 4-5, of the fracture surfaces show some "necking" or a Poisson effect of the fiber near the region of fiber failure. This feature, which is observed for many of the pulled-out fibers after 5 wet/dry cycles, suggests that fiber failure behavior remains ductile. Additionally, pulled-out fibers with no wet/dry exposure, Figure 4-2a, also exhibit this "necking".

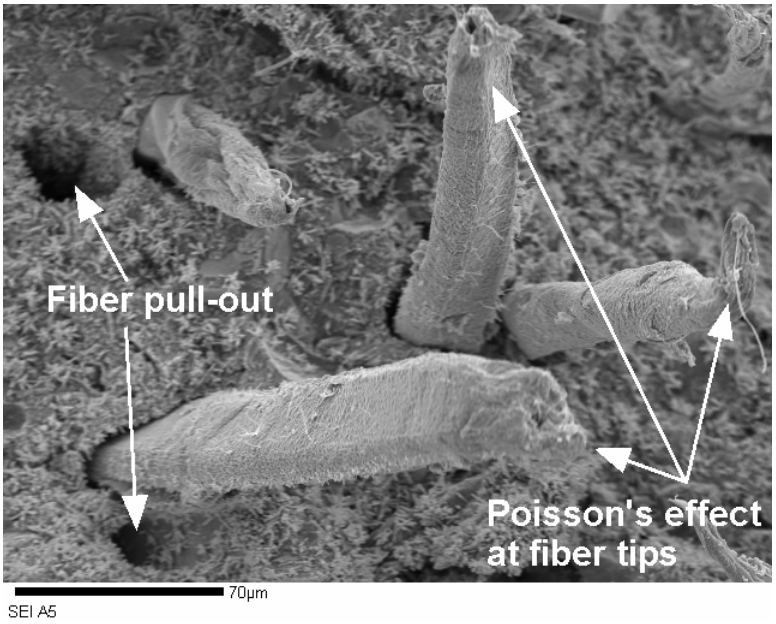

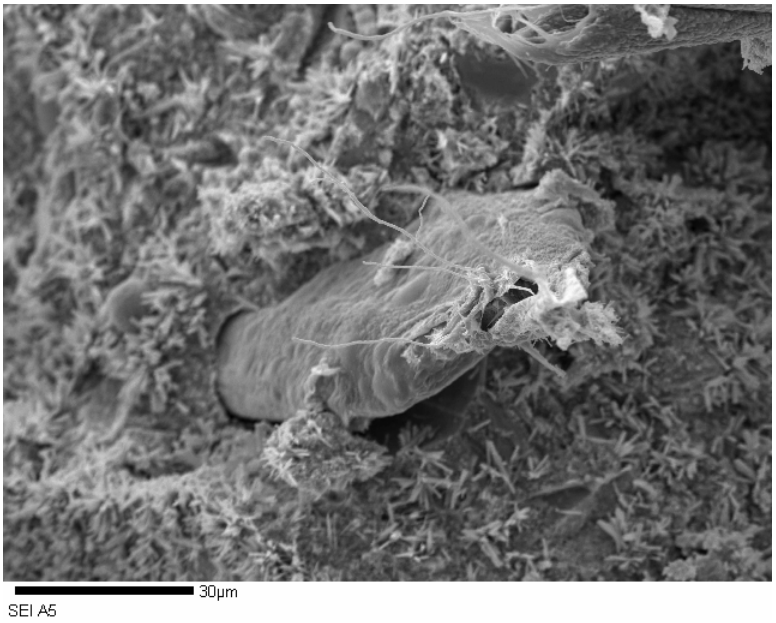

Figure 4-5. SEM micrograph of kraft pulp fiber-cement composite fracture surface after 5 wet/dry cycles.

4.1.2 Effect of Fiber Beating

Refinement or beating of the pulp fibers fibrillates the fiber surface [Coutts, 1983; 1984; 1987]. The outermost later, S1, may become damaged by beating, thereby increasing the fiber surface area. Thus, it may be proposed that beaten fibers should exhibit increased fiber-cement bonding due to this increase in fiber surface area. This increased bonding would be characterized by higher strength, but lower toughness and decreased tendency for fiber pull-out as compared to unbeaten fibers. However, beating may decrease the average fiber length. Additionally, beaten fibers tend to be more conformable. In terms of post-cracking toughness, it is possible that these changes in fiber length and conformability may present competing effects to the increased fiber surface area [El-Ashkar *et al.*, 2003]. However, Coutts [1984] has generated evidence to the contrary, showing that unbeaten fiber composites exhibit greater toughness as compared to beaten fiber composites. Thus, as the anticipated effect of beating is unclear, the goal of this part of the research was to assess how the initial mechanical behavior and behavior after wet/dry cycling is influenced by fiber beating.

Results from flexural testing of cement composites reinforced with beaten (fiber B) and unbeaten (fiber C) kraft fibers are shown in Figure 4-6 – 4-8. Prior to wet/dry cycling, the composites containing unbeaten fibers show a 61.3% greater average peak strength and a 80.3% greater average post-cracking toughness than those containing beaten fibers. Average first crack strength values were similar for both beaten (5.637±0.271 MPa) and unbeaten (5.947±0.323 MPa) fiber composites.

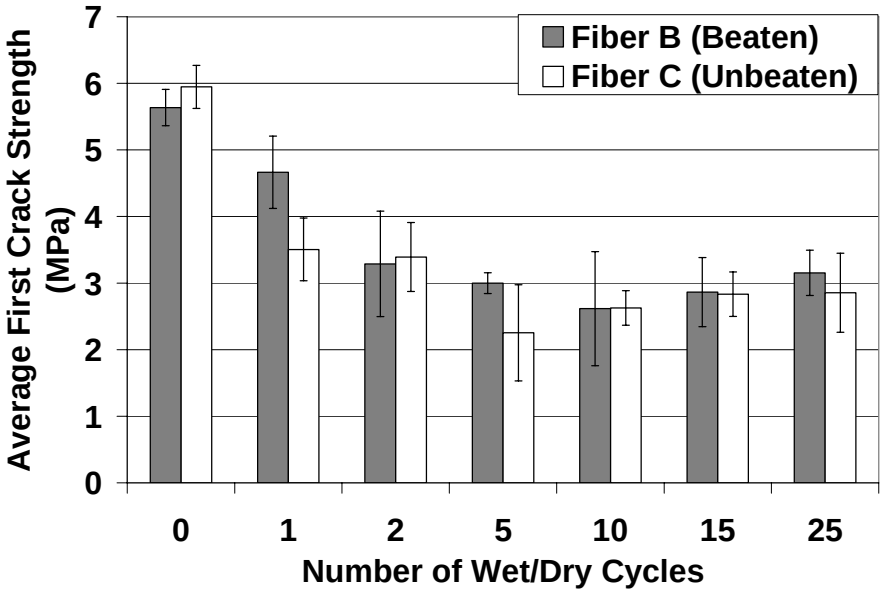

Figure 4-6. Flexure test results for kraft fiber B (beaten) and kraft fiber C (unbeaten). Average first crack strength (MPa) versus number of wet/dry cycles.

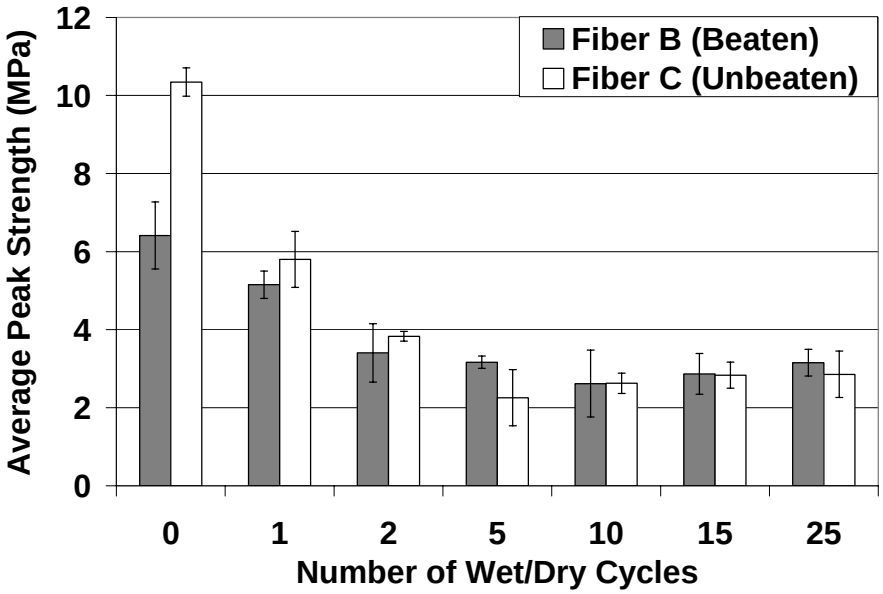

Figure 4-7. Flexure test results for kraft fiber B (beaten) and kraft fiber C (unbeaten). Average peak strength (MPa) versus number of wet/dry cycles.

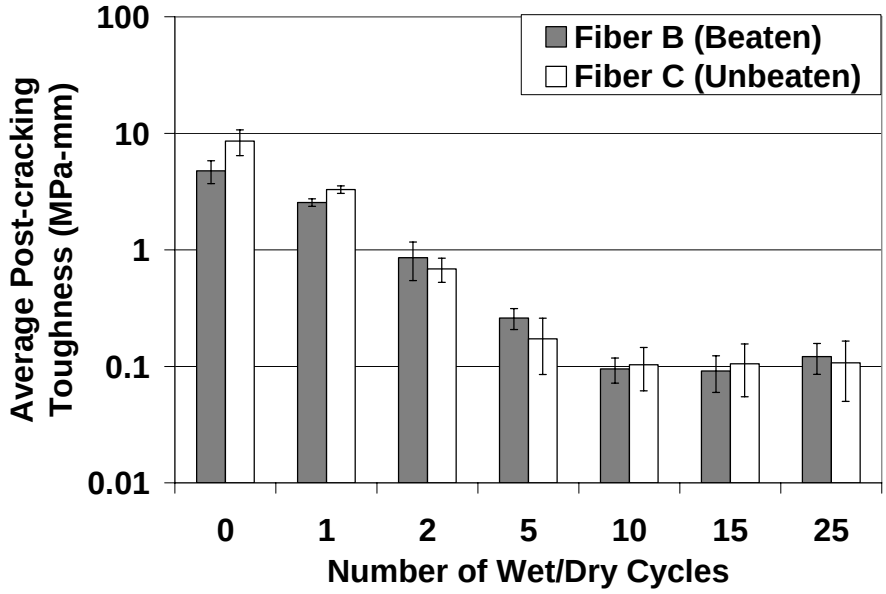

Figure 4-8. Flexure test results for kraft fiber B (beaten) and kraft fiber C (unbeaten). Average post-cracking toughness (MPa-mm) versus number of wet/dry cycles.

SEM micrographs in Figure 4-9 illustrate typical fracture surfaces of composites containing either beaten or unbeaten fibers without any wet/dry exposure. While bulk observation of fracture surfaces yields no apparent differentiation with beating, microscopy does show some variations in failure mode. Specifically, with the beaten fiber composites, it is often observed that the S1 layer separates from the fiber upon failure, remaining bonded to the matrix. Additionally, the beaten fiber pull-out length ranges from 400-600 μm, whereas the pull-out length of the unbeaten fibers ranges from 700-900 μm. Thus, the beaten fiber-cement paste bond seems to be stronger than the unbeaten fiber-cement paste bond. It is believed that the larger surface area of the beaten fiber is the primary contributing factor to this observed behavior.

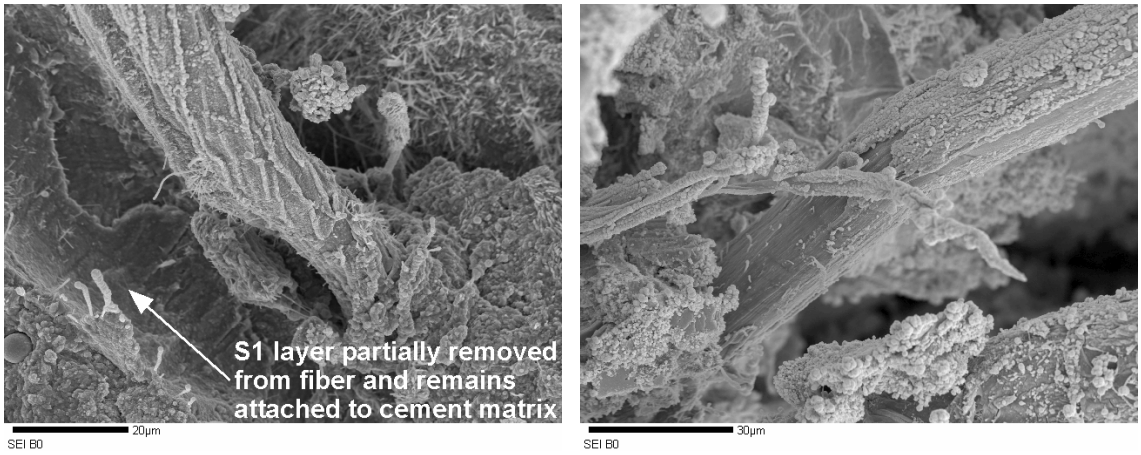

(a)

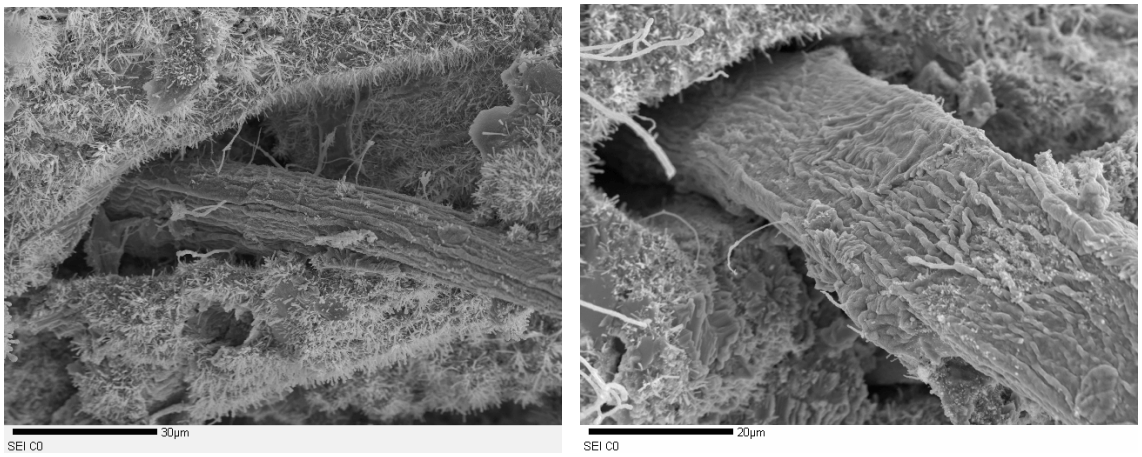

(b)

Figure 4-9. SEM micrographs of kraft pulp fiber-cement composite fracture surfaces after 0 wet/dry cycles. (a) Beaten kraft fiber. (b) Unbeaten kraft fiber.

Figures 4-6 – 4-8 also shows data describing the progressive effect of wet/dry cycling on mechanical behavior. After 5 wet/dry cycles, the composites containing beaten fibers generally show increased strength and toughness values as compared to those of the unbeaten fiber composites. Beyond 10 wet/dry cycles, no appreciable difference between the beaten and unbeaten fiber composites is apparent from these data. It is worth noting, however, that the beaten fiber composites exhibit a 10.5% increase in peak/first crack strength and a 12.9% increase in post-cracking toughness after 25 wet/dry cycles, as compared to the unbeaten fiber composites.

Micrographs of typical fracture surfaces for each of these samples after 25 wet/dry cycles are shown in Figure 4-10. For the beaten fibers, it is commonly observed that the S1 and S2 layers are partially removed from the fiber during composite failure, while such observations are not made for unbeaten fibers. Similar observations were made without wet/dry cycling (Figure 4-9). Thus, the fiber-cement paste bond appears to be stronger for the beaten fiber-cement composite prior to and after cycling. The mechanical testing data collected support this supposition. That is, the beaten fiber composites exhibited greater peak/first crack strength and toughness in flexure after 25 wet/dry cycles. The increased fiber/matrix bonding with beaten fibers could result in a larger fiber failure surface area and greater energy dissipation during composite failure, given that both the beaten and unbeaten fibers fail by brittle fracture.

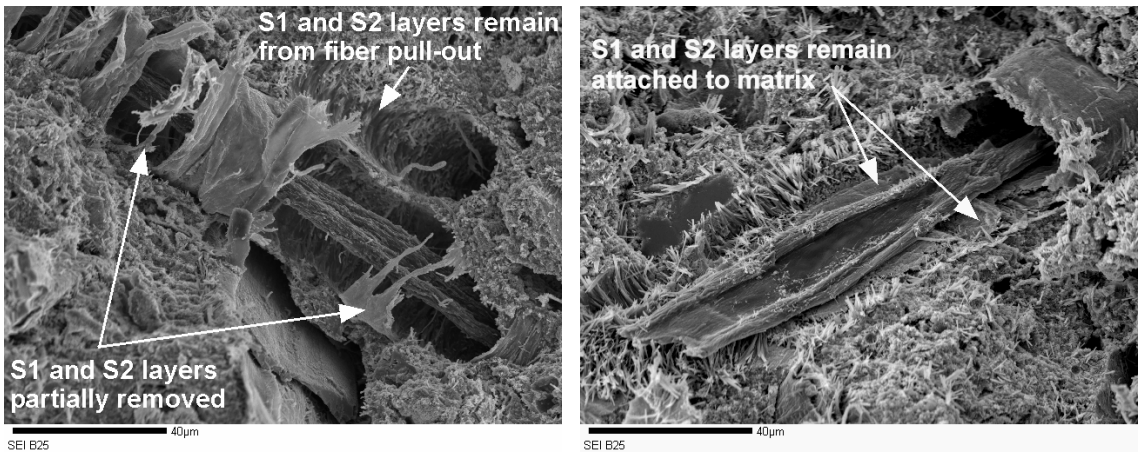

(a)

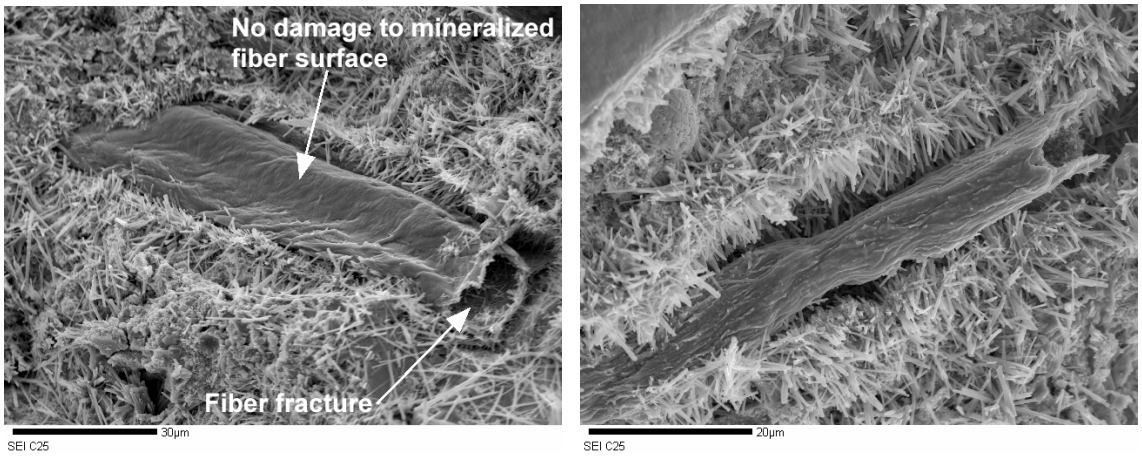

(b)

Figure 4-10. SEM micrographs of kraft pulp fiber-cement composite fracture surfaces after 25 wet/dry cycles. (a) Beaten kraft fiber. (b) Unbeaten kraft fiber.

4.1.3 Effect of Fiber Drying History

The potential for fiber/matrix debonding and microcracking at the interface during wet/dry cycling of composites is dependent upon (among other factors) the dimensional stability of the fiber reinforcement in response to moisture fluctuations. Wood fibers are hygroscopic, taking up moisture from a wet environment and giving up moisture to a drier environment. As a result, wood fibers swell with increasing moisture content and shrink upon its loss, below the fiber saturation point. Swelling/shrinking occurs primarily diametrically, with little dimensional change in the longitudinal direction. That is, 2-3% longitudinal expansion with swelling is typical, while the fiber cross section may change by 40-60%, depending on species, pulp type, and moisture content, among other factors. The initial drying state of a fiber, too, affects its dimensional stability during subsequent wetting and drying. Fibers which have been dried once (market pulp) prior to introduction to a matrix material are expected to swell less upon re-wetting, as compared to fibers which have not been previously dried (mill pulp). This improved dimensional stability is due to increased S1-S2 interlayer bonding in once-dried fibers compared to never-dried fibers. As a result, once-dried fibers tend to show a degree of concavity in their cross-section (prior to re-wetting), while never-dried fibers tend to be cylindrical or elliptical. Thus, never-dried fiber may hasten the formation of hydration products within the cell wall and lumen drying wetting and drying due to their larger swelling capacity, larger fiber diameter, and smaller cell wall thickness.

Savastano and Agopyan [1999] have shown that the transition zone around vegetable fibers was significantly larger than that of hydrophobic polypropylene fibers. Due to vegetable fibers releasing water into the surrounding matrix, it is assumed that an area of increased water-to-cement ratio forms. This may lead to a localized increase in transition zone porosity around hygroscopic fibers, as compared to polypropylene fibers. Thus, it is possible that the larger swelling capacity of never-dried pulp fibers may cause a larger and less dense transition zone, as compared to once-dried pulp fibers. Mechanical testing and microstructural characterization was performed to determine if once-dried fibers would impart improved performance as compared to never-dried fibers when used to reinforce cement paste.

First, the characteristics of the different fiber types were examined indirectly while determining an appropriate wet/dry cycle length for the composites. In a plot of percent mass change with time over the course of wetting and subsequent drying, Figure 3-1, composites containing never-dried fibers (fibers A and D), increase approximately 32-35% in mass during soaking, while composites containing once-dried fibers (fibers B and C) increase approximately 4-6% in mass. These data agree with the supposition that once-dried fibers are more dimensionally stable, gaining less water (mass) over the exposure period.

Bending test results comparing fiber C (once-dried) and fiber D (never-dried) are shown in Figure 4-11 – 4-13. Without any wet/dry cycling, the once-dried fiber composites exhibited 9.3%, 32.7%, and 56.3% greater first cracking strength, peak strength, and post-cracking toughness, respectively, compared to the never-dried fiber composites.

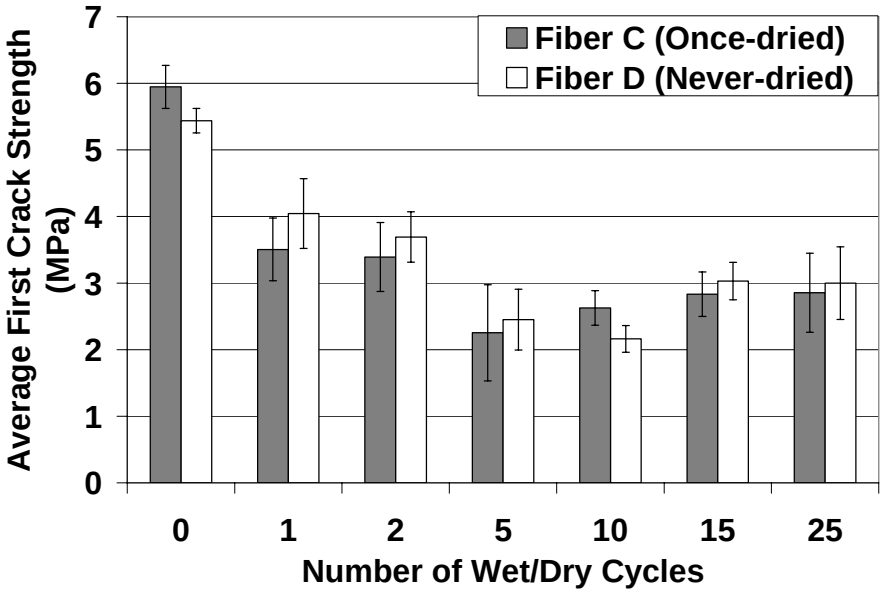

Figure 4-11. Flexure test results for kraft fiber C (once-dried) and kraft fiber D (never-dried). First crack strength (MPa) versus number of wet/dry cycles.

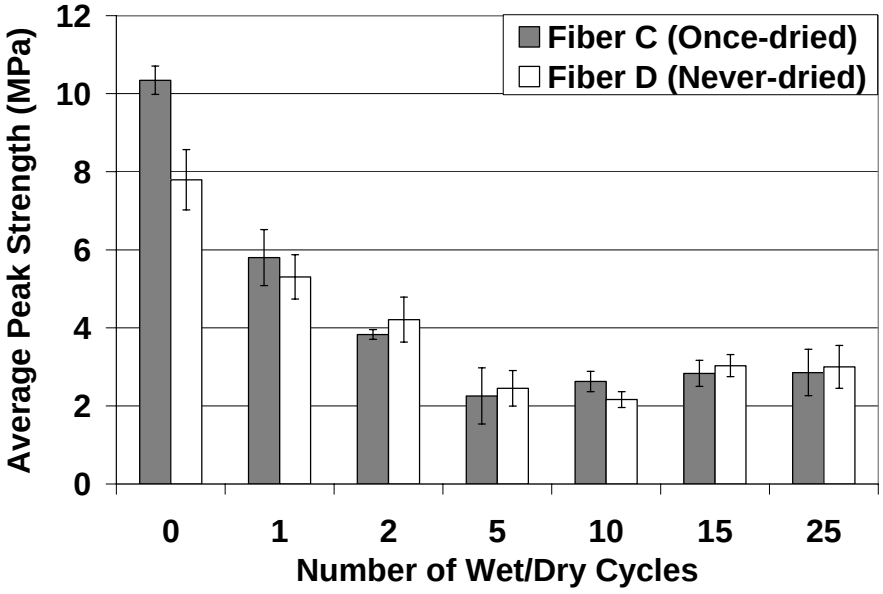

Figure 4-12. Flexure test results for kraft fiber C (once-dried) and kraft fiber D (never-dried). Peak strength (MPa) versus number of wet/dry cycles.

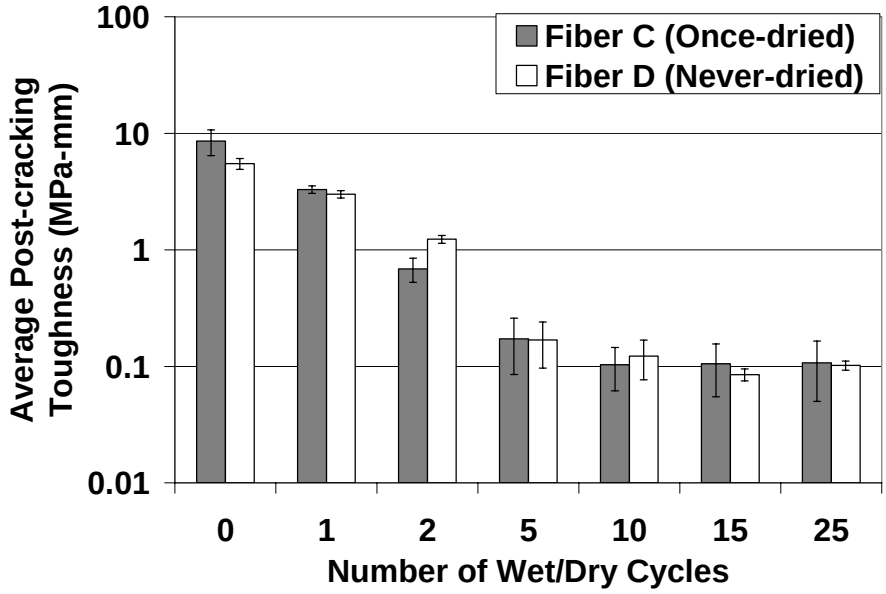

Figure 4-13. Flexure test results for kraft fiber C (once-dried) and kraft fiber D (never-dried. Post-cracking toughness (MPa-mm) versus number of wet/dry cycles.

No apparent differences were observed by SEM, except for the fiber morphology as mentioned previously. These results appear to indicate that the larger swelling capacity of never-dried fibers tends to weaken the transition zone around these fibers. This weak interface may impart less friction during ductile never-dried fiber pull-out, as suggested by Savastano and Agopyan [1999], leading to greater strength and toughness of once-dried fiber composites prior to wet/dry cycling.

The data in Figures 4-11 – 4-13 show that with exposure to wet/dry cycling, the strength and post-cracking toughness of the two fiber types are virtually indistinguishable. SEM micrographs of fracture surfaces of never-dried and once-dried fiber composites after 25 wet/dry cycles are found in Figure 4-14. Images like the one in Figure 4-14a verify that once-dried fibers tend to exhibit concavity in their cross-section.

No separation between fiber layers was observed to occur during failure of once-dried fiber composites. This suggests that the strengthening of the interlayer bonding during the initial drying does influence the mode of failure. However, the effect of this interlayer bonding within the fibers is not directly observed in the flexural test data, suggesting that other factors overshadow this effect. In contrast, damage to and separation between the S1 and S2 layers is observed in the never-dried fiber samples (Figure 4-14b). This seems to indicate that the fiber-cement bonding is stronger for the never-dried fibers after cycling. This should manifest itself in lower toughness of the never-dried fiber-cement composite relative to the once-dried fiber-cement composite, but the toughness values are so similar in these samples after 10, 15, and 25 cycles that no conclusive determination can be made about the role drying on performance.

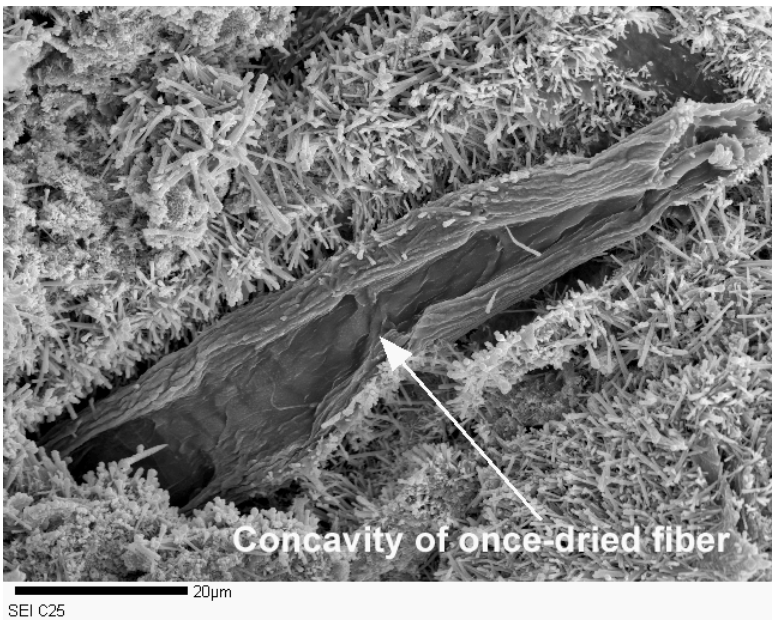

(a)

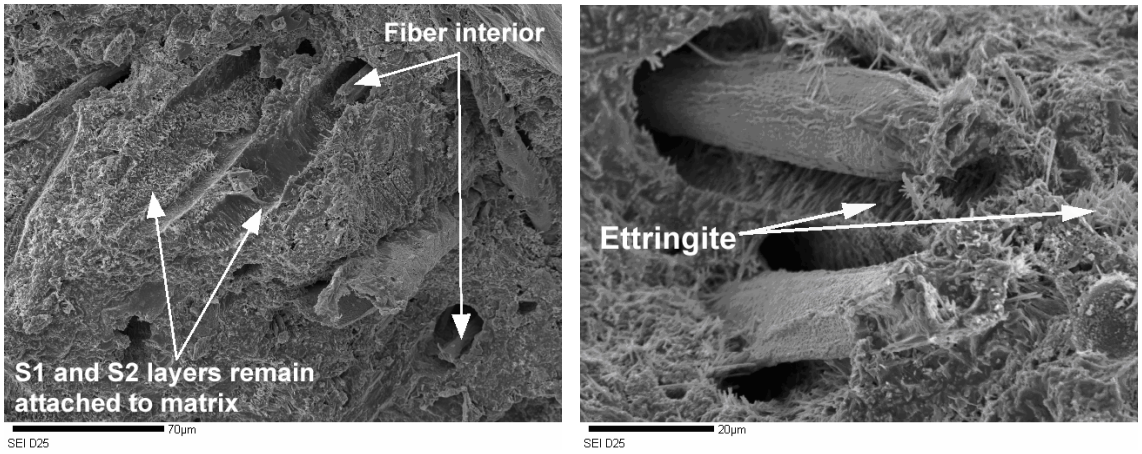

(b)

Figure 4-14. SEM micrographs of kraft pulp fiber-cement composite fracture surfaces after 25 wet/dry cycles. (a) Once-dried kraft fiber. (b) Never-dried kraft fiber.

4.1.4 Effect of Fiber Bleaching

Bleaching, commonly used to increase the brightness of pulp, largely removes lignin from wood fibers. Lignin is a highly crosslinked polymer that binds the fibers together. Typically, unbleached fibers consist of 65-75% cellulose, 17-32% hemicellulose, and 3-8% lignin, while bleached kraft fibers contain 70-80% cellulose and 20-30% hemicellulose, by mass [Stenius, 2000]. Lignin-containing by-products of paper pulping, such as lignosulfonates, are commonly used as chemical admixtures in concrete to retard cement hydration.

The effect of fiber bleaching on initial fiber-cement composite performance and performance after wet/dry cycling is difficult to anticipate. First, the removal of lignin from the fiber is suspected to increase fiber/matrix bonding. It is possible that the removal of lignin results in both a physical and chemical mechanism of increased fiber-cement bonding. Physically, the loss of lignin may result in a more open or rougher fiber surface, allowing for increased physical bonding with the cement paste. Also, chemically, due to the retarding effect of lignin on cement hydration, it is anticipated that the presence of lignin in an unbleached fiber may slow or prevent localized cement hydration and subsequent embrittlement of the fiber. However, bleached fibers have been shown to be stronger but less ductile than unbleached fibers [Mai *et al.*, 1983]. Furthermore, bleached fibers tend to be more collapsible due to the removal of lignin. Also, lignin has been found to be more susceptible to alkali attack than cellulose, which may present a competing effect in terms of long-term performance [ACI 544, 1996].

Without wet/dry cycling, it seems that the flexural behavior for composites reinforced with bleached or unbleached fibers is largely indistinguishable (Figures 4-15 – 4-17), while some variations in microstructure are apparent. Flexural test data, without wet/dry cycling, show that the peak strength, first cracking strength, and post-cracking toughness are each slightly (13.3%, 2.3%, and 26.0%, respectively) greater for the composites containing unbleached fibers (fiber A) as compared to bleached fibers (fiber D). Therefore, these data do support the concept that lignin impedes fiber-cement bonding or cement hydration near the fiber-cement interface, in the absence of wet/dry cycling. The presence of lignin leads to slightly longer unbleached fiber pull-out lengths (approximately 600-800 μm) as compared to pull-out lengths of 500-700 μm for bleached fibers.

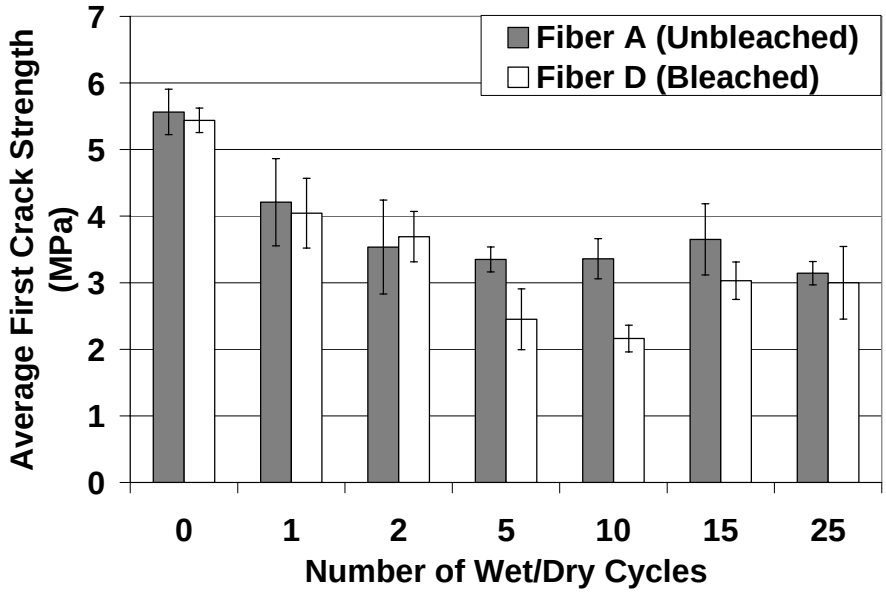

Figure 4-15. Flexure test results for kraft fiber A (unbleached) and kraft fiber D (bleached). First crack strength (MPa) versus number of wet/dry cycles.

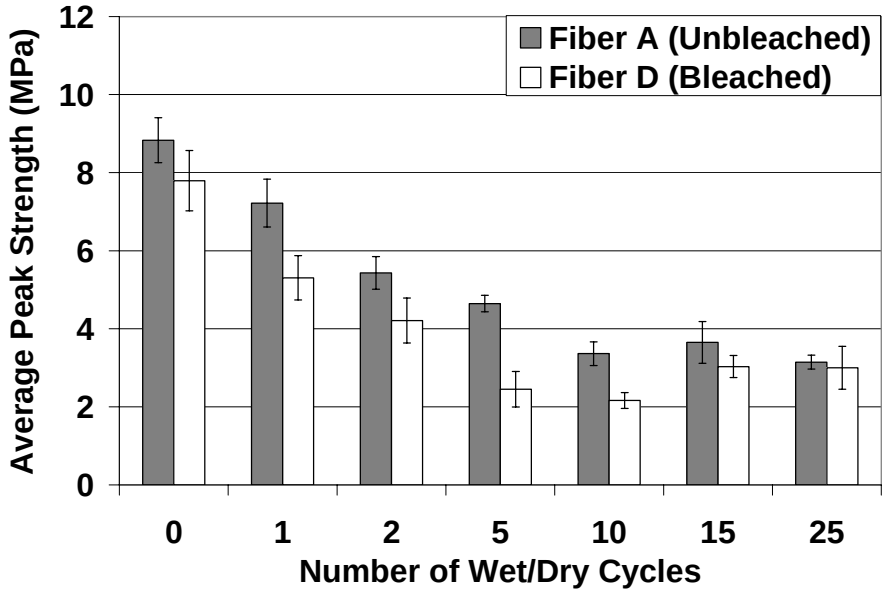

Figure 4-16. Flexure test results for kraft fiber A (unbleached) and kraft fiber D (bleached). Peak strength (MPa) versus number of wet/dry cycles.

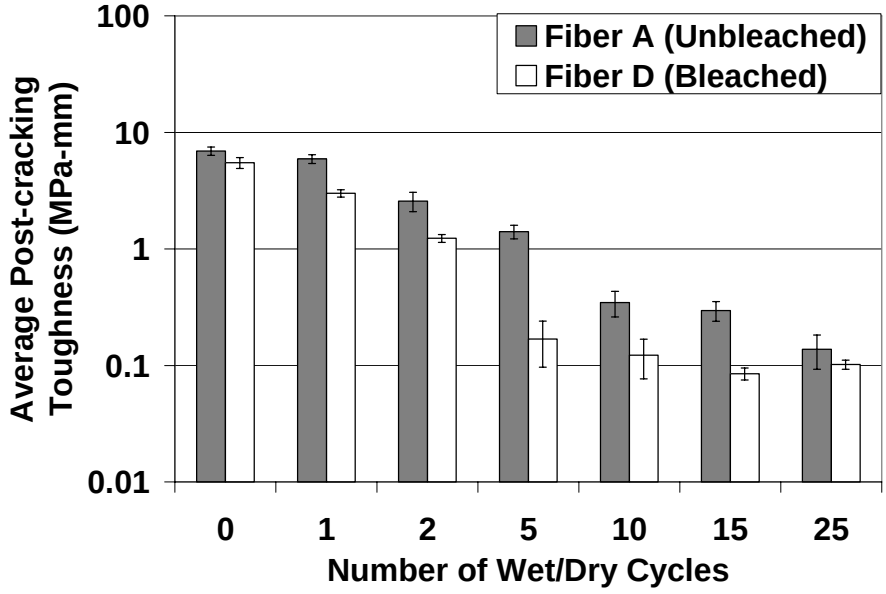

Figure 4-17. Flexure test results for kraft fiber A (unbleached) and kraft fiber D (bleached). Post-cracking toughness (MPa-mm) versus number of wet/dry cycles.

Characterization of bleached and unbleached fiber-cement composite fracture surfaces without wet/dry cycling was performed by SEM (Figure 4-18). With the bleached fibers, Figure 4-18b, microfibrils in the S1 layer are clearly visible as striations on the fiber surface. However, with the unbleached fibers (Figure 4-18a), cement hydration products – rather than cellulosic microstructure – are apparent on the surface of the pulled-out unbleached fibers.

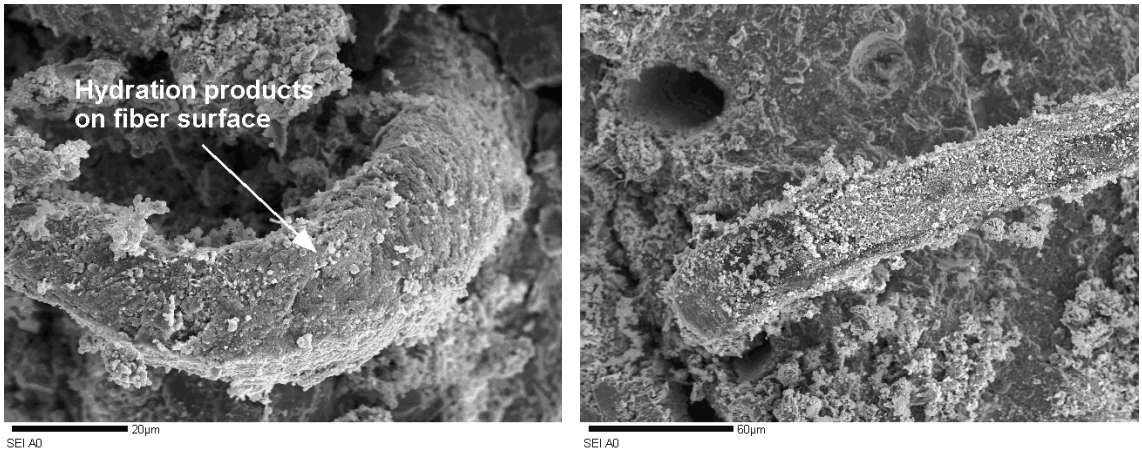

(a)

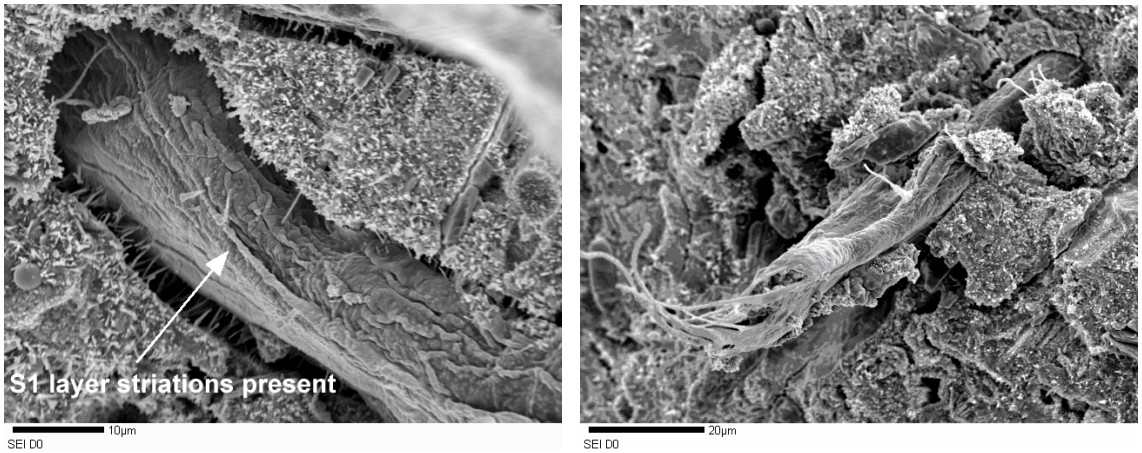

(b)

Figure 4-18. SEM micrographs of kraft pulp fiber-cement composite fracture surfaces after 0 wet/dry cycles. (a) Unbleached kraft fiber. (b) Bleached kraft fiber.

Figures 4-15 – 4-17 show the progression of degradation with wet/dry cycling for unbleached and bleached fiber composites. The trend in loss of strength and toughness with increasing numbers of cycles is slower for unbleached fiber-cement composites as compared to bleached fiber composites. Like the data without wet/dry

cycling (presented previously), these data also support the notion that cement hydration and fiber-cement bonding is impeded in the presence of lignin. It is important to note, however, that the progressive decrease in these properties is indeed slowed, but not prevented. The mechanism for this slower degradation trend has not been definitely established. However, it may be related to lignin present on the fiber surface and in the fiber cell wall acting as a physical chemical barrier to hydration product formation, or it may be related to local retardation of cement hydration in the fiber by lignin. Generally, over the range of wet/dry cycles examined here, the unbleached fiber composite exhibited greater strength and toughness. The relatively greater strength and toughness with unbleached fibers is particularly apparent between 2 and 15 wet/dry cycles. After 25 cycles, the unbleached fiber composites exhibit 4.8% greater peak/first crack strength and 34.9% greater toughness, as compared to the bleached fiber composite. The unbleached fiber-cement composite exhibited minimum flexural property values after 25 cycles, whereas, the bleached fiber-cement composites reached minimum values between 10 and 15 cycles and increased moderately with additional cycling.

Figure 4-19 shows typical fiber-cement composite fracture surfaces after 25 wet/dry cycles. Images of unbleached fiber-cement composite fracture surfaces show significant damage to the fiber. In Figure 4-19a, specifically, the removal of the S1 layer from the fiber, separation of S1 and S2 layers, and the formation of hydration products within the fiber are apparent. However, fracture surfaces for bleached fiber-cement composites exhibit similar forms of damage. For example, Figure 4-19b shows that separation of S1 and S2 layers as well as interior fiber mineralization. However, from observation of a range of fracture surfaces for bleached and unbleached fiber reinforced

composites, it appears that significantly more bleached fibers exhibit interior mineralization after 25 cycles, as compared to unbleached fibers.

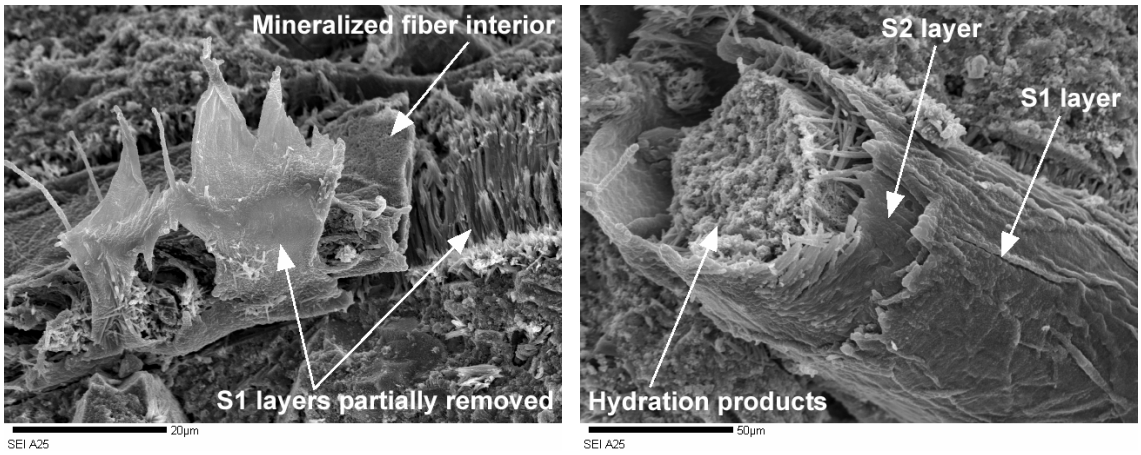

(a)

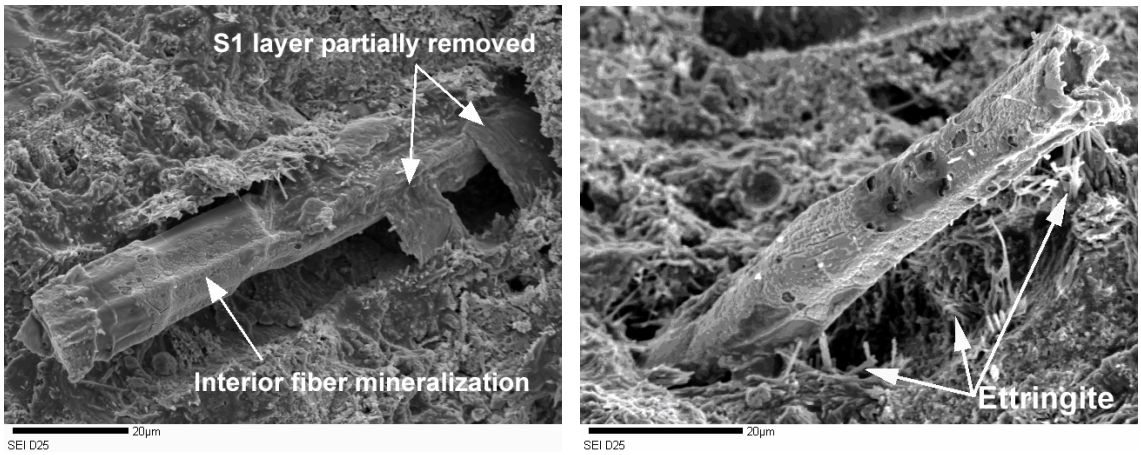

(b)

Figure 4-19. SEM micrographs of kraft pulp fiber-cement composite fracture surfaces after 25 wet/dry cycles. (a) Unbleached kraft fiber. (b) Bleached kraft fiber.

4.1.5 Effect of Fiber Pulping Process

As discussed in Sections 2.1.3 and 2.1.4, there are two primary processes to extract fibers from wood. The most common method, kraft pulping, yields a relatively long (4-5 mm) fiber as compared to TMP pulping (1-2 mm). This fiber length effect may influence the flexural behavior as discussed below.

More importantly, the pulping processes affect the fiber chemistry. Since the TMP fiber pulping process is mechanical in nature, the resulting fibers contain a much higher percentage of lignin (25-31%) compared to bleached and unbleached kraft pulp fibers, containing 0-1 and 3-8% lignin by mass, respectively. Lignin is thought to be the chemical component most prone to alkali degradation. However, little research is available concerning the durability of TMP fiber-cement composite degradation due to wet/dry cycling. Thus, a comparative investigation was warranted and the results are described below.

Typical load-deflection curves for each fiber composite after 0 cycles are illustrated in Figure 4-20a. TMP composites initially (after 0 wet/dry cycles) exhibited higher first crack strength, but lower peak strength and lower toughness as compared to unbleached and bleached kraft pulp composites (Figures 4-21 – 4-23), in general agreement with the findings reported by Campbell and Coutts [1980] and Soroushian and Marikunte [1992].

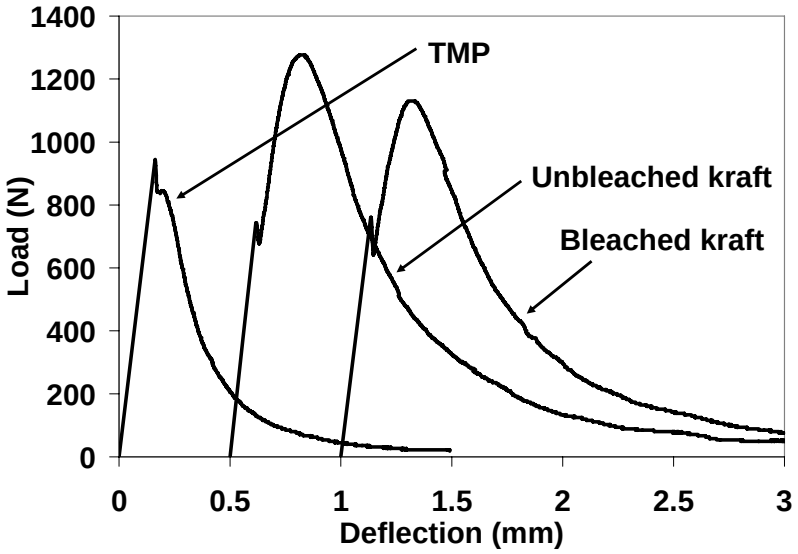

(a)

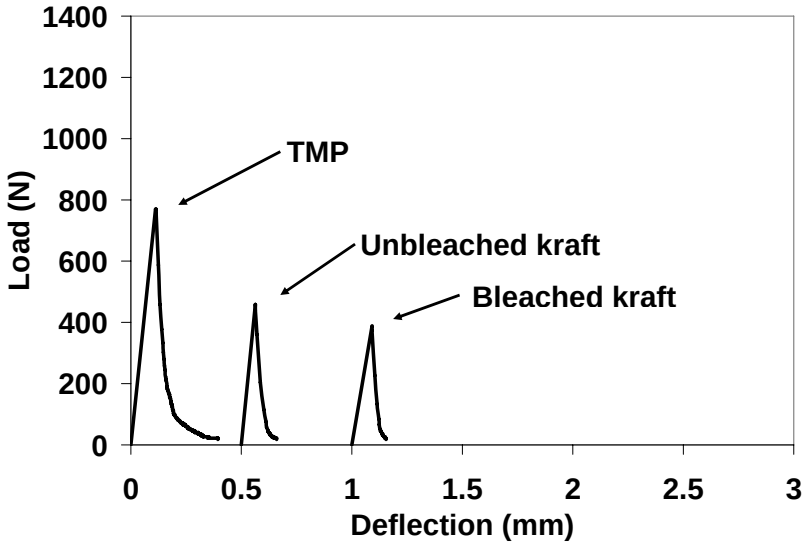

(b)

Figure 4-20. Typical load-deflection curves (offset) for TMP, unbleached kraft, and bleached kraft composites with 4% fibers by volume. (a) After 0 wet/dry cycles. (b) After 25 wet/dry cycles.

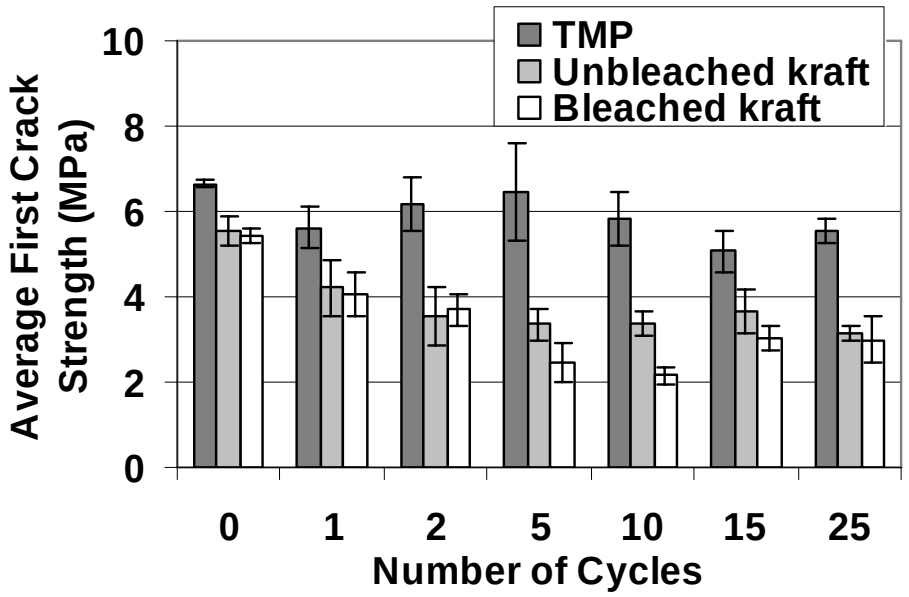

Figure 4-21. Flexural testing results for TMP fiber-cement composites. Average first crack strength (MPa) versus number of cycles. Note: First crack and peak strength are the same for TMP samples.

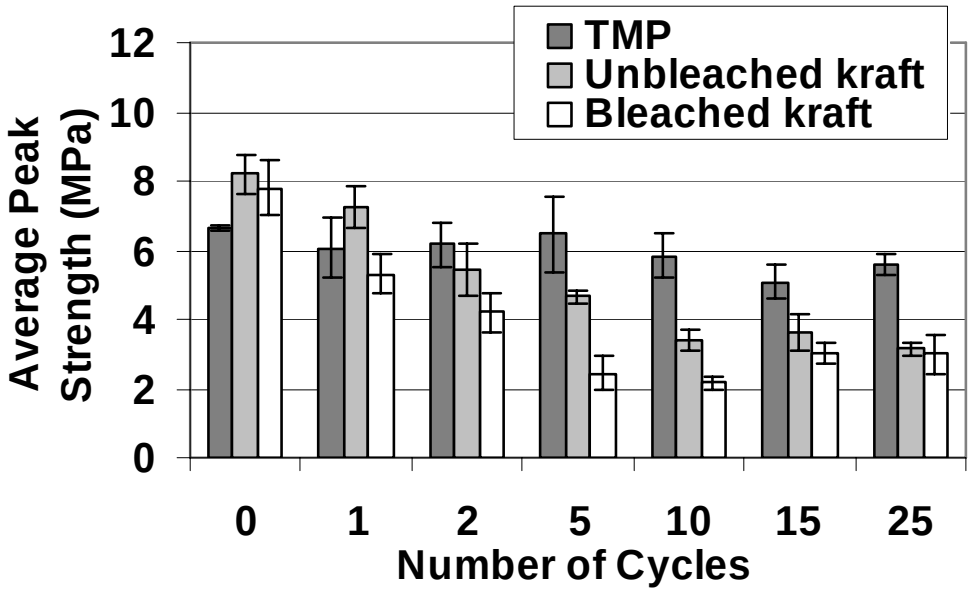

Figure 4-22. Flexural testing results for TMP fiber-cement composites. Average peak strength (MPa) versus number of cycles. Note: First crack and peak strength are the same for TMP samples.

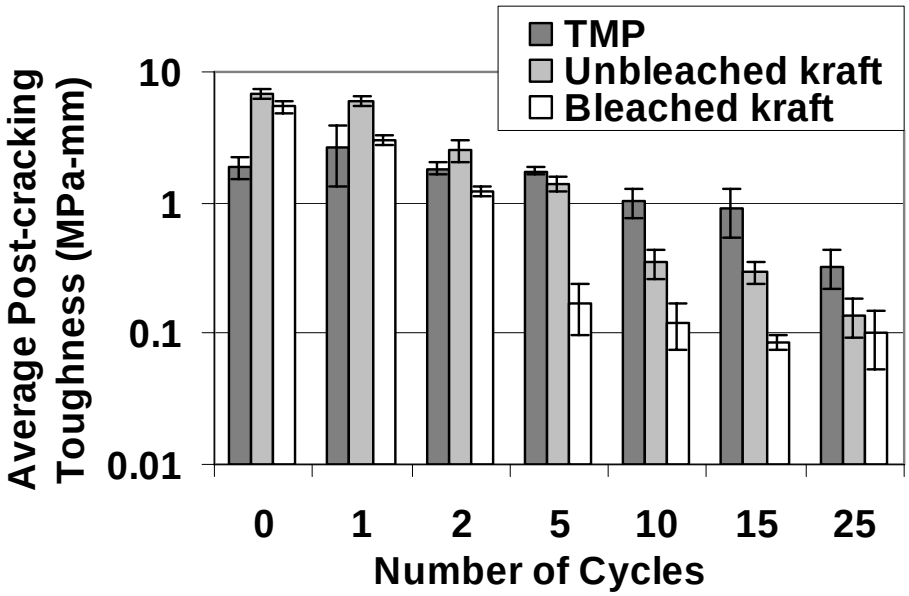

Figure 4-23. Flexural testing results for TMP fiber-cement composites. Average post-cracking toughness (MPa-mm) versus number of cycles.

Differences in first crack strength and post-crack behavior when comparing the kraft and TMP fiber composites are apparent. The higher first crack strength for the TMP composites may result from the shorter length of TMP fibers. The variation in fiber length is due to the differences in the TMP and kraft pulping operations. As more shorter (*i.e.*, TMP) fibers are present in a sample for a given fiber volume fraction, microcrack bridging may be improved, resulting in a higher first crack strength. In the post-cracking region, peak strength and toughness are decreased with TMP fibers. It is proposed that this is due to lower tensile strengths and shorter fiber pull-out lengths (also due to a shorter fiber length), as compared to the higher strength, longer kraft fibers. Since TMP fibers typically contain less cellulose by mass (40-45%) than kraft fibers (65-80%), TMP

fiber tensile strength is approximately 50-70% that of kraft fibers [McDonough *et al.*, 1987; Lehtonen, 2003].

With wet/dry cycling, all composites, regardless of fiber type, showed some degradation in mechanical properties. However, the relative losses for the TMP fiber composites were less than for the bleached or unbleached kraft fiber composites. Typical load-deflection curves after 25 wet/dry cycles can be seen in Figure 4-12b. These curves show that the composites exhibited lower strength and post-crack toughening than samples prior to cycling. As seen in Figures 4-21 – 4-23, TMP fiber-cement composites exhibited a 16.3% and 82.2% loss in first crack (peak) strength and post-cracking toughness, respectively, after 25 cycles compared to TMP specimens of the same age which were not subjected to cycling. For comparison, after 25 cycles, unbleached kraft pulp composites showed a 43.5% decrease in first crack strength, a 64.4% decrease in peak strength, and a 98.0% decrease in post-cracking toughness. Similarly, bleached kraft pulp composites lost 44.9% of first crack strength, 61.5% of peak strength, and 98.1% of post-cracking toughness after 25 wet/dry cycles.

However, as clearly seen in Figures 4-21 – 4-23, TMP composites generally exhibited a slower progression of degradation, as measured by mechanical performance, than both bleached and unbleached kraft fiber composites. That is, losses of 50% or more in post-cracking toughness, compared to that prior to cycling, were observed after 1 and 2 cycles for the bleached and unbleached kraft pulp composites, respectively. However, the TMP composites exhibited toughness losses of more than 50% after 15 wet/dry cycles. Similarly, bleached and unbleached kraft pulp composites exhibited losses of more than 25% in peak strength after 1 and 2 cycles, respectively, while TMP

composites did *not* exhibit strength losses greater than 25% over the range of wet/dry cycles investigated here.

Comparing the data after 25 wet/dry cycles, TMP composite strength and toughness exceeded that of the kraft pulp composites. Relative to unbleached and bleached kraft composites, TMP composite first crack (peak) strength was 77.1% and 85.7% greater, respectively, and toughness was 138.6% and 221.7% greater, respectively, after 25 cycles. These results suggest that TMP fibers may afford enhanced durability as compared to kraft pulp fiber-cement composites. It is proposed that the lignin in TMP and unbleached kraft fibers may slow the progression of composite degradation due to wet/dry cycling.

4.1.6 Effect of Aligned Pulp Fiber Sheets

The use of aligned fiber sheets has already proved effective in reinforcing cement mortars [Mohr *et al.,* 2003]. Significant improvements in post-cracking toughness were seen for relatively low equivalent fiber volume fractions [Mohr et al., 2003]. Aligned pulp fiber sheet composites have also been evaluated for wet/dry cycling durability. A basis weight of 30 g/m^2 was used for all fiber sheets. The sheets were made with the four kraft pulp fiber types described previously.

Results for the three fiber variations are shown in Figures 4-24 and 4-25. It can be seen that flexural strength after 25 cycles decreased by 26.5-38.5% as compared to that prior to cycling. Post-cracking toughness decreased by 28.7-53.8%. It should be noted that prior to mechanical testing, during wet/dry cycling, samples tended to

delaminate along the fiber sheet most likely due to fiber-cement debonding and subsequent microcracking.

By 25 wet/dry cycles, there are negligible differences between the different kraft fiber types, including the effect of bleaching. Thus, the fiber variations appear not to have an effect of fiber-cement bonding during wet/dry cycling.

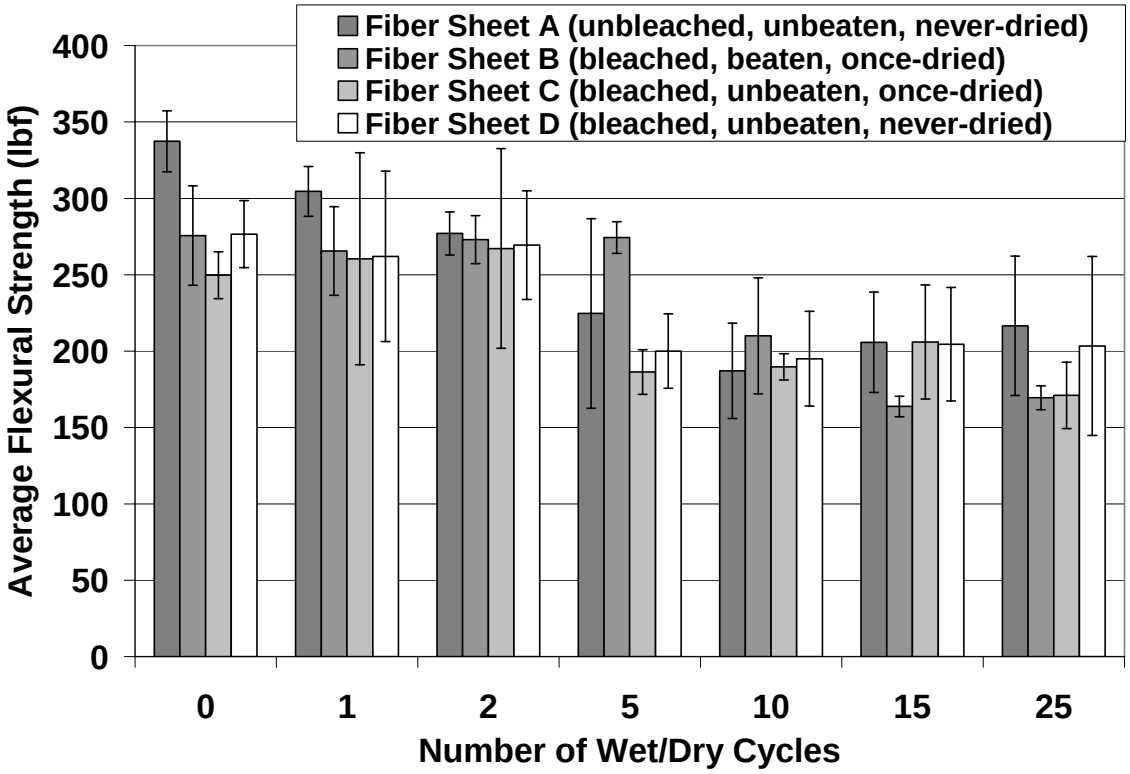

Figure 4-24. Flexural testing results for aligned kraft pulp fiber sheet composites. Average flexureal strength (lbf) versus number of cycles.

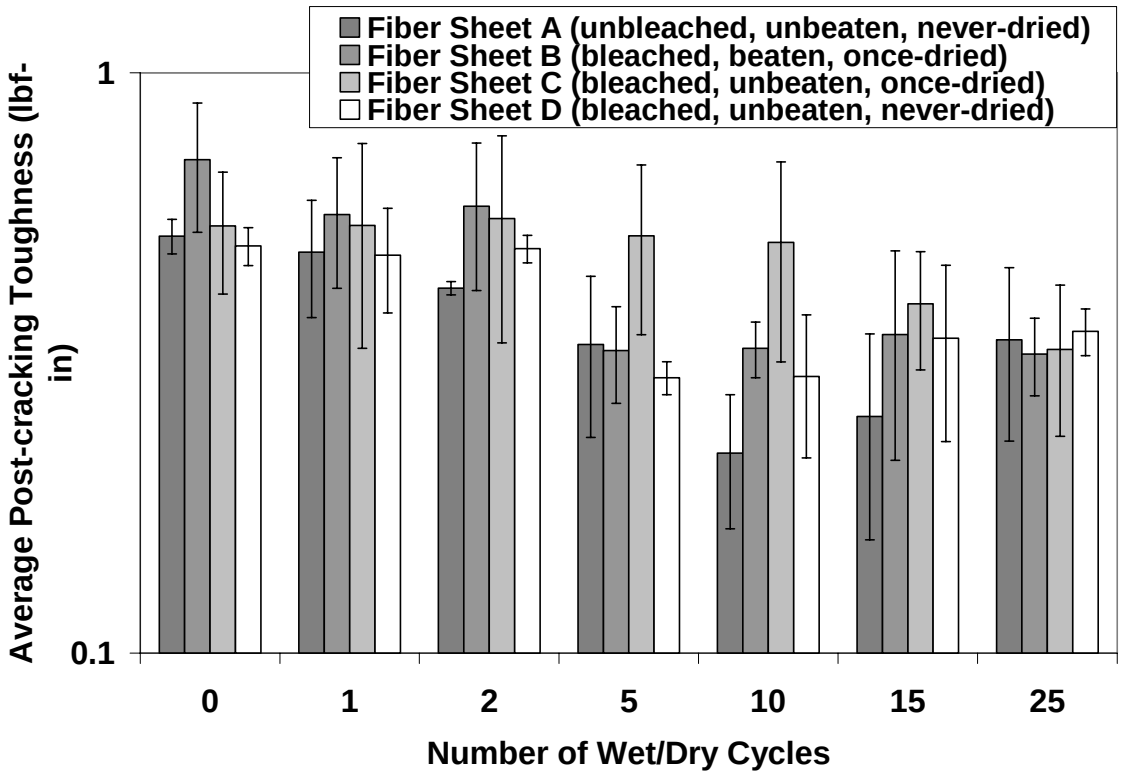

Figure 4-25. Flexural testing results for aligned kraft pulp fiber sheet composites. Average post-cracking toughness (lbf-in) versus number of cycles.

4.2 Proposed Degradation Mechanisms

To explain the mechanical behavior and microstructure discussed in Section 4.1, a progressive series of degradation mechanisms has been proposed: (1) initial fiber-cement debonding (due to fiber shrinkage during drying), as indicated by decreases in strength between 0 and 2 cycles, (2) reprecipitation of relatively low-strength hydration products (*i.e.*, secondary ettringite) within this new void space, introduced at the former fiber-cement interface, minimizing fiber dimensional changes during subsequent wetting,

and (3) fiber mineralization by the reprecipitation of hydration products, likely primarily calcium hydroxide, within the fiber cell wall structure.

During the initial wet/dry cycles, prior to the reprecipitation of hydration products around the fiber, the fibers are largely free to shrink and swell without impedance. Upon drying, diametrical fiber shrinkage may create a capillary expulsive pressure on the pore solution residing within the fiber lumen. Such a pressure would cause the pore solution to be primarily expelled through the fiber ends and pits along the fiber. During this drying, reprecipitation of hydration products can occur in this space at the former fiber-cement interface. However, the reprecipitation of hydration products such as ettringite can restrain fiber swelling upon rewetting. During subsequent drying, then, fiber shrinkage is also reduced. Thus, the driving force for pore solution expulsion is minimized. That is, the pore solution resides within the fiber for a longer period of time. Therefore, the pore solution will not only migrate from the fiber lumen to the matrix through the ends and fiber pits, but the solution can also diffuse from the lumen through the cell wall, resulting in a deposition of hydration products within the fiber cell wall. This deposition or reprecipitation decreases fiber ductility and leads to shorter fiber pull-out lengths in the composite. Complete fiber mineralization may not take place until beyond approximately 10 wet/dry cycles in this research, as suggested by observations of small increases in strength between 10 and 25 cycles. The following sections will highlight the research which forms the basis for these proposed mechanisms.

4.2.1 Pulp Fiber Characteristics

ESEM observations and EDS measurements were conducted on unbleached and bleached kraft pulp fibers as well as TMP fibers to qualify fiber chemical composition prior to incorporation in the cement matrix. The fibers were also investigated for dimensional changes during wetting and drying.

Results, shown in Figure 4-26, indicate that the kraft fibers exhibited higher net intensities of Al and Si, than the TMP fibers. It should be noted that the kraft fibers were treated with a process described in [Kurtis *et al.*, 2001; El-Ashkar *et al.*, 2003] to improve dispersion. This process involves treating the fibers with cationic starch and fly ash to improve their dispersion during mixing. Therefore, the increased levels of Al and Si on the kraft fiber surface can be attributed to the fly ash treatment. The TMP fibers were not treated by this process, thus explaining the lower levels of inorganic elements on the fiber surface. In addition, the kraft fibers did not yield any evidence of high alkali surface compositions that may have been present due to the particular pulping process.

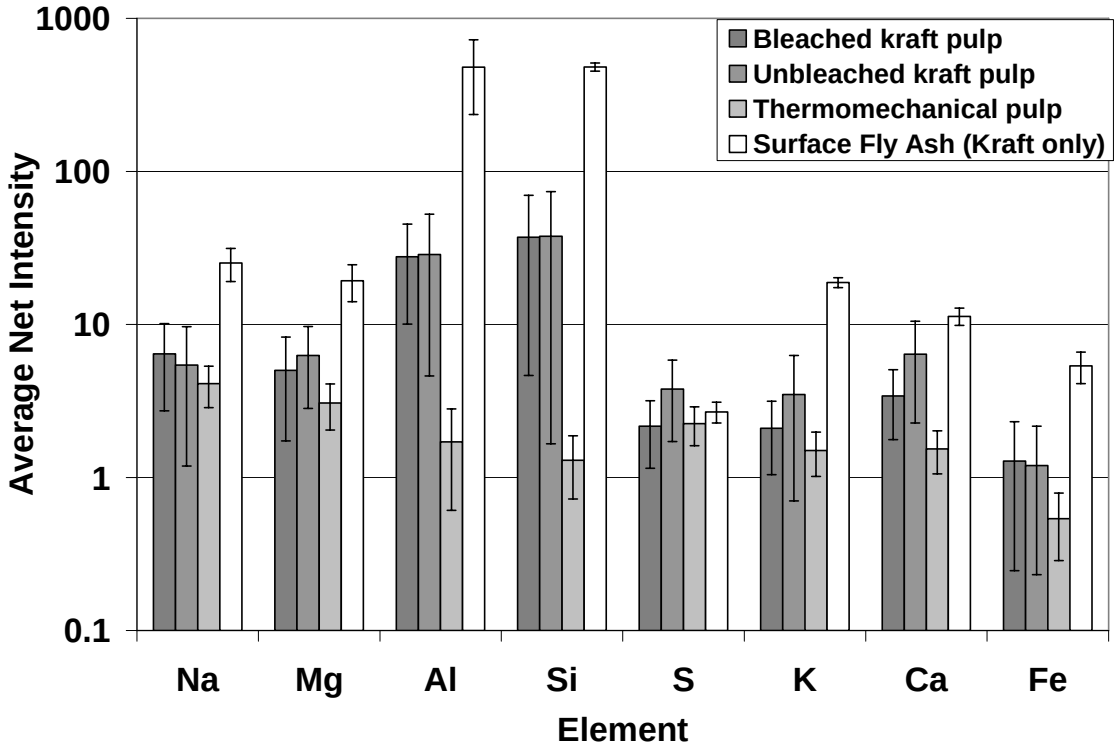

Figure 4-26. ESEM EDS average elemental net intensity for fibers prior to mixing.

Furthermore, dimensional changes during wetting and drying were observed for the kraft and TMP fibers. As seen in Figure 4-27, the apparent dimensional changes in TMP fibers were much less than that of kraft fibers (Figure 4-28). The average TMP fiber lateral swelling was approximately 10% compared to 135% for the kraft fibers. It should also be noted that TMP fiber swelling resulted in an apparent "straightening" of the fibers, whereas kraft fiber swelling was primarily observed as an increase in the lateral fiber dimension. These differences in dimensional stability are primarily due to the fiber lignin content [Nanko *et al.*, 1991]. Lignin stiffens the fiber cell wall by filling the spaces between the cellulose microfibrils improving dimensional stability, albeit at

the sacrifice of fiber tensile strength. Typically, unbleached and bleached kraft pulp contains 3-8% and 0-1% lignin by mass, respectively, while TMP fibers contain 25-31% lignin [Stenius, 2000].

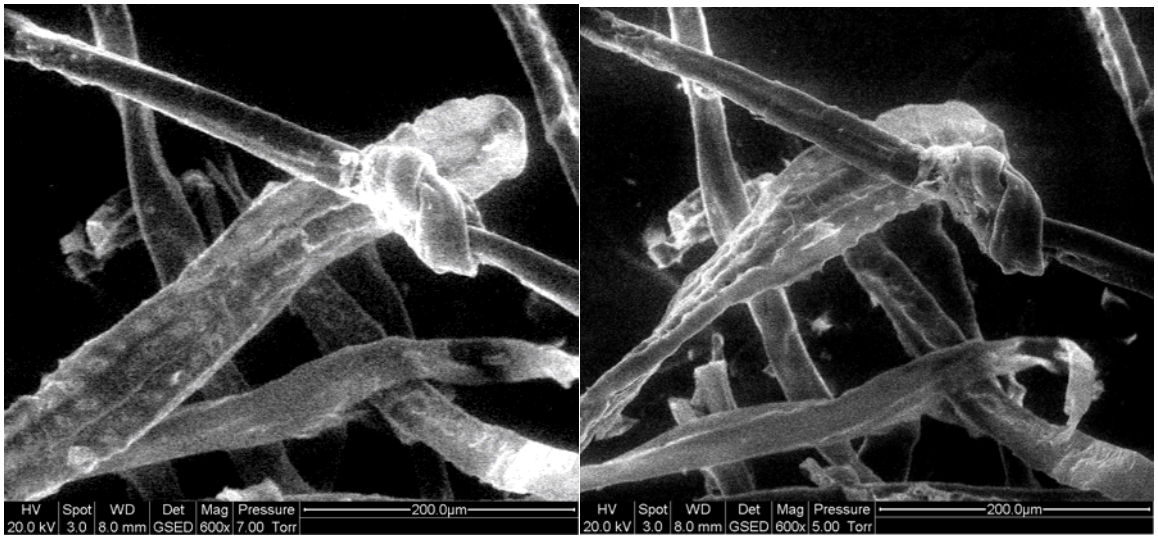

(a) (b)

Figure 4-27. ESEM micrographs of TMP fiber dimensional change capacity. (a) After 30 minutes at 100% RH. (b) After 5 minutes at 10% RH.

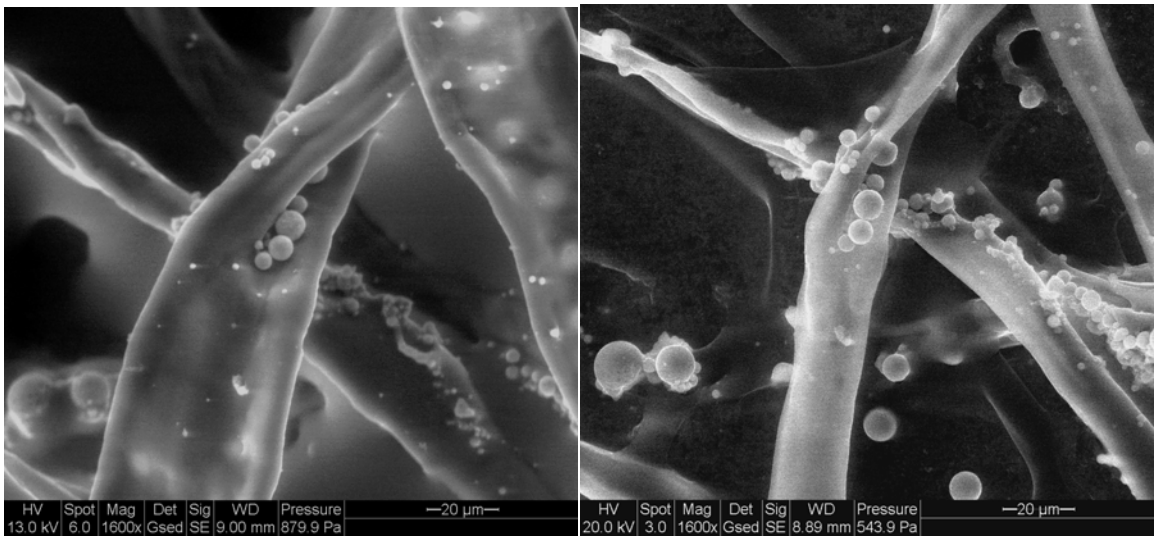

(a) (b)

Figure 4-28. ESEM micrographs of kraft pulp fiber dimensional change capacity. (a) After 30 minutes at 100% RH. (b) After 5 minutes at 10% RH.

4.2.2 Matrix Composition

The composition of C-S-H in the matrix was determined to investigate any changes in the chemical composition during wet/dry cycling. From BSE EDS, Si/Ca in the C-S-H was determined to be 0.520±0.031 both prior to and after wet/dry cycling. The determined ratio falls within the range of previously reported data [Taylor, 1997]. In addition, C-S-H was assumed to have substituted and/or absorbed some Al^{+3} for Si^{+4} and adsorbed some sulfur [Richardson, 1999]. For cement pastes cured at room temperature, Al/Ca and S/Ca trace compositions have been found to range from 0.04-0.06 and 0.01-0.04, respectively, for C-S-H [Richardson and Groves, 1993; Bonen and Diamond, 1994]. Prior to cycling, Al/Ca and S/Ca were determined to be 0.0788±0.0165 and

0.0389±0.0118, respectively. After 25 wet/dry cycles, these ratios were 0.0693±0.0145 and 0.0306±0.0101, respectively. However, no definitive conclusion can be drawn concerning any desorption due to the ranges of these determined values. It should be noted that the determined ratios of Al to Ca are greater than previously reported. This may indicate that an Al-rich product, presumably an AFm phase such as C_4AH_x, is intermixed in the matrix.

4.2.3 Composite Microstructure Prior to Wet/Dry Cycling

EDS spot analyses for samples not exposed to wet/dry cycling can be seen in Figures 4-29 and 4-30. Figure 4-29 indicates that the dominant phases present on all fiber surfaces are typical of cement matrices: $Ca(OH)_2$, C-S-H, and AFm/AFt phases.

The unbleached kraft pulp fibers appear to contain higher levels of the AFm/AFt phase than the other two fiber types. As for Figure 4-29, it appears that the unbleached kraft fibers contain small amounts of ettringite (an AFt phase) on their fiber surface. The bleached fibers appear to contain both monosulfate (an AFm phase) and ettringite phases. The TMP fibers contain the lowest amount of monosulfate/ettringite and appear to primarily contain $Ca(OH)_2$ and C-S-H on the fiber surface. During fiber pull-out, prior to initial drying, the observed hydration products are assumed to be indicative of the surrounding interface transition zone matrix composition.

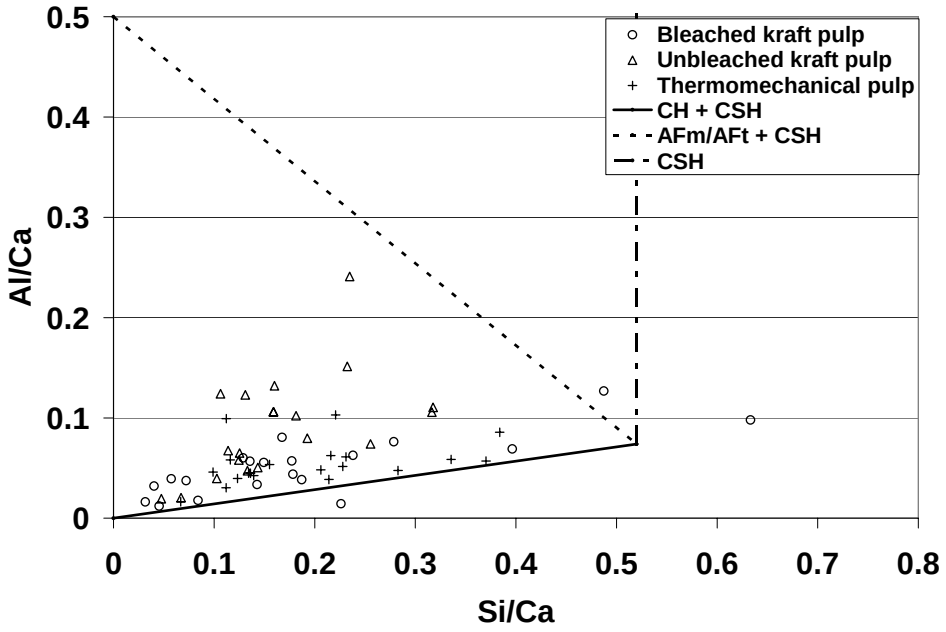

Figure 4-29. ESEM EDS analysis - average Al/Ca versus Si/Ca molar ratios after 0 cycles.

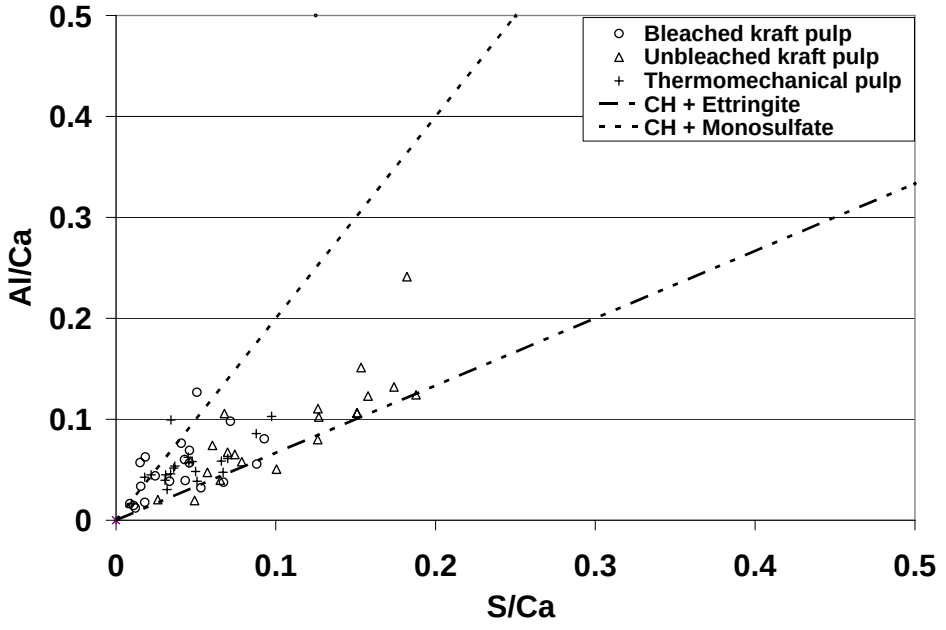

Figure 4-30. ESEM EDS analysis - average Al/Ca versus S/Ca molar ratios after 0 cycles.

4.2.4 Initial Fiber-Cement Debonding

It is believed that fiber dimensional changes during wet/dry cycling, as discussed previously, leads to fiber-cement debonding upon the initial drying cycle. ESEM observations also indicate that fiber interlayer debonding is also possible.

The debonding mode is most likely related to the degree of fiber-cement bonding. That is, if the particular fiber-cement bond is stronger than the fiber interlayer bonding, interlayer debonding would be expected, and vice versa. Due to a physically rougher surface as a result of lignin removal, bleached kraft fibers are expected to exhibit increased fiber-cement bonding and an increased tendency for fiber interlayer debonding, as compared to unbleached kraft fibers.

EDS measurements obtained on samples subjected to 1 wet/dry cycle are shown in Figures 4-31 and 4-32. For the kraft fibers, there are significant reductions in the amount of monosulfate, ettringite, and C-S-H present on the fiber surface, compared to Figures 4-29 and 4-30, prior to cycling. Thus, it appears that CH is the dominant hydration product on the fiber surface in this sample.

It should also be noted that increases in the Na/Ca and K/Ca molar ratios occurred after 1 wet/dry cycle. This appears to indicate that Na and K-rich products as well as $Ca(OH)_2$ have leached from the matrix and precipitated from the pore solution onto the kraft fiber surface. However, for the TMP fibers, there does not appear to be any observable changes in the relative abundance of alkali-rich products, C-S-H, and $Ca(OH)_2$ on the fiber surface.

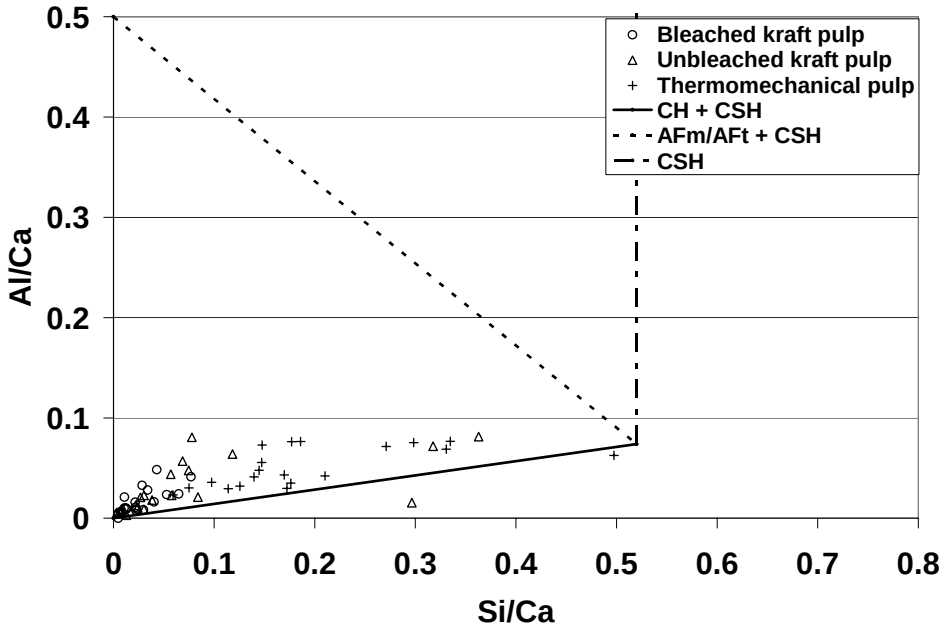

Figure 4-31. ESEM EDS analysis - average Al/Ca versus Si/Ca molar ratios after 1 cycle.

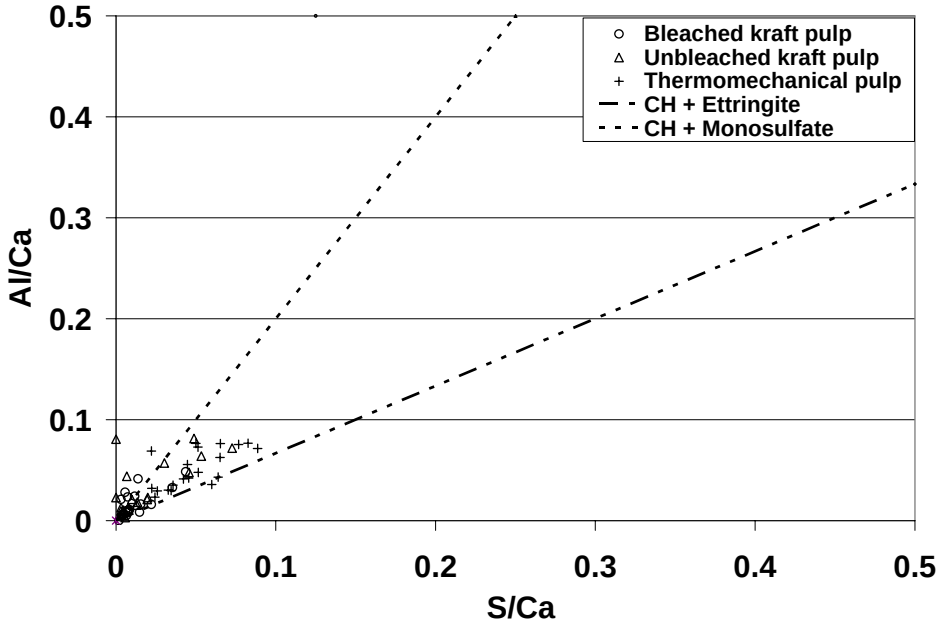

Figure 4-32. ESEM EDS analysis - average Al/Ca versus S/Ca molar ratios after 1 cycle.

4.2.5 Reprecipitation of Secondary Ettringite

After fiber-cement or fiber interlayer debonding, the new void space created around or within the fibers acts as a reservoir during subsequent wetting for the pore solution and a repository of free ions during subsequent wetting. As seen in Figures 4-33 and 4-34, significant changes in the chemical composition of the fiber surface are apparent after 2 wet/dry cycles compared to that after 0 and 1 wet/dry cycle. As seen in these figures, there are noticeable increases in the Al/Ca and S/Ca ratios and decreases in Si/Ca for both kraft fiber types.

Figure 4-34 definitively indicates the presence of ettringite on the surface of the kraft fibers. Ettringite appears to be reprecipitating in the void space created at the former fiber-cement interface. Again, there does not appear to be any observable change in TMP fiber surface chemistry. Secondary ettringite formation appears to minimize further fiber-cement debonding, as indicated by a leveling of the first crack strength beyond 2 cycles and peak strength beyond 5 cycles, as previously discussed.

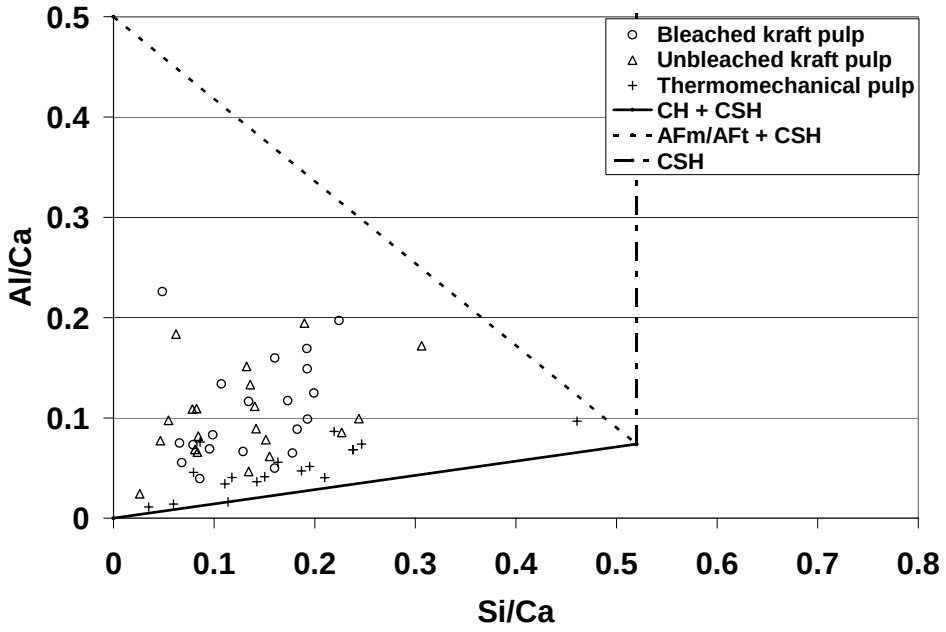

Figure 4-33. ESEM EDS analysis - average Al/Ca versus Si/Ca molar ratios after 2 cycles.

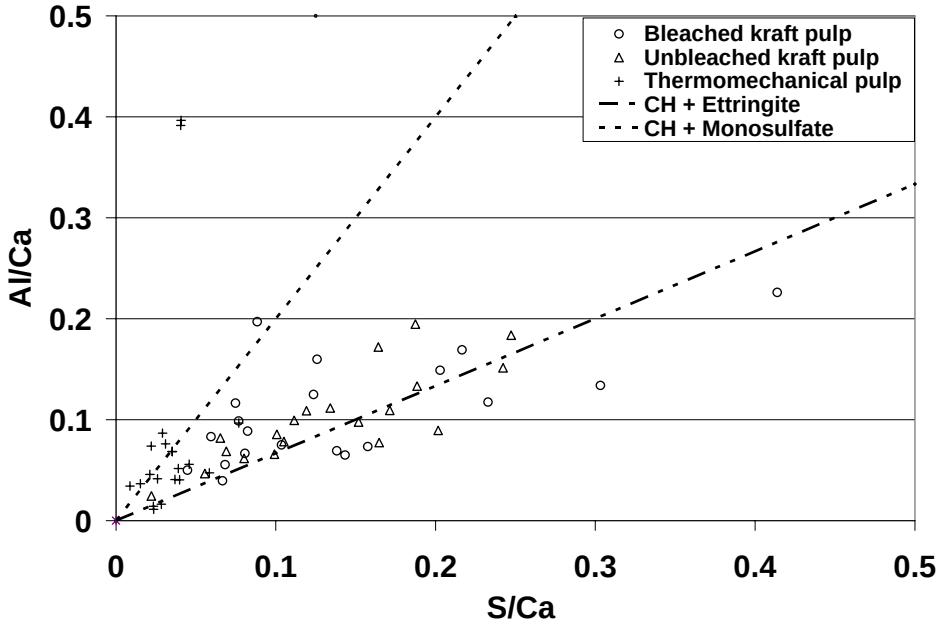

Figure 4-34. ESEM EDS analysis - average Al/Ca versus S/Ca molar ratios after 2 cycles.

Batic *et al.* [2000] have shown that the reprecipitation of ettringite in microcracks and voids of cement paste can occur under normal (*i.e.*, non-elevated temperatures) curing conditions. As discussed previously, desorption of sulfur and aluminum ions from C-S-H was not observed after 25 wet/dry cycles. Thus, the additional sulfate required for ettringite formation may be provided by (1) monosulfate and/or (2) ions in the pore solution. The AFm phases (monosulfate and C_4AH_x) are also most likely providing a source of Al, as Al^{+3} ions are not abundant in the pore solution [Ramlochan *et al.*, 2004].

Upon rewetting after the initial drying cycle, Ca^{+2} (primarily from $Ca(OH)_2$) and SO_4^{-2} ions in the pore solution, may react with aluminum provided by the AFm phases to form ettringite. Additionally, it is thought that leaching of sodium and potassium ions due to cycling (calcium ions are maintained due to limewater saturation) and the subsequent lowering of pore solution pH occurs within the first 2 wet/dry cycles. These aspects favor ettringite formation and the destabilization of monosulfate [Taylor *et al.*, 2001].

Figure 4-35 illustrates the formation of ettringite needle-like crystals near kraft fibers after 2 wet/dry cycles. Based on visual observation, the typical needle-like ettringite crystals only appear to form in locations of fiber interlayer debonding where the S1 fiber layer remained attached to the matrix. However, the needle-like crystals are not observed on all fiber surfaces (Figure 4-36), despite EDS spot analyses indicating the presence of ettringite.

Figure 4-35. ESEM micrographs of needle-like ettringite crystals around kraft pulp fibers after 2 wet/dry cycles.

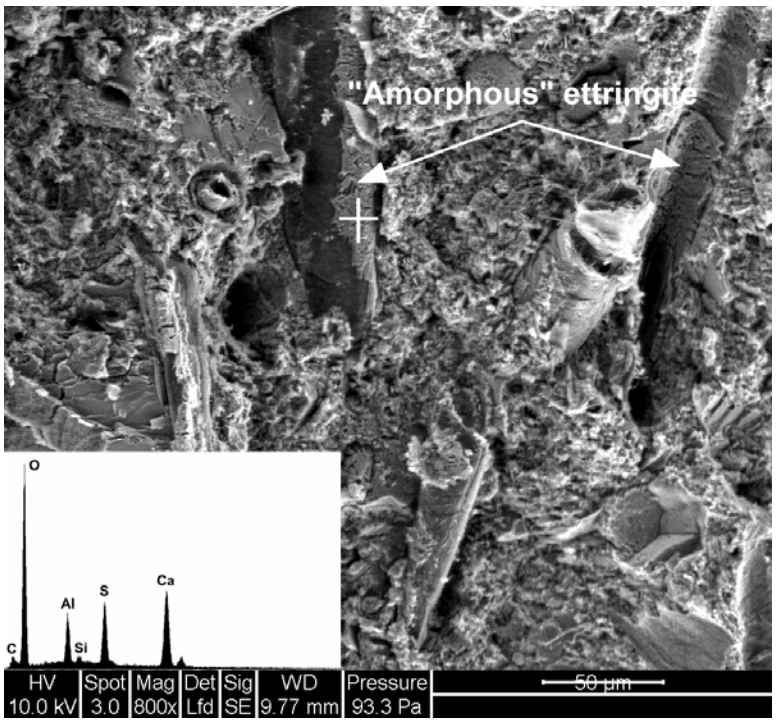

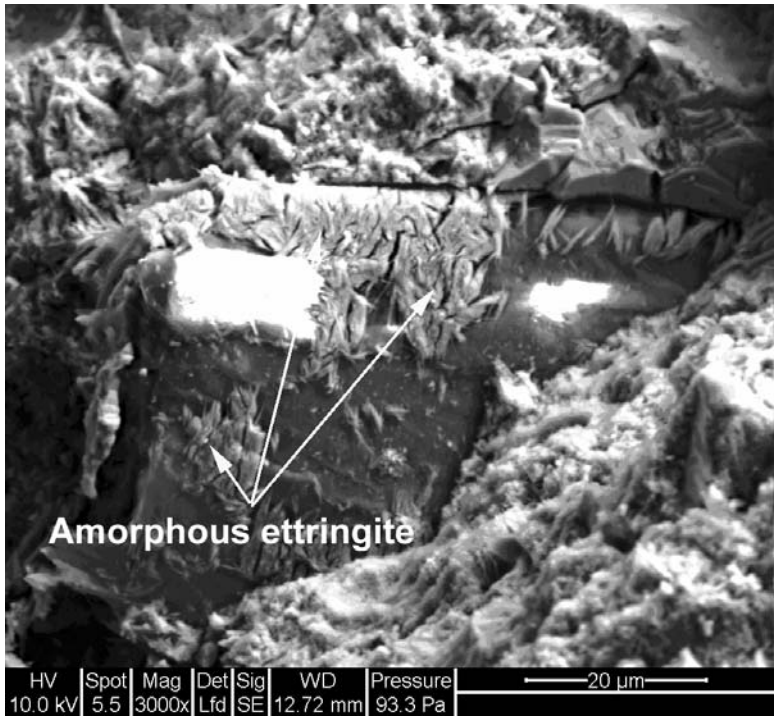

Figure 4-36. ESEM micrographs of amorphous / sheath-like ettringite around kraft pulp fibers after 2 wet/dry cycles.

It is also observed that ettringite is present in an apparently amorphous morphology, similar to ASR gel [Marusin, 1994], as seen in Figure 4-36 and confirmed by EDS. It is possible that ettringite crystals could be wrapping circumferentially around the fibers, appearing as a sheath-like form. However, for the purposes of simplifying this discussion, it will be referred to "apparently amorphous" ettringite

The form of ettringite reprecipitation appears to be dependent upon the fiber-cement debonding mechanism. Apparently amorphous ettringite appears to only form in the case of fiber-cement debonding. It was previously mentioned that needle-like crystals formed when fiber interlayer debonding was observed. In addition, the form of ettringite may also be inherently related to the available space for reprecipitation. Fiber interlayer debonding creates a space of up to 10-15 μm, while fiber-cement debonding appears to create a void space width of only a few microns.

Ettringite formation was also verified via chemical elemental mapping of polished samples. Figure 4-37 shows distinct rings of ettringite around several kraft pulp fibers after 2 wet/dry cycles. As for the TMP fibers, ettringite formation was not observed, even after 25 cycles as seen in Figure 4-38.

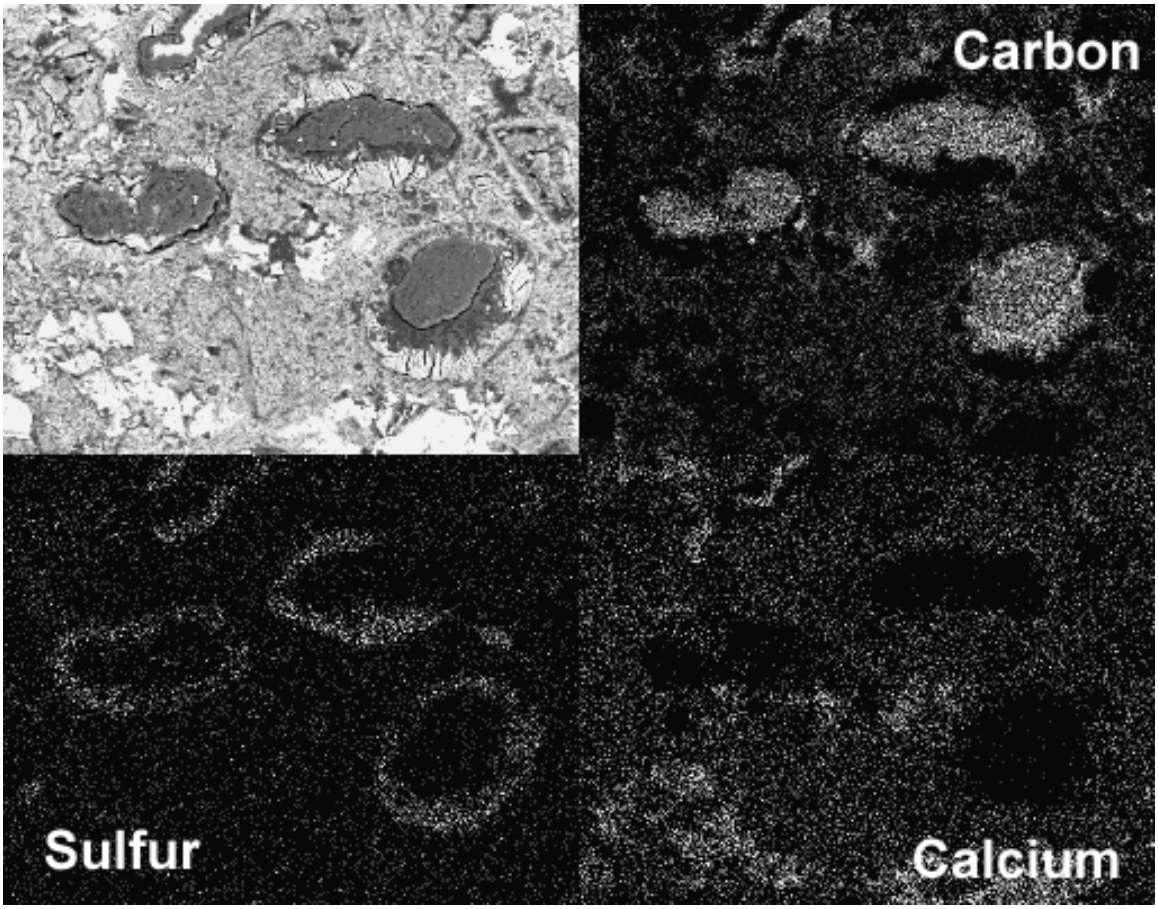

Figure 4-37. ESEM BSE chemical mapping of polished kraft pulp fiber composite after 2 wet/dry cycles (upper right: carbon, lower left: sulfur, lower right: calcium).

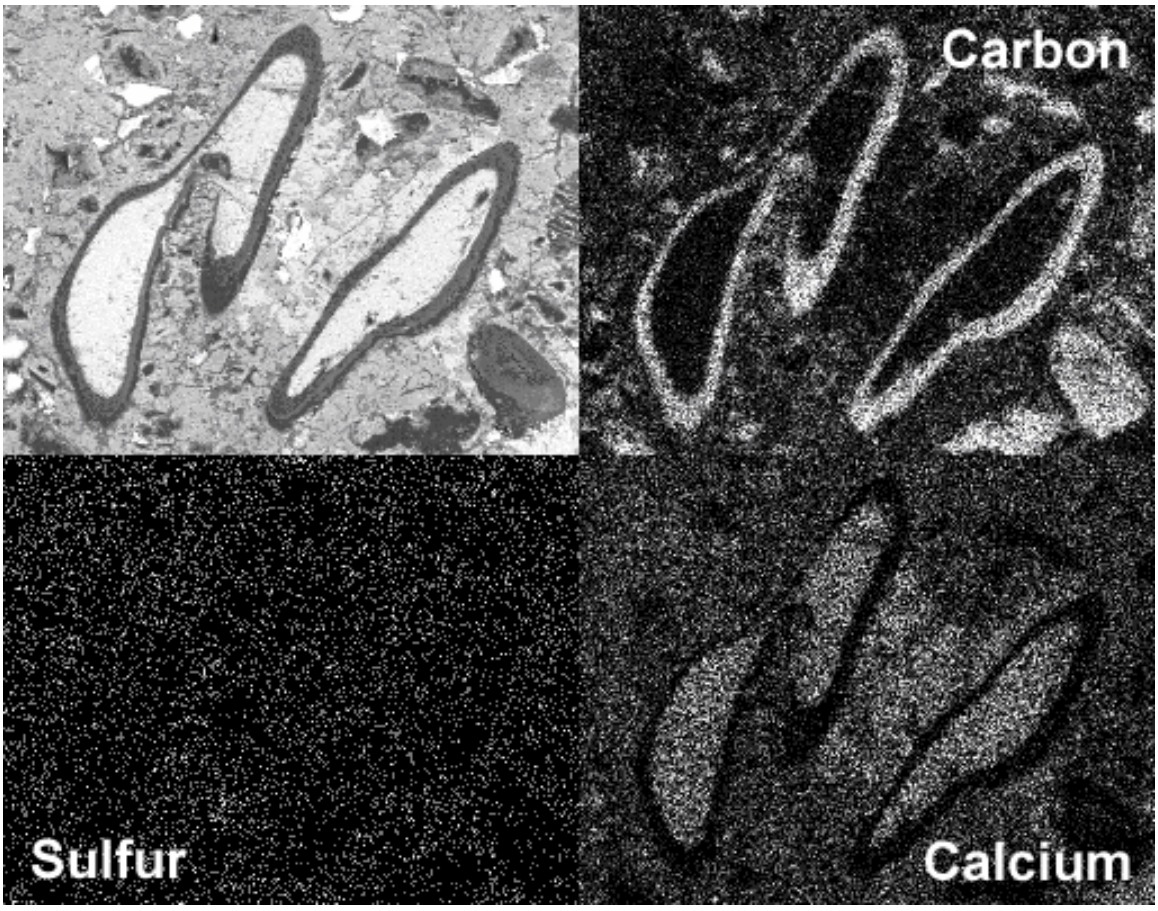

Figure 4-38. ESEM BSE chemical mapping of polished TMP fiber composite after 25 wet/dry cycles (upper right: carbon, lower left: sulfur, lower right: calcium).

In addition, no radial microcracking was observed around the kraft pulp fibers after 25 wet/dry cycles, as indicated in Figure 4-39. Thus, ettringite formation does not appear to be exerting any tensile stresses against the cement matrix. Since the pulp fibers are more compliable, ettringite formation only exerts pressure on the fiber, eventually restricting fiber swelling.

No apparent changes in the chemical composition of the fiber surface, as indicated by individual EDS data points, are observed after 5 (Figures 4-40 and 4-41) and 10 cycles (Figures 4-42 and 4-43), compared to that after 2 cycles. However, average molar ratios for Si/Ca and Al/Ca progressively decrease from 2 to 10 cycles for both kraft fiber types. At the same time, the S/Ca molar ratio remains constant over this wet/dry cycling range.

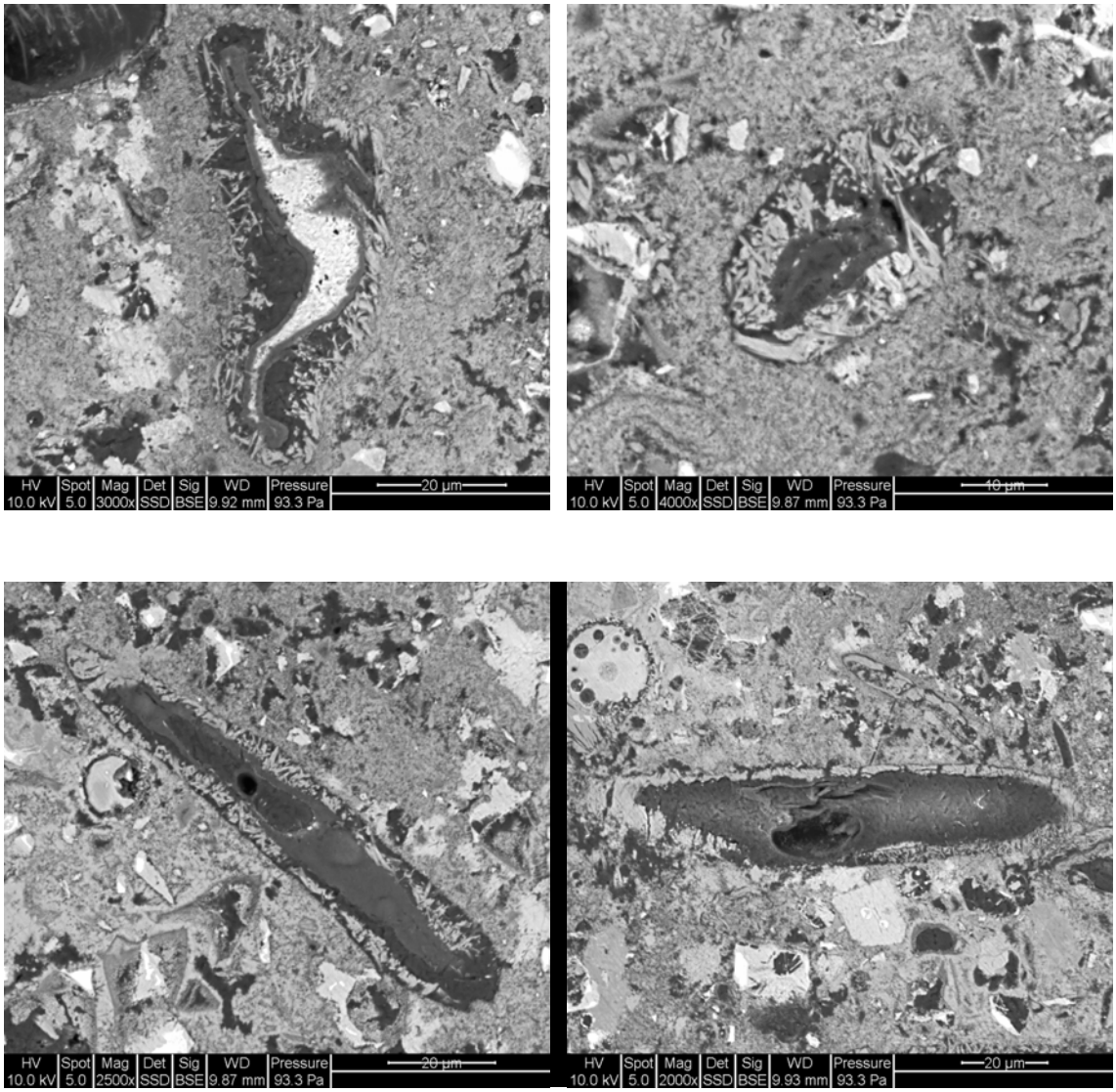

Figure 4-39. ESEM BSE micrographs of kraft pulp composites indicating absence of microcracking around fibers due to ettringite reprecipitation.

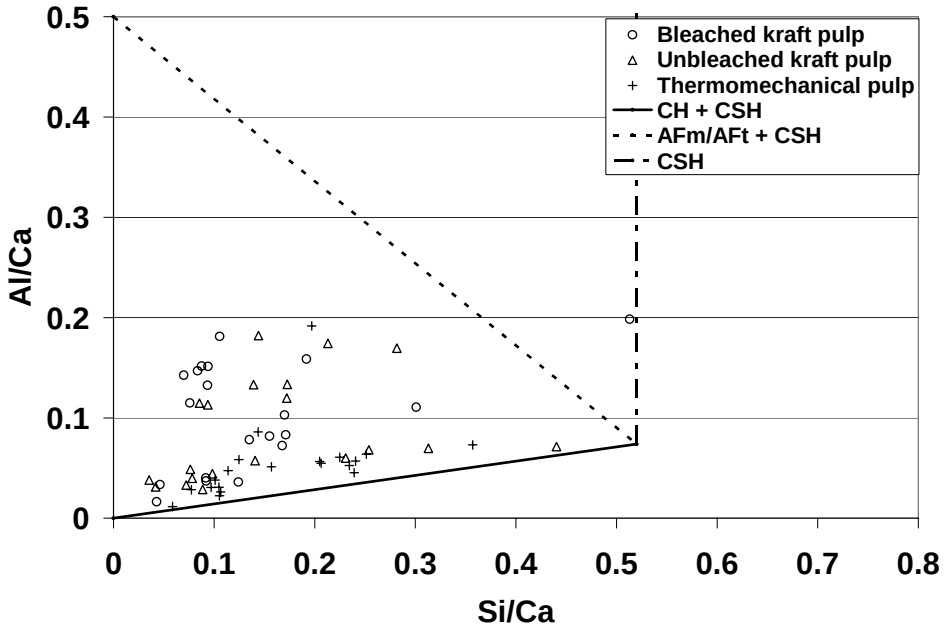

Figure 4-40. ESEM EDS analysis - average Al/Ca versus Si/Ca molar ratios after 5 cycles.

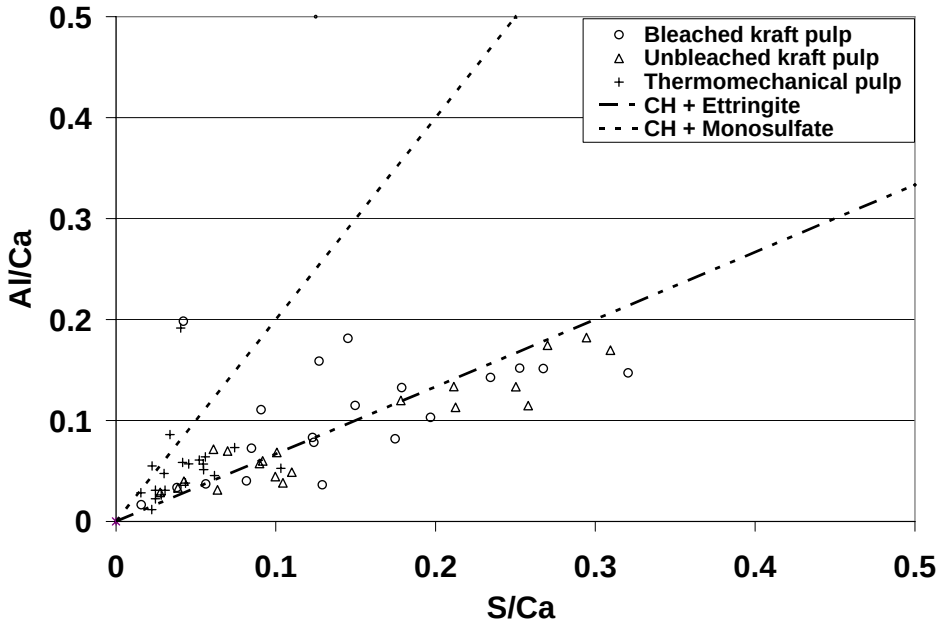

Figure 4-41. ESEM EDS analysis - average Al/Ca versus S/Ca molar ratios after 5 cycles.

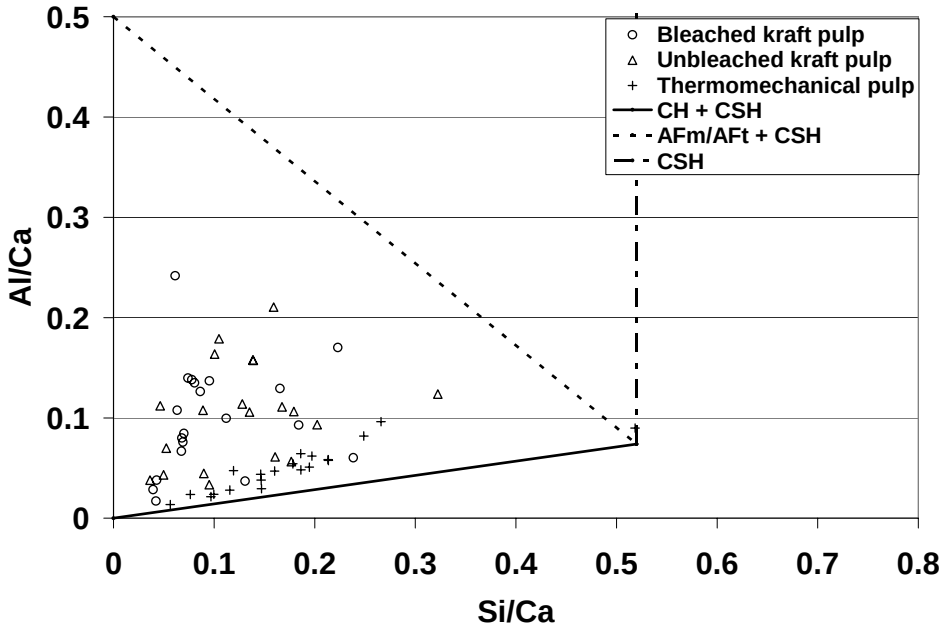

Figure 4-42. ESEM EDS analysis - average Al/Ca versus Si/Ca molar ratios after 10 cycles.

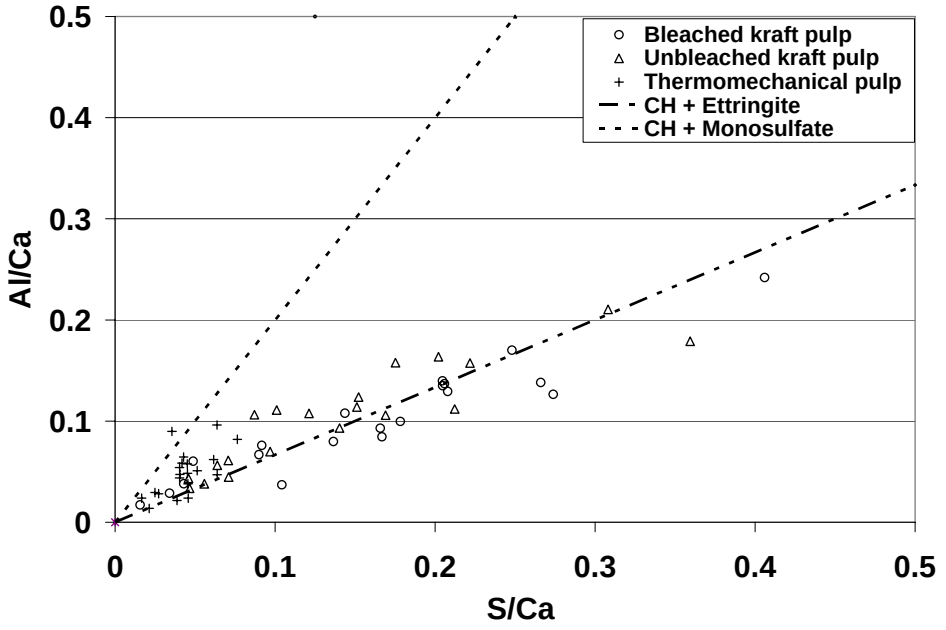

Figure 4-43. ESEM EDS analysis - average Al/Ca versus S/Ca molar ratios after 10 cycles.

4.2.6 Fiber Mineralization

After ettringite reprecipitates around the fibers, fiber swelling upon rewetting is expected to be prevented entirely or to a great extent. During subsequent drying, fiber shrinkage is, then, also reduced. Thus, the driving force for pore solution expulsion is minimized. That is, the pore solution will reside within the fiber for a longer period of time. Therefore, the pore solution may diffuse from the lumen through the cell wall, as opposed to primarily exiting through the fiber ends and pits. This movement of pore solution through the fiber cell wall results in a deposition of hydration products, likely $Ca(OH)_2$.

It was previously proposed (Section 4.1) that fiber mineralization may not occur until after 10 wet/dry cycles as indicated by slight increases in flexural strength. EDS measurements of fiber surfaces exposed to 15 and 25 wet/dry cycles (Figures 4-44 – 4-47) indicate increasing amounts of $Ca(OH)_2$. Additional semi-quantitative EDS measurements of $Ca(OH)_2$ abundances with wet/dry cycling will be performed to further substantiate this hypothesis.

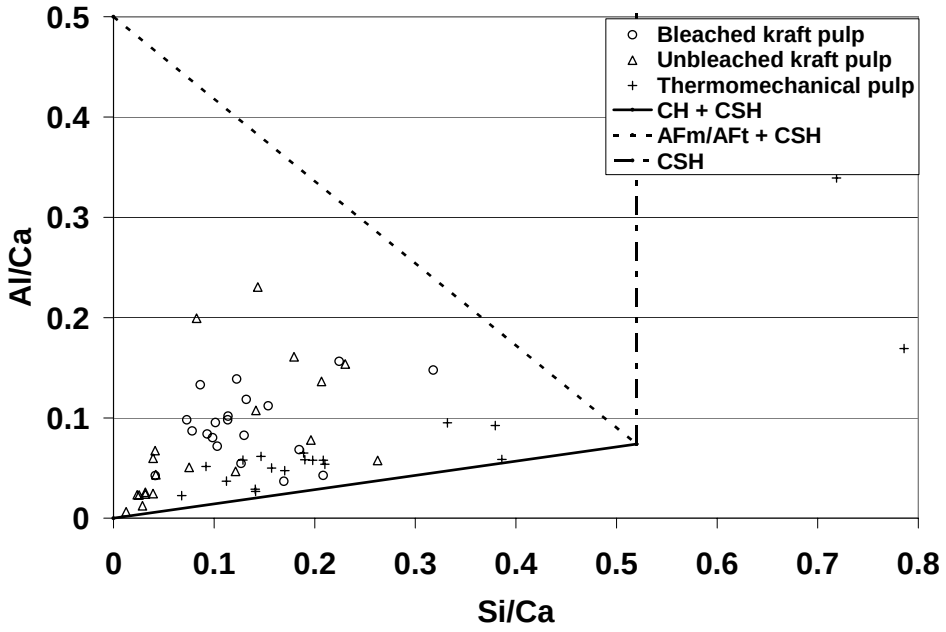

Figure 4-44. ESEM EDS analysis - average Al/Ca versus Si/Ca molar ratios after 15 cycles.

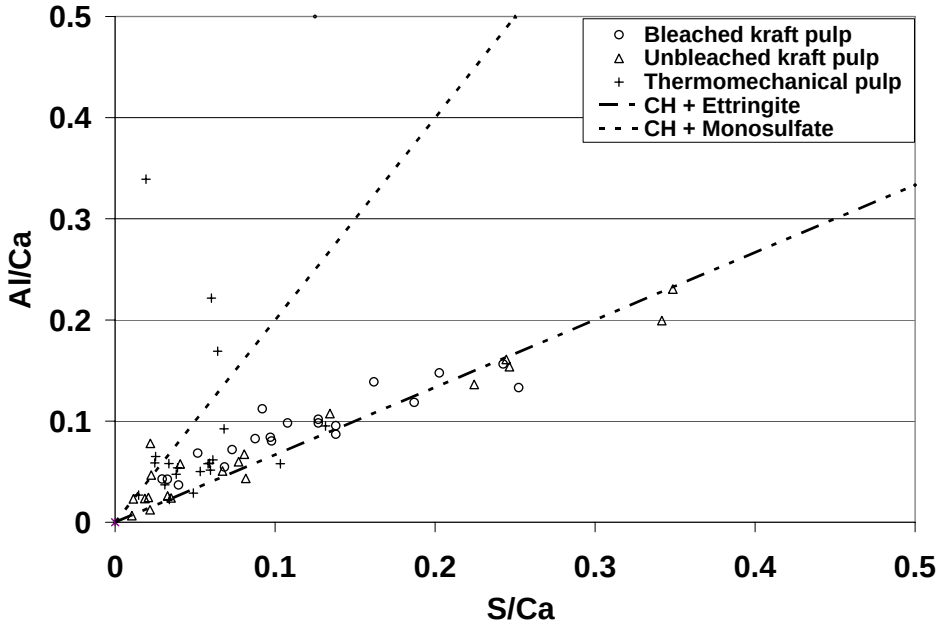

Figure 4-45. ESEM EDS analysis - average Al/Ca versus S/Ca molar ratios after 15 cycles.

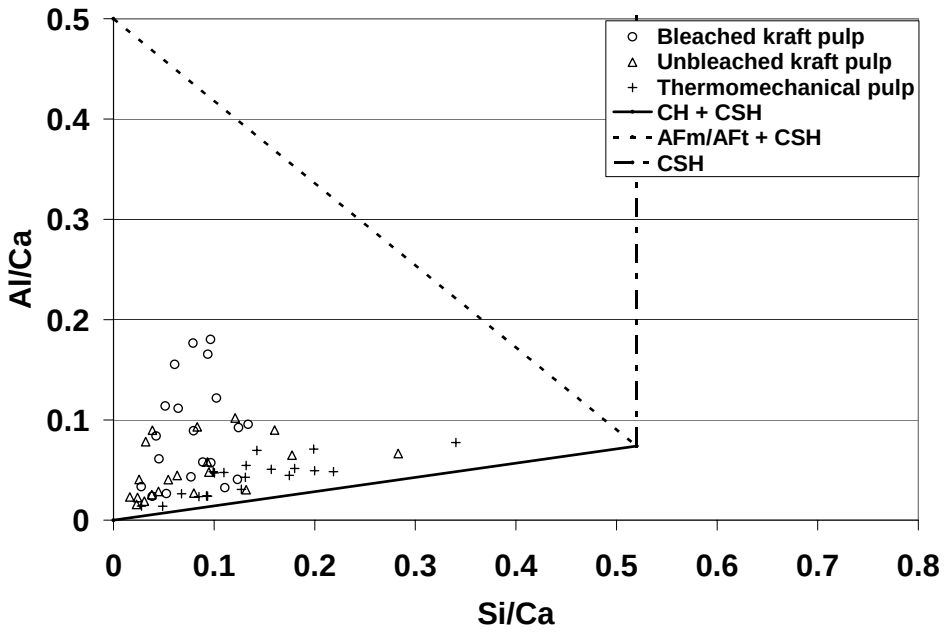

Figure 4-46. ESEM EDS analysis - average Al/Ca versus Si/Ca molar ratios after 25 cycles.

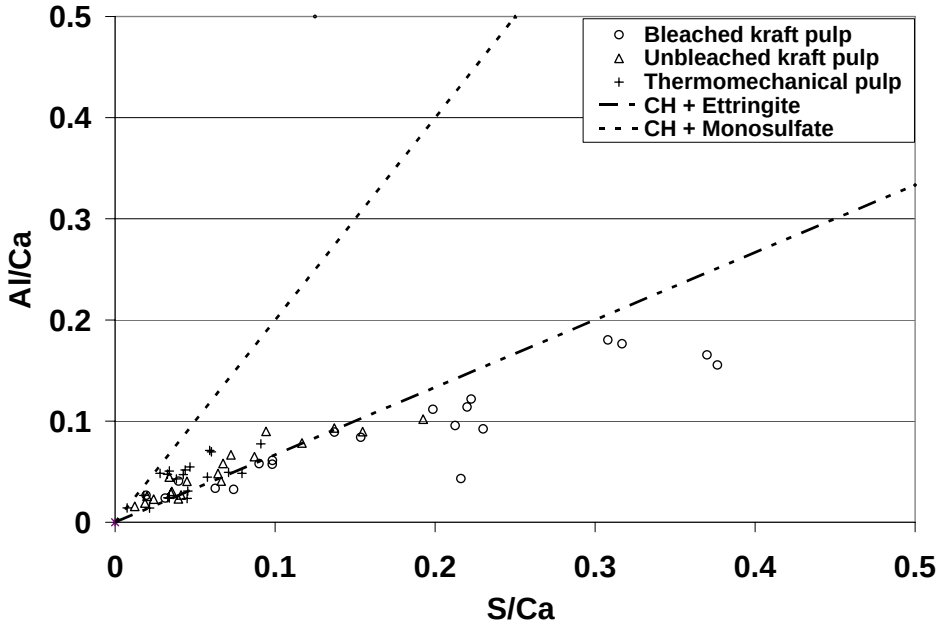

Figure 4-47. ESEM EDS analysis - average Al/Ca versus S/Ca molar ratios after 25 cycles.

Additional ESEM observations were made during *in situ* wetting and drying of composite fracture surface to observe the swelling behavior and extent of fiber mineralization of kraft pulp fibers after 25 wet/dry cycles. It can be seen in Figure 4-48 that localized kraft fiber swelling is apparent, but the overall fiber swelling is restricted. Complete fiber mineralization (*i.e.*, no fiber swelling) by the reprecipitation of $Ca(OH)_2$ in the fiber cell wall is also apparent in most kraft fibers. Figure 4-49 shows a completely mineralized kraft fiber and a respective EDS spectrum of the fiber surface. However, levels of organic materials remain relatively high, indicating that replacement of organic with inorganic components is not occurring. Instead, it is believed that $Ca(OH)_2$ reprecipitates within the fiber wall by filling the space between the cellulose microfibrils. This space would have been occupied by lignin prior to kraft pulping.

In TMP fibers, the space within the fiber cell wall is occupied by lignin, as it is not removed during thermomechanical pulping. TMP fibers, after 25 cycles (Figure 4-50), exhibit minimal levels of calcium on the fiber surface and/or in the fiber cell wall as evidenced by the EDS spectrum. However, TMP fibers do show evidence of $Ca(OH)_2$ formation within the fiber lumen. This is particularly evident in Figure 4-50, where calcium is the predominant element observed within the fiber lumen. Thus, it is proposed that lignin within the TMP fiber cell wall acts as a barrier to pore solution ingress and by its very presence prevents reprecipitation of mineral phases within the fiber cell wall, minimizing fiber mineralization.

Calcium hydroxide may be accumulating in the TMP fiber lumen due to the superior dimensional stability of TMP fibers. Since TMP fibers exhibit negligible fiber shrinkage upon drying, the driving force for pore solution expulsion is minimized. This is

similar to what has been proposed concerning ettringite reprecipitation around kraft fibers preventing subsequent fiber swelling/shrinkage. However, in the case of kraft fibers during latter drying cycles (after ettringite formation), the pore solution may filter through the fiber, depositing CH within the fiber cell wall. Pore solution movement through the TMP fiber cell wall is minimized due to lignin, leading to the accumulation of CH within the fiber lumen.

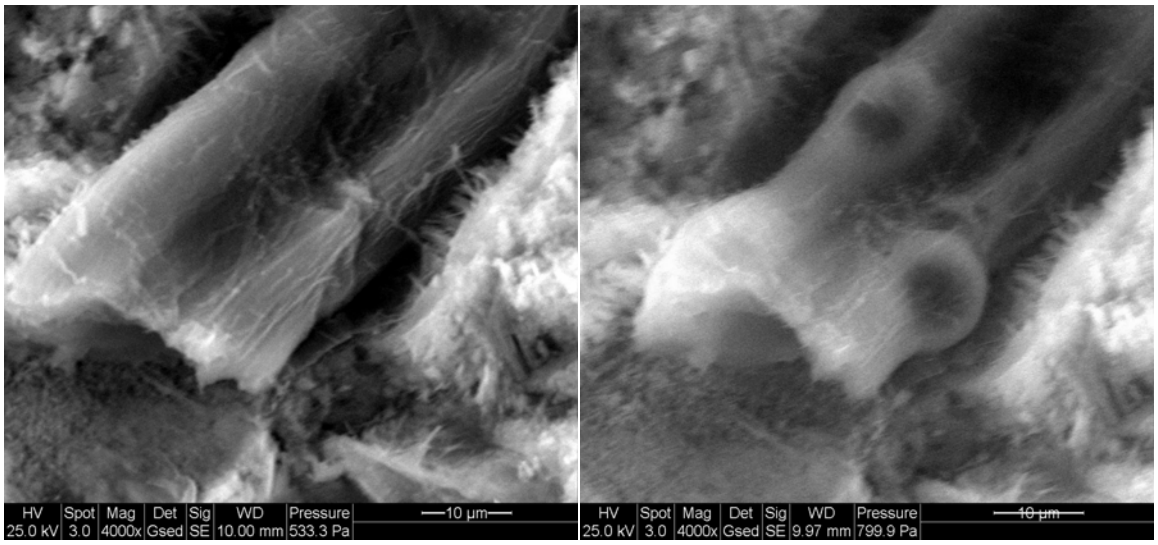

(a) (b)

Figure 4-48. ESEM micrograph of kraft pulp fiber after 25 wet/dry cycles. (a) Prior to saturation (10% RH). (b) After 1 hour at 98% RH.

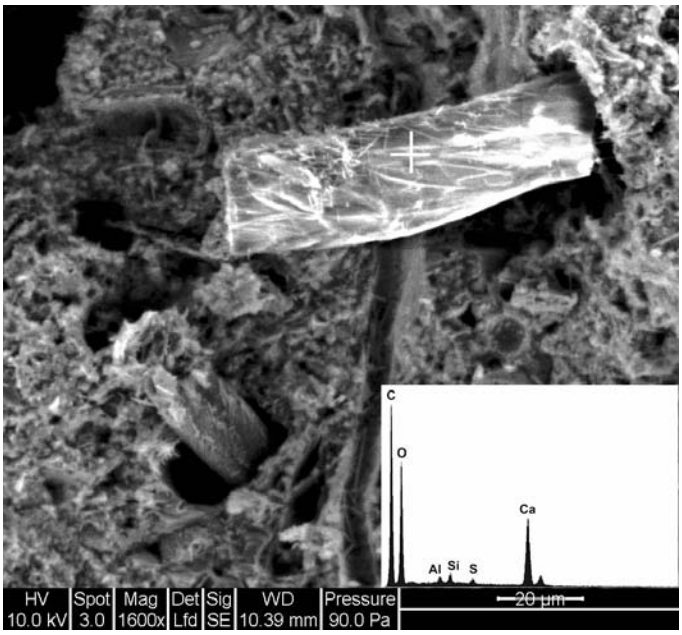

Figure 4-49. ESEM micrograph of kraft fiber after 25 wet/dry cycles.

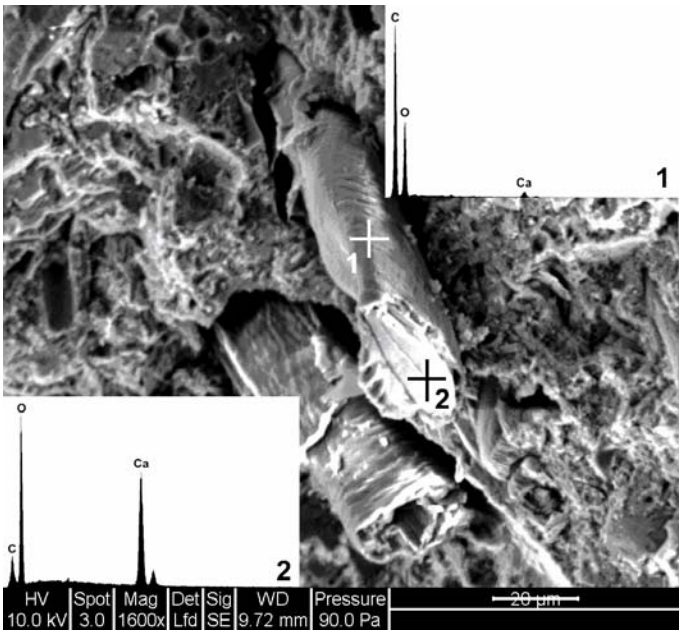

Figure 4-50. ESEM micrograph of TMP fiber after 25 wet/dry cycles.

CHAPTER 5

WET/DRY CYCLING – MATRIX MODIFICATIONS

In order to develop methods for mitigating pulp-fiber cement composite degradation, it was necessary to develop a degradation mechanism that correlates with the observed mechanical testing results. Thus, in the previous chapter a three-part progressive degradation model characterizing degradation due to wet/dry cycling in cast-in-place kraft pulp and thermomechanical pulp (TMP) fiber-cement composites was proposed. This model consists of (1) initial fiber-cement debonding, (2) reprecipitation of secondary ettringite within the void space at the former fiber-cement interface (kraft fibers only), and (3) fiber embrittlement due to reprecipitation of calcium hydroxide within the fiber lumen and/or fiber cell wall.

In order to mitigate fiber-cement composite degradation, there are two avenues for composite modifications: (1) fiber modifications and (2) matrix modifications. Modifications to the pulp fibers have been used in order to minimize fiber-cement debonding and/or moisture migration around and through the fibers during wetting and drying. Fiber modifications have included fiber impregnation [Gram, 1983], fiber treatments [Ziraba *et al.*, 1985], and fiber fibrillation. Modifications affecting fiber chemical composition and fiber dimensional stability were discussed in Chapter 4. Matrix modifications, the focus of the work presented here, have included the use of high alumina cement [Gram, 1983], matrix sealants [Canovas *et al.*, 1992], and supplementary

cementitious materials (SCMs) as a partial replacement for portland cement. These modifications have been employed in order to reduce pore solution pH and/or composite permeability. From the existing literature, only silica fume [Gram, 1983; Bergstrom and Gram, 1984; Tolêdo Filho *et al.*, 2003], slag [Gram, 1983; Tolêdo Filho *et al.*, 2003], and rice husk ash [Ziraba *et al.*, 1985] have been evaluated for their effect on composite durability.

Despite scattered mechanical testing results for composites containing supplementary cementitious materials, there has been no comprehensive evaluation of the potential benefits of this matrix modification technique. Therefore, the objective of this phase of the research was to evaluate the mechanical performance of kraft pulp fiber-cement composites containing SCMs after exposure to wet/dry cycling. Ternary and quaternary SCM blends were also investigated in order to optimize cost and performance. In addition, the effect of composite permeability due to changing the water-to-cement ratio has also been evaluated.

5.1 Effect of Water-to-Cement Ratio (Permeability)

The effect of changing the water-to-cement ratio was evaluated to assess permeability changes on composite degradation. In other words, do decreases in composite permeability affect the movement of pore solution ions that may minimize certain degradation processes as discussed in Chapter 4? This particular aspect is important is isolate as SCMs (Section 5.2) have a similar effect on permeability in addition to changing the pore solution chemistry and matrix microstructure.

5.1.1 Kraft Pulp Fiber-Cement Composites

Results for various water-to-cement ratios ranging from 0.50 to 0.70 with kraft fiber reinforcement are shown in Figures 5-1 – 5-3. It can be seen that, as expected, after 0 cycles, the water-to-cement ratio of 0.50 composite exhibited higher first crack and peak strengths, as compared to the higher water-to-cement ratio composites. As the number of cycles increased, it appears that the differences in strength between the water-to-cement ratio of 0.60 and 0.70 composites are negligible. However, the water-to-cement ratio of 0.50 composite strengths appear to exhibit a slower progression of degradation. Though, by 25 wet/dry cycles, there were no longer any observable differences. In terms of post-cracking toughness, there were no significant differences between any of the water-to-cement ratios evaluated over the range of wet/dry cycling investigated. Therefore, within this range of water-to-cement ratios, composite permeability may not play a significant role in composite durability.

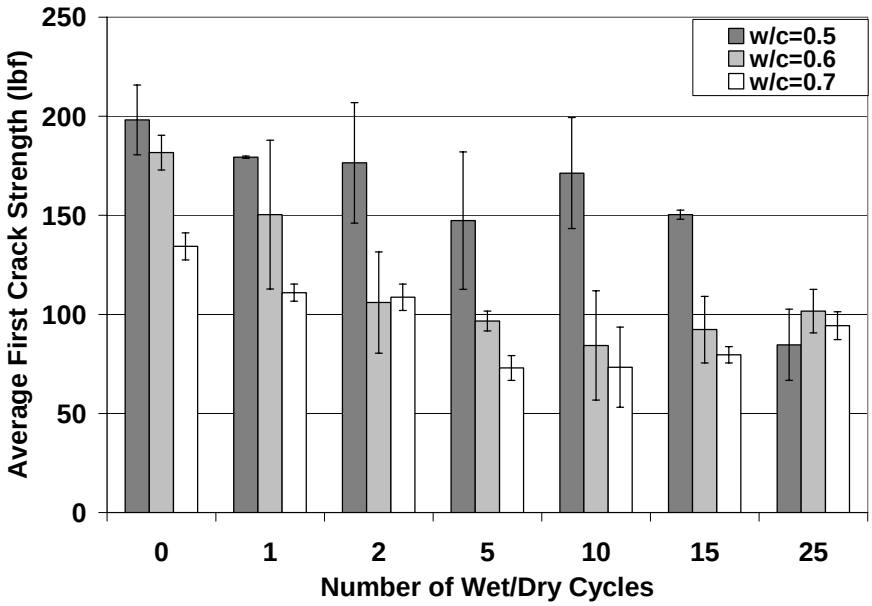

Figure 5-1. Flexural testing results for bleached kraft pulp fiber-cement composites with varying water-to-cement ratios. Average first crack strength (MPa) versus number of cycles.

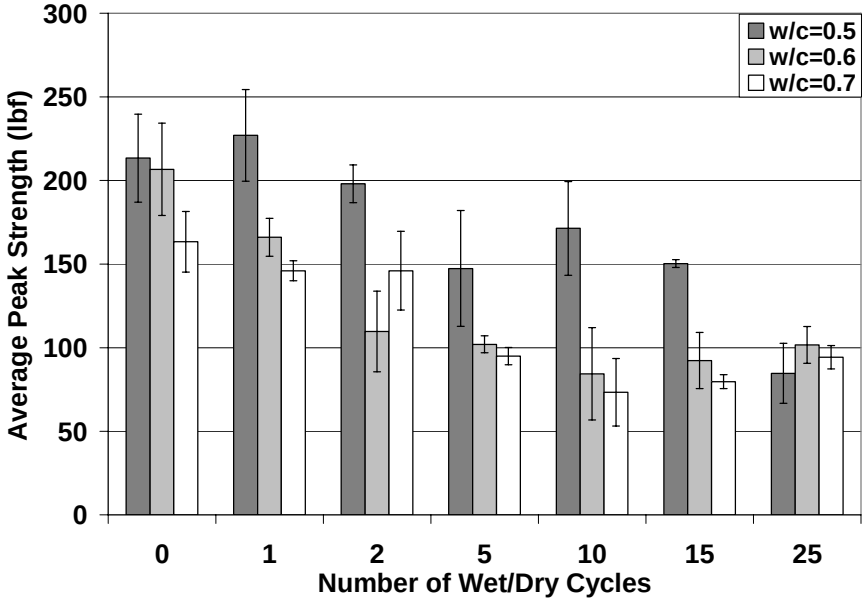

Figure 5-2. Flexural testing results for bleached kraft pulp fiber-cement composites with varying water-to-cement ratios. Average peak strength (MPa) versus number of cycles.

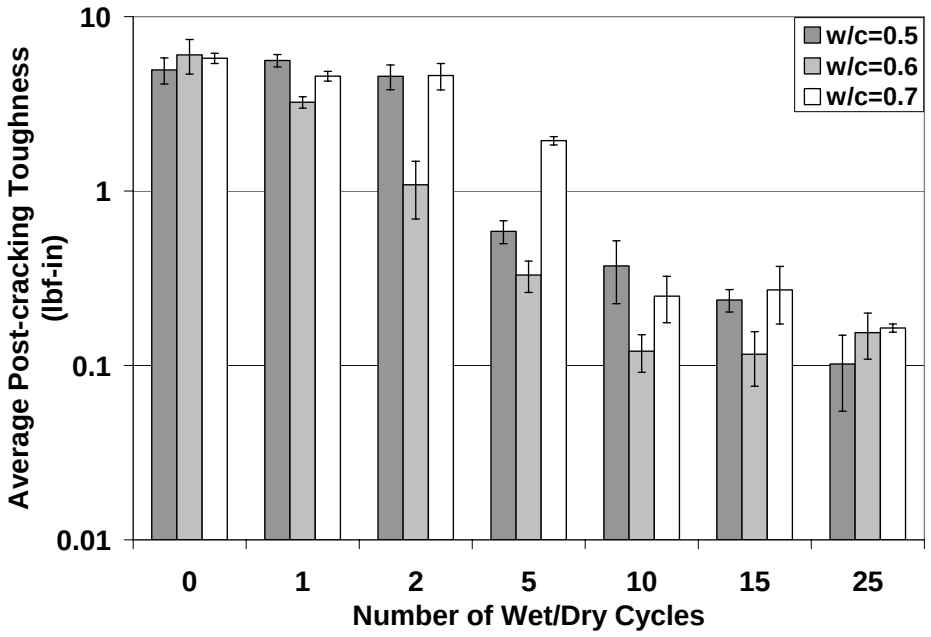

Figure 5-3. Flexural testing results for bleached kraft pulp fiber-cement composites with varying water-to-cement ratios. Average post-cracking toughness (MPa-mm) versus number of cycles.

5.1.2 TMP Fiber-Cement Composites

Thermomechanical pulp (TMP) fibers, which have a shorter fiber length and stiffer cell wall, have also been evaluated. These characteristics generally allow TMP to be used at higher fiber volumes than kraft pulp for a given water-to-cement ratio, due to less fiber clumping. It was found that a minimum water-to-cement ratio of 0.26 was easily achieved while maintaining adequate fiber dispersion. A maximum water-to cement ratio of 0.60 was used.

Flexural results in Figures 5-4 and 5-5, show that below a water-to-cement ratio of 0.40, composite permeability does appear to affect post-cracking toughness durability.

Though the lower water-to-cement ratio composites exhibit minimal toughness prior to cycling, these composites show smaller relative losses in toughness after 25 cycles, than samples with a water-to-cement ratio greater than 0.40. Thus, there appears to be a threshold water-to-cement ratio above which the composite post-cracking toughness durability does not change. Below this threshold, lower water-to-cement ratios appear to lead to improved toughness with wet/dry cycling. This trend was not apparent with kraft pulp fiber composites as the water-to-cement ratio investigated using kraft fibers appears to be above this threshold.

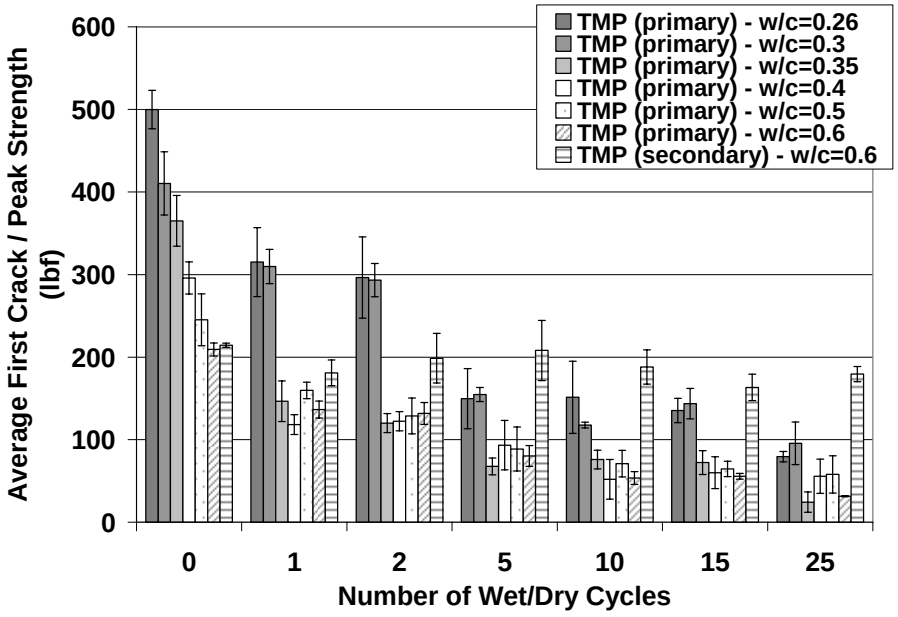

Figure 5-4. Flexural testing results for TMP fiber-cement composites with varying water-to-cement ratios. Average first crack strength (MPa) versus number of cycles.

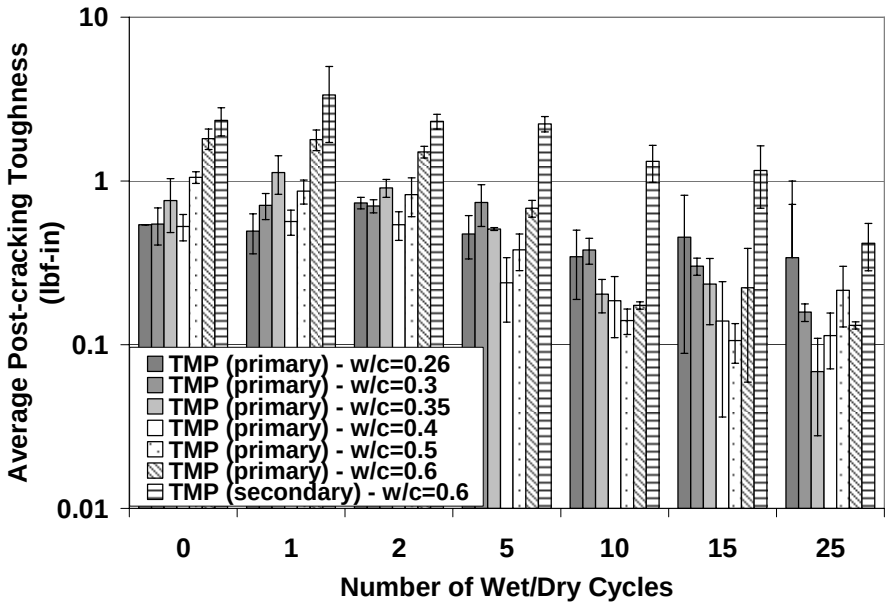

Figure 5-5. Flexural testing results for TMP fiber-cement composites with varying water-to-cement ratios. Average post-cracking toughness (MPa-mm) versus number of cycles.

5.2 Effect of Supplementary Cementitious Materials (SCMs)

It should be noted that all specimens containing SCMs were cured for a minimum of 28 days prior to wet/dry cycling commenced. Thus, the slower rates of the pozzolanic or latent hydraulic reactions can be considered insignificant since these reactions achieve equivalent or higher degree of hydration compared to a pure portland cement paste.

5.2.1 Mechanical Testing

5.2.1.1 Silica Fume (SF) Replacement

Blended SF-cement composites were tested at cement weight replacement values of 10, 30, and 50%. At replacement values above 10%, workability was significantly degraded due to the incorporation of silica fume. Though adequate for academic purposes, 10% silica fume is typically the maximum amount used in the concrete industry. Thus, ternary and quaternary blends containing 10% silica fume will be discussed in subsequent sections.

Prior to wet/dry cycling, SF composite first crack strengths (Figure 5-6) were similar to that of the control. After the first wet/dry cycle, a decrease in first crack strength was observed for all composites. As cycling progressed, first crack strengths remained relatively unchanged for all SF composites, up to 10 cycles. Beyond 10 cycles, the 10% SF first crack strength decreased to a level comparable to the control, while the 30 and 50% SF composite first crack strengths continued to remain unchanged. After 25 cycles, the 30 and 50% SF composites exhibited 60.9% and 86.2% higher first crack strength, respectively, compared to the control.

In terms of peak strength (Figure 5-7), there was a gradual progression of degradation for all SF composites, up to 5 cycles. Beyond 5 cycles, the 30 and 50% SF composites exhibited no additional mechanical property losses. However, the 10% SF composite continued to show losses in peak strength. By 25 cycles, the differences between the 10% SF composite and the control were negligible. After 25 cycles, the 30

and 50% SF composite peak strength were 200.4% and 159.4% greater, respectively, than the control.

Without wet/dry exposure, post-cracking toughness values for the SF composites (Figure 5-8), except at 50% replacement, were 35.4% and 27.4% lower for the 10 and 30% replacements than the control, respectively. The 50% replacement exhibited similar toughness as the control. After 1 wet/dry cycle, as decreases in first crack strength were seen, post-cracking toughness increased for the SF composites. After this initial increase, the rate of SF composite degradation was similar to the strength trends. That is, the 10% SF composite exhibited a gradual degradation, while the 30 and 50% SF composites did not exhibit any further observable changes. After 25 cycles, the 10% SF composite toughness was similar to that of the control. The 30% SF composite toughness was similar to that prior to cycling, while the 50% SF composite toughness showed a 34.5% increase compared to that without wet/dry exposure.

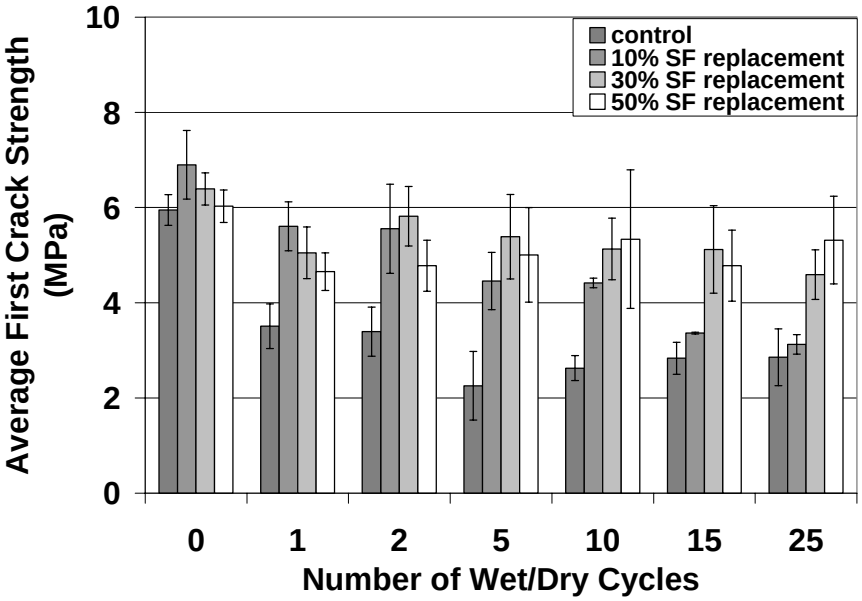

Figure 5-6. Silica fume composite flexural testing results. Average first crack strength (MPa) versus number of cycles.

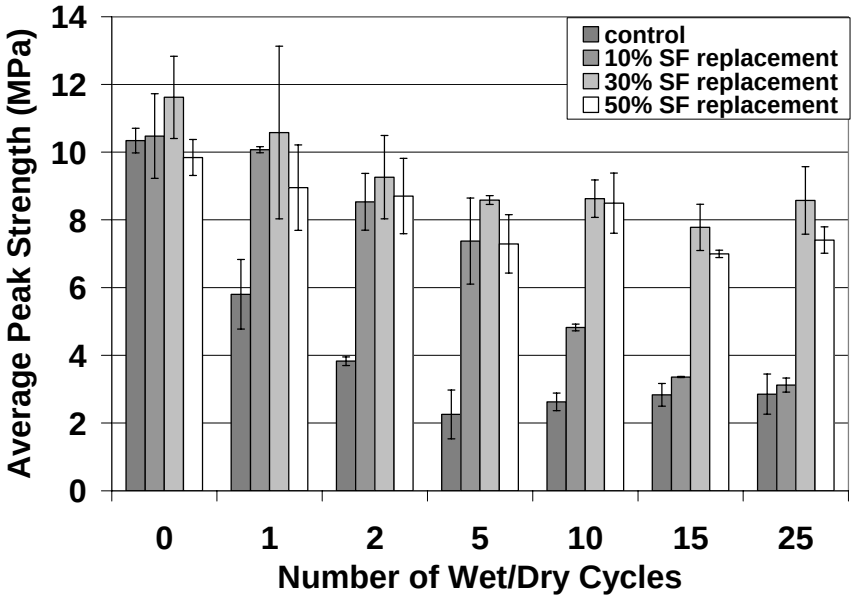

Figure 5-7. Silica fume composite flexural testing results. Average peak strength (MPa) versus number of cycles.

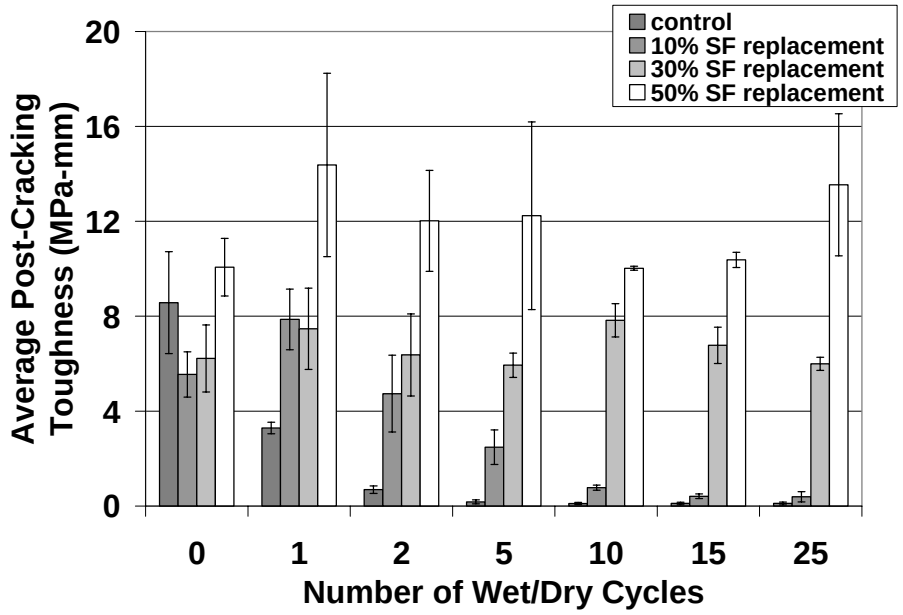

Figure 5-8. Silica fume composite flexural testing results. Average post-cracking toughness (MPa-mm) versus number of cycles.

5.2.1.2 Slag (SL) Replacement

For this work, SL composites were tested with 10, 30, 50, 70, and 90% SL replacement for cement by weight. Results, seen in Figure 5-9, indicate that initial (*i.e.*, 0 cycles) SL composite first crack strengths were similar to the control. Generally, the SL composites exhibited similar values and trends as the control as wet/dry cycling progressed. That is, all composites showed a notable decrease in strength after 1 wet/dry cycle. Degradation continued with increasing number of wet/dry cycles. However, only the 90% SL composites did not show any further first crack strength degradation following the initial decrease after 1 wet/dry cycle.

Figure 5-10 shows that, prior to cycling, all SL composites (except for 90% SL) exhibited 23.3-37.3% lower peak strength than the control. The 90% SL composite peak strength was comparable to the control. As cycling progressed, generally, the SL composite strengths were similar to the control. However, following a decrease after 1 wet/dry cycle, no further changes in the 90% SL composite peak strength were observed. After 25 cycles, the 90% SL strength was 123.2% greater than that of the control. All other SL composite strengths were similar to the control.

As for post-cracking toughness (Figure 5-11), all the SL composites, except for 90% SL, exhibited a slightly slower progression of degradation than the control between 1 and 5 cycles. Beyond 5 cycles, the differences between the control and the SL composites (except 90% SL) were indistinguishable. For the 90% SL composite, there was no observable degradation over the range of wet/dry cycles. After 25 cycles, the 90% SL toughness was significantly greater than that of the control.

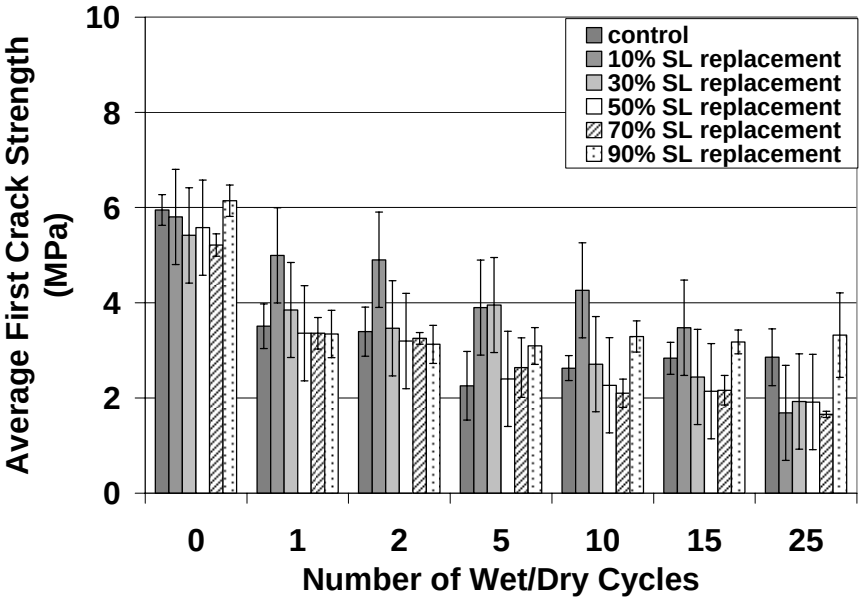

Figure 5-9. Slag composite flexural testing results. Average first crack strength (MPa) versus number of cycles.

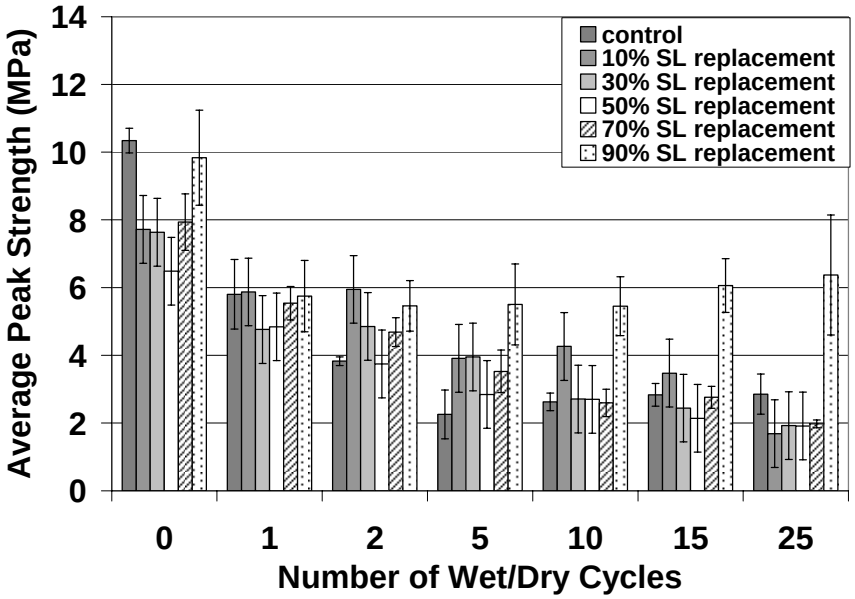

Figure 5-10. Slag composite flexural testing results. Average peak strength (MPa) versus number of cycles.

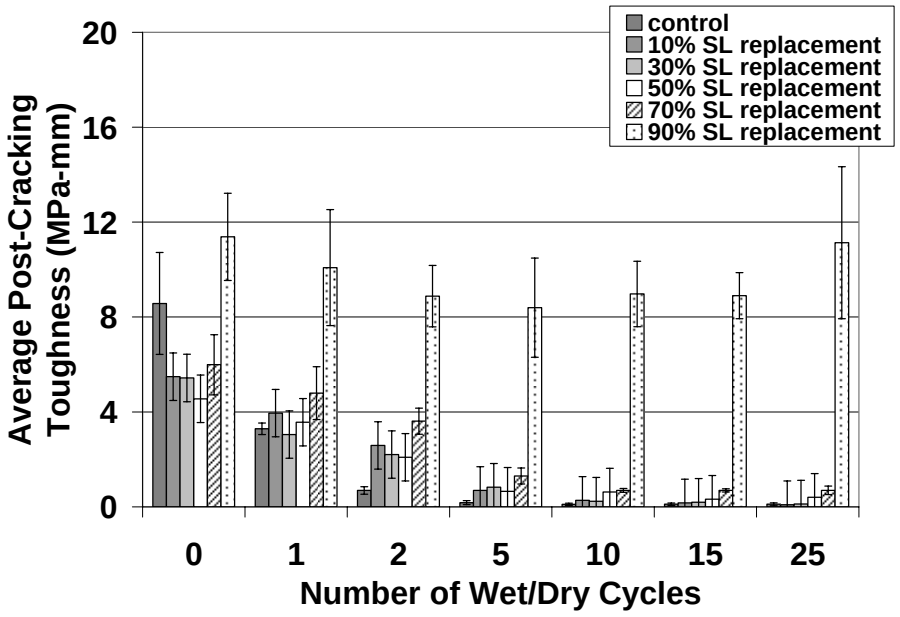

Figure 5-11. Slag composite flexural testing results. Average post-cracking toughness (MPa-mm) versus number of cycles.

5.2.1.3 Class F (FA) and Class C (CA) Fly Ash Replacement

Both fly ashes were tested at 10, 30, 50, and 70% cement replacement values. Upon mechanical testing, both types of composites exhibited similar first crack strength results, as seen in Figures 5-12 and 5-15. Prior to cycling, first crack strength decreased with increasing replacement amounts. That is, the 10% FA/CA composite first crack strengths were similar to the control, while the 70% FA/CA composite strengths were significantly less than the control. It should be noted that the CA composite showed greater first crack strength than the FA composite, without exposure. These differences in strength are also evident as cycling progressed. By 25 cycles, the FA/CA composites

exhibited strengths similar to the control. However, the rate of composite degradation was slowed with the replacement of cement with fly ash.

Again, peak strength trends (Figures 5-13 and 5-16) were similar to that observed with the first crack strength data. Prior to cycling, peak strength decreased with increasing replacement amounts. All FA/CA composites exhibited a slower progression of degradation than the control. However, by 25 wet/dry cycles, peak strength differences between the fly ash composites and the control were negligible.

In terms of post-cracking toughness (Figures 5-14 and 5-17), all fly ash composites prior to cycling, except for the 10 and 30% CA composites, showed lower toughness that the control. As cycling commenced and progressed, all FA/CA composites exhibited a slower rate of degradation than the control. Contrary to the strength trends, increasing replacement amounts led to improvements in toughness with wet/dry cycling. However, only the 70% FA/CA composite toughness was greater than the control, after 25 cycles. In addition, it is evident that 70% FA improved toughness more so that than 70% CA. However, the toughness of the 70% FA/CA composites was significantly less than that of the control prior to cycling.

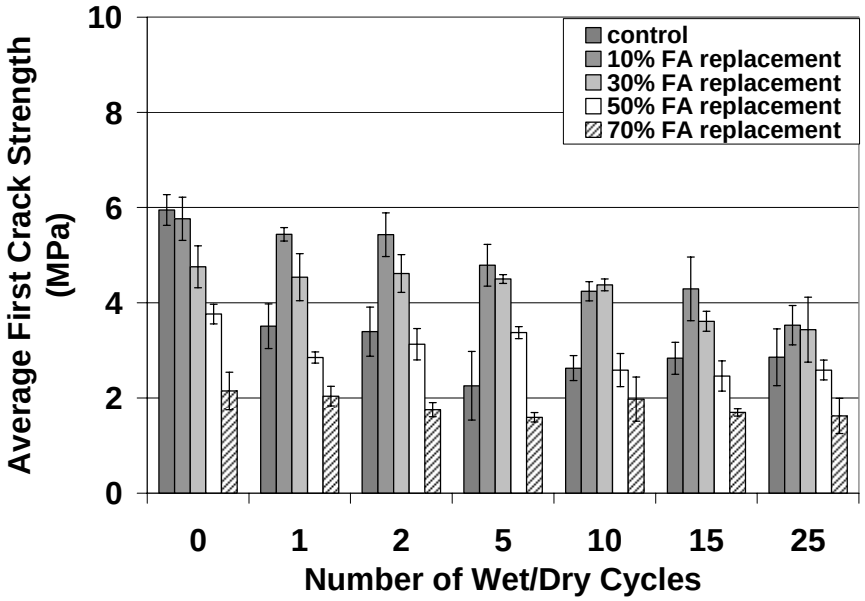

Figure 5-12. Class F fly ash composite flexural testing results. Average first crack strength (MPa) versus number of cycles.

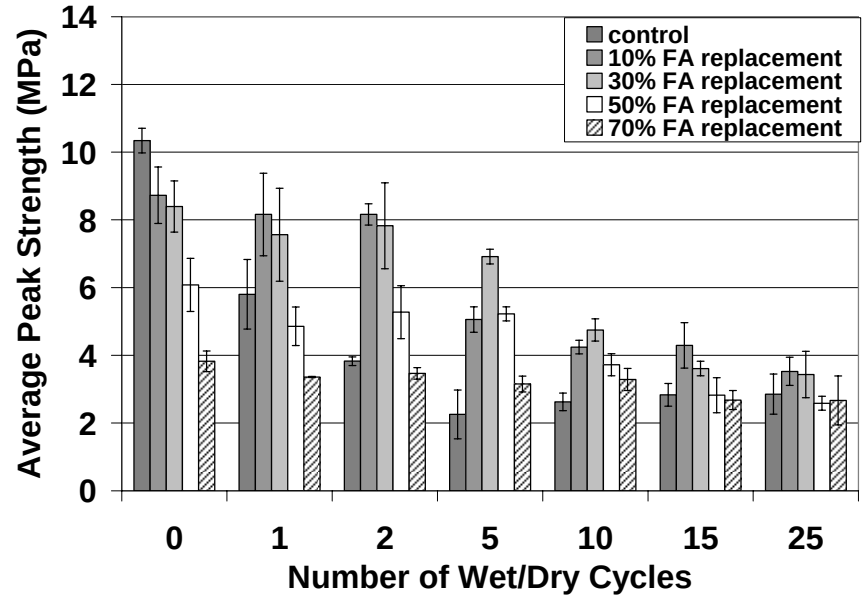

Figure 5-13. Class F fly ash composite flexural testing results. Average peak strength (MPa) versus number of cycles.

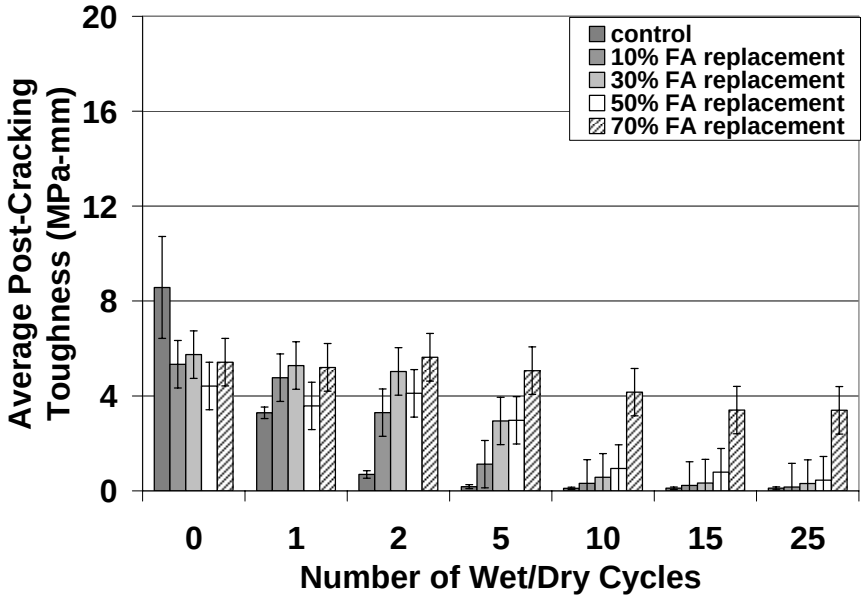

Figure 5-14. Class F fly ash composite flexural testing results. Average post-cracking toughness (MPa-mm) versus number of cycles.

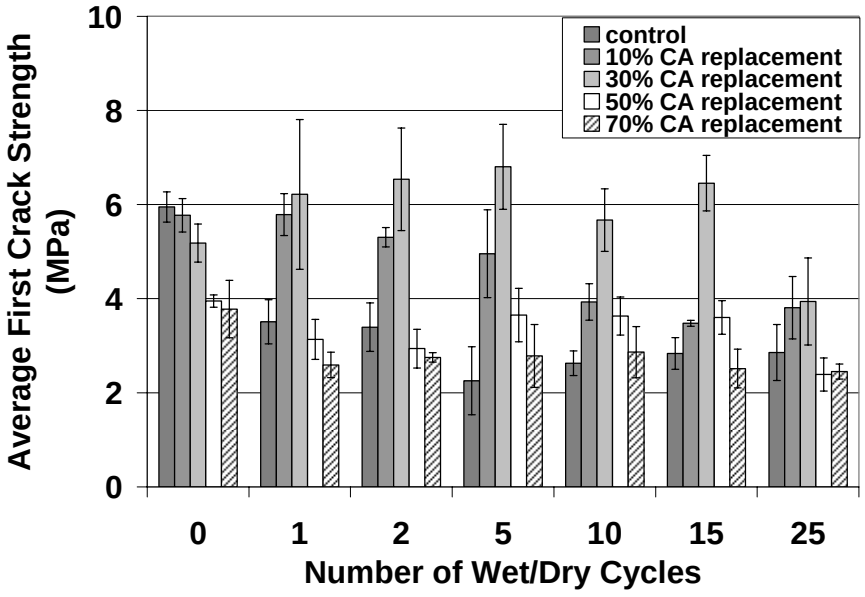

Figure 5-15. Class C fly ash composite flexural testing results. Average first crack strength (MPa) versus number of cycles.

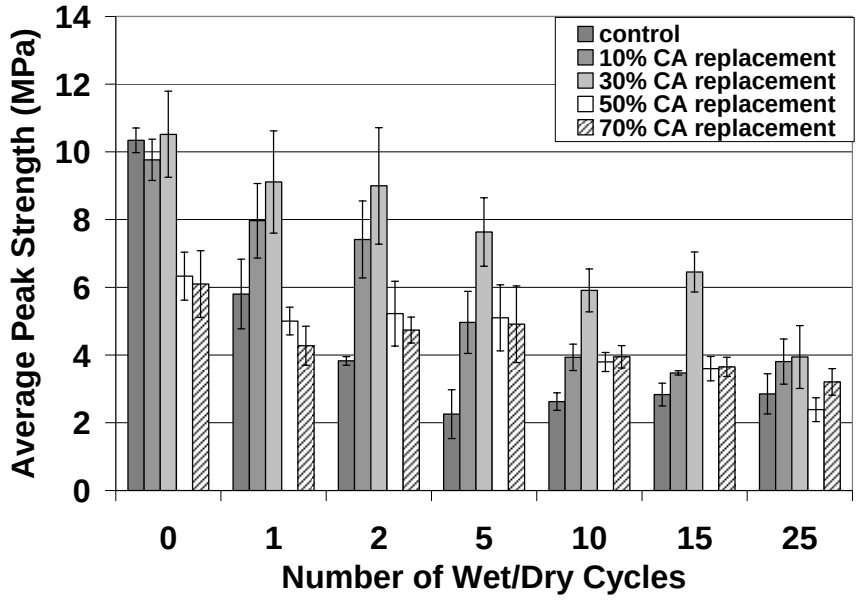

Figure 5-16. Class C fly ash composite flexural testing results. Average peak strength (MPa) versus number of cycles.

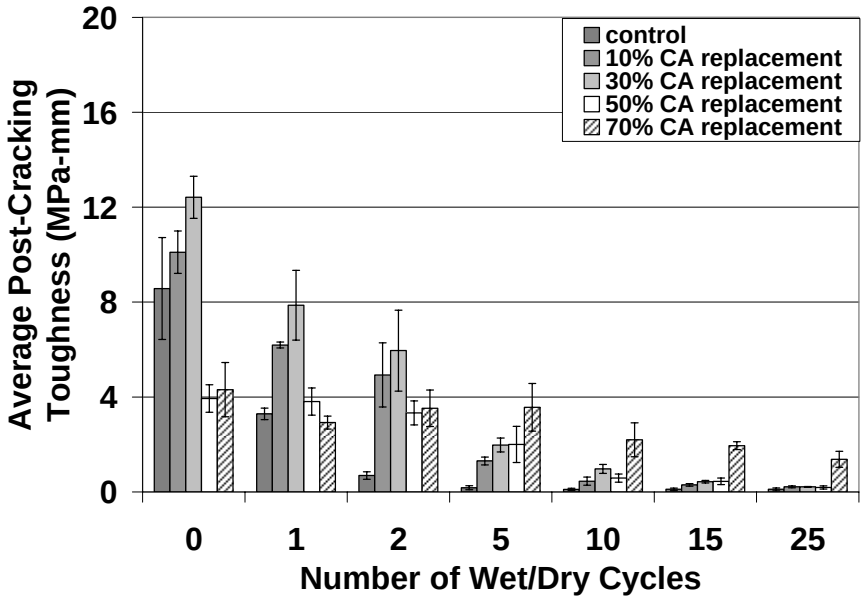

Figure 5-17. Class C fly ash composite flexural testing results. Average post-cracking toughness (MPa-mm) versus number of cycles.

5.2.1.4 Metakaolin (MK235 and MK349) Replacement

Two types of metakaolin were evaluated at cement replacement values of 10 and 30%. The types are distinguished by a number code – MK235 or MK349 – and differ primarily in their surface area. MK235 has a surface area of 11.1 m^2/g, while MK349 has a surface area of 25.4 m^2/g.

Prior to cycling (Figure 5-18), it is observed that the MK composites generally showed slightly lower first crack strength than the control. In addition, for both types of MK, the 30% composite first crack strength was lower than the 10% composite. Over the range of wet/dry cycles investigated here, the 10% MK235 and both MK349 first crack strengths were similar to the control. However, the 30% MK349 did exhibit a marked increase in strength between 2 and 5 cycles, though strength decreased with additional cycling. After 1 wet/dry cycle, the 30% MK235 composite exhibited an increase in first crack strength. No observable changes occurred with increasing numbers of cycles. By 25 cycles, the 30% MK235 composite first crack strength was comparable to the control without wet/dry exposure. However, all other metakaolin composites exhibited similar strengths as the control.

Figure 5-19 illustrates the MK peak strength results. Without wet/dry exposure, all MK composites showed similar peak strength values as the control. No changes in strength were observed after 1 wet/dry cycle. Additional cycling led to decreases in peak strength for both 10% MK composites. By 10 cycles, the 10% MK composite peak strength were comparable to that of the control. The 30% MK composites exhibited negligible changes, up to 15 cycles. After 25 cycles, the 30% MK349 composite

exhibited a significant decrease in peak strength. However, the 30% MK235 composite, over the range of wet/dry cycles investigated here, did not exhibit any composite peak strength degradation.

Post-cracking toughness results (Figure 5-20) show that, prior to cycling, the MK235 composites exhibited lower toughness than the control, while the MK349 composite toughness was similar to the control. With progressive cycling, the 10% MK toughness values decreased significantly, after a slight increase with 1 wet/dry cycle. Up to 5 cycles, the 30% MK composites did not exhibit any degradation. However, beyond 5 cycles, the 30% MK349 toughness decreased, while the 30% MK235 toughness remained unchanged. After 25 cycles, the 30% MK235 composite toughness was comparable to the control prior to cycling.

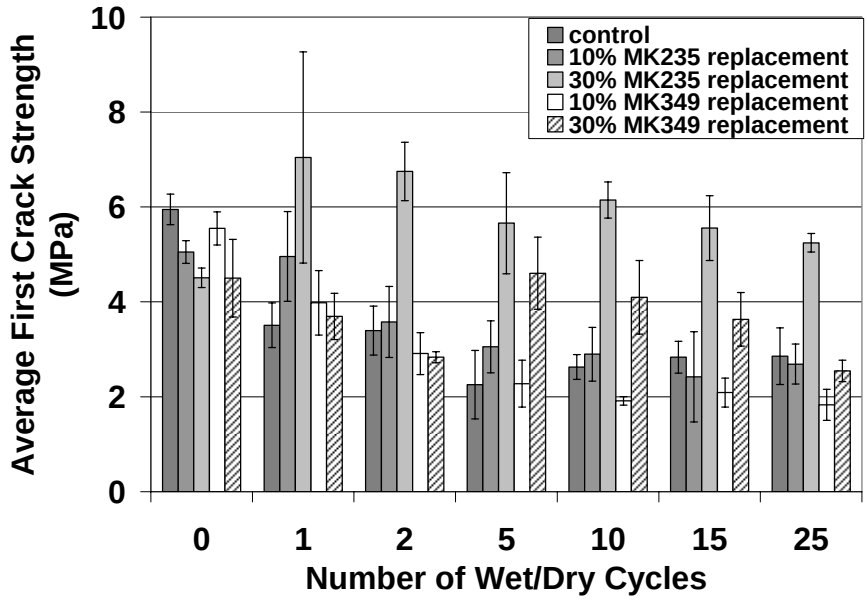

Figure 5-18. Metakaolin composite flexural testing results. Average first crack strength (MPa) versus number of cycles.

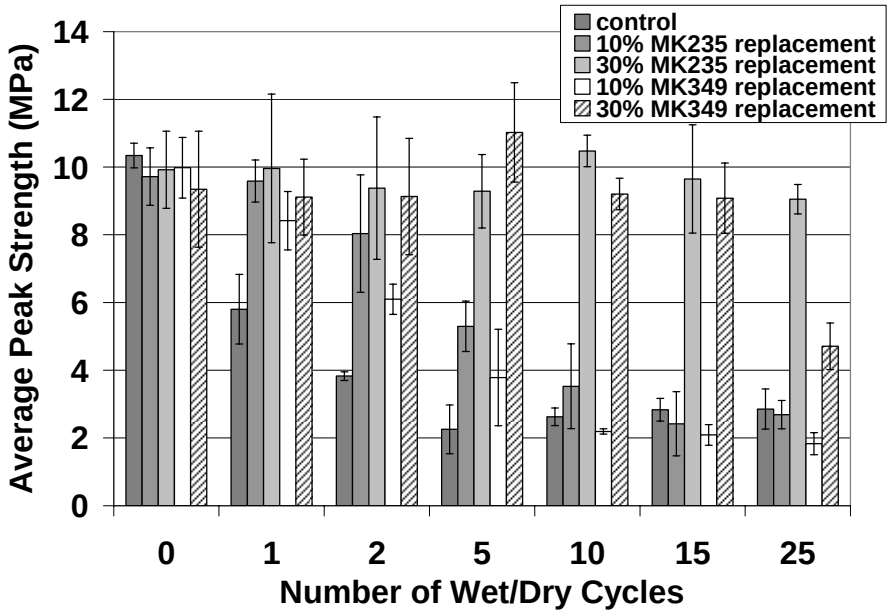

Figure 5-19. Metakaolin composite flexural testing results. Average peak strength (MPa) versus number of cycles.

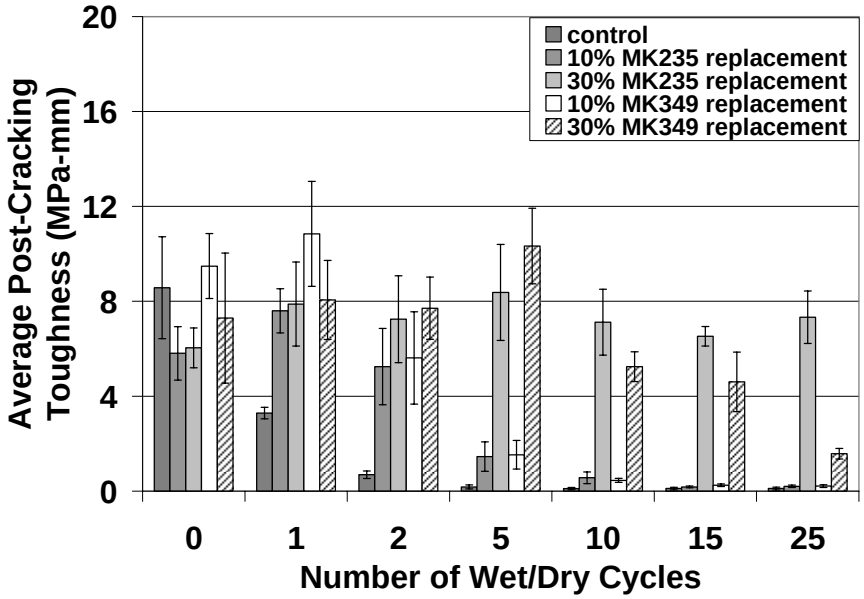

Figure 5-20. Metakaolin composite flexural testing results. Average post-cracking toughness (MPa-mm) versus number of cycles.

5.2.1.5 DEVA Blend (Raw and Calcined) Replacement

Proprietary blends of diatomaceous earth and volcanic ash were tested at 10, 30, and 50% replacements by weight of cement and differed primarily in their surface area. The raw blend had a larger surface area (2.654 m^2/g) than the calcined variety (0.999 m^2/g).

As with the fly ash samples, the different DEVA blends exhibited similar results. For both first crack strength (Figures 5-21 and 5-24) and peak strength (Figure 5-22 and 5-25), increasing replacement amounts led to lower strengths. All DEVA replacements, though, did slow the progression of composite degradation, as compared to the control. However, by 25 cycles, DEVA strengths were similar to or slightly greater than the control. Only the 50% DEVA composites exhibited significantly greater peak strength than the control.

Up to 2 wet/dry cycles, the DEVA composites did not exhibit considerable changes in post-cracking toughness as seen in Figures 5-23 and 5-26. Beyond this point, all DEVA composites showed decreases in toughness. After 25 cycles, only the 50% DEVA composites were showed improved toughness as compared to the control. However, these toughness values were still lower than that of the control prior to cycling.

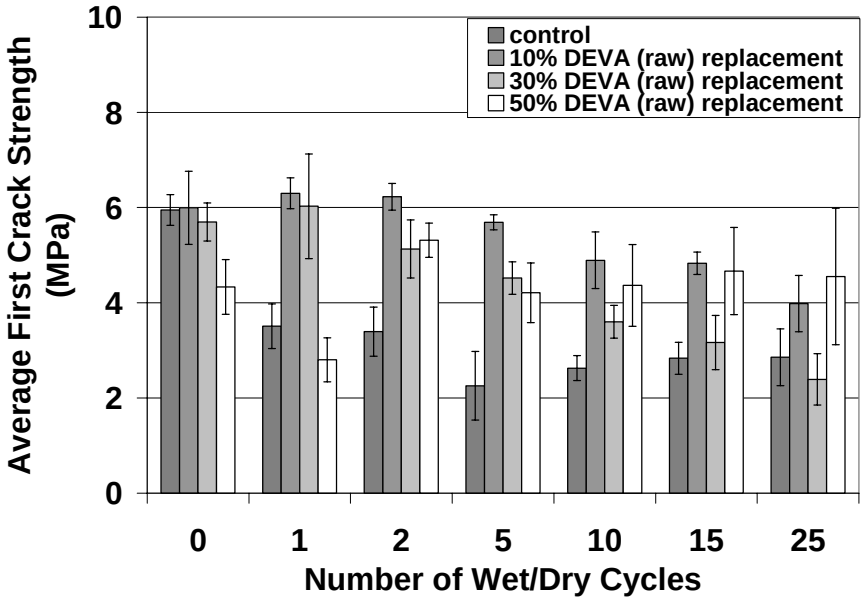

Figure 5-21. Raw DEVA blend composite flexural testing results. Average first crack strength (MPa) versus number of cycles.

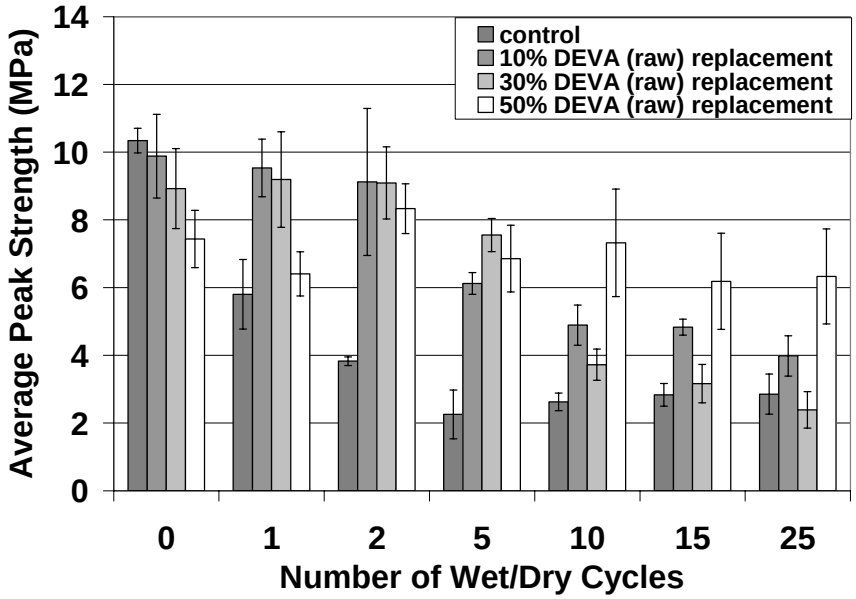

Figure 5-22. Raw DEVA blend composite flexural testing results. Average peak strength (MPa) versus number of cycles.

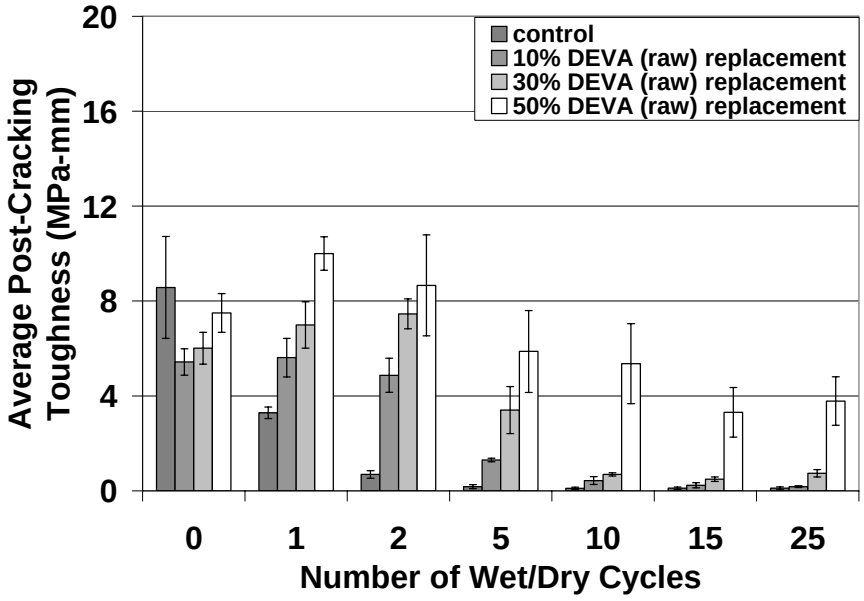

Figure 5-23. Raw DEVA blend composite flexural testing results. Average post-cracking toughness (MPa-mm) versus number of cycles.

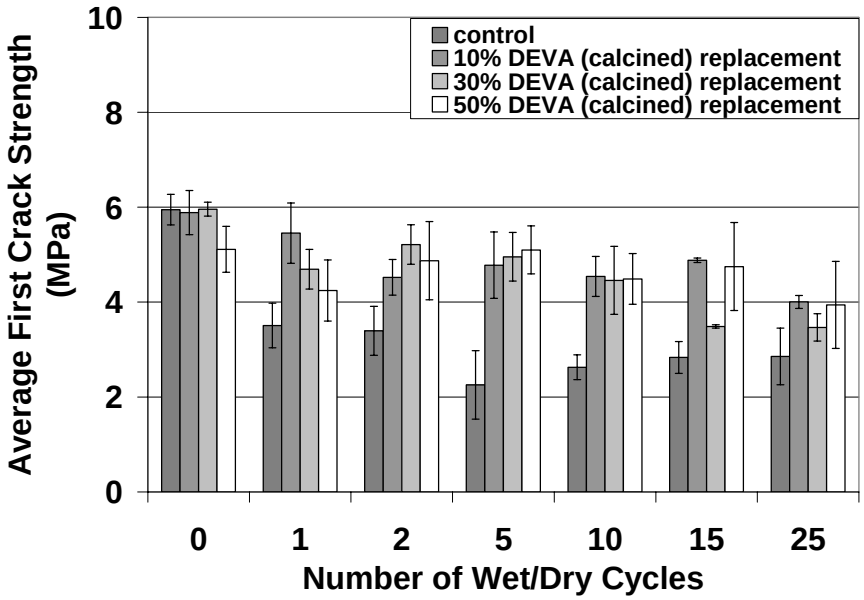

Figure 5-24. Calcined DEVA blend composite flexural testing results. Average first crack strength (MPa) versus number of cycles.

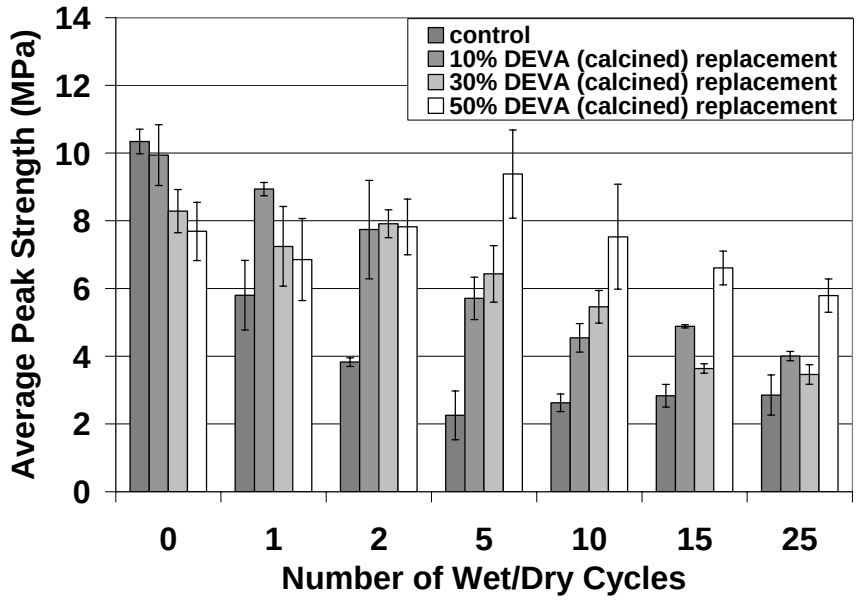

Figure 5-25. Calcined DEVA blend composite flexural testing results. Average peak strength (MPa) versus number of cycles.

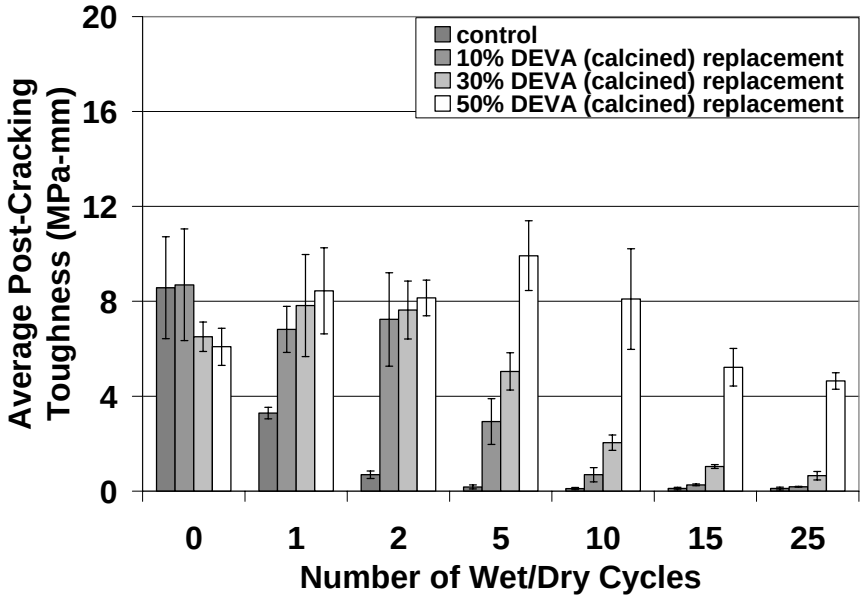

Figure 5-26. Calcined DEVA blend composite flexural testing results. Average post-cracking toughness (MPa-mm) versus number of cycles.

5.2.1.6 Ternary and Quaternary Blend Replacements

Ternary and quaternary SCM blends were also investigated in order to optimize cost and performance. For example, though the 30 and 50% SF composites showed no signs of degradation, these replacement values are not commercially practical and dramatically increase the cost of such a composite. Thus, blends of fly ash/slag, silica fume/slag, silica fume/fly ash, metakaolin/slag, metakaolin/silica fume, and metakaolin/silica fume/slag were investigated.

Results for these SCM blended kraft pulp fiber-cement composites are shown in Figures 5-27 – 5-44. However, it can be seen that the fly ash/slag, silica fume/fly ash, and metakaolin/silica fume blends (Figures 5-27 – 5-36) did not produce results that would indicate these SCM blends were effective. Figures 5-37 – 5-44 show the mechanical testing data for the silica fume/slag, metakaolin/slag, and metakaolin/silica fume/slag SCM blend composites.

These results show that the 10% SF/70% SL and 10% MK235/70% SL composites minimized the progression of composite degradation during wet/dry cycling. The 10% MK235/10% SF/70% SL quaternary blend composite did not exhibit any signs of composite degradation over the range of wet/dry cycles investigated in this study. After 25 cycles, first crack and peak strengths for the quaternary blend composite were slightly lower than the control without exposure. Toughness, after 25 cycles, for the quaternary blend composite was similar to the unexposed control.

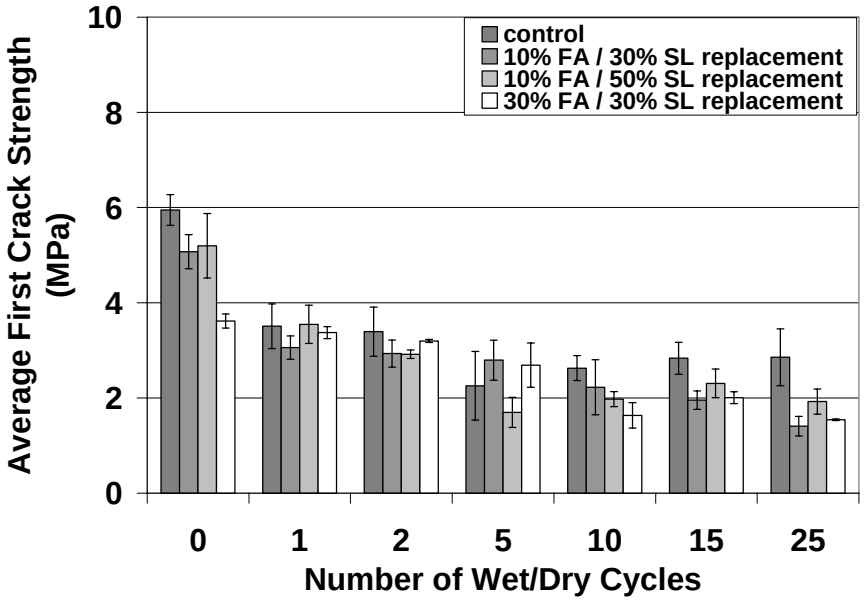

Figure 5-27. Fly ash and slag ternary blend composite flexural testing results. Average first crack strength (MPa) versus number of cycles.

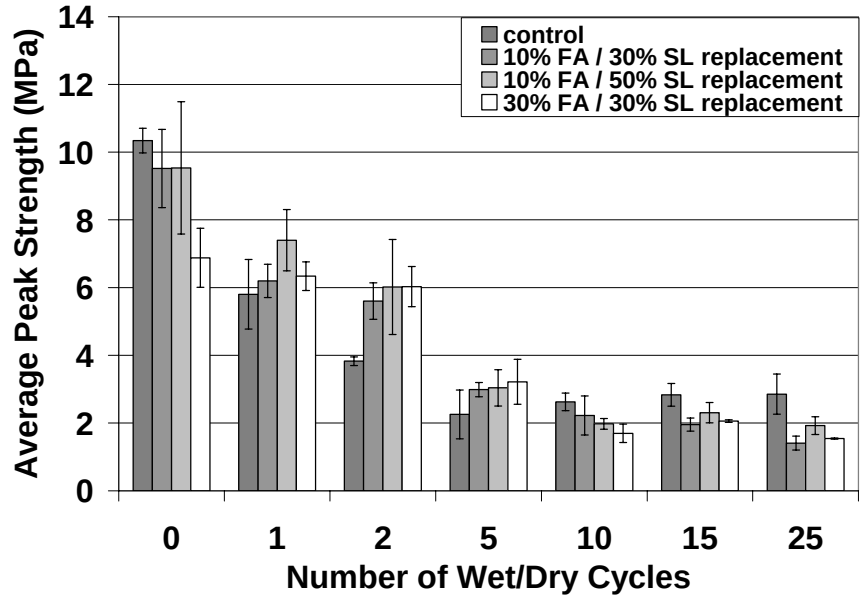

Figure 5-28. Fly ash and slag ternary blend composite flexural testing results. Average peak strength (MPa) versus number of cycles.

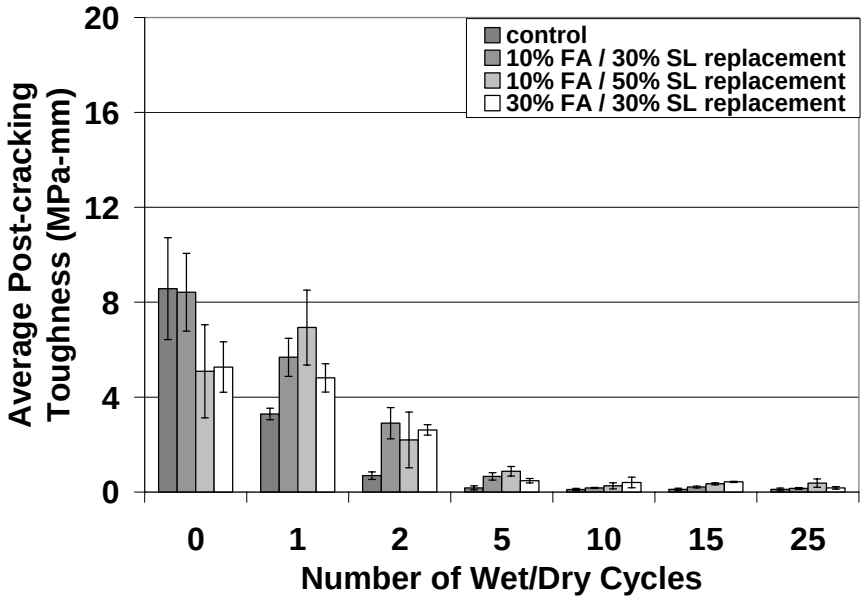

Figure 5-29. Fly ash and slag ternary blend composite flexural testing results. Average post-cracking toughness (MPa-mm) versus number of cycles.

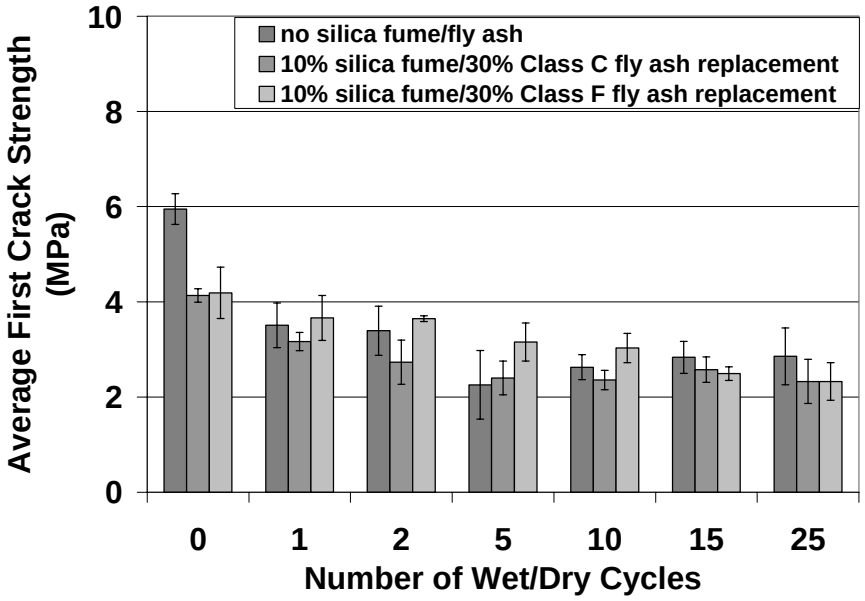

Figure 5-30. Fly ash and silica fume ternary blend composite flexural testing results. Average first crack strength (MPa) versus number of cycles.

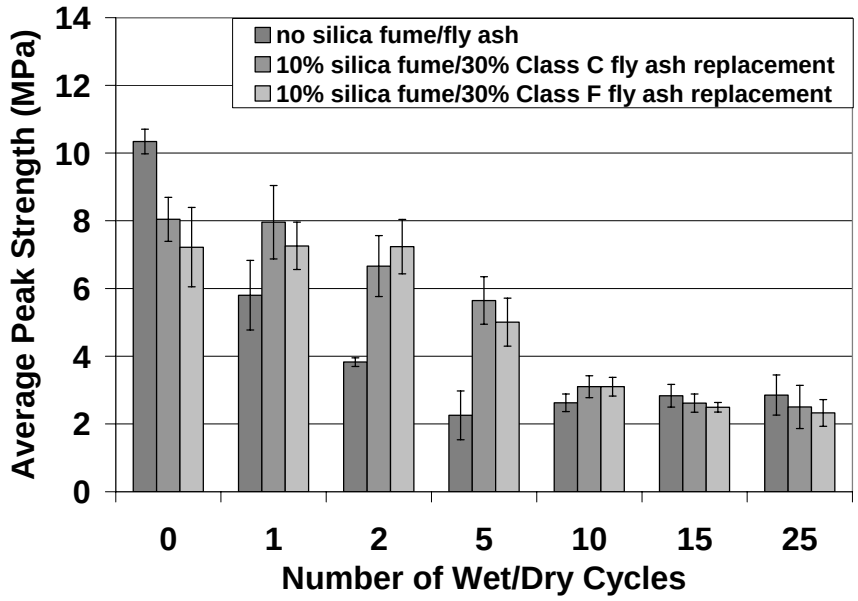

Figure 5-31. Fly ash and silica fume ternary blend composite flexural testing results. Average peak strength (MPa) versus number of cycles.

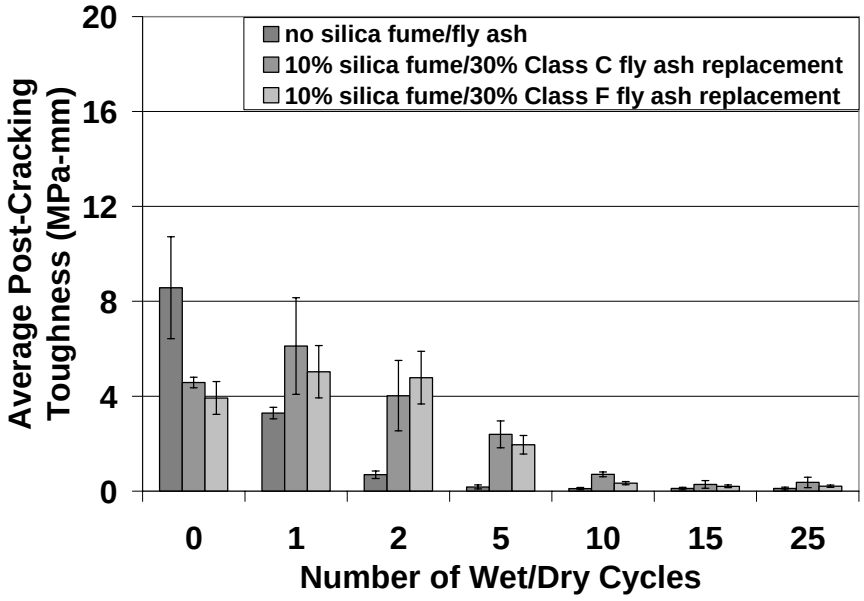

Figure 5-32. Fly ash and silica fume ternary blend composite flexural testing results. Average post-cracking toughness (MPa-mm) versus number of cycles.

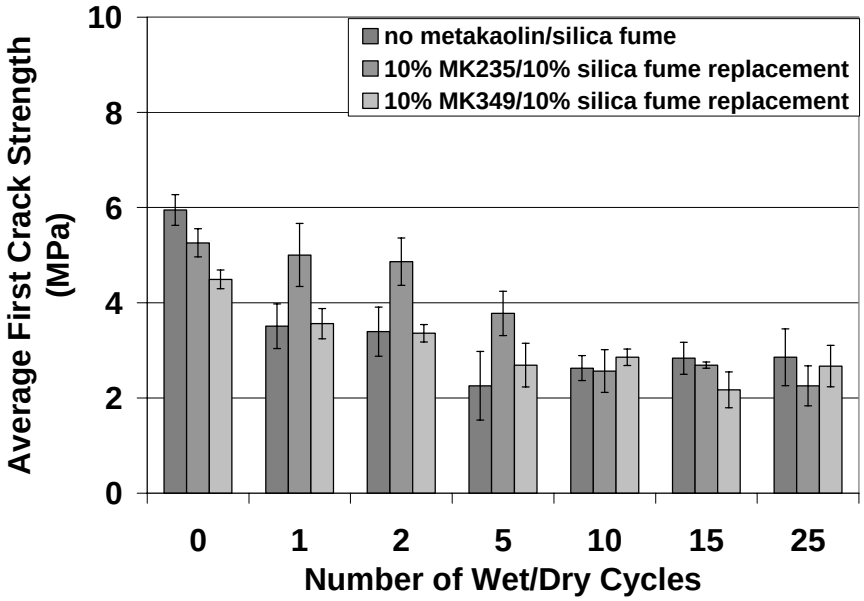

Figure 5-33. Metakaolin (MK235) and silica fume ternary blend composite flexural testing results. Average first crack strength (MPa) versus number of cycles.

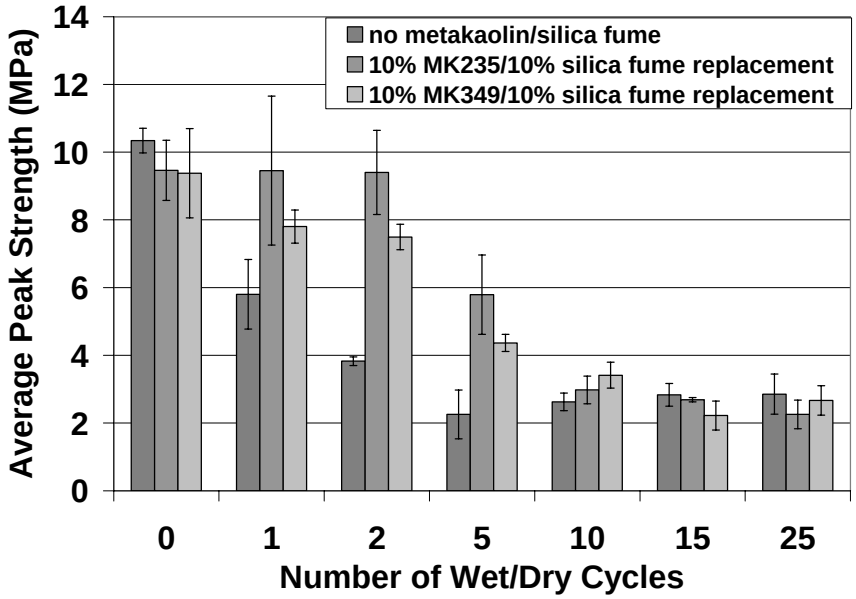

Figure 5-34. Metakaolin (MK235) and silica fume ternary blend composite flexural testing results. Average peak strength (MPa) versus number of cycles.

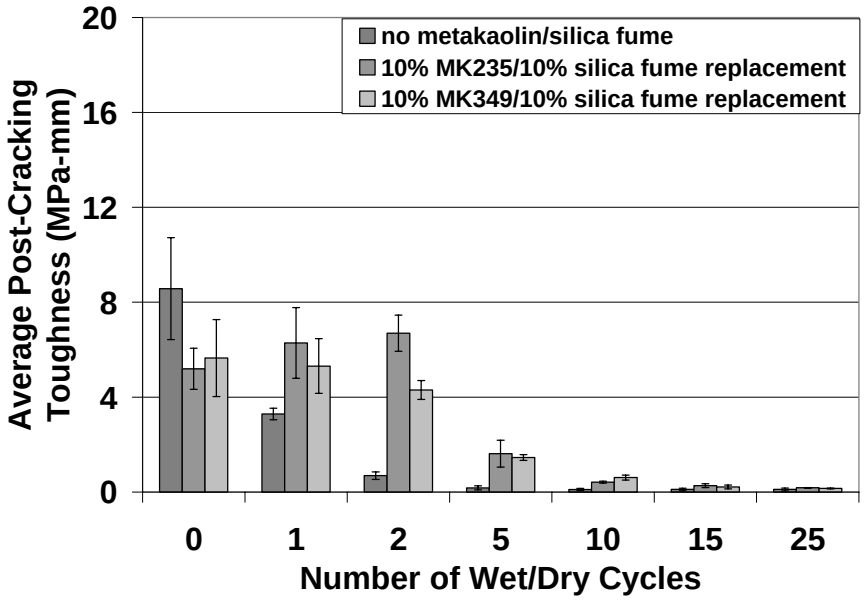

Figure 5-35. Metakaolin (MK235) and silica fume ternary blend composite flexural testing results. Average post-cracking toughness (MPa-mm) versus number of cycles.

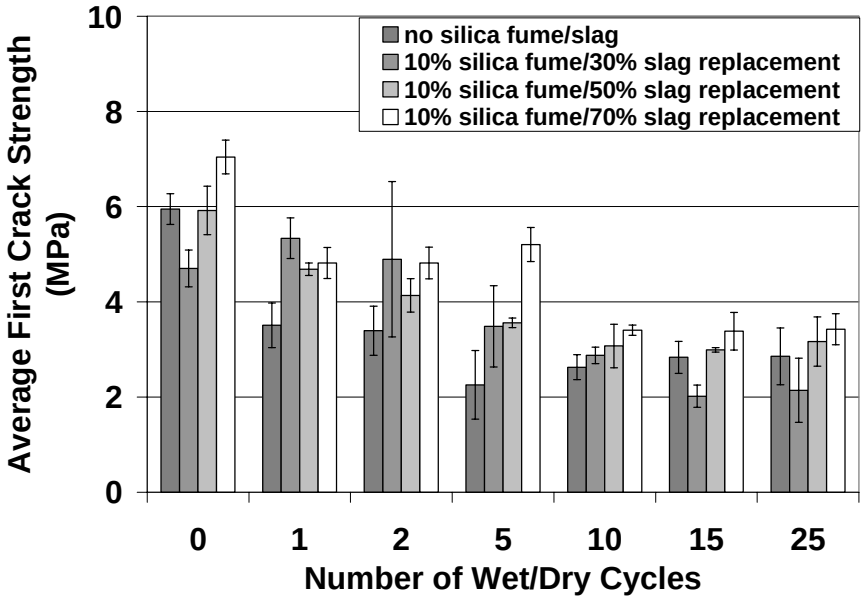

Figure 5-36. Silica fume and slag ternary blend composite flexural testing results. Average first crack strength (MPa) versus number of cycles.

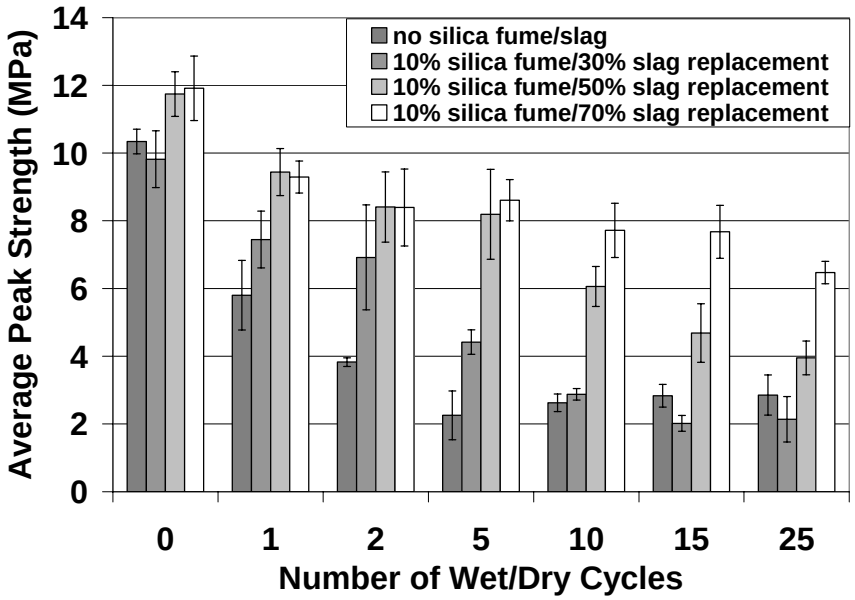

Figure 5-37. Silica fume and slag ternary blend composite flexural testing results. Average peak strength (MPa) versus number of cycles.

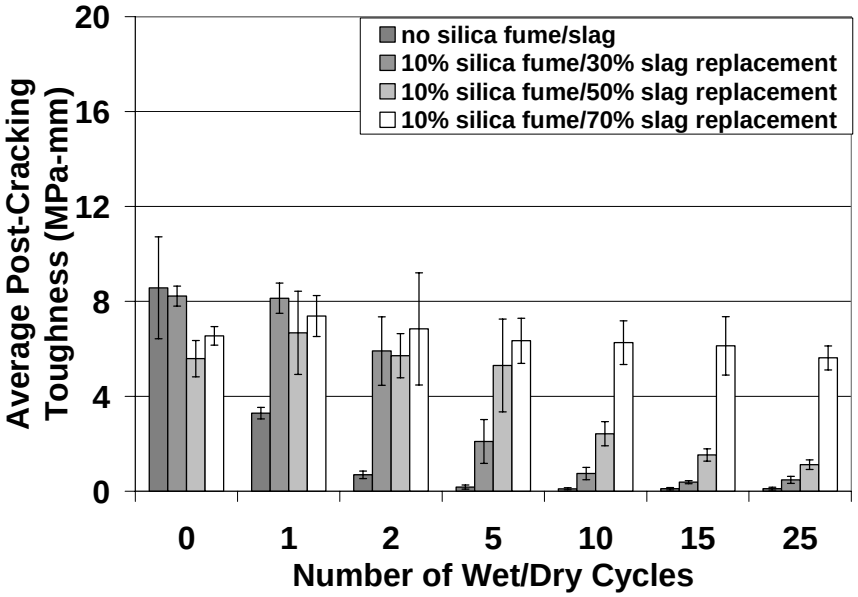

Figure 5-38. Silica fume and slag ternary blend composite flexural testing results. Average post-cracking toughness (MPa-mm) versus number of cycles.

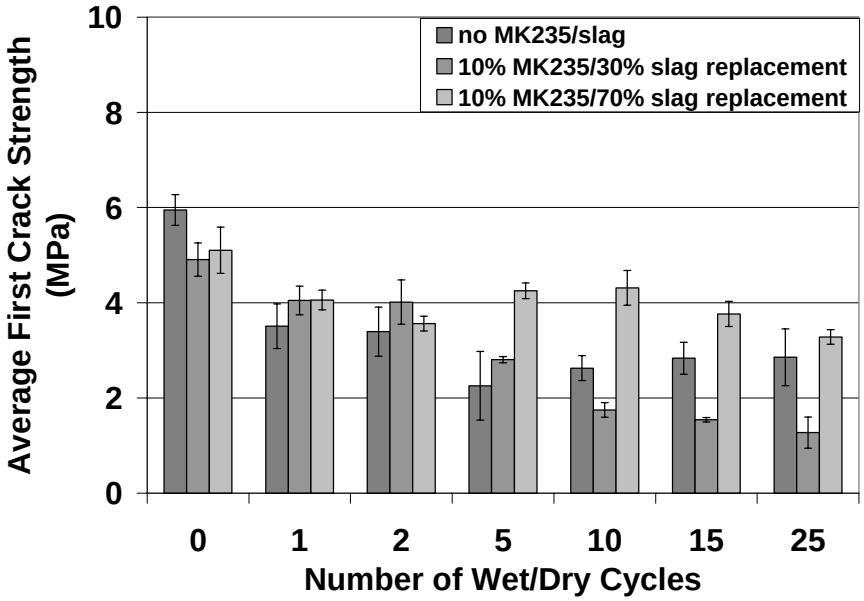

Figure 5-39. Metakaolin (MK235) and slag ternary blend composite flexural testing results. Average first crack strength (MPa) versus number of cycles.

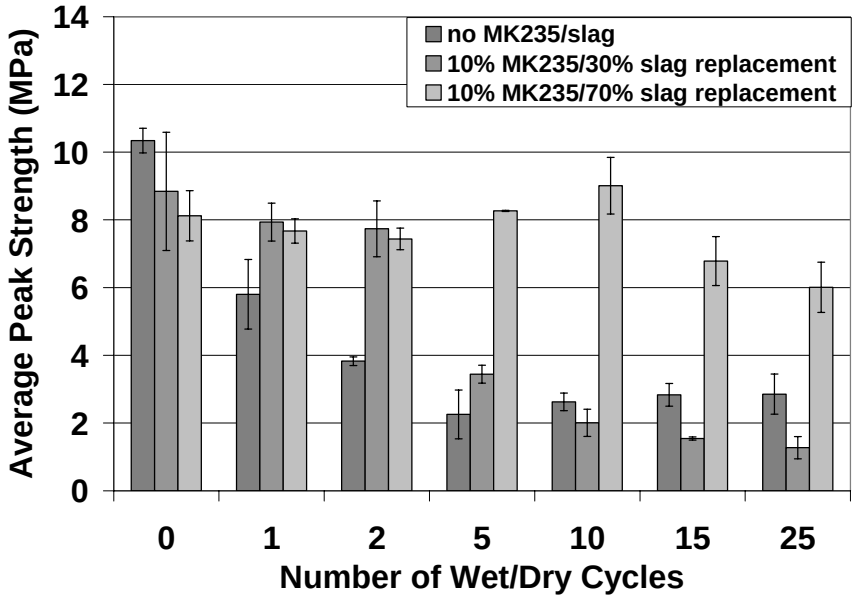

Figure 5-40. Metakaolin (MK235) and slag ternary blend composite flexural testing results. Average peak strength (MPa) versus number of cycles.

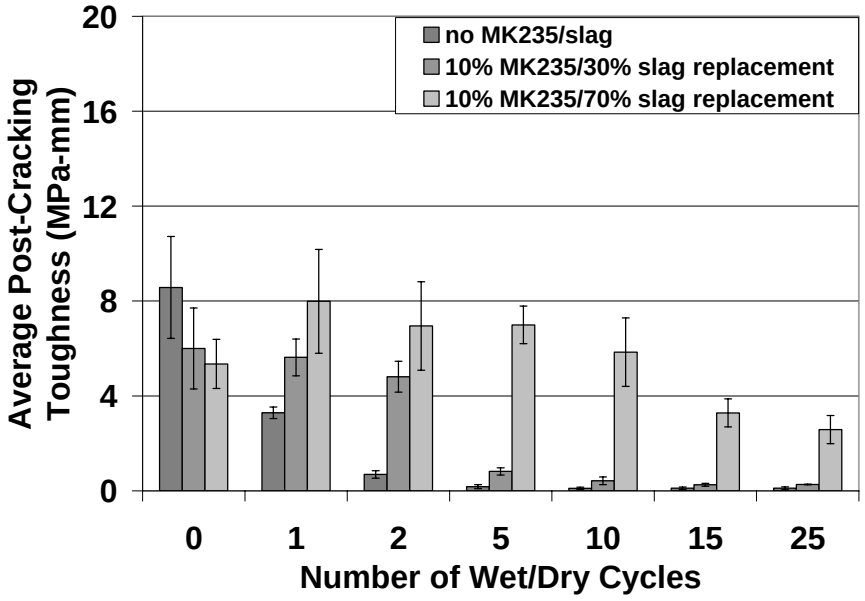

Figure 5-41. Metakaolin (MK235) and slag ternary blend composite flexural testing results. Average post-cracking toughness (MPa-mm) versus number of cycles.

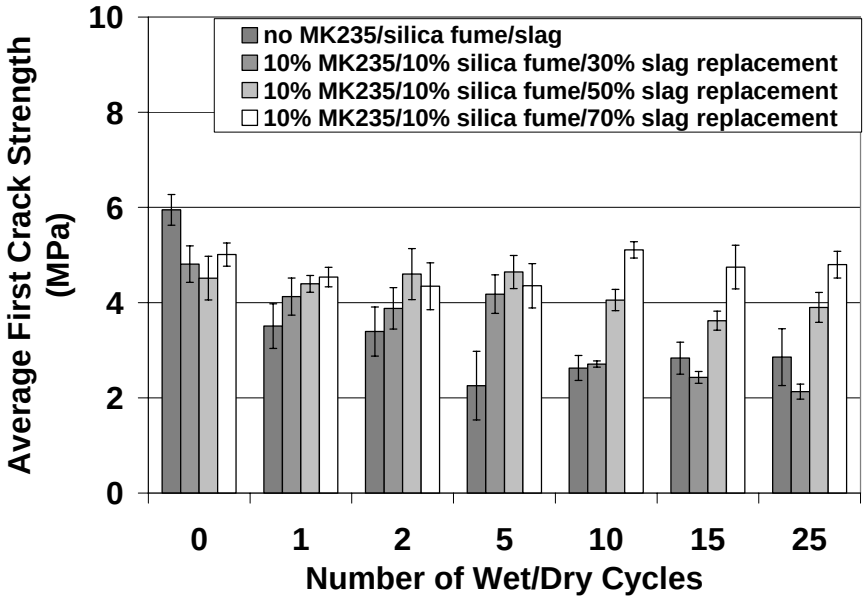

Figure 5-42. Metakaolin, silica fume, and slag quaternary blend composite flexural testing results. Average first crack strength (MPa) versus number of cycles.

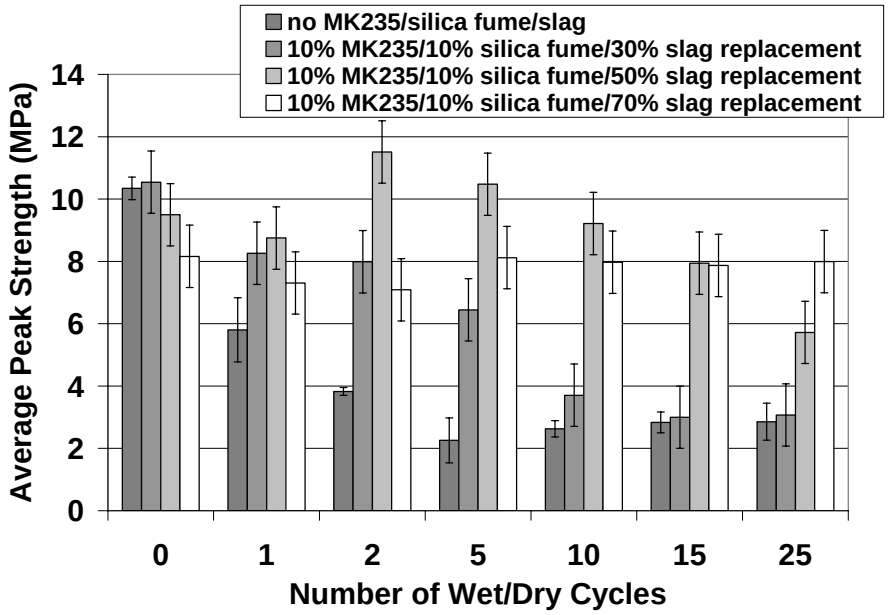

Figure 5-43. Metakaolin, silica fume, and slag quaternary blend composite flexural testing results. Average peak strength (MPa) versus number of cycles.

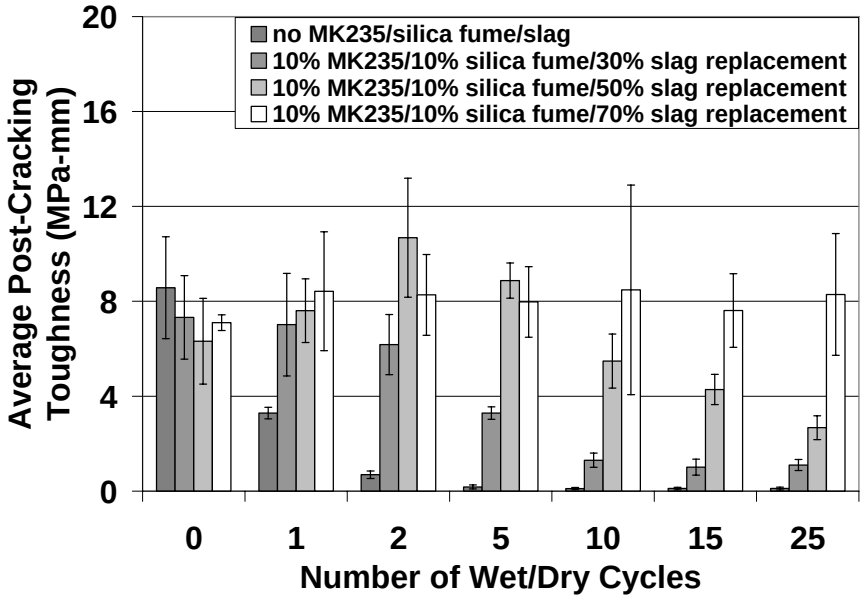

Figure 5-44. Metakaolin, silica fume, and slag quaternary blend composite flexural testing results. Average post-cracking toughness (MPa-mm) versus number of cycles.

5.2.2 Chemical Analysis

5.2.2.1 EDS Analysis

Preliminary EDS analyses have been conducted on kraft pulp fiber-cement composites containing silica fume and slag to assess the propensity of SCMs at minimizing ettringite and calcium hydroxide reprecipitation on the fiber surface. Results for composites after 25 wet/dry cycles containing silica fume at 10% and 50% replacement values (Figures 5-45 and 5-46) indicate that silica fume minimizes the reprecipitation of ettringite. Ettringite formation is believed to be minimized through the stabilization of monosulfate. Monosulfate is stabilized by the maintaining of a relatively high matrix alkali content after 25 cycles (*i.e.*, leaching is minimized) as seen in Figure 5-47. In addition, as expected, it appears that Si/Ca has increased relative to the pure cement composite due to the formation of supplementary C-S-H.

Similar results were seen in Figure 5-48 – 5-50 using 10, 50, and 90% slag as a partial weight replacement for cement. It can be seen in Figure 5-49 that as the percent of slag increased, ettringite formation was increasingly prevented and aluminate-rich phases, such as monosulfate and C_4AH_x, were stabilized.

Thus, the EDS results indicate that, at a minimum, silica fume and slag are both effective in minimizing the formation of ettringite after 25 cycles. In addition, the alkali content of the composite remains high, indicating that the pore solution pH remains relatively constant over the range of wet/dry cycles. Thus, stabilization of the pore solution pH minimizes conversion of monosulfate to ettringite.

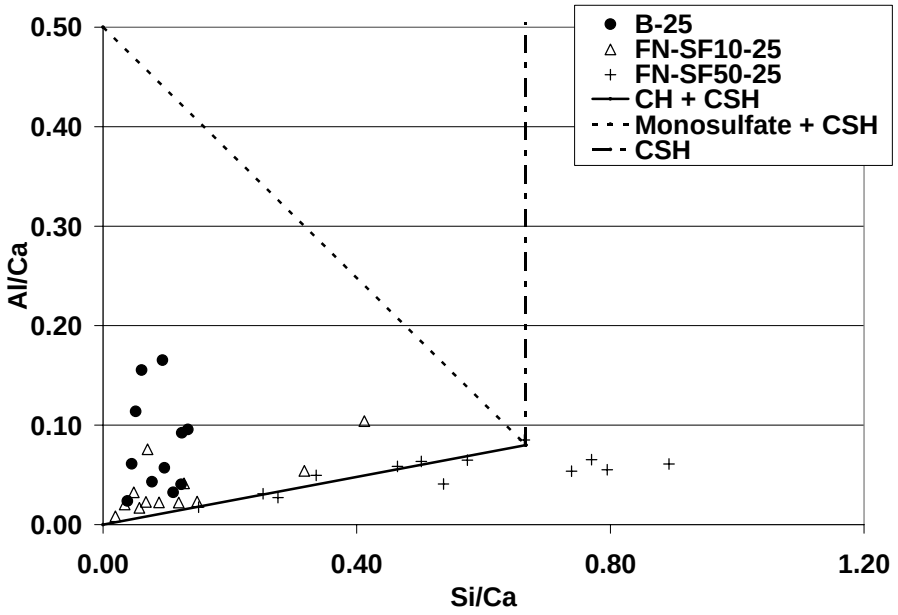

Figure 5-45. ESEM EDS analysis after 25 cycles for composites containing silica fume - average Al/Ca versus Si/Ca molar ratios.

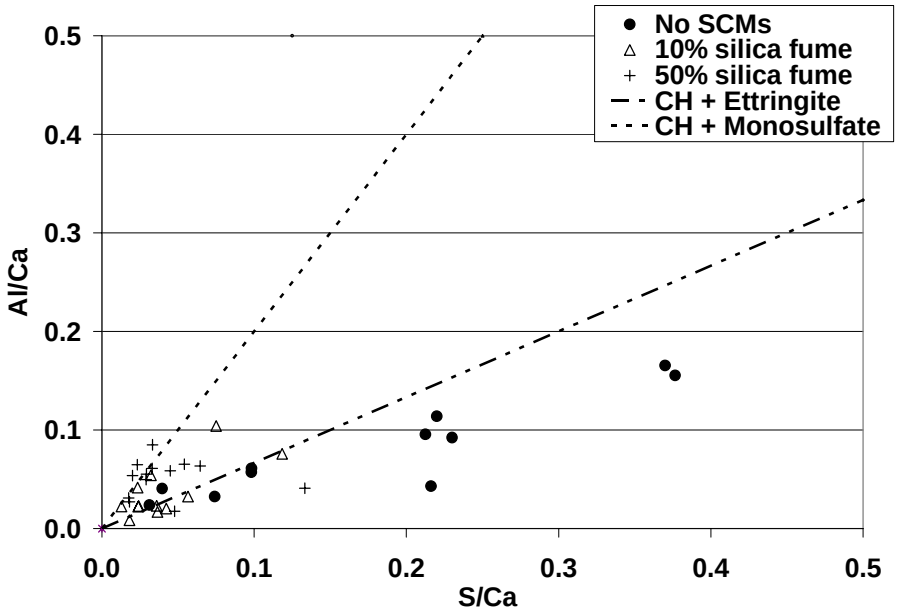

Figure 5-46. ESEM EDS analysis after 25 cycles for composites containing silica fume - average Al/Ca versus S/Ca molar ratios.

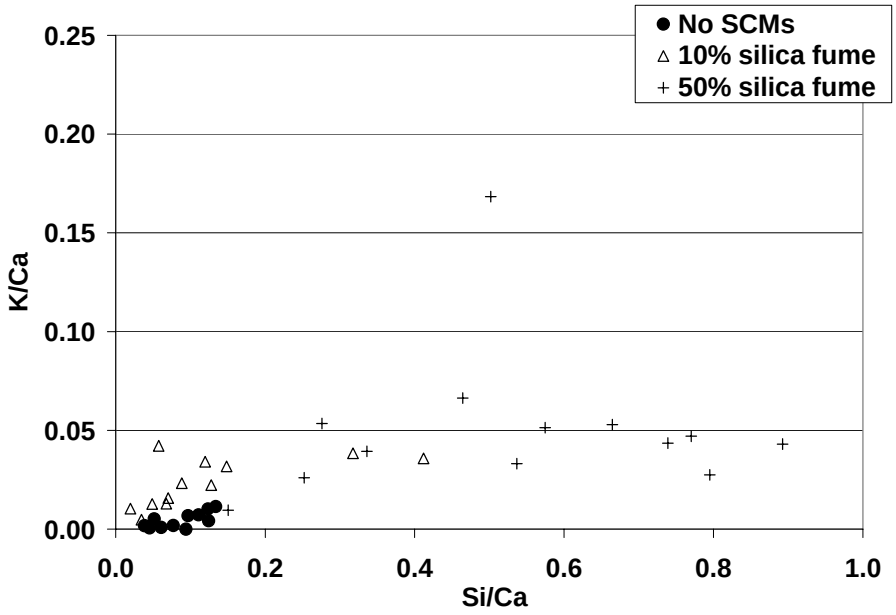

Figure 5-47. ESEM EDS analysis after 25 cycles for composites containing silica fume - average Si/Ca versus K/Ca molar ratios.

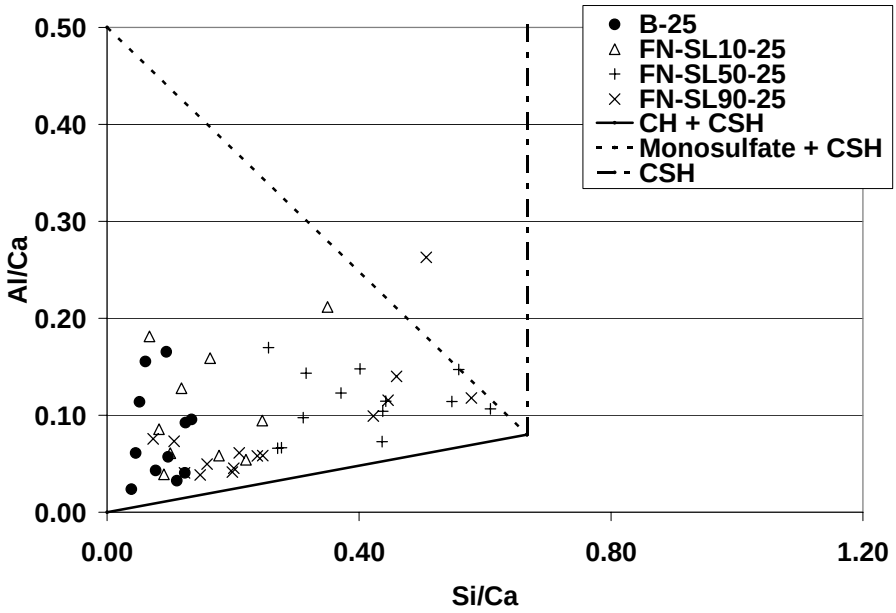

Figure 5-48. ESEM EDS analysis after 25 cycles for composites containing slag - average Al/Ca versus Si/Ca molar ratios.

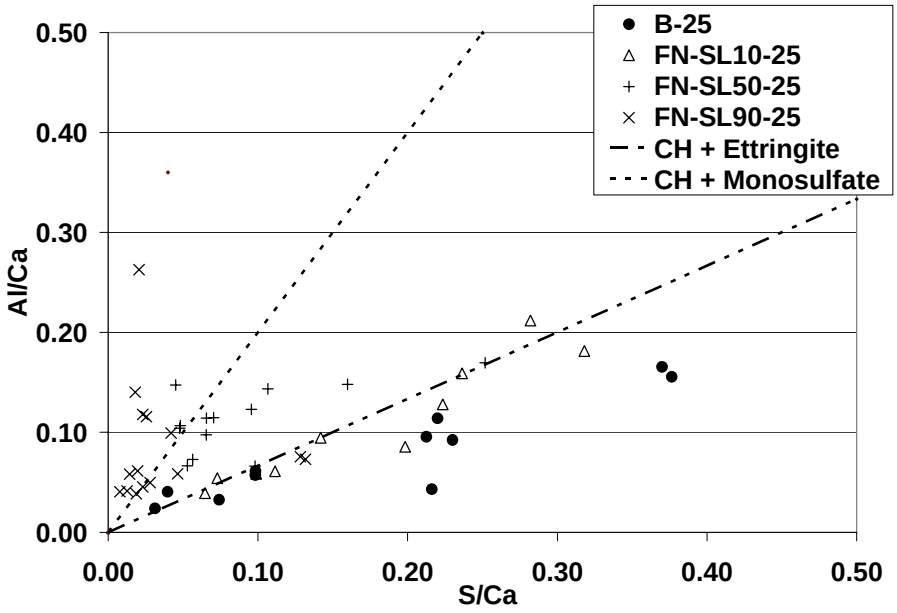

Figure 5-49. ESEM EDS analysis after 25 cycles for composites containing slag - average Al/Ca versus S/Ca molar ratios.

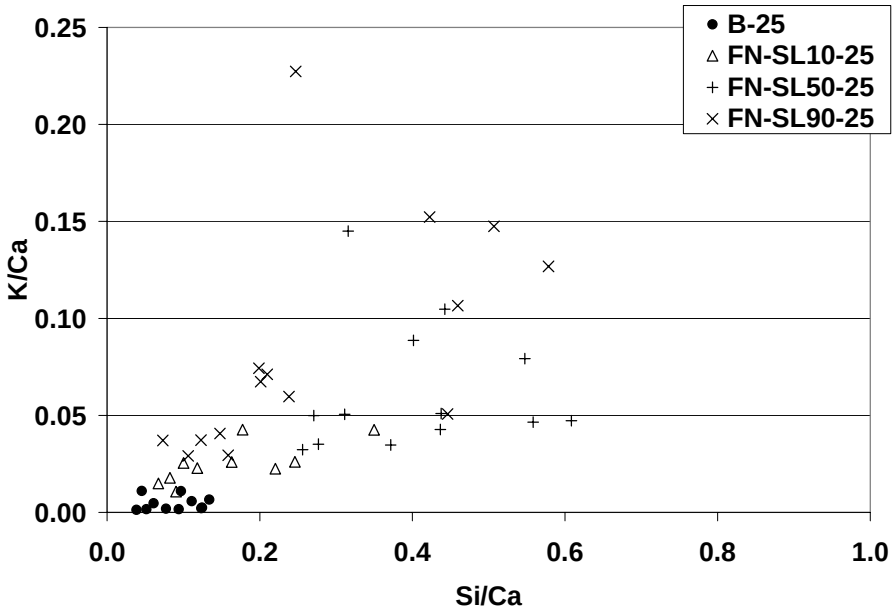

Figure 5-50. ESEM EDS analysis after 25 cycles for composites containing slag - average Si/Ca versus K/Ca molar ratios.

5.2.2.2 DSC Analysis

Furthermore, preliminary DSC results indicate, as expected, that the addition of SCMs (as indicated by increased flexural toughness) led to a reduction of CH content as shown in Figure 5-51. Thus, CH cannot reprecipitate within the fiber cell wall and/or fiber lumen of the kraft pulp fibers. Thermal analysis of these composites will be redone with TGA/DTA in order to account for calcium carbonate that was previously neglected. In addition, the higher temperatures allowed by TGA/DTA will facilitate the quantification of unreacted SCMs.

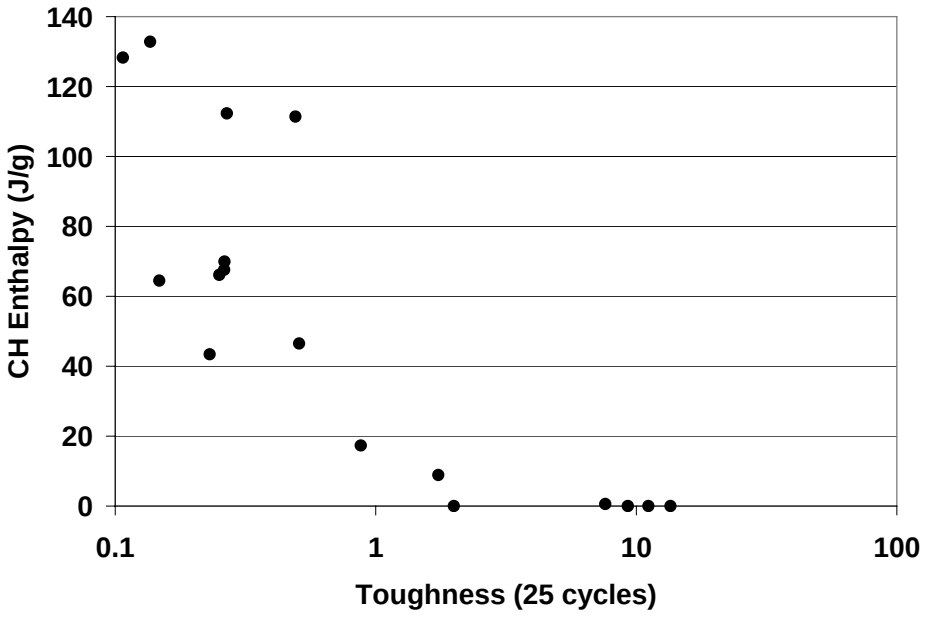

Figure 5-51. CH enthalpy (prior to cycling) as determined by DSC versus flexural post-cracking toughness (after 25 cycles).

5.2.3 Fracture Surface Fractography

5.2.3.1 Fracture Surface Roughness Number

Based on preliminary results as seen in Figure 5-52, a strong correlation exists between the fracture surface roughness and the composite post-cracking toughness. This fractography measurement is an important parameter as toughness is also related to fracture energy (*e.g.*, K_{Ic}). This correlation appears to be linear in nature. One interesting aspect of this linear behavior is the roughness number intercept with no toughness. Theoretically, a fracture surface with no toughness should exhibit a flat fracture surface as would be indicated by a roughness number of 1. However, in the observed measurements, the roughness number intercept is much greater than 1. For these composites, the increased roughness may be related to the imaging technique (*i.e.*, maximum observable resolution). In addition, the inherent porosity and cement hydration product crystals may add to the roughness of the fracture surface while not contributing to fracture energy dissipation.

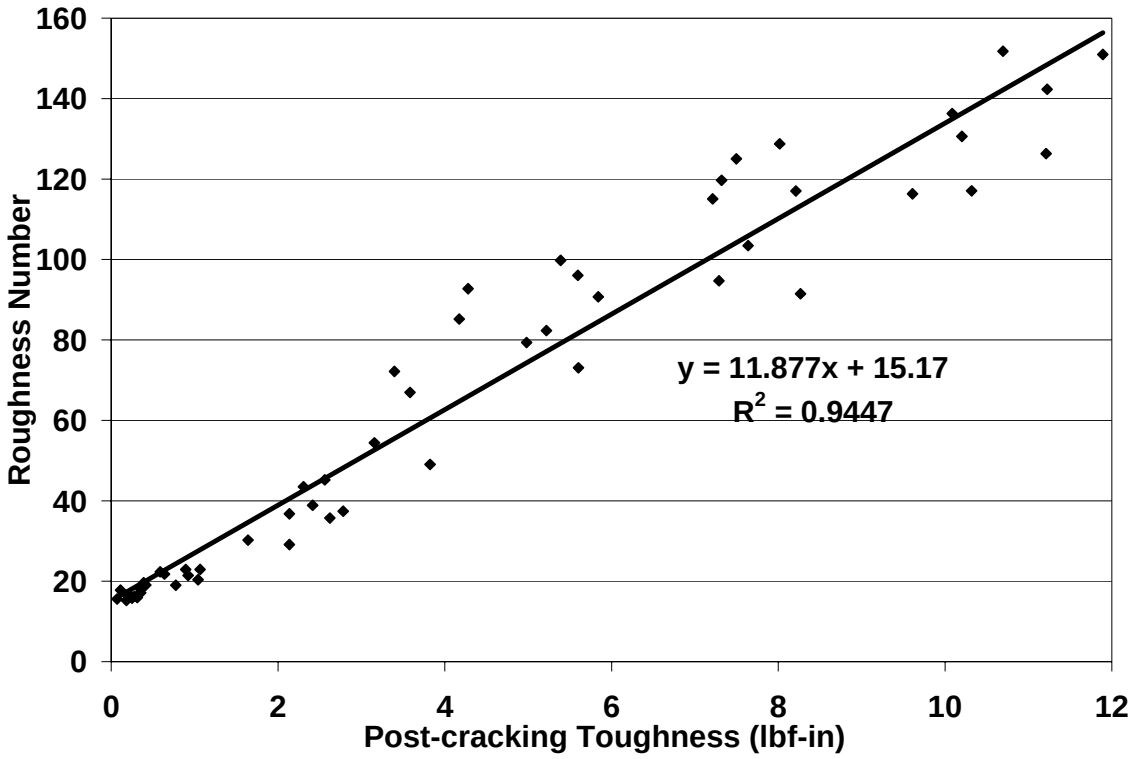

Figure 5-52. Fracture surface roughness versus composite post-cracking roughness.

5.2.3.2 Fracture Surface Fractal Dimension

Another fractography parameter that was investigated was the fracture surface fractal dimension, which allowed for the extrapolation of matrix roughness from the net fracture surface roughness. As seen in Figure 5-22, there are apparent differences in the roughness of the net fracture surface (including fiber effects) as compared to the matrix roughness. In theory, a matrix roughness line with zero slope would indicate that the fibers do not contribute to energy dissipation during fracture due to pure fiber pull-out.

In this case, it can be seen the fibers do contribute some to the energy dissipation, indicating that composite fracture was a combination of fiber pull-out and fiber fracture.

More research is necessary to elucidate the mechanisms of fracture behavior as measured by the fractal dimension. In addition, by measuring the differences in fractal dimension as a function of the number of wet/dry cycles, the fracture behavior can be assessed.

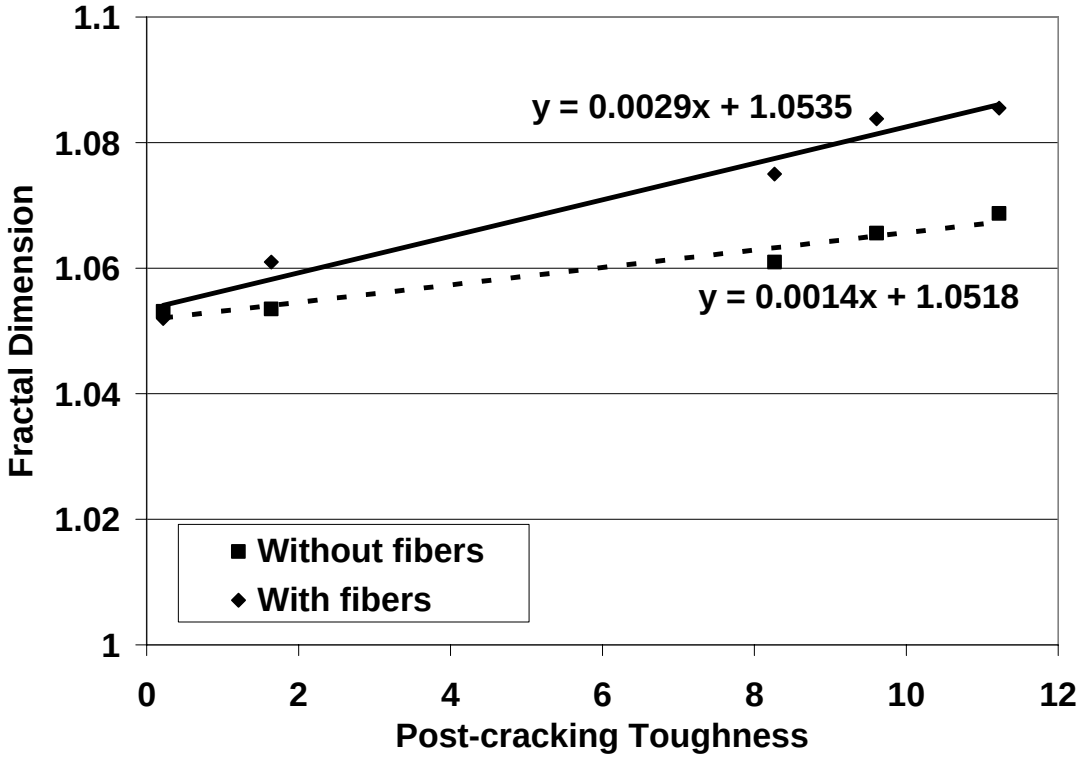

Figure 5-53. Fracture surface fractal dimension versus composite post-cracking toughness.

CHAPTER 6

INTERNAL CURING

The previous chapters have dealt specifically with the wet/dry cycling durability of pulp fiber-cement composites. Though degradation of these composites was found to be severe, the incorporation of pulp fibers to cementitious matrices can still be a viable possibility so long as the fibers mitigate durability concerns prior to substantial environmental exposure. In this chapter, one such aspect – internal curing – will be investigated.

When concrete experiences substantial autogenous shrinkage, cracking results, which compromises both mechanical properties and durability [Jensen and Hansen, 2002]. Portland cement hydration products occupy a lesser volume than the reactants, producing a net chemical shrinkage. In the plastic state, the material is able to contract to accommodate this strain, but, after setting, the chemical shrinkage induces an increase in internal capillary porosity (i.e, those voids ~50μm or smaller) [Bentz *et al.*, 2001]. When the internal relative humidity of the concrete decreases, shrinkage results. Changes in surface tension, disjoining pressure, and capillary tension in the water/air menisci created in these capillary pores have each been proposed as mechanisms leading to this autogenous or self-desiccation shrinkage [Lura *et al.*, 2003]. If the member is subject to internal (*i.e.*, by aggregate or reinforcing steel) or external restraint, cracking can result from tensile stresses induced during shrinkage. Autogenous shrinkage is particularly

problematic in higher strength concrete due to its inherently fine pore structure, use of very fine reactive particles, high cement content, and low water content [Bentz and Jensen, 2004].

Thus, to overcome autogenous shrinkage and related cracking, some have recently proposed "internal curing" of concrete, whereby moisture-rich materials are introduced to the fresh mixture [Jensen and Hansen, 2001; 2002; Jensen and Lura, 2003]. The objective is to provide an adequate internal reservoir of water to compensate for the water lost by self-desiccation.

One well-recognized approach is the use of saturated highly porous minerals or aggregate (*e.g.*, pumice, perlite, expanded clay aggregate, expanded shale aggregate, expanded slate aggregate) in the mixture [Bentz *et al.*, 2005]. These materials may, over time, release water to the hydrating paste, mitigating the effects of autogenous shrinkage. However, control of moisture content with these variable materials is difficult, leading to problems in maintaining consistency. Also, due to their large porosity and relatively large size, their use substantially reduces the strength and elastic modulus of concrete. Due to their ability to adsorb water, clays have been proposed for this purpose, but their tendency for agglomeration in highly ionic media precludes their use [Jensen and Lura, 2003]. Thus, alternative materials which may also act as moisture reservoirs, but which are expected to less negatively impact strength and durability been proposed. These include superabsorbent polymers (SAPs) and diatomaceous earth [Jensen and Hansen, 2001; 2002; Jensen and Lura, 2003].

Wood-derived fibers and powders may also be likely suitable for this application and may be able to provide internal curing water at lower cost than SAPs and

with more control over concrete performance as compared to lightweight aggregate. Wood-derived fibers and powders contain both free and bound water. The free water (*i.e.*, water held in large pores and in the lumen) and weakly bound water may be released into the surrounding, self-desiccating cement matrix over time, providing relief from self-desiccation and subsequent autogenous shrinkage. The objective of this research, then, was to assess the suitability of wood-derived fibers and powders for internal curing [Mohr *et al.,* 2005c].

6.1 Heat of Hydration

Calorimetry was performed to assess the effect of the addition of the wood-derived materials on the rate of hydration of cement paste. Results in Figures 6-1 and 6-2 show that there are negligible differences between the control and the samples containing the fibers or powder. Wood powder appears to be the most deleterious by slightly delaying setting, though overall hydration (*i.e.*, heat evolved) is not significantly suppressed. Therefore, overall, the inclusion of these materials within the cement matrix does not present any notable incompatibilities that would prohibit their use.

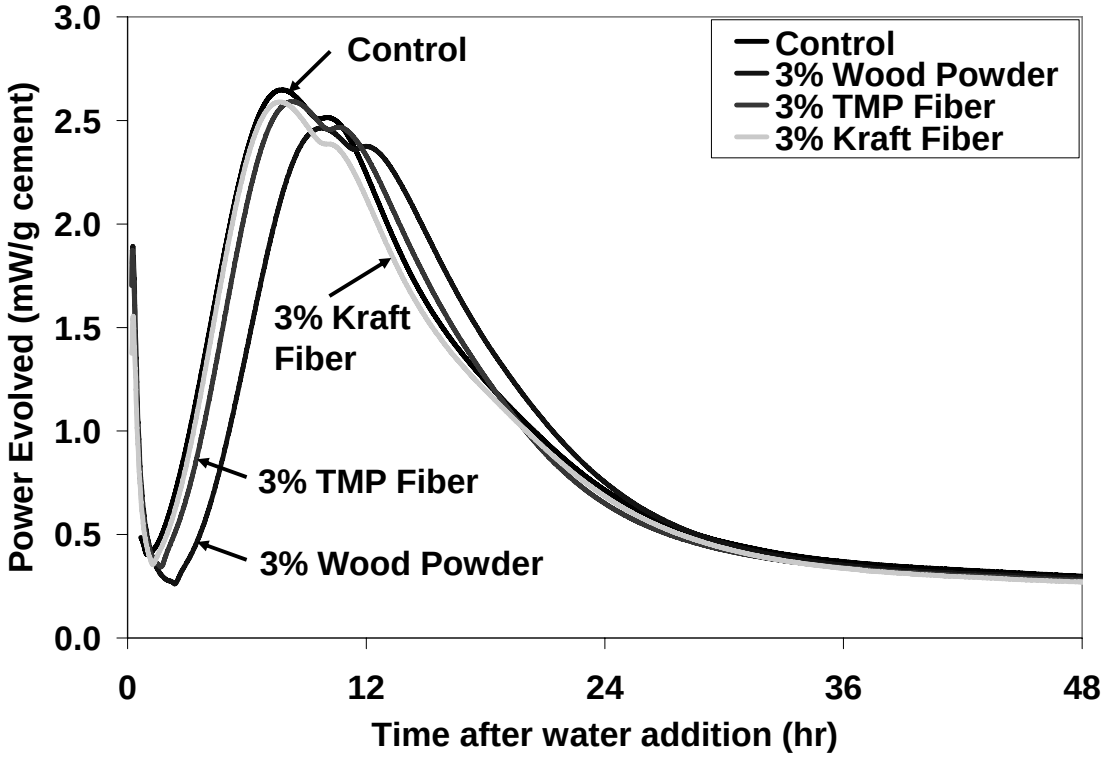

Figure 6-1. Isothermal calorimetry results (power evolved) for composites containing internal curing materials.

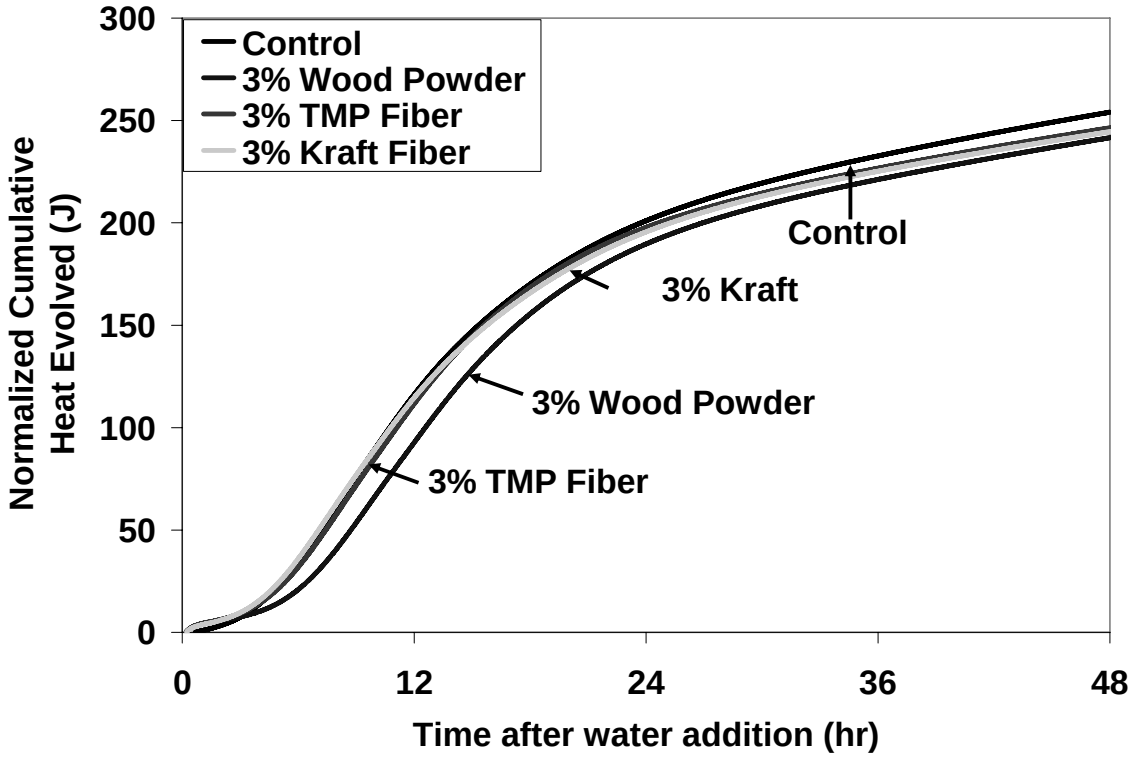

Figure 6-2. Isothermal calorimetry results (cumulative heat evolved) for composites containing internal curing materials.

6.2 Autogenous / Self-Desiccation Deformation

Autogenous deformations were measured for cement pastes containing TMP fibers, kraft pulp fibers, cellulose powder, wood powder, and superabsorbent polymers (SAPs). The mass fractions varied between materials as discussed previously. Final setting times were also measured for the autogenous shrinkage samples. Length measurements began at this time (*i.e.*, zero measurements were taken at final set).

6.2.1 Kraft Fibers and Cellulose Powder

Kraft fibers and cellulose powder did not prove to be effective wood-derived materials for internal curing. This ineffectiveness is most likely due to poor workability at low water-to-cement ratios and minimal absorption of pore solution by these materials. The maximum mass fraction achieved with both materials was only 1.0%, equivalent to $w/c_e = 0.010$. At higher addition rates, the cement paste mix was clumpy and was not workable. Additional superplasticizer, up to the maximum dosage rate, did not produce any improvements in workability.

After 40 days, as seen in Figure 6-3, the kraft fiber composites exhibited autogenous shrinkage of -1021.8 ± 62.1 με ($\mu\varepsilon = 10^{-6}$ mm/mm). The cellulose powders exhibited slightly less shrinkage of -861.8 ± 44.1 με and -848.8 ± 43.0 με for the two types of powders, respectively. Thus, because similar behavior was observed for the fibers and powders, it is realized that fiber length does not seem to influence autogenous shrinkage. That is, there does not appear to be any mechanical effect (*i.e.*, internal restraint) of fiber addition, at least for the lower dosage rates and short fiber lengths (i.e, less than 1.0 mm).

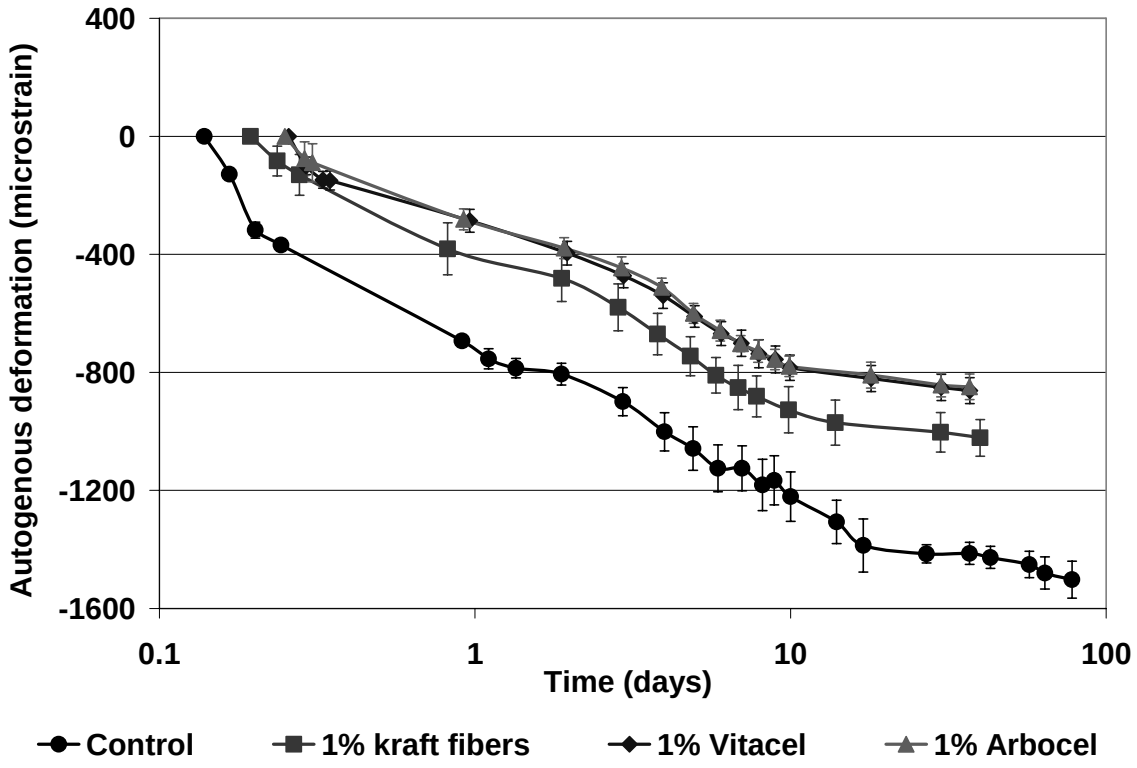

Figure 6-3. Autogenous shrinkage for pastes containing kraft fibers and cellulose powder (*Vitacel* and *Arbocel*).

6.2.2 TMP Fibers and Wood Powder

TMP fibers were previously found to be more easily incorporated into fresh cement due to a stiffer fiber cell well (due to the presence of lignin) and shorter fiber length [McDonough *et al.*, 1997]. Thus, good workability was easily achieved at relatively high mass fractions. Results are shown in Figures 6-4 and 6-5 for TMP and wood powder composites, respectively. It can be seen that as the addition rate increased, autogenous shrinkage decreased for both the TMP fiber and wood powder composites. All TMP and wood powder composites exhibited noticeable expansion during the first

several days. Sample length expansion and time of observed expansion increased with increasing dosage rates, up to 2.25%, as well. After 40 days, the minimum shrinkage observed was -196.6 ± 25.9 με and -211.0 ± 53.1 με, for the TMP fiber and wood powder pastes, respectively. This appears to indicate that the entrained water contained within the fiber/powder lumen and cell wall is being slowly released to the self-desiccating matrix and providing the water needed for continued internal curing. It is interesting to note that the 3.0% TMP composite did not provide additional benefits as compared to the 2.25% TMP composite. This behavior will be addressed later as this behavior was also observed for pastes containing SAPs.

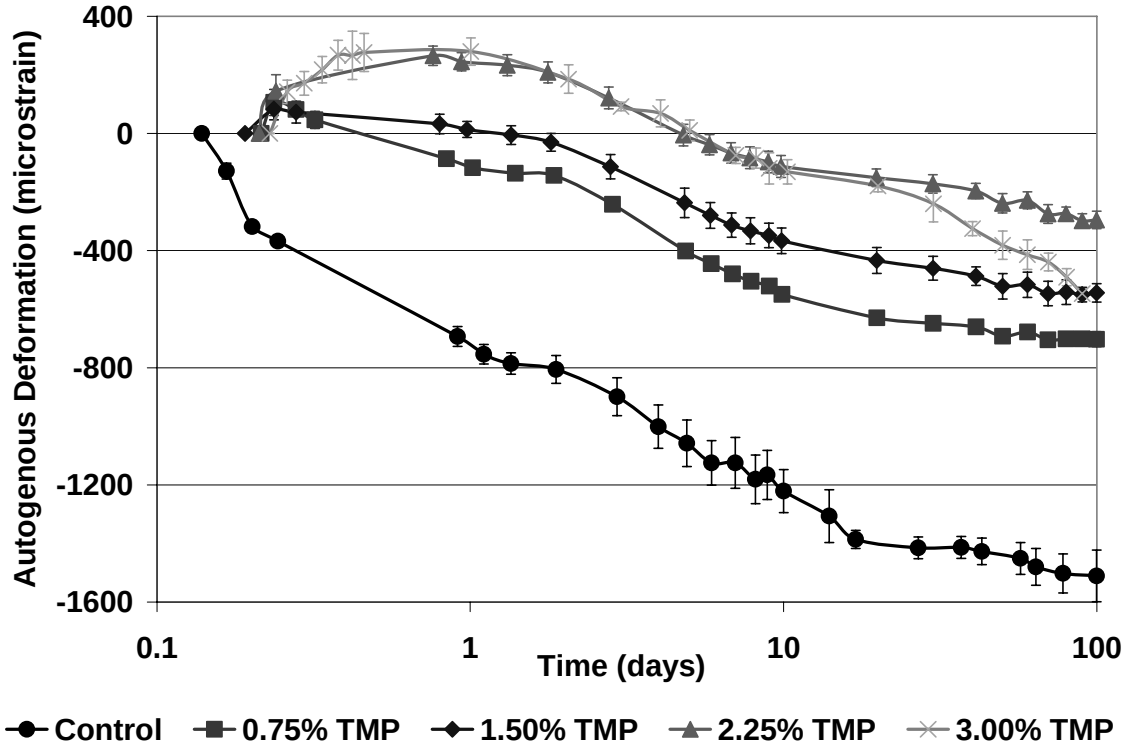

Figure 6-4. Autogenous shrinkage for pastes containing TMP fibers.

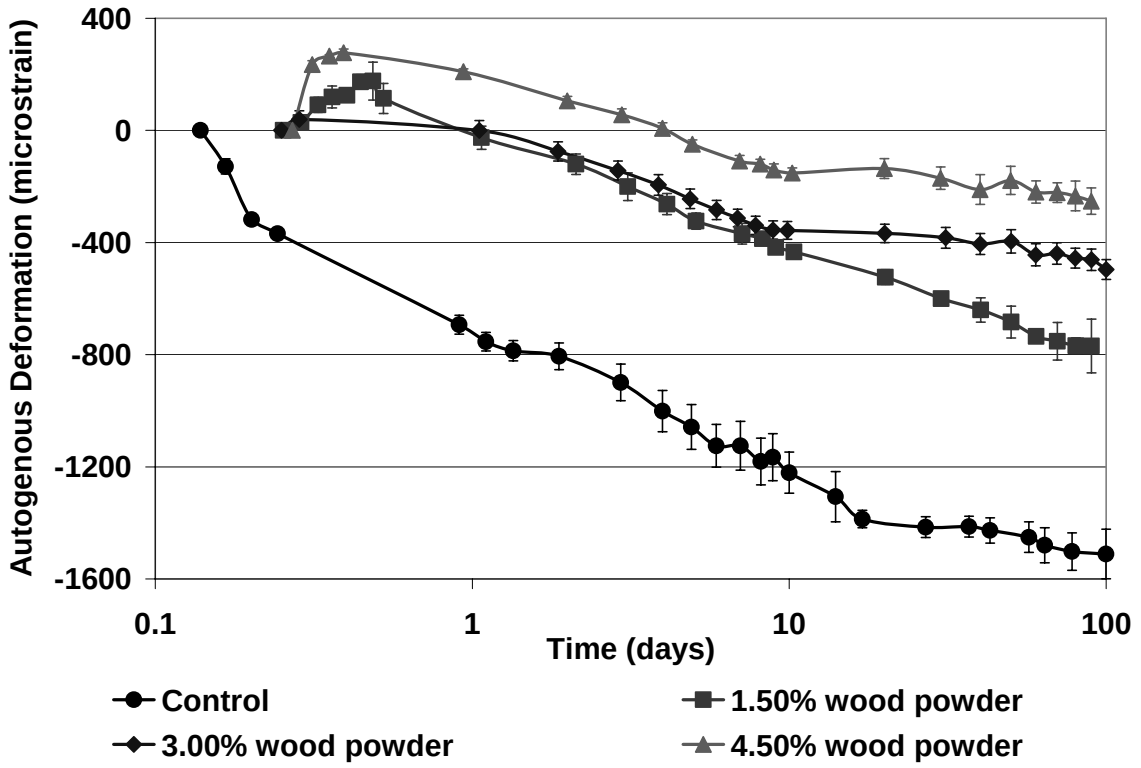

Figure 6-5. Autogenous shrinkage for pastes containing wood powder.

6.2.3 Super Absorbent Polymers (SAPs)

The previous results have shown the effectiveness of certain wood-derived materials at mitigating autogenous shrinkage. However, one of the most commonly used materials for this application has been SAPs. These polymers were tested in conjunction with the wood-derived materials in order to provide a basis for comparison. As seen in Figure 6-6, the addition of SAPs to cement did provide some reduction in autogenous shrinkage. However, after 40 days, minimum autogenous shrinkage strains were reduced to -763.3 ± 114.2 με, as compared to -1427.3 ± 45.1 με in the control at this age.

As with the TMP results, there appears to be a threshold water entrainment dosage above which the addition of water does not lead to increased benefits. For SAPs, this water entrainment threshold value is 0.05 (0.50% SAP) and for the TMP fiber composites, it is 0.075 (2.25% TMP). The differences in threshold values may be related to the water release rate of the particular material. That is, the TMP fibers are thought to release water more slowly than SAPs, thus explaining initial TMP expansion and subsequent minimal shrinkage. In addition, the threshold value may also be a function of material distribution and spacing. In this situation, the SAPs achieve maximum spacing at lower water entrainment rates than the TMP fibers. Further research in under way to elucidate this threshold mechanism. It is anticipated that the use of coatings for the wood-derived materials – used to control the water release rate – will provide insight into this mechanism.

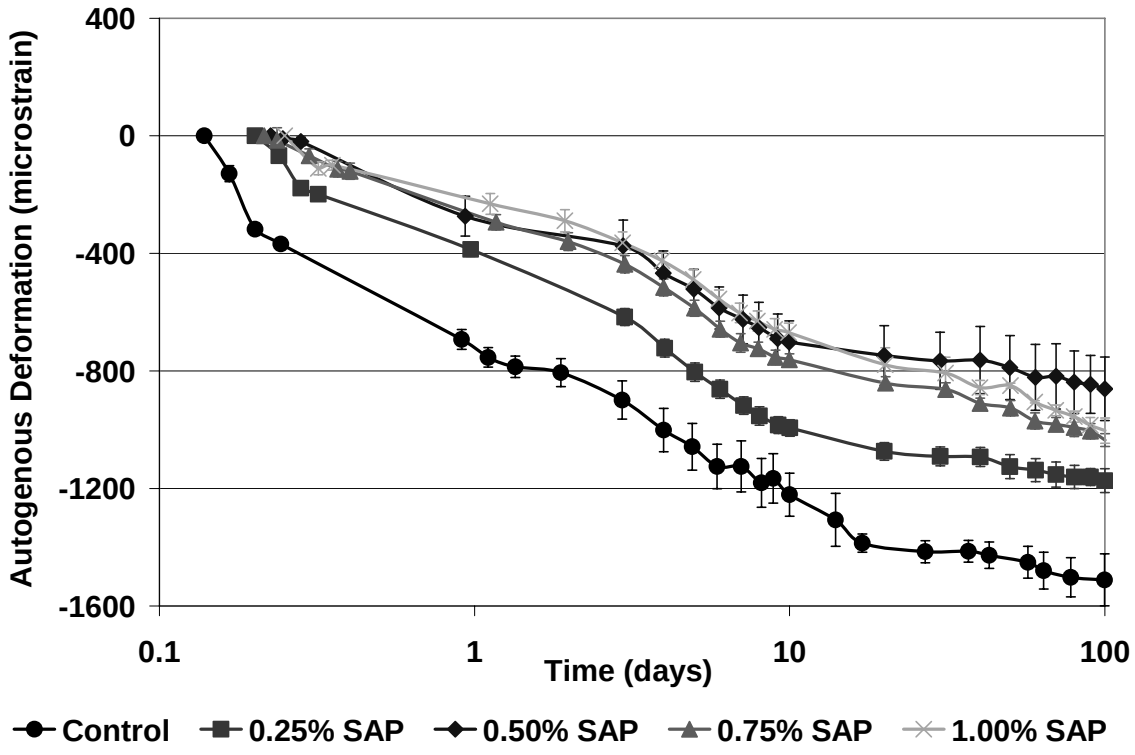

Figure 6-6. Autogenous shrinkage for pastes containing SAPs.

6.3 Compressive Strength

Compressive strength was measured to probe the efficiency of the internal curing materials at increasing the degree of hydration of the cement paste as well as to identify any incompatibilities between the internal curing materials and cement hydration. As stated previously, only relative strength differences should be considered due to the non-standard specimen geometry. Specimens were tested in compression at 3, 7, and 14 days and at the same dosage rates as that evaluated for autogenous shrinkage.

Figure 6-7 illustrates the strength trends for the kraft fiber and cellulose powder cement composites. It can be seen that the addition of kraft fibers led to a decrease in strength at all ages. The cellulose powder sample strengths were similar to the control beyond 3 days. As realized in the previous section concerning autogenous shrinkage, the differences between the two types of cellulose powders, varying in fiber length only, are negligible.

As for the wood-derived materials that decreased autogenous shrinkage, the compressive strength results for the TMP fiber and wood powder composites are shown in Figures 6-8 and 6-9, respectively. In Figure 6-8, it appears that the 0.75% and 1.5% TMP dosage rates led to a similar decrease (~15-20%) in strength as compared to the control at 14 days. As the dosage rate incrementally increased above 1.5%, further progressive decreases in strength were observed. The addition of 3% TMP fibers by mass led to an approximate 30% decrease in strength at 14 days compared to the control. Similarly in Figure 6-10, the strength of the wood powder composites progressively decreased with increased dosage rate. However, there is no clear strength leveling with the wood powder data, as was observed with TMP fibers. This may be due to the increased water entrainment amounts relative to the TMP samples.

In Figure 6-10, the strength of the cement samples containing SAPs is shown. At lower dosage rates – water entrainment less than 0.05 – there is no decrease in strength relative to the control. This was expected, as previously shown as the equivalence of competing mechanisms (*i.e.*, increased porosity versus increased degree of hydration) by [Jensen and Hansen 2001]. At higher dosage rates, strength decreased noticeably due to increased porosity and no change in the degree of hydration at these

early ages. These strength values were similar to the TMP composites entraining the same amount of water. That is, at 14 days, the compressive strength of the 0.75% and 1.0% SAP samples were approximately 25% less than the control.

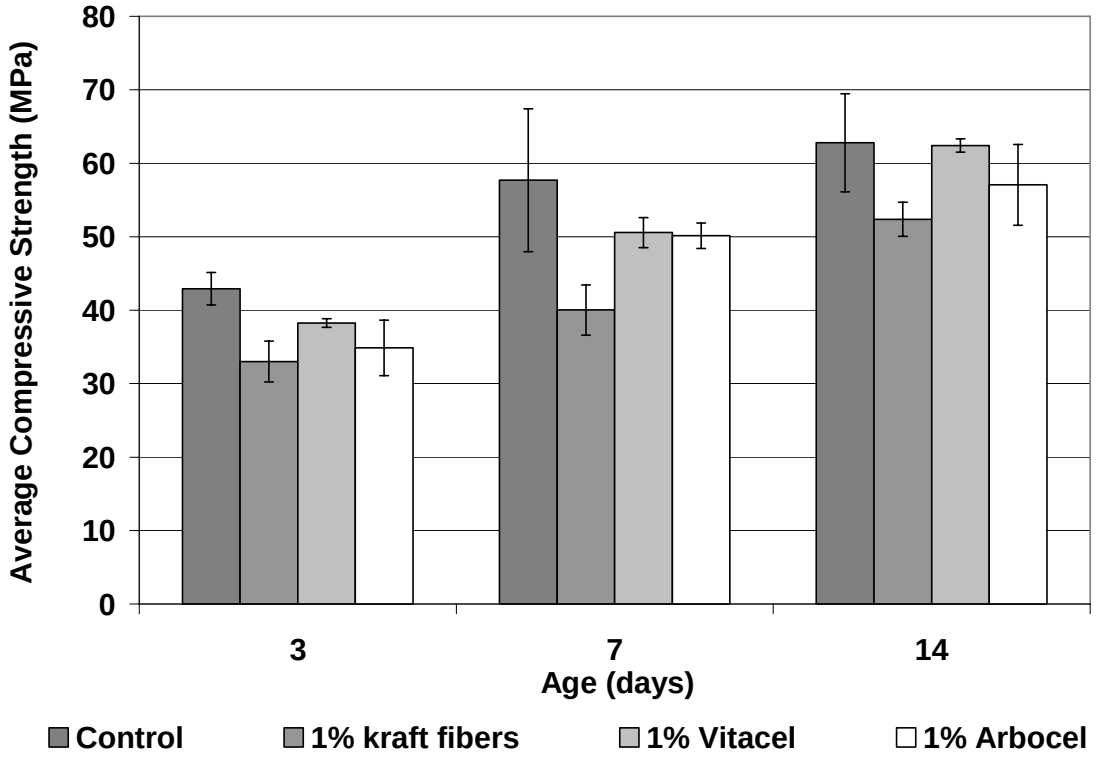

Figure 6-7. Compressive strength for pastes containing kraft fibers and cellulose powder (*Vitacel* and *Arbocel*).

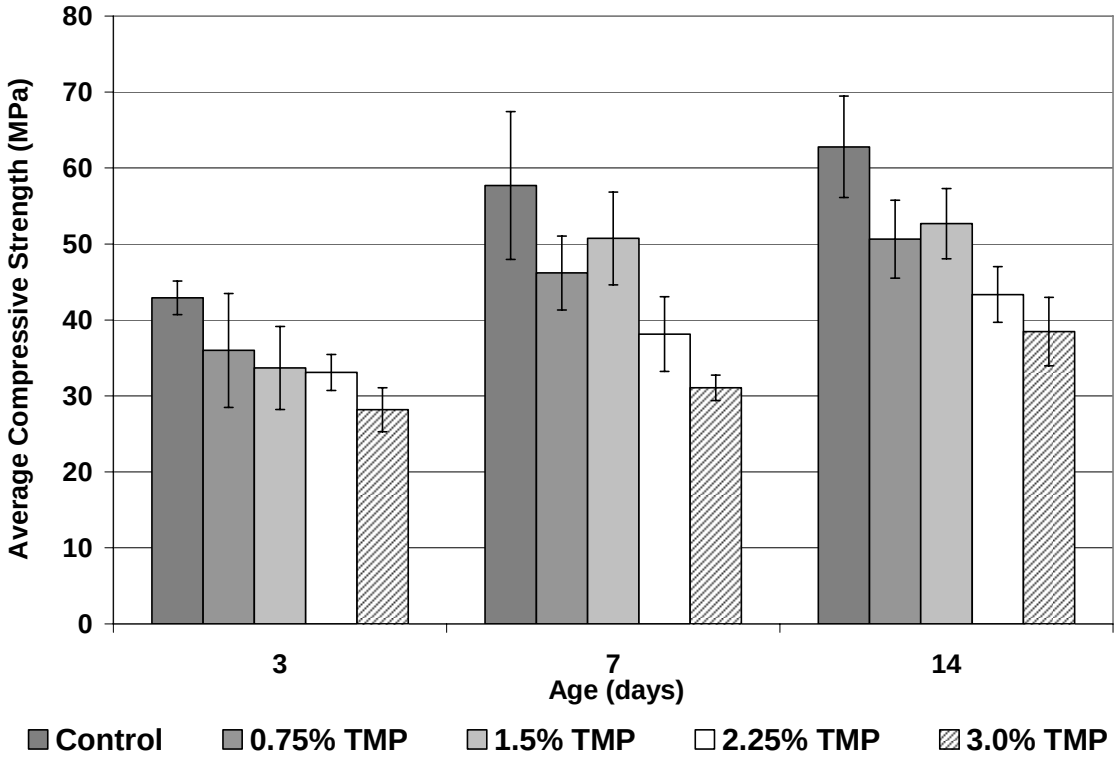

Figure 6-8. Compressive strength for pastes containing TMP fibers.

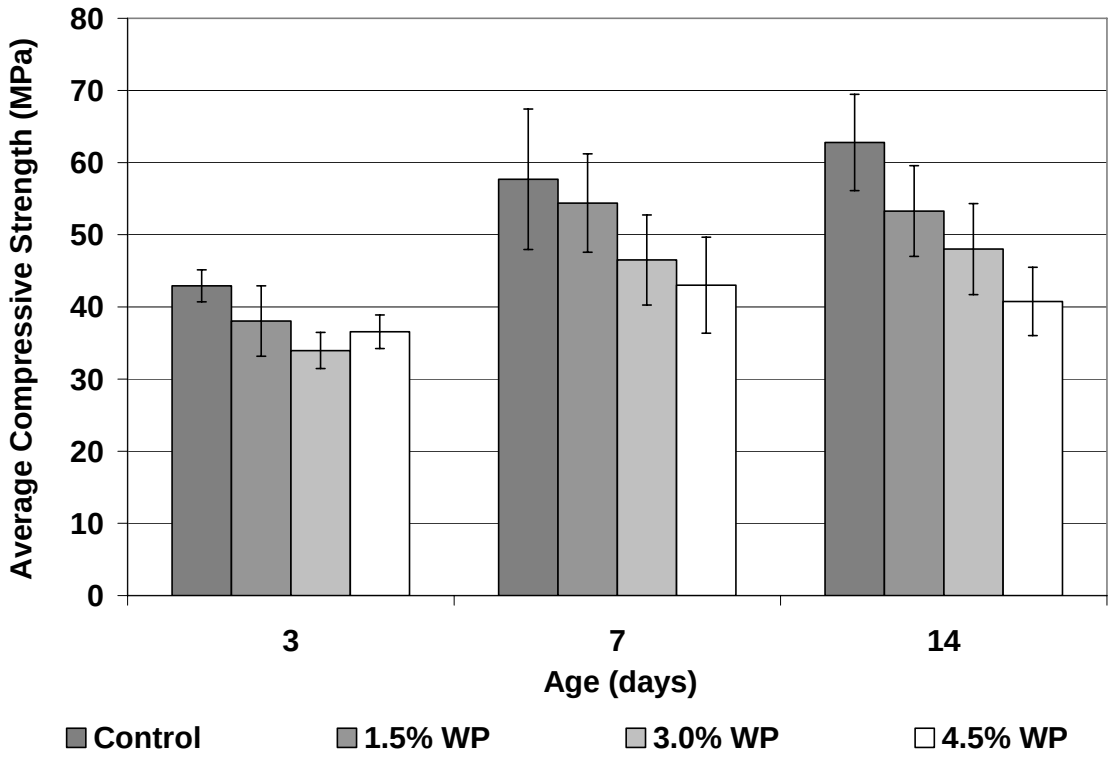

Figure 6-9. Compressive strength for pastes containing wood powder.

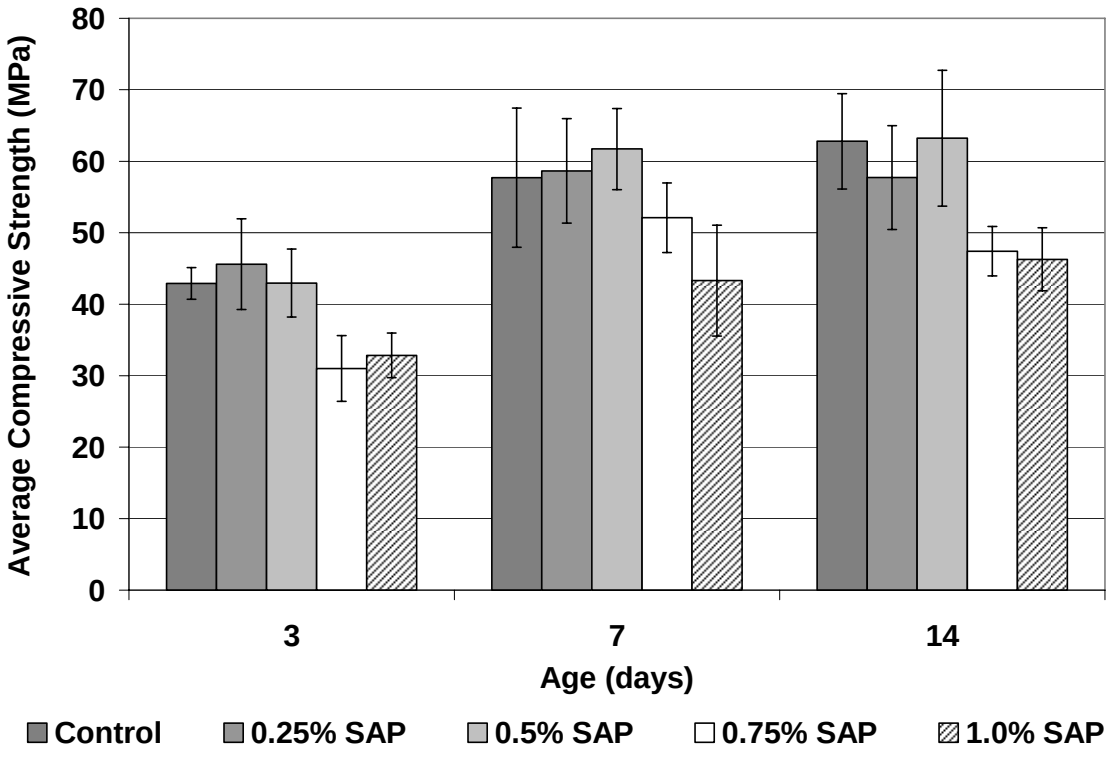

Figure 6-10. Compressive strength for pastes containing SAPs.

CHAPTER 7

CONCLUSIONS, RECOMMENDATIONS, AND FUTURE RESEARCH

Pulp fibers are unique reinforcing materials as they are non-hazardous, renewable, and readily available at relatively low cost compared to other commercially available fibers. However, to ensure the satisfactory performance of pulp fiber-cement materials, improved understanding of their expected long-term performance was essential. In particular adequate understanding of the effect of moisture fluctuations expected during exterior exposure on performance over time was critical to ensure durability of these pulp fiber-cement composites and to gain market acceptance for these materials. Although natural fibers have been used historically to reinforce various building materials, little scientific effort has been devoted to the examination of natural fibers to reinforce cement-based engineered materials. Thus, one of the objectives of this research program was to thoroughly investigate the durability of pulp fiber-cement composites and the mechanisms of degradation due to wet/dry cycling. In addition to the wet/dry cycling durability aspects, pulp fibers were also investigated for their ability to mitigate self-desiccation and subsequent autogenous shrinkage in high-performance cement pastes.

7.1 Conclusions

7.1.1 Wet/Dry Cycling – Fiber Modifications

7.1.1.1 Kraft Pulp Fiber-Cement Composites

Three pulp fiber treatments were evaluated to identify those treatments that may minimize composite degradation due to wet/dry cycling. Mechanical testing of specimens was conducted after 0, 1, 2, 5, 10, 15, and 25 wet/dry cycles. SEM observation of fracture surfaces was done to verify the mechanical testing results. From testing and microstructural characterization, these conclusions may be drawn:

- With the exception of fiber A (unbleached), the majority of first crack and peak strength loss and decrease in post-cracking toughness occurred within a low number of wet/dry cycles (typically less than 5 cycles).

- Beating did not appear to significantly affect mechanical behavior of the composite after exposure, although variations in fiber damage (including separation of S1 from S2 layer) were observed by SEM. Prior to wet/dry cycling, unbeaten fiber composites exhibited greater peak strength and post-cracking toughness.

- Bleached (*i.e.* low-lignin) fibers exhibited accelerated progression of fiber mineralization as compared to unbleached fibers. Unbleached fiber-cement composites exhibited greater toughness, particularly for low numbers of wet/dry cycles. Without exposure, unbleached fiber composites exhibit greater flexural properties than bleached fiber composites.

- Once-dried fiber composites exhibited superior dimensional stability compared to never-dried fiber composites. However, the drying state of the fibers did not appear to have any significant effect composite performance during wet/dry exposure. Thus, initial fiber swelling/shrinking does not seem to play any role in composite degradation.

- For all kraft pulp fiber-cement composites, the majority of losses in strength and toughness were found to occur at a low number of cycles (*i.e.*, less than 5 wet/dry cycles). Fiber pull-out lengths were also found to shorten significantly up to 5 cycles while displaying ductile fiber failure.

- It is proposed that a three-part progressive series of degradation mechanisms exists for these fiber-cement composites: (1) fiber-cement debonding up to 2 cycles, (2) subsequent reprecipitation of hydration products within the void space at the former fiber-cement interface, prior to 10 wet/dry cycles, as evidenced by observations of ductile fiber failure at the same time as significant decreases in strength and toughness, and (3) fiber embrittlement due to

mineralization, which appears to occur beyond 10 cycles as indicated by relatively small increases in strength and no recovered toughness.

7.1.1.2 TMP Fiber-Cement Composites

Flexural testing of specimens was conducted after 0, 1, 2, 5, 10, 15, and 25 wet/dry cycles. Prior to cycling, the shorter fiber length of TMP fibers, as compared to kraft fibers, is believed to lead to higher first crack strength, but lower peak strength and post-cracking toughness. After 25 cycles, TMP composites exhibited higher strength and toughness than kraft pulp composites.

In general, losses in mechanical properties (*i.e.*, peak strength, post-cracking toughness) progressed more slowly in TMP composites than for bleached or unbleached kraft pulp composites. Losses of 50% or more in post-cracking toughness, compared to that prior to cycling, were observed after 1 and 2 cycles for the bleached and unbleached kraft pulp composites, respectively. However, the TMP composites exhibited toughness losses of more than 50% after 15 wet/dry cycles. Similarly, bleached and unbleached kraft pulp composites exhibited losses of more than 25% in peak strength after 1 and 2 cycles, respectively, while TMP composites did *not* exhibit strength losses greater than 25% over the range of wet/dry cycles investigated here.

These results run contrary to ACI 544 recommendations on natural fiber chemical composition. Based on the results presented here, the component – lignin – mostly though to be extremely susceptible to alkali degradation, was shown to be the primary factor responsible for the improved rates of degradation of TMP fiber composites

as compared to composites containing kraft pulp fibers. It is anticipated that this work will be of particular interest to this ACI committee and will be incorporated into future recommendations.

7.1.1.3 Proposed Composite Degradation Mechanisms

Much of the previously published research has focused on the mechanical properties of natural fiber-cement composites. Thus, few results are available concerning the microstructural durability of these composites during wet/dry cycling, particularly the progression of degradation. The progressive series of degradation mechanisms presented in Chapter 4 has been the first comprehensive explanation of composite degradation due to wet/dry cycling. Previous examinations of composite degradation only investigated composite behavior prior to and after a set number of wet/dry cycles. This research is believed to be the first thorough examination of the progression of degradation as evaluated by mechanical testing, microstructural characterization, and chemical analysis.

This series of mechanisms proposed: (1) initial fiber-cement debonding (due to fiber shrinkage during drying), as indicated by decreases in strength between 0 and 2 cycles, (2) reprecipitation of relatively low-strength hydration products (*i.e.*, secondary ettringite) within this new void space, introduced at the former fiber-cement interface, minimizing fiber dimensional changes during subsequent wetting, and (3) fiber mineralization by the reprecipitation of hydration products, likely primarily calcium hydroxide, within the fiber cell wall structure.

During the initial wet/dry cycles, prior to the reprecipitation of hydration products around the fiber, the fibers are largely free to shrink and swell without impedance. Upon drying, diametrical fiber shrinkage may create a capillary expulsive pressure on the pore solution residing within the fiber lumen. Such a pressure would cause the pore solution to be primarily expelled through the fiber ends and pits along the fiber. During this drying, reprecipitation of hydration products can occur in this space at the former fiber-cement interface. However, the reprecipitation of hydration products such as ettringite can restrain fiber swelling upon rewetting. During subsequent drying, then, fiber shrinkage is also reduced. Thus, the driving force for pore solution expulsion is minimized. That is, the pore solution resides within the fiber for a longer period of time. Therefore, the pore solution will not only migrate from the fiber lumen to the matrix through the ends and fiber pits, but the solution can also diffuse from the lumen through the cell wall, resulting in a deposition of hydration products within the fiber cell wall. This deposition or reprecipitation decreases fiber ductility and leads to shorter fiber pull-out lengths in the composite. Complete fiber mineralization may not take place until beyond approximately 10 wet/dry cycles in this research, as suggested by increases in strength between 10 and 25 cycles.

7.1.2 Wet/Dry Cycling – Matrix Modifications

In this study, supplementary cementitious materials as a partial weight replacement for cement and variations in the water-to-cement ratio were investigated as a means to mitigate kraft pulp fiber-cement degradation due to wet/dry cycling. Single,

ternary, and quaternary blends of silica fume, fly ash, metakaolin, and a diatomaceous earth/volcanic ash blend were used. Mechanical testing was conducted after exposure to 0, 1, 2, 5, 10, 15, and 25 wet/dry cycles. From mechanical testing, the following was observed:

- Composites containing 30% SF, 50% SF, 90% SL, and 30% MK235 completely eliminated degradation due to wet/dry cycling. However, all but the SL composite are not practical for large-scale production.

- Ternary and quaternary blends of 10% SF/70% SL, 10% MK235/70% SL, and 10% MK235/10% SF/70% SL also completely eliminated composite degradation at more practical replacement values.

- Composite pore structure and permeability do not seem have an effect on durability for these cast-in-place composites.

- There is not an observable direct correlation between SCM oxide composition and composite mechanical performance. Instead, improvements in SCM composite durability are most likely related to specific chemical reactions that reduce the matrix calcium hydroxide content and minimize ettringite reprecipitation.

- Laser scanning confocal microscopy of composite fracture surfaces revealed a strong correlation between composite post-cracking toughness and surface roughness. Additional fractography of the surfaces showed that matrix cracking was a contributing factor for increased toughness, as measured by fractal dimension.

7.1.3 Internal Curing

In the work presented here, several wood-derived materials were investigated as economical alternatives to superabsorbent polymers for internal curing applications. This research is believed to be the first investigation to assess the use of wood-derived materials for internal curing. Materials were evaluated for their ability to minimize autogenous shrinkage and investigated for effects on compressive strength. From the testing conducted, the following conclusions may be drawn:

- The wood-derived materials did not appreciably influence cement hydration as measured by isothermal calorimetry.

- Kraft pulp fibers and cellulose powders were ineffective for internal curing applications. Mass fractions capable of mitigating autogenous shrinkage could not be achieved due to low absorption capacity and poor workability.

- TMP fibers and wood powder reduced autogenous shrinkage to a greater extent than the superabsorbent polymers, when comparing equivalent water entrainment rates (*i.e.*, w/cm_e).

- The wood-derived materials tended to adversely influence compressive strength more so than the superabsorbent polymers at low mass fractions (minimal water entrainment). At higher mass fractions, above the critical entrainment amount, ($w/cm + w/cm_e = 0.35$), all materials showed decreased compressive strength due to an increased in the net water-to-cementitious materials ratio.

7.2 Recommendations

7.2.1 Wet/Dry Cycling

The fiber modifications investigated in this research did not mitigate composite degradation after wet/dry cycling. However, the use of high-lignin fibers may be used as an alternative to kraft pulp fibers in commercial products. The slower rates of degradation for the high-lignin fibers may enhance and prolong the life cycle for these commercial materials, such as siding and roofing products. In addition, TMP fibers could be used in conjunction with supplementary cementitious materials to complete mitigate composite degradation.

For large scale commercial production of these composites, the use of greater than 90% slag by weight of portland cement as a matrix is a viable alternative to a pure

portland cement composite. This composite could also be manufactured at a significant economical savings as slag is an industrial by-product with a commercial value approximately half that of portland cement. In addition, ternary and quaternary blends of 10% SF/70% SL, 10% MK235/70% SL, and 10% MK235/10% SF/70% SL also completely eliminated composite degradation. However, due to the high cost of silica fume and metakaolin, these composites could be manufactured at a slightly higher cost than that containing only portland cement. Though, considering the severe degradation of the pure portland cement composites, the increased initial costs may significantly offset the long-term life cycle costs of using a material with poor durability.

7.2.2 Internal Curing

For this particular cementitious system, based solely on autogenous shrinkage performance, the optimum TMP fiber and wood powder dosage rates were found to be 2.25% and 4.50%, respectively. However, these rates led to a 31-35% reduction in compressive strength at 14 days.

By including compressive strength as a factor in the recommendations, 1.5% TMP fibers by mass may be an appropriate dosage rate as it does not compromise strength as much as higher fiber mass fractions. Wood powder may not be an appropriate material when compressive strength is of concern.

7.3 Future Research

7.3.1 Wet/Dry Cycling

In an effort to further substantiate the reprecipitation of calcium hydroxide with the kraft fiber cell wall from 10 to 25 cycles, additional ESEM EDS measurements should be conducted. In order to quantify the relative amount of $Ca(OH)_2$ present within the kraft fiber cell wall, the Ca net intensities at the different numbers of wet/dry cycles should be directly compared. Quantification is possible by controlling the collection time of the EDS spectra. It is anticipated that the calcium net intensity will progressively increase beyond 10 wet/dry cycles, indicating that calcium hydroxide is reprecipitating within the fiber cell wall.

Future research needs to be conducted to identify the role of SCM addition in the modification of the chemical composition of the composites. The research presented here indicated that composite permeability does not appear to play a role in the progression of composite degradation. Thus, this variable has been isolated and its effect on durability may be considered negligible. However, the effect of SCM replacement on the pore solution chemistry and matrix chemical composition needs further evaluation.

To accomplish this goal, additional ESEM EDS measurements should be conducted on all kraft fiber-cement composites containing SCMs. The relative amounts of ettringite and monosulfate will be analyzed as well as the trace composition of the C-S-H.

In addition, as discussed in Chapter 5, the DSC analyses should be replaced with TGA/DTA measurements in order to account for calcium carbonate, which is expected to form from the reaction of calcium hydroxide with carbon dioxide. Thus, previously, the DSC measurements neglected calcium carbonate allowing for only relative trends, not absolute. Future research should definitively quantify the amounts of calcium hydroxide (plus calcium carbonate) present in the samples.

In addition, x-ray diffraction (XRD) measurements should be conducted to determine if any additional phases are involved with the mechanisms of degradation. The role of alkalis is of particular interest and is difficult to evaluate through other means. Thus, XRD measurements should facilitate phase identification of these phases which can be correlated to thermal analysis peaks.

Going beyond the addition of SCMs as a partial weight replacement for cement as a means to mitigate degradation, additional cement types (compositions) should be evaluated. These include cement compositions with low/high C_3A and C_4AF values and low/high sulfate contents. Calcium aluminate and polymer-modified cements are anticipated to be an alternative to SCM-modified cements and should be evaluated for their respective effect on the progression of kraft pulp fiber-cement composite degradation.

7.3.2 Internal Curing

The proof-of-concept research presented here indicated that wood-derived materials are possibly more effective than other materials currently used to mitigate

autogenous shrinkage. However, before wood-derived materials are recommended for commercial applications, more work must be conducted in order to understand the internal curing mechanisms.

In addition, the present work should be scaled up from cement paste to mortar and concrete. This would allow for comparisons to saturated lightweight aggregates which are also commonly used as internal curing materials. Since autogenous shrinkage is relatively difficult to measure, care should be taken in specimen preparation to minimize any moisture migration from or to the self-desiccating concrete specimens. It is anticipated that concretes would be cast in sealed molds and wrapped in aluminum tape after demolding to prevent moisture changes. Also, it is possible to assess autogenous shrinkage through the use of embedded strain gages that would allow for the specimens to be cured in sealed molds.

Not only would the mechanical effects (*i.e.*, autogenous shrinkage and compressive strength) of internal curing with wood-derived materials be investigated, but microstructural aspects should be assessed. For example, applying new techniques for cement-based materials characterization, such as MRI, would allow the tracking of moisture movement through cement paste. Moisture movement tracking is particularly useful to determine an appropriate water release rate from a particular material.

REFERENCES

AASTHO PP 34-99, Standard practice for estimating the cracking tendency of concrete, American Association of State Transportation and Highway Officials, Washington, DC, 2003.

ACI544.1R, State-of-the-art report on fiber reinforced concrete, American Concrete Institute, Detroit, Michigan, USA, 1996.

Andonian R, Mai YW, Cotterell B. Strength and fracture properties of cellulose fibre reinforced cement composites. The International Journal of Cement Composites 1979;1(3):151-158.

ASTM C 191, Standard test method for time of setting of hydraulic cement by vicat needle, American Society for Testing and Materials, West Conshohocken, PA, 2003.

ASTM C 293, Standard test method for flexural strength of concrete (using simple beam with center-point loading), American Society for Testing and Materials, West Conshohocken, PA, 2002.

ASTM C 348, Standard test method for flexural strength of hydraulic-cement mortars, American Society for Testing and Materials, West Conshohocken, PA, 2002.

ASTM C 1260, Standard test method for alkali reactivity of aggregates (mortar-bar method), American Society for Testing and Materials, West Conshohocken, PA, 2001.

ASTM C 1581, Standard Test Method for Determining Age at Cracking and Induced Tensile Stress Characteristics of Mortar and Concrete under Restrained Shrinkage, American Society for Testing and Materials, West Conshohocken, PA, 2004.

Balaguru P. Contribution of fibers to crack reduction of cement composites during the initial and final setting period. ACI Materials Journal 1994;91(3):280-288.

Batic OR, Milanesi CA, Maiza PJ, Marfil SA. Secondary ettringite formation in concrete subjected to different curing conditions. Cement and Concrete Research 2000;30:1407-1412.

Bentur A, Akers SAS. The microstructure and ageing of cellulose fibre reinforced cement composites cured in a normal environment. International Journal of Cement Composites and Lightweight Concrete 1989;11(2):99-109.

Bentz DP, Jensen OM, Hansen KK, Olesen JF, Stang H, Haecker CJ. Influence of cement particle-size distribution on early age autogenous strains and stresses in cement-based materials. Journal of the American Ceramic Society 2001;84:129-135.

Bentz DP, Jensen OM. Mitigation strategies for autogenous shrinkage cracking. Cement and Concrete Research 2004;26:677-685.

Bentz DP, Lura P, Roberts JW. Mixture proportioning for internal curing. Concrete International 2005;27:35-40.

Bergstrom SG, Gram H. Durability of alkali-sensitive fibres in concrete. International Journal of Cement Composites and Lightweight Concrete 1984;6(2):75–80.

Blankenhorn PR, Blankenhorn BD, Silsbee MR, DiCola M. Effects of fiber surface treatments on mechanical properties of wood fiber-cement composites. Cement and Concrete Research 2001;31:1049-1055.

Bledzki AK, Gassan J. Composites reinforced with cellulose based fibres. Progress in Polymer Science 1999;24:221-274.

Bonen D, Diamond S. Interpretation of compositional patterns found by quantitative energy dispersive x-ray analysis for cement paste constituents. Journal of the American Ceramic Society 1994;77(7):1875-1882.

Cabrera JG, Cusens AR, Brookes-Wang Y. Effect of superplasticizers on the plastic shrinkage of concrete. Magazine of Concrete Research 1992;44(160):149-155.

Campbell MD, Coutts RSP. Wood fibre-reinforced cement composites. Journal of Materials Science 1980;15(8):1962-1970.

Canovas SK, Selva NH, Kawiche GM. New economical solutions for improvement of durability of Portland cement mortars reinforced with sisal fibres. Materials and Structures 1992;25:417–22.

Coutts RSP, Kightly P. Microstructure of autoclaved refined wood-fibre cement mortars. Journal of Materials Science 1982;17(6):1801-1806.

Coutts RSP. Wood fibres in inorganic matrices. Chemistry in Australia 1983;50(5):143-148.

Coutts RSP, Kightly P. Bonding in wood fibre-cement composites. Journal of Materials Science 1984;19(10):3355-3359.

Coutts RSP. Autoclaved beaten wood fibre-reinforced cement composites. Composites 1984;15(2):139-143.

Coutts RSP, Warden PG. Air-cured, wood pulp fibre cement composites. Journal of Materials Science Letters 1985;4(1):117-119.

Coutts RSP. Eucalyptus wood fibre-reinforced cement. Journal of Materials Science Letters 1987a;6(8):955-957.

Coutts RSP. Air-cured wood pulp fibre-cement mortars. Composites 1987b;18(4):325-328.

Coutts RSP. Fibre-matrix interface in air-cured wood-pulp fibre-cement composites. Journal of Materials Science Letters 1987c;6:140-142.

Coutts RSP, Warden PG. Effect of compaction on the properties of air-cured wood fibre reinforced cement. Cement and Concrete Composites 1990;12:151-156.

Davies GW, Campbell MD, Coutts RSP. A SEM study of wood fibre reinforced cement composites. Holzforschung 1981;35:201-204.

De Gutierrez RM, Diaz LN, Delvasto S. Effect of pozzolans on the performance of fiber-reinforced mortars. Cement and Concrete Composites 2005;27(5):593-598.

El-Ashkar NH. Wood pulp microfibers in cement-based composites: improving fiber distribution and characterizing composite behavior. Ph.D. Thesis, Georgia Institute of Technology, Atlanta, GA, 2002a, p. 343.

El-Ashkar NH, Mohr BJ, Nanko H, Kurtis KE. Durability of pulp fiber-cement composites to wet/dry cycling. In: Proceedings of the International Conference on Advances in Building Technology 2002b;1: 233-237.

El-Ashkar NH, Nanko H, Kurtis KE. Investigation of Flexural Properties of Wood Pulp Microfiber Cement-Based Composites. In: El-Dieb AS, Lissel SL, Reda Taha MM, editors. Proceedings of the International Conference on Performance of Construction Materials in the New Millennium. Cairo, Egypt, 2003. p. 1055-1064.

Graham MS. Fiber cement product performance. Professional Roofing, October 2000.

Gram H. Methods for reducing the tendency towards embrittlement in sisal fibre concrete. Nordic Concrete Research 1983;2:62–71.

Hearle JWS, Sparrow JT. Mechanics of the extension of cotton fibres, Part II: theoretical modeling. Journal of Applied Polymer Science 1979;8(2):1857-1874.

Hojaji H, James Hardie Corporation. Personal communication, April 2005.

Illston JM, Domone PLJ. Construction Materials: Their Nature and Behavior. New York: Spon Press, 2001.

Jensen OM, Hansen PF. A dilatometer for measuring autogenous deformation in hardening cement paste. Materials and Structures 1995;28(181):406-409.

Jensen OM, Hansen PF. Water entrained cement-based materials, I: Principles and theoretical background. Cement and Concrete Research 2001;31:647-654.

Jensen OM, Hansen PF. Water entrained cement-based materials, II: Experimental observations, Cement and Concrete Research 2002;32:973-978.

Jensen OM, Lura P. Techniques for internal water curing of concrete. Proc. ECI Advances in Cement and Concrete: Copper Mountain, Colorado, USA, Eds: Lange, D.A., Scrivener, K.L., Marchand, J., 2003:67-78.

Justice JM, Kennison LH, Mohr BJ, Beckwith S, McCormick L, Wiggins B, Zhang ZZ, Kurtis KE. "Comparison of Two Metakaolins and Silica Fume Used as Supplementary Cementitious Materials." In: Proceedings of the ACI 7th International Symposium on Utilization of High-Strength/High Performance Concrete, SP-228, Detroit: American Concrete Institute, 2005:213-235.

Kubotsu A, Ueda M. A new conductive treatment of the specimen for scanning electron microscopy. Journal of Electron Microscopy 1980;29(1):45-53.

Kurpiel FT. Diffusion of cellulose fiber-cement siding and roofing into North America. In: Moslemi AA, editor. Proceedings of Inorganic-Bonded Wood and Fiber Composite Materials. 1997. p. 41-44.

Kurpiel FT. Fiber-cement siding is tomorrow's growth product. Wood Technology 1998;125(1):50-54.

Kurtis KE, El-Ashkar NH, Collins CL, Naik NN. Examining cement-based materials by laser scanning confocal microscopy. Cement and Concrete Composites 2002;25:695-701.

Kurtis KE, Nanko H, El-Ashkar, NH. US Patent 20020160174, 6 November 2001.

Lee AWC, Hong Z. Compressive strength of cylindrical samples as an indicator of wood-cement compatibility. Forest Products Journal 1986;36(11/12):87-90.

Lehtonen L, unpublished results, 2003.

Lin X, Silsbee MR, Roy D.M, Kessler K, Blankenhorn PR. Approaches to improve the properties of wood fiber reinforced cementitious composites. Cement and Concrete Research 1994;24(8):1558-1566.

Lura P, Jensen OM, Van Breugel K. Autogenous shrinkage in high performance cement paste: An evaluation of basic mechanisms. Cement and Concrete Research 2003:33:223-232.

MacVicar R, Matuana LM, Balatinecz JJ. Aging mechanisms in cellulose fiber reinforced cement composites. Cement and Concrete Composites 1999;21:189-196.

Mai YW, Hakeem MI, Cotterell B. Effects of water and bleaching on the mechanical properties of cellulose fibre cements. Journal of Materials Science 1983;18:2156-2162.

Marikunte S, Soroushian P. Statistical evaluation of long-tern durability characteristics of cellulose fiber reinforced cement composites. ACI Materials Journal 1994;91(6):607-616.

Marusin SL. A simple treatment to distinguish alkali-silica gel from delayed ettringite formation in concrete. Magazine of Concrete Research 1994;46(168):163-167.

McDonough TJ, Aziz S, Rankin KL. The strength of mechanical pulp fibers. ICP Technical Paper Series #267, The Institute of Paper Chemistry, Appleton, WI, 1987.

Mohr BJ, Nanko H, Kurtis KE. Aligned Kraft Pulp Fiber Sheets for Reinforcing Mortar. Submitted to Cement and Concrete Composites, December 2003.

Mohr BJ, Nanko H, Kurtis KE. Durability of Kraft Pulp Fiber-Cement Composites to Wet/Dry Cycling. Cement and Concrete Composites 2005a;27(4):435-448.

Mohr BJ, Nanko H, Kurtis KE. Durability of Thermomechanical Pulp Fiber-Cement Composites to Wet/Dry Cycling. Cement and Concrete Research 2005b;35(8):1646-1649.

Mohr BJ, Premenko L, Nanko H, Kurtis KE. Examination of Wood-Derived Powders and Fibers for Internal Curing of Cement-Based Materials. In: Proceedings of the 4th International Seminar on Self-Desiccation and Its Importance in Concrete Technology, Eds. Persson, B., Bentz, D., Nilsson, L.O., 2005c:229-244.

NAHBRC. Moisture-related problems with engineered wood. ToolBase TechNotes, http://www.nahbrc.org/ToolBase/hotline/TechNote/moisture_prob_engwood.htm, April 2005.

Naik TR, Friberg, TS, Chun Y. Use of pulp and paper mill residual solids in production of cellucrete. Cement and Concrete Research 2004;34:1229-1234.

Nanko H, Asano S, Ohsawa J. Shrinkage behavior of pulp fibers during drying. In: Proceedings of TAPPI International Paper Physics Conference. Kona, HI, 1991. p. 365-374.

Nevell TP, Zeronian SH. Cellulose chemistry and its applications. New York: Wiley, 1985.

Ramlochan T, Thomas MDA, Hooton RD. The effect of pozzolans and slag on the expansion of mortars cured at elevated temperature, Part II: Microstructural and microchemical investigations. Cement and Concrete Research 2004;34:1341-1356.

Richardson IG, Groves GW. Incorporation of minor and trace elements into calcium silicate hydrate (C-S-H) gel in hardened cement pastes. Cement and Concrete Research 1993;23(1):131-138.

Richardson IG. The nature of C-S-H in hardened cement pastes. Cement and Concrete Research 1999;29(8):1131-1147.

Richardson JM, Biernacki JJ, Stutzmann PE, Bentz DP. Stoichiometry of slag hydration with calcium hydroxide. Journal of the American Ceramic Society 2002;85(4):947-953.

Sarigaphuti M, Shah SP, Vinson KD. Shrinkage cracking and durability characteristics of cellulose fiber reinforced concrete. ACI Materials Journal 1993;90(4):309-318.

Savastano H, Agopyan V. Transition zone studies of vegetable fibre-cement paste composites. Cement and Concrete Composites 1999;21:49-57.

Savastano H, Warden PG, Coutts RSP. Mechanically pulped sisal as reinforcement in cementitious matrices. Cement and Concrete Composites 2003;25:311-319.

Savastano H, Warden PG, Coutts RSP. Microstructure and mechanical properties of waster fibre-cement composites. Cement and Concrete Composites 2005;27(5):583-592.

Simatupang MH, Lange H. Lignocellulosic and plastic fibres for manufacturing of fibre cement boards. The International Journal of Cement Composites and Lightweight Concrete 1987;9(2):109-112.

Soroushian P, Marikunte S. Reinforcement of cement-based materials with cellulose fibers. Thin-section fiber reinforced concrete and ferrocement, SP-124, Detroit: American Concrete Institute, 1990:99-124.

Soroushian P, Marikunte S. Moisture sensitivity of cellulose fiber reinforced cement. Durability of Concrete V.2, SP-126, Detroit: American Concrete Institute, 1991:821-835.

Soroushian P, Marikunte S. Moisture effects on flexural performance of wood fiber-cement composites. Journal of Materials in Civil Engineering 1992;4(3):277-291.

Soroushian P, Marikunte S, Won JP. Wood fiber reinforced cement composites under wetting-drying and freezing-thawing cycles. Journal of Materials in Civil Engineering 1994;6(4):595-611.

Soroushian P, Shah Z, Won J. Optimatization of wastepaper fiber-cement composites. ACI Materials Journal 1995:92(1):82-97.

Soroushian P, Ravanbakhsh S. Control of plastic shrinkage cracking with specialty cellulose fibers. ACI Materials Journal 1998;95(4):429-435.

Soroushian P, Ravanbakhsh S. High-early-strength concrete: Mixture proportioning with processed cellulose fibers for durability. ACI Materials Journal 1999;96(5):593-599.

Soroushian P. Reinforcing effects on processed cellulose fibers in mortar (stucco), thin sheet products, and concrete. High-performance fiber-reinforced concrete thin sheet products, SP-190, Detroit: American Concrete Institute, 2000:203-214.

Stenius P. Forests Products Chemistry. Atlanta: TAPPI, 2000.

TAPPI T211, Ash in Wood, Pulp, Paper and Paperboard: Combustion at 525 Degrees C, Technical Association of the Pulp and Paper Industry, Atlanta, Georgia, USA, 2002.

TAPPI T412, Moisture in Pulp, Paper and Paperboard, Technical Association of the Pulp and Paper Industry, Atlanta, Georgia, USA, 2002.

Taylor HFW, Famy C, Scrivener KL. Delayed ettringite formation. Cement and Concrete Research 2001;31:683-693.

Taylor HFW. Cement Chemistry. London: Thomas Telford, 1997.

Thorp BA, Kocurek MJ, ed. Pulp and Paper Manufacture, V. 7: Paper Machine Operations. Montreal: Technical Section Canadian Pulp and Paper Association, 1998.

Tolêdo Filho RD, Scrivener K, England GL, Ghavami K. Durability of alkali-sensitive sisal and coconut fibres in cement mortar composites. Cement and Concrete Composites 2000;22(6):127-143.

Tolêdo Filho RD, England GL, Ghavami K, Scrivener K. Development of vegetable fibre–mortar composites of improved durability. Cement and Concrete Composites 2003;25:185–96.

Tolêdo Filho RD, Ghavami K, Sanjuan MA, England GL. Free, restrained and drying shrinkage of cement mortar composites reinforced with vegetable fibres. Cement and Concrete Composites 2005;27(5):537-546.

Vinson KD, Daniel JI. Specialty cellulose fibers for cement reinforcement. Thin-section fiber reinforced concrete and ferrocement, SP-124, Detroit: American Concrete Institute, 1990: 1-18.

Voigt T, Bui VK, Shah SP. Drying shrinkage of concrete reinforced with fibers and welded-wire fabric. ACI Materials Journal 2004;101(3):233-241.

Young JF, Mindess S, Gray RJ, Bentur A. The Science and Technology of Civil Engineering Materials. Upper Saddle River, NJ: Prentice Hall, 1998.

Ziraba YN, Baluch MH, Azad AK. Use of plasticized sulphur in sisal-fibre concrete. Durability of Building Materials 1985;3:65–76.